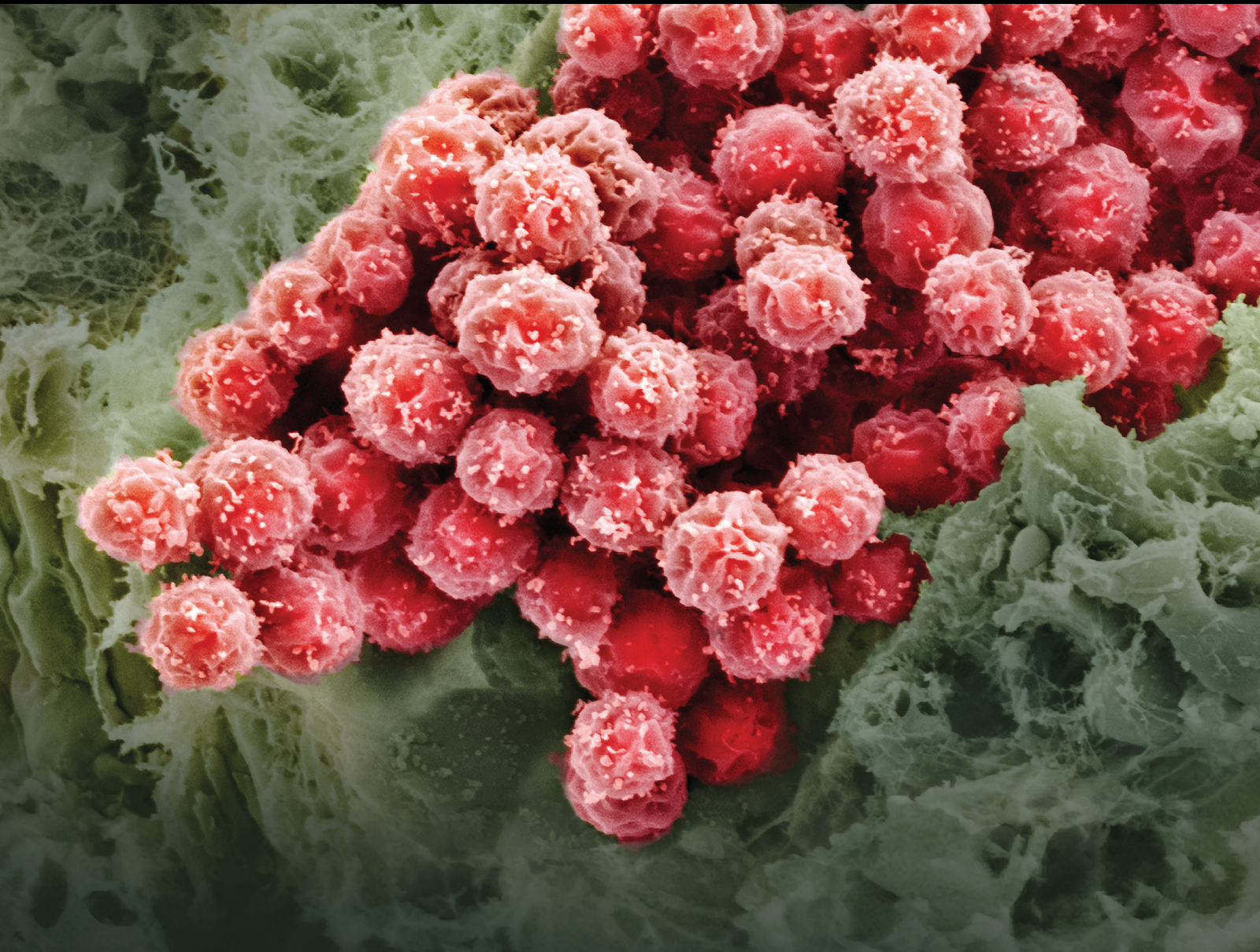


Stem Cell Therapies for Connective Tissue Regeneration toward Joint Preservation

Lead Guest Editor: Liang Gao

Guest Editors: Rebekah Decker, Francesca Taraballi, Riccardo Levato, and Zhenxing Shao





Stem Cell Therapies for Connective Tissue Regeneration toward Joint Preservation

Stem Cells International

**Stem Cell Therapies for Connective
Tissue Regeneration toward Joint
Preservation**

Lead Guest Editor: Liang Gao

Guest Editors: Rebekah Decker, Francesca
Taraballi, Riccardo Levato, and Zhenxing Shao







Copyright © 2021 Hindawi Limited. All rights reserved.

This is a special issue published in “Stem Cells International.” All articles are open access articles distributed under the Creative Commons Attribution License, which permits unrestricted use, distribution, and reproduction in any medium, provided the original work is properly cited.





Chief Editor

Renke Li , Canada

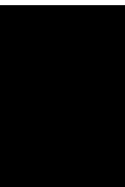
Associate Editors




James Adjaye , Germany
Andrzej Lange, Poland
Tao-Sheng Li , Japan
Heinrich Sauer , Germany
Holm Zaehres , Germany

Academic Editors

Cinzia Allegrucci , United Kingdom
Eckhard U Alt, USA
Francesco Angelini , Italy
James A. Ankrum , USA
Stefan Arnhold , Germany
Marta Baiocchi, Italy
Julie Bejoy , USA
Philippe Bourin , France
Benedetta Bussolati, Italy
Leonora Buzanska , Poland
Stefania Cantore , Italy
Simona Ceccarelli , Italy
Alain Chapel , France
Sumanta Chatterjee, USA
Isotta Chimenti , Italy
Mahmood S. Choudhery , Pakistan
Pier Paolo Claudio , USA
Gerald A. Colvin , USA
Joery De Kock, Belgium
Valdo Jose Dias Da Silva , Brazil
Leonard M. Eisenberg , USA
Alessandro Faroni , United Kingdom
Ji-Dong Fu , USA
Marialucia Gallorini , Italy
Jacob H. Hanna , Israel
David A. Hart , Canada
Zhao Huang , China
Elena A. Jones , United Kingdom
Oswaldo Keith Okamoto , Brazil
Alexander Kleger , Germany
Laura Lasagni , Italy
Shinn-Zong Lin , Taiwan
Zhao-Jun Liu , USA
Valeria Lucchino, Italy
Risheng Ma, USA
Giuseppe Mandraffino , Italy

Katia Mareschi , Italy
Pasquale Marrazzo , Italy
Francesca Megiorni , Italy
Susanna Miettinen , Finland
Claudia Montero-Menei, France
Christian Morszeck, Germany
Patricia Murray , United Kingdom
Federico Mussano , Italy
Mustapha Najimi , Belgium
Norimasa Nakamura , Japan
Karim Nayernia, United Kingdom
Toru Ogasawara , Japan
Paulo J Palma Palma, Portugal
Zhaoji Pan , China
Gianpaolo Papaccio, Italy
Kishore B. S. Pasumarthi , Canada
Manash Paul , USA
Yuriy Petrenko , Czech Republic
Phuc Van Pham, Vietnam
Alessandra Pisciotta , Italy
Bruno P#ault, USA
Liren Qian , China
Md Shaifur Rahman, Bangladesh
Pranela Rameshwar , USA
Syed Shadab Raza Raza , India
Alessandro Rosa , Italy
Subhadeep Roy , India
Antonio Salgado , Portugal
Fermin Sanchez-Guijo , Spain
Arif Siddiqui , Saudi Arabia
Shimon Slavin, Israel
Sieghart Sopper , Austria
Valeria Sorrenti , Italy
Ann Steele, USA
Alexander Storch , Germany
Hirotaka Suga , Japan
Gareth Sullivan , Norway
Masatoshi Suzuki , USA
Daniele Torella , Italy
H M Arif Ullah , USA
Aijun Wang , USA
Darius Widera , United Kingdom
Wasco Wruck , Germany
Takao Yasuhara, Japan
Zhaohui Ye , USA



Shuiqiao Yuan , China
Dunfang Zhang , China
Ludovic Zimmerlin, USA
Ewa K. Zuba-Surma , Poland




Contents

Mechanical Stress-Induced IGF-1 Facilitates col-I and col-III Synthesis via the IGF-1R/AKT/mTORC1 Signaling Pathway

Bin Yan , Canjun Zeng , Yuhui Chen , Minjun Huang , Na Yao , Jie Zhang , Bo Yan , Jiajun Tang , Liang Wang , and Zhongmin Zhang 






Research Article (11 pages), Article ID 5553676, Volume 2021 (2021)

Neu5Ac Induces Human Dental Pulp Stem Cell Osteo-/Odontoblastic Differentiation by Enhancing MAPK/ERK Pathway Activation

Changzhou Li, Xinghuan Xie, Zhongjun Liu, Jianhua Yang , Daming Zuo , and Shuaimei Xu 







Research Article (12 pages), Article ID 5560872, Volume 2021 (2021)

Bone Mesenchymal Stem Cells Contribute to Ligament Regeneration and Graft–Bone Healing after Anterior Cruciate Ligament Reconstruction with Silk–Collagen Scaffold

Fanggang Bi , Yangdi Chen , Junqi Liu , Wenhao Hu , and Ke Tian 

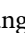




Research Article (11 pages), Article ID 6697969, Volume 2021 (2021)

Potency of Bone Marrow-Derived Mesenchymal Stem Cells and Indomethacin in Complete Freund's Adjuvant-Induced Arthritic Rats: Roles of TNF- α , IL-10, iNOS, MMP-9, and TGF- β 1

Eman A. Ahmed , Osama M. Ahmed , Hanaa I. Fahim , Tarek M. Ali , Basem H. Elesawy , and Mohamed B. Ashour 

Research Article (11 pages), Article ID 6665601, Volume 2021 (2021)

Research Progress on Stem Cell Therapies for Articular Cartilage Regeneration

Shuangpeng Jiang , Guangzhao Tian , Xu Li, Zhen Yang, Fuxin Wang, Zhuang Tian, Bo Huang, Fu Wei, Kangkang Zha, Zhiqiang Sun, Xiang Sui, Shuyun Liu , Weimin Guo , and Quanyi Guo 

Review Article (25 pages), Article ID 8882505, Volume 2021 (2021)











Bioengineering Approaches to Accelerate Clinical Translation of Stem Cell Therapies Treating Osteochondral Diseases

Meng Wang , Yixuan Luo , Yin Yu , and Fei Chen 

Review Article (13 pages), Article ID 8874742, Volume 2020 (2020)

Research Article

Mechanical Stress-Induced IGF-1 Facilitates col-I and col-III Synthesis via the IGF-1R/AKT/mTORC1 Signaling Pathway

Bin Yan ¹, Canjun Zeng ², Yuhui Chen ³, Minjun Huang ¹, Na Yao ⁴, Jie Zhang ¹,
Bo Yan ¹, Jiajun Tang ¹, Liang Wang ¹, and Zhongmin Zhang ⁵

¹Department of Spine Surgery, Center for Orthopedic Surgery, The Third Affiliated Hospital of Southern Medical University, Guangzhou, Guangdong, China

²Department of Foot and Ankle Surgery, Center for Orthopedic Surgery, The Third Affiliated Hospital of Southern Medical University, Guangzhou, Guangdong, China

³Department of Traumatic Surgery, Center for Orthopedic Surgery, The Third Affiliated Hospital of Southern Medical University, Guangzhou, Guangdong, China

⁴Guangdong Food and Drug Vocational-Technical School, Guangzhou, Guangdong, China

⁵Department of Spine Surgery, Nanfang Hospital of Southern Medical University, Guangzhou, Guangdong, China

Correspondence should be addressed to Liang Wang; liang091@aliyun.com and Zhongmin Zhang; nfzzm@163.com

Received 14 January 2021; Revised 13 September 2021; Accepted 12 November 2021; Published 6 December 2021

Academic Editor: Andrea Ballini

Copyright © 2021 Bin Yan et al. This is an open access article distributed under the Creative Commons Attribution License, which permits unrestricted use, distribution, and reproduction in any medium, provided the original work is properly cited.

Mechanical stress promotes human ligamentum flavum cells (LFCs) to synthesize multitype collagens, leading to ligamentum flavum hypertrophy (LFH). However, the mechanism of mechanical stress in the formation of collagen remains unclear. Therefore, we investigated the relationship between mechanical stress and collagen synthesis in the present study. First, LFCs were isolated from 9 patients and cultured with or without mechanical stress exposure for different times. IGF-1, collagen I (col-I), and collagen III (col-III) protein and mRNA levels were then detected via ELISA and qPCR, respectively. Moreover, the activation of pIGF-1R, pAKT, and pS6 was examined by Western blot analysis. To further explore the underlying mechanism, an IGF-1 neutralizing antibody, NVP-AEW541, and rapamycin were used. IGF-1, col-I, and col-III were significantly increased in stressed LFCs compared to nonstressed LFCs. In addition, the activation of pIGF-1R, pAKT, and pS6 was obviously enhanced in stressed LFCs. Interestingly, col-I protein, col-I mRNA, col-III protein, col-III mRNA, and IGF-1 protein, but not IGF-1 mRNA, were inhibited by IGF-1 neutralizing antibody. In addition, col-I and col-III protein and mRNA, but not IGF-1, were inhibited by both NVP-AEW541 and rapamycin. Moreover, the activation of pIGF-1R, pAKT, and pS6 was reduced by the IGF-1 neutralizing antibody and NVP-AEW541, and the activation of pS6 was reduced by rapamycin. In summary, these results suggested that mechanical stress promotes LFCs to produce IGF-1, which facilitates col-I and col-III synthesis via the IGF-1R/AKT/mTORC1 signaling pathway.

1. Introduction

Currently, an increasing number of elderly individuals have lumbar spinal stenosis (LSS) [1, 2]. The clinical symptoms of LSS include lower limb numbness with pain, low back pain, and claudication [3]. LSS causes tremendous discomfort for patients, and LSS is often caused by ligamentum flavum hypertrophy (LFH) [4, 5]. Previous studies [6–9] have shown that mechanical stress promotes collagen I (col-I) and collagen III

(col-III) synthesis which contributes to LFH. However, the exact mechanisms remain unclear.

According to a previous study [10], IGF-1 is important for anabolism and stimulates the IGF-1R/AKT/mTORC1 signaling pathway, resulting in muscle or bone formation [11–13]. Moreover, increased IGF-1 promotes hypertrophy of various tissues [14–17], and mechanical stress plays a vital role in IGF-1 formation [18, 19]. We have previously reported that [20] exogenous IGF-1 promotes col-I and

col-III synthesis in LFCs, which are fibrous connective tissue stem cells. However, in LFH, the relationship of mechanical stress and IGF-1 has not been sufficiently studied.

In the present study, we hypothesized that mechanical stress plays a pivotal role in IGF-1 synthesis. In addition, IGF-1 may promote col-I and col-III synthesis by the IGF-1R/AKT/mTORC1 signaling pathway. To test these hypotheses, col-I and col-III as the important indicator of LFH were detected, and related marker activation of the IGF-1R/AKT/mTORC1 signaling pathway was examined. In addition, the relationship of mechanical stress and IGF-1 in LFH as well as the potential mechanism involved was investigated.

2. Materials and Methods

2.1. LFC Cultivation and Identification. First, nonthickened ligamentum flavum (LF) samples were aseptically obtained from 9 lumbar surgery patients (5 males and 4 females with an average age of 47.2 years). The LF samples were washed with physiological saline 3 times before being minced into 0.5 mm³ pieces. The LF samples were then digested with 0.2% collagenase-I for 1.5 h at 37°C and washed 2 times with PBS. The LF samples were centrifuged 3 times at 1000 r/min for 5 min before being placed in cell culture plates with DMEM containing 20% fetal bovine serum (FBS). Subsequently, the LF samples were incubated, and the medium was changed every 3 days. Approximately one week later, LFCs migrated out from the LF samples. When the LFCs reached 80% confluence, they were passaged 1:2. Moreover, some of the LFCs were cryopreserved in media (10%DMSO + 20%FBS + 70%DMEM) at -80°C. LFC morphology was inspected, and the expression of vimentin and col-I in LFCs was detected by immunostaining [21].

2.2. Mechanical Stress Application. Experiments were performed with LFCs from each individual patient. The LFCs were grouped into experimental and control groups, and they were cultured in BioFlex I 6-well plates at 1×10^5 cells per well. After LFCs reached 80% confluence, they were subjected to serum starvation (DMEM with 0.2% FBS) for 12 h. The experimental groups were subjected to cycles of relaxation for 10 s and 20% elongation for 10 s by a tension system (FX5K, Flexcell International Corporation, USA) [22–25] for 6 h, 12 h, and 24 h. Control groups were cultured in the same environment without mechanical stress.

2.3. IGF-1 Neutralizing Antibody Treatment. LFCs were grouped into the following 3 groups: nonstress group, stress group, and stress+IGF-1 neutralizing antibody (10 µg/ml, Abcam, Cambridge, UK) group. LFCs in the stress group and the stress+IGF-1 neutralizing antibody group were subjected to cycles of relaxation for 10 s and 20% elongation for 10 s by the tension system for 24 h, and LFCs in the nonstress group were not subjected to mechanical stress. IGF-1, col-I and col-III protein, and mRNA levels were detected by ELISA and RT-qPCR, respectively, in each group. In addition, the activation of pIGF-1R, pAKT, and pS6 in each group was evaluated by Western blot analysis.

2.4. NVP-AEW541 Treatment. LFCs were grouped into the following 3 groups: nonstress group, stress group, and stress+100 ng/ml NVP-AEW541 (a specific inhibitor of IGF-1R, dissolved in DMSO, MedChem Express, Monmouth Junction, NJ) group. LFCs in the stress group and the stress+100 ng/ml NVP-AEW541 group were subjected to cycles of relaxation for 10 s and 20% elongation for 10 s by the tension system for 24 h, and LFCs in the nonstress group were not subjected to mechanical stress. IGF-1, col-I and col-III protein, and mRNA levels were detected by ELISA and RT-qPCR, respectively, in each group. Moreover, the activation of pIGF-1R, pAKT, and pS6 in each group was evaluated by Western blot analysis.

2.5. Rapamycin Treatment. LFCs were grouped into the following 3 groups: nonstress group, stress group, and stress+10 ng/ml rapamycin (a specific inhibitor of mTORC1, dissolved in DMSO, Alexis Biochemicals, Lausen, Switzerland) group. LFCs in the stress group and the stress+10 ng/ml rapamycin group were subjected to cycles of relaxation for 10 s and 20% elongation for 10 s by the tension system for 24 h, and LFCs in the nonstress group were not subjected to mechanical stress. IGF-1, col-I and col-III protein, and mRNA levels were detected by ELISA and RT-qPCR, respectively, in each group. Moreover, the activation of pS6 in each group was evaluated by Western blot analysis.

2.6. RT-qPCR Analysis. IGF-1, col-I, and col-III mRNA was measured by RT-qPCR in each group. First, we extracted total RNA from LFCs and detected its concentration and purity. Reverse transcription was then performed followed by qPCR. The primer sequences used in the present study are listed in Table 1 [21]. Sangon Biotech (Sangon Biotech, China) synthesized all primers in the study. All assays in the study were performed in triplicate. The samples were normalized to GAPDH and analyzed by the $2^{-\Delta\Delta Cq}$ method [26].

2.7. Enzyme-Linked Immunosorbent Assay. Culture supernatants from LFCs in each group were collected. To remove insoluble impurities and cell debris, the supernatants were centrifuged at 1000 g at 4°C for 20 min. The cleared supernatants were immediately used to measure IGF-1, col-I, and col-III protein levels by a Human IGF-1 ELISA Kit (Elabscience Biotechnology, China), Collagen I ELISA Kit (Elabscience Biotechnology, China), and Collagen III ELISA Kit (Elabscience Biotechnology), respectively.

2.8. Western Blot Assays. LFCs from each group were lysed on ice in lysis buffer, and the lysates were then added to Laemmli buffer at 100°C for 10 min. The LFC lysates were separated by electrophoresis, and the proteins were then transferred to nitrocellulose membranes. The membranes were blocked with TBS containing 5% nonfat milk for 2 h at 25°C. Subsequently, the membranes were incubated with primary antibodies for 12 h at 4°C followed by incubation with secondary antibodies for 1.5 h at 25°C. Finally, a chemiluminescence kit (Beyotime, China) was used to visualize the nitrocellulose membranes.

TABLE 1: Primers used in the study.

Gene	Sequence (5' to 3')
IGF-1	Forward GTG TTG CTT CCG GAG CTG TG
	Reverse CAA ATG TAC TTC CTT CTG AGT C
Collagen I	Forward GTC GAG GGC CAA GAC GAA G
	Reverse CAG ATC ACG TCA TCG CAC AAC
Collagen III	Forward ATG TTC CAC GGA AAC ACT GG
	Reverse GGA GAG AAG TCG AAG GAA TGC
GAPDH	Forward ACA CCC ACT CCT CCA CCT TT
	Reverse TTA CTC CTT GGA GGC CAT GT

2.9. Statistical Analyses. Data were statistically analyzed and graphed using GraphPad Prism 5.01 (GraphPad Software Inc., San Diego, CA, USA). Protein and mRNA changes with or without mechanical stress at different times were analyzed by one-way ANOVA, and Tukey's honestly significant difference was used as the post hoc method. The remaining data were analyzed by Student's *t*-test. The results were considered significant when $P < 0.05$, and the data are presented as the mean \pm SD.

3. Results

3.1. Identification and Morphology of LFCs with or without Mechanical Stress. Immunofluorescence staining showed that LFCs expressed high levels of col-I and vimentin (Figure 1), which indicated that highly purified LFCs were cultured. Without mechanical stress, most LFCs were polygonal (Figure 2(a)). Under mechanical stress, LFCs became fusiform and arranged along the direction of stress (Figure 2(b)).

3.2. Mechanical Stress Promotes IGF-1, col-I, and col-III Protein and mRNA Production as well as Activation of pIGF-1R, pAKT, and pS6. IGF-1, col-I, and col-III mRNA was examined via RT-qPCR in the stress group and the nonstress group at 6h, 12h, and 24h. Mechanical stress upregulated IGF-1, col-I, and col-III mRNA production in a time-dependent manner (Figures 3(e)–3(g)). Moreover, IGF-1, col-I, and col-III protein levels were examined by ELISA at 6h, 12h, and 24h. Mechanical stress increased IGF-1, col-I, and col-III protein production in a time-dependent manner (Figures 3(h)–3(j)). The activation of pIGF-1R, pAKT, and pS6 was evaluated in the stress group and the nonstress group by Western blot analysis at 6h, 12h, and 24h. Mechanical stress increased the activation of pIGF-1R (Figures 3(a) and 3(b)), pAKT (Figures 3(a) and 3(c)), and pS6 (Figures 3(a) and 3(d)) in a time-dependent manner.

3.3. IGF-1 Neutralizing Antibody Reduces col-I and col-III mRNA Production; Reduces IGF-1, col-I, and col-III Protein Production; and Suppresses the Activation of pIGF-1R, pAKT, and pS6. IGF-1, col-I, and col-III mRNA and protein levels were examined by RT-qPCR and ELISA, respectively, at 24h for the nonstress group, the stress group, and the stress+10 μ g/ml IGF-1 neutralizing antibody group. The

IGF-1 neutralizing antibody reduced the mRNA levels of col-I/col-III (Figures 4(f) and 4(g)), but not IGF-1 (Figure 4(e)). Moreover, IGF-1, col-I, and col-III protein levels were reduced by the IGF-1 neutralizing antibody (Figures 4(h)–4(j)). Furthermore, IGF-1 neutralizing antibody suppressed the activation of pIGF-1R (Figures 4(a) and 4(b)), pAKT (Figures 4(a) and 4(c)), and pS6 (Figures 4(a) and 4(d)).

3.4. NVP-AEW541 Reduces IGF-1, col-I, and col-III Protein and mRNA Production and Suppresses the Activation of pIGF-1R, pAKT, and pS6. IGF-1, col-I, and col-III mRNA and protein levels were examined by RT-qPCR and ELISA, respectively, at 24h in the nonstress group, the stress group, and the stress+100 ng/ml NVP-AEW541 group. NVP-AEW541 reduced the mRNA levels of col-I/col-III mRNA (Figures 5(f) and 5(g)), but not IGF-1 (Figure 5(e)), and it reduced the protein levels of col-I/col-III protein (Figures 5(i) and 5(j)), but not IGF-1 (Figure 5(h)). In addition, the activation of pIGF-1R (Figures 5(a) and 5(b)), pAKT (Figures 5(a) and 5(c)), and pS6 (Figures 5(a) and 5(d)) was reduced by NVP-AEW541.

3.5. Rapamycin Reduces IGF-1, col-I, and col-III Protein and mRNA Production and Suppresses the Activation of pS6. IGF-1, col-I, and col-III mRNA and protein levels were detected by RT-qPCR and ELISA, respectively, at 24h in the nonstress group, the stress group, and the stress+10 ng/ml rapamycin group. Rapamycin decreased the mRNA levels of col-I/col-III (Figures 6(d) and 6(e)), but not IGF-1 (Figure 6(c)), and it reduced the protein levels of col-I/col-III (Figures 6(g) and 6(h)), but not IGF-1 (Figure 6(f)). In addition, the induction of pS6 was suppressed by rapamycin (Figures 6(a) and 6(b)).

4. Discussion

In previous studies, LFH has been identified as a common cause of LSS [3–5]. LFH is caused by increased collagen levels, mainly col-I and col-III [8, 21, 27–29]. Many inflammatory and growth factors such as IL-1, IL-6, TGF- β 1, VEGF, PDGF-BB, CTGF, and TNF- α have been reported to promote col-I and col-III production, eventually leading to LFH [8, 21, 27, 30–36]. Chuang et al. [37] showed that oxidative stress activates the Akt and MAPK pathways to upregulate inflammatory mediator (iNOS and NF- κ B) and fibrotic marker (TGF- β , β -catenin, α -SMA, and vimentin) expression levels, thereby contributing to LFH. Habibi et al. [38] confirmed that acidic fibroblast growth factor (FGF-1) expression is higher in LSS patient tissues than in nonhypertrophied ligamentum flavum tissues.

IGF-1 is a vital growth factor that promotes collagen production via the mTORC1 signaling pathway [11–13]. According to previous studies [14–17], IGF-1 is released by various types of cells under mechanical stress and IGF-1 increases collagen expression levels, which contributes to the hypertrophy of various tissues. Some studies have also reported [6–9] that mechanical stress may play a vital role in LFH. Nakatani et al. [8] indicated that mechanical stress

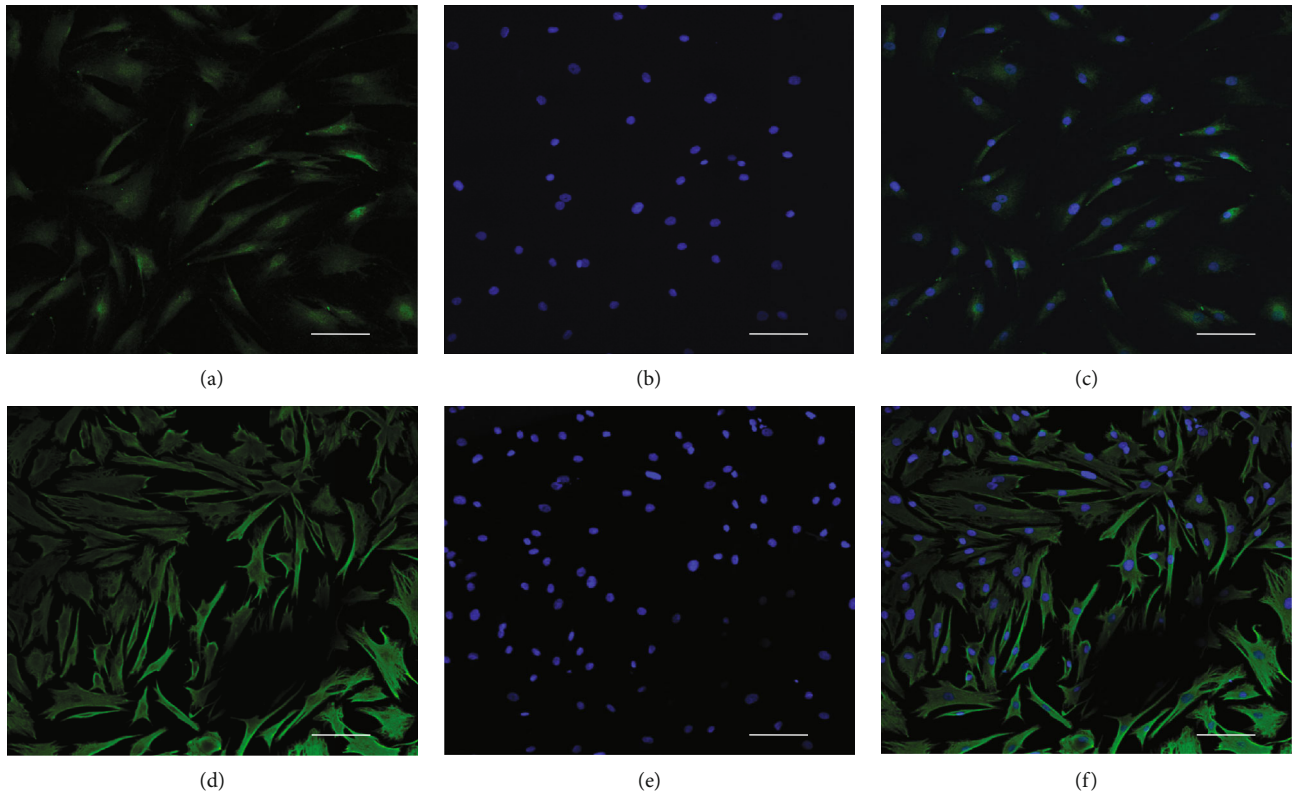


FIGURE 1: Identification of LFCs. Collagen I (a) and vimentin (d) immunofluorescence staining. Immunofluorescence is shown in green (a, d), and DAPI-stained nuclei are shown in blue (b, e). Merged pictures are shown (c, f). LFCs: ligamentum flavum cells; DAPI: 4',6-diamidino-2-phenylindole. Scale bar = 50 μm .

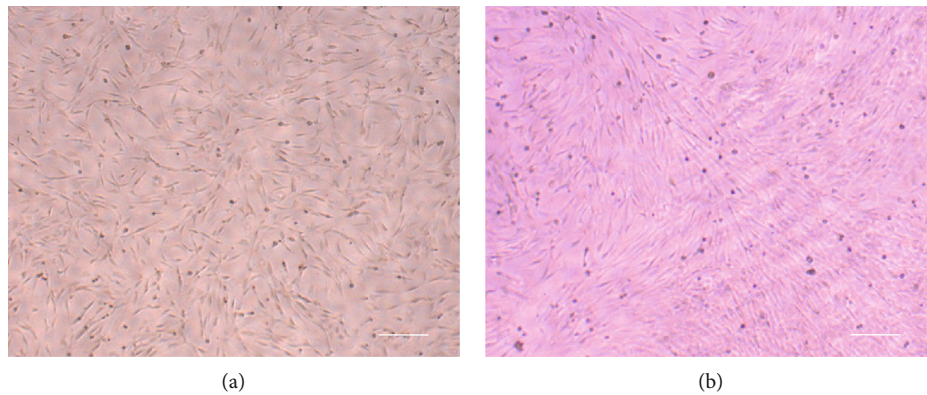


FIGURE 2: Morphology of LFCs with or without mechanical stress. LFCs were cultured without mechanical stress (a). LFCs were subjected to cycles of relaxation for 10 s and 20% elongation for 10 s (b). LFCs: ligamentum flavum cells. Scale bar = 100 μm .

stimulates LFCs to produce TGF- β 1, which increases the synthesis of collagens, resulting in LFH. Hayashi et al. [9] reported that fibroblast growth factor 9 (FGF9) and its pathway contribute to LFH under mechanical stress. Reijnders et al. [18] reported that mechanical stress results in IGF-1 mRNA upregulation in osteocytes of rat tibia and that IGF-1 is involved in the translation of mechanical stress to bone formation. Juffer et al. [19] showed that mechanical stress stimulates MLO-Y4 osteocytes to express IGF-1 isoform, which is an important factor in anabolism and metab-

olism in muscle, at the mRNA and protein levels. However, the interaction between mechanical stress and IGF-1 has not been previously studied in LFH. In the present study, we researched the correlation of mechanical stress, IGF-1, and the IGF-1R/AKT/mTORC1 signaling pathway in LFH.

First, we isolated primary LFCs from 9 patients who underwent lumbar spinal surgery. LFCs are fibrous connective tissue stem cells. According to the study conducted by Zhong and Chen [39], LFCs can be identified by detecting col-I and vimentin expression. Therefore, in the present

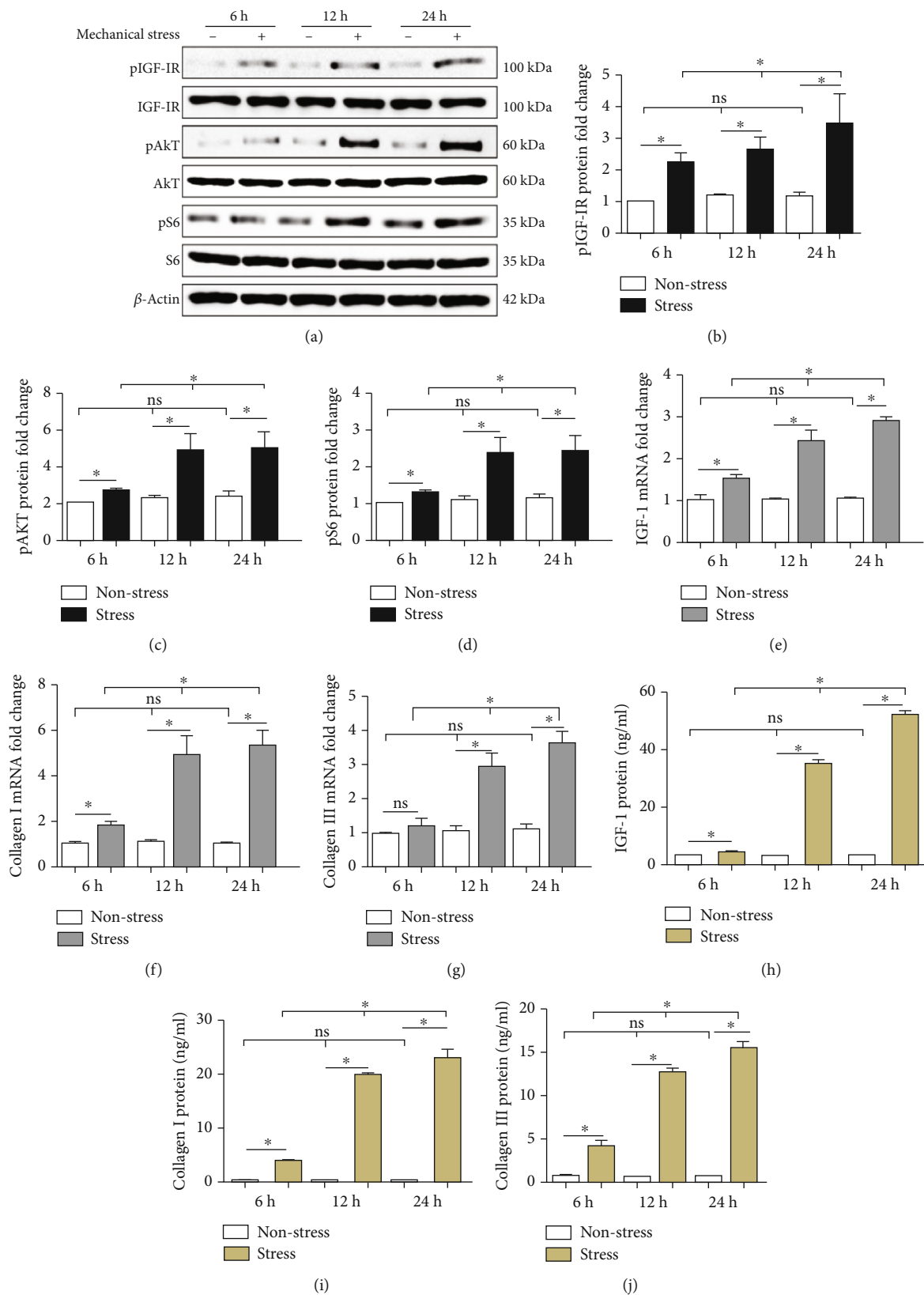


FIGURE 3: IGF-1R/AKT/mTORC1 signaling pathway-related mRNA and protein changes in LFCs with or without mechanical stress. Mechanical stress upregulated the activation of pIGF-1R (a, b), pAKT (a, c), and pS6 (a, d), as well as the mRNA levels of IGF-1 (e), col-I (f), and col-III (g) and the protein levels of IGF-1 (h), col-I (i), and col-III (j) in a time-dependent manner. Columns represent the mean ± SD of 3 samples, and each experiment was performed in triplicate. LFCs: ligamentum flavum cells; IGF-1: insulin-like growth factor 1; col-I: collagen I; col-III: collagen III. “*” represents $P < 0.05$; “ns” indicates $P > 0.05$.

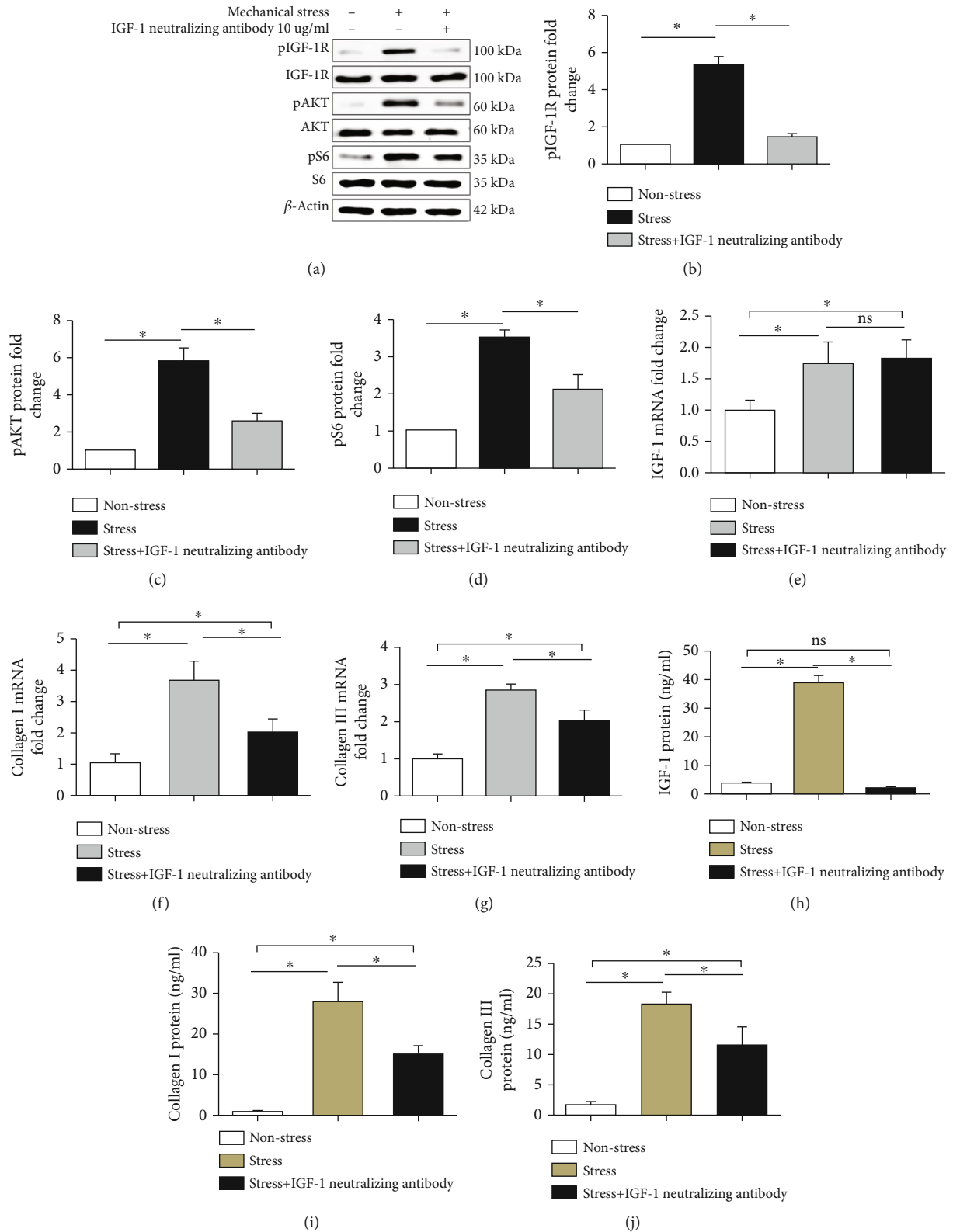


FIGURE 4: IGF-1 neutralizing antibody treatment. Mechanical stress in the nonstress group, the stress group, and the stress+10 μ g/ml IGF-1 neutralizing antibody group. The IGF-1 neutralizing antibody reduced the mRNA levels of col-I (f) and col-III (g), but not IGF-1 (e). The IGF-1 neutralizing antibody also reduced the protein expression of IGF-1 (h), col-I (i), and col-III (j). In addition, the activation of pIGF-1R (a, b), pAKT (a, c), and pS6 (a, d) was reduced by the IGF-1 neutralizing antibody. Columns represent the mean \pm SD of 3 samples, and each experiment was performed in triplicate. LFCs: ligamentum flavum cells; IGF-1: insulin-like growth factor 1; col-I: collagen I; col-III: collagen III. "*" represents $P < 0.05$; "ns" indicates $P > 0.05$.

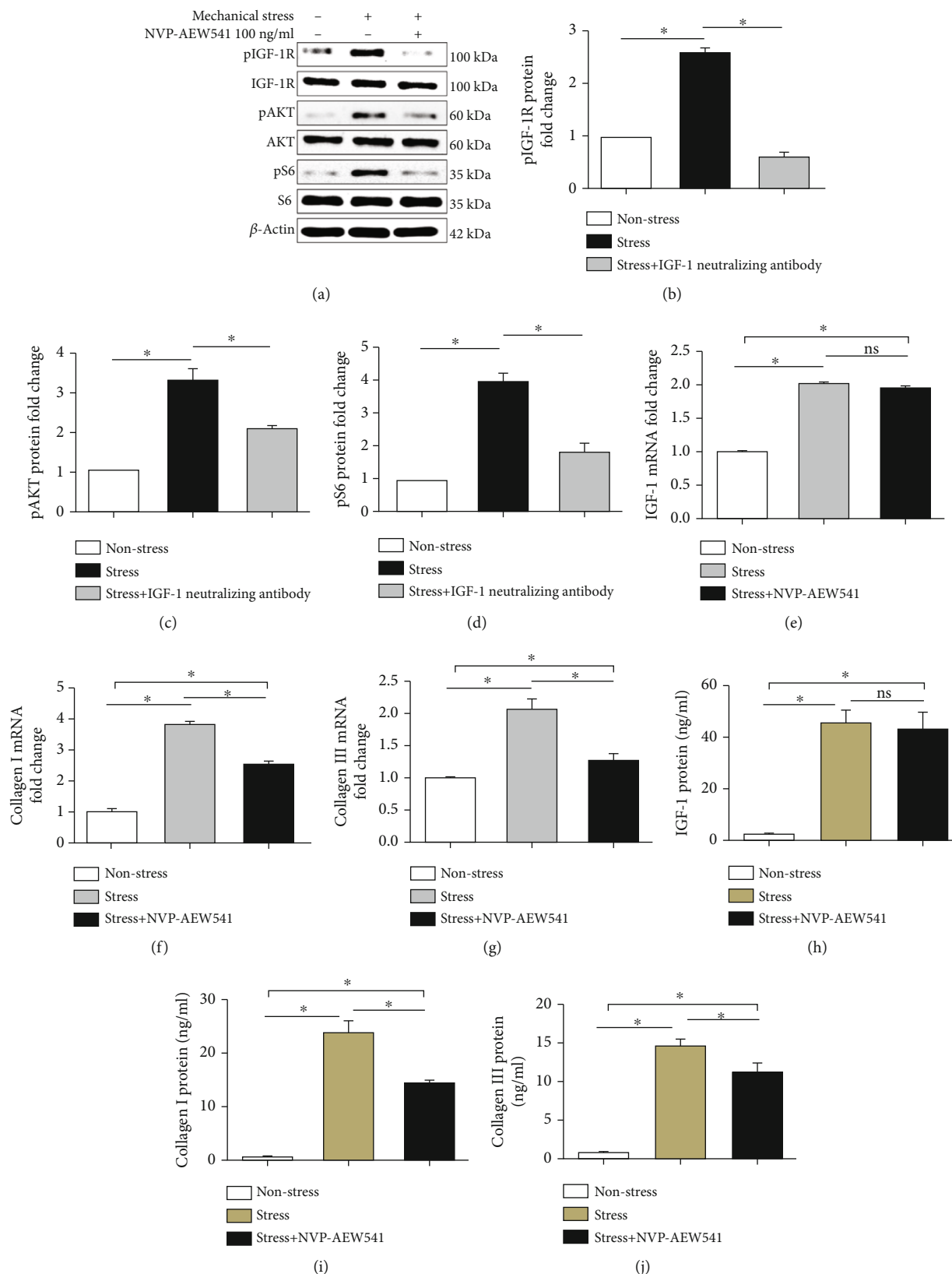


FIGURE 5: NVP-AEW541 treatment. Mechanical stress in the nonstress group, the stress group, and the stress+100 ng/ml NVP-AEW541 group. NVP-AEW541 reduced the mRNA levels of col-I (f) and col-III (g), but not IGF-1 (e). col-I (i) and col-III (j) protein levels, but not IGF-1 (h) protein levels, were attenuated by NVP-AEW541. In addition, NVP-AEW541 reduced the activation of pIGF-1R (a, b), pAKT (a, c), and pS6 (a, d). Columns represent the mean \pm SD of 3 samples, and each experiment was performed in triplicate. LFCs: ligamentum flavum cells; IGF-1: insulin-like growth factor 1; col-I: collagen I; col-III: collagen III. “*” represents $P < 0.05$; “ns” indicates $P > 0.05$.

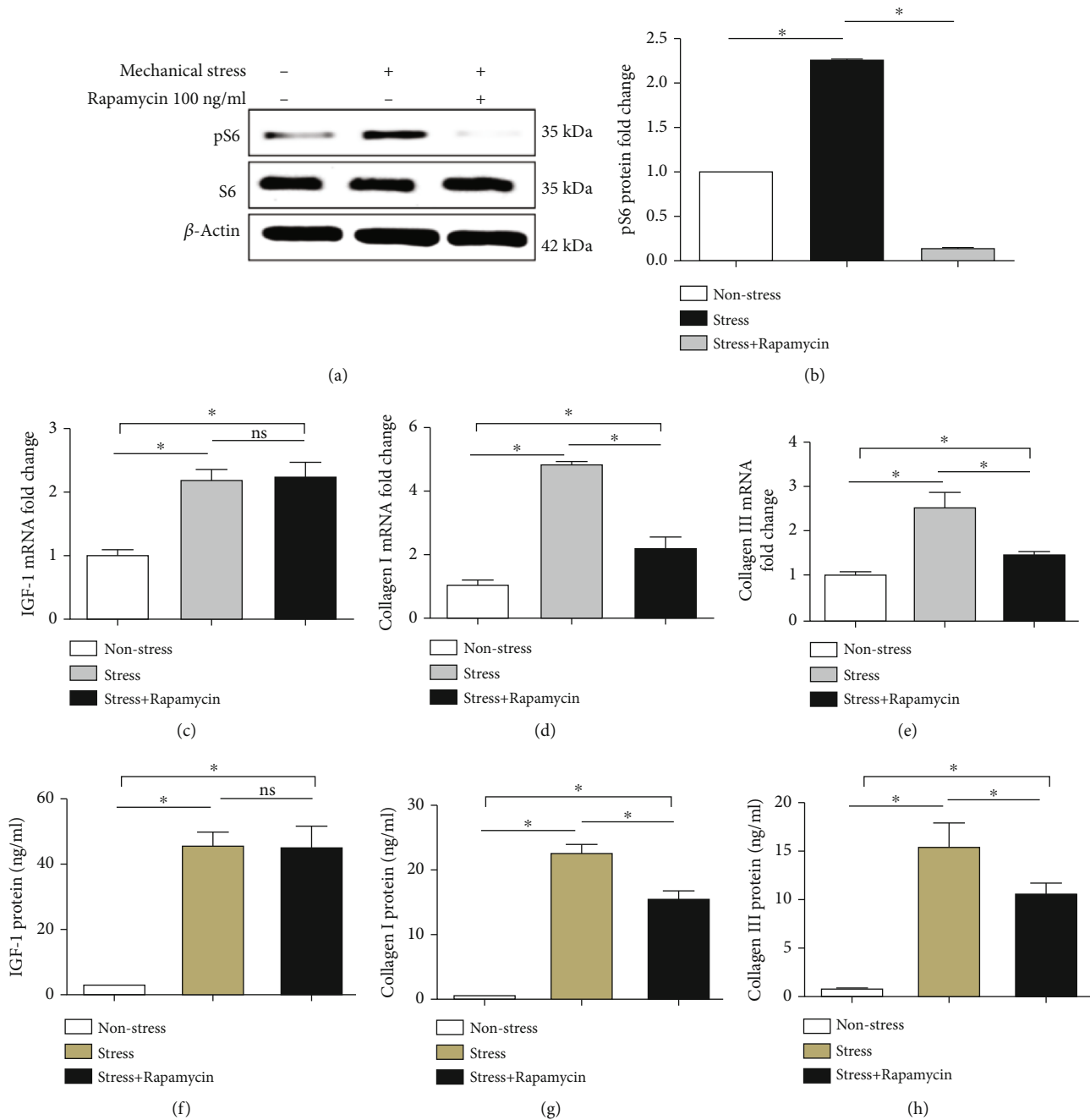


FIGURE 6: Rapamycin treatment. Mechanical stress in the nonstress group, the stress group, and the stress+rapamycin group. Rapamycin reduced the mRNA levels of col-I (d) and col-III (e), but not IGF-1 (c). Rapamycin reduced the protein levels of col-I (g) and col-III (h), but not IGF-1 (f). In addition, rapamycin reduced the activation of pS6 (a, b). Columns represent the mean \pm SD of 3 samples, and each experiment was performed in triplicate. LFCs: ligamentum flavum cells; IGF-1: insulin-like growth factor 1; col-I: collagen I; col-III: collagen III. "*" represents $P < 0.05$; "ns" indicates $P > 0.05$.

study, LFC purity was examined by col-I and vimentin expression. Immunofluorescence results showed that the LFCs were of high purity (Figure 1). In addition, LFC viability was evaluated by the MTT assay (Solarbio, China), which demonstrated that there were no changes in LFC viability in each group.

LFCs were also subjected to cyclic mechanical stress at different times. Compared to nonstressed cells, cyclic mechanical stress promoted the synthesis of IGF-1 in LFCs

in a time-dependent manner, which eventually led to col-I/col-III accumulation via the IGF-1R/AKT/mTORC1 signaling pathway. To understand the molecular mechanism involved, we used an IGF-1 neutralizing antibody. Compared to the nonstress group, IGF-1, col-I, and col-III protein and mRNA levels were increased in the stress group. In addition, col-I and col-III protein and mRNA levels were significantly reduced in the stress+IGF-1 neutralizing antibody group compared to the stress group. Interestingly,

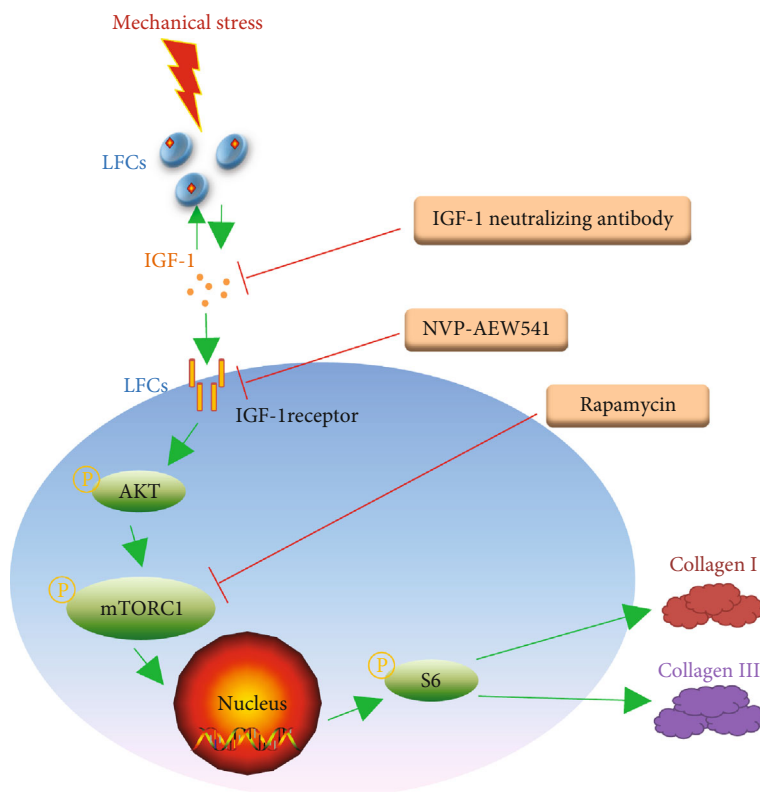


FIGURE 7: Potential mechanism by which mechanical stress promotes collagen I and collagen III synthesis.

IGF-1 protein expression, but not mRNA expression, was reduced in the stress+IGF-1 neutralizing antibody group compared to the stress group. Correspondingly, the activation of pIGF-1R, pAKT, and pS6 was decreased in the stress+IGF-1 neutralizing antibody group compared to the stress group. For further investigation, NVP-AEW541 (a specific inhibitor of IGF-1R) and rapamycin (a specific inhibitor of mTORC1) were used in the present study. Although 100 ng/ml NVP-AEW541 and 10 ng/ml rapamycin almost completely blocked the IGF-1R/AKT/mTORC1 signaling pathway, col-I and col-III protein and mRNA levels were only partially reduced. col-I and col-III protein and mRNA levels were still higher in both groups compared to the nonstress group. Moreover, neither NVP-AEW541 nor rapamycin reversed IGF-1 expression, which was induced by mechanical stress.

Based on the above findings, we hypothesized that mechanical stress may promote col-I and col-III production via other signaling pathways, and the potential mechanism involved requires further study. In addition, due to the lack of an animal model of LFH, only cytological experiments were performed in the present study. Thus, it is necessary to build an effective animal model for further research.

5. Conclusion

In summary, the present study showed that mechanical stress upregulated IGF-1, col-I, and col-III protein and mRNA production. The IGF-1 neutralizing antibody, NVP-AEW541, and rapamycin blocked the IGF-1R/AKT/

mTORC1 signaling pathway and reduced col-I and col-III production in LFCs. These findings demonstrated that cyclic mechanical stress promotes LFCs to secrete IGF-1, which induces col-I and col-III synthesis via the IGF-1R/AKT/mTORC1 signaling pathway (Figure 7). These results provide a new understanding of LFH and may facilitate the development of novel methods to treat LSS.

Data Availability

Data are available on request (detail contact information: nfzzm@163.com).

Conflicts of Interest

The authors in the study declare that they have no conflicts of interest.

Authors' Contributions

Bin Yan, Canjun Zeng, and Yuhui Chen contributed equally to this work.

Acknowledgments

The National Natural Science Foundation of China (No. 31801012) and Science and Technology Program of Guangzhou, China (201804010390), supported this study.

References

- [1] J. Deasy, "Acquired lumbar spinal stenosis," *Journal of the American Academy of Physician Assistants*, vol. 28, no. 4, pp. 19–23, 2015.
- [2] Y. Yabe, Y. Hagiwara, M. Tsuchiya et al., "Decreased elastic fibers and increased proteoglycans in the ligamentum flavum of patients with lumbar spinal canal stenosis," *Journal of Orthopaedic Research*, vol. 34, no. 7, pp. 1241–1247, 2016.
- [3] P. Jatteau and A. Bardonnnet, "Pathomechanism of ligamentum flavum hypertrophy: a multidisciplinary investigation based on clinical, biomechanical, histologic, and biologic assessments," *Spine*, vol. 30, no. 23, p. 2649, 2005.
- [4] S. Costandi, B. Chopko, M. Mekhail, T. Dews, and N. Mekhail, "Lumbar spinal stenosis: therapeutic options review," *Pain Practice*, vol. 15, no. 1, pp. 68–81, 2015.
- [5] M. Szpalski and R. Gunzburg, "Lumbar spinal stenosis in the elderly: an overview," *European Spine Journal*, vol. 12, no. 2, pp. S170–S175, 2003.
- [6] T. Okuda, I. Baba, Y. Fujimoto et al., "The pathology of ligamentum flavum in degenerative lumbar disease," *Spine*, vol. 29, no. 15, pp. 1689–1697, 2004.
- [7] J. W. Hur, B. J. Kim, J. H. Park et al., "The mechanism of ligamentum flavum hypertrophy," *Neurosurgery*, vol. 77, no. 2, pp. 274–282, 2015.
- [8] T. Nakatani, T. Marui, T. Hitora, M. Doita, K. Nishida, and M. Kurosaka, "Mechanical stretching force promotes collagen synthesis by cultured cells from human ligamentum flavum via transforming growth factor-beta1," *Journal of Orthopaedic Research*, vol. 20, no. 6, pp. 1380–1386, 2002.
- [9] K. Hayashi, A. Suzuki, H. Terai et al., "Fibroblast growth factor 9 is upregulated upon intervertebral mechanical stress-induced ligamentum flavum hypertrophy in a rabbit model," *Spine*, vol. 44, no. 20, pp. E1172–E1180, 2019.
- [10] Z. Zhang, L. Li, W. Yang et al., "The effects of different doses of IGF-1 on cartilage and subchondral bone during the repair of full-thickness articular cartilage defects in rabbits," *Osteoarthritis and Cartilage*, vol. 25, no. 2, pp. 309–320, 2017.
- [11] A. D. Bakker, T. Gakes, J. M. A. Hogervorst, G. M. J. de Wit, J. Klein-Nulend, and R. T. Jaspers, "Mechanical stimulation and IGF-1 enhance mRNA translation rate in osteoblasts via activation of the AKT-mTOR pathway," *Journal of Cellular Physiology*, vol. 231, no. 6, pp. 1283–1290, 2016.
- [12] M. Ding, R. K. Bruick, and Y. Yu, "Secreted IGFBP5 mediates mTORC1-dependent feedback inhibition of IGF-1 signalling," *Nature Cell Biology*, vol. 18, no. 3, pp. 319–327, 2016.
- [13] L. Xian, X. Wu, L. Pang et al., "Matrix IGF-1 maintains bone mass by activation of mTOR in mesenchymal stem cells," *Nature Medicine*, vol. 18, no. 7, pp. 1095–1101, 2012.
- [14] C. D. Blackstock, Y. Higashi, S. Sukhanov et al., "Insulin-like Growth Factor-1 Increases Synthesis of Collagen Type I via Induction of the mRNA-binding Protein LARP6 Expression and Binding to the 5' Stem-loop of *COL1a1* and *COL1a2* mRNA*," *Journal of Biological Chemistry*, vol. 289, no. 11, pp. 7264–7274, 2014.
- [15] S. Doessing, L. Holm, K. M. Heinemeier et al., "GH and IGF1 levels are positively associated with musculotendinous collagen expression: experiments in acromegalic and GH deficiency patients," *European Journal of Endocrinology*, vol. 163, no. 6, pp. 853–862, 2010.
- [16] P. Li, "Resveratrol inhibits collagen I synthesis by suppressing IGF-1R activation in intestinal fibroblasts," *World Journal of Gastroenterology*, vol. 20, no. 16, p. 4648, 2014.
- [17] S. Honscho, S. Nishikawa, K. Amano et al., "Pressure-mediated hypertrophy and mechanical stretch induces IL-1 release and subsequent IGF-1 generation to maintain compensative hypertrophy by affecting Akt and JNK pathways," *Circulation Research*, vol. 105, no. 11, pp. 1149–1158, 2009.
- [18] C. M. A. Reijnders, N. Bravenboer, A. M. Tromp, M. A. Blankenstein, and P. Lips, "Effect of mechanical loading on insulin-like growth factor-I gene expression in rat tibia," *Journal of Endocrinology*, vol. 192, no. 1, pp. 131–140, 2007.
- [19] P. Juffer, R. T. Jaspers, P. Lips, A. D. Bakker, and J. Klein-Nulend, "Expression of muscle anabolic and metabolic factors in mechanically loaded MLO-Y4 osteocytes," *American Journal of Physiology. Endocrinology and Metabolism*, vol. 302, no. 4, pp. E389–E395, 2012.
- [20] B. Yan, M. Huang, C. Zeng et al., "Locally produced IGF-1 promotes hypertrophy of the ligamentum flavum via the mTORC1 signaling pathway," *Cellular Physiology and Biochemistry*, vol. 48, no. 1, pp. 293–303, 2018.
- [21] Z.-M. Zhong, D. S. Zha, W. D. Xiao et al., "Hypertrophy of ligamentum flavum in lumbar spine stenosis associated with the increased expression of connective tissue growth factor," *Journal of Orthopaedic Research*, vol. 29, no. 10, pp. 1592–1597, 2011.
- [22] K. Iwasaki, K. I. Furukawa, M. Tanno et al., "Uni-axial cyclic stretch induces Cbfa1 expression in spinal ligament cells derived from patients with ossification of the posterior longitudinal ligament," *Calcified Tissue International*, vol. 74, no. 5, pp. 448–457, 2004.
- [23] H. Ohishi et al., "Role of prostaglandin I_{in} the gene expression induced by mechanical stress in spinal ligament cells derived from patients with ossification of the posterior longitudinal ligament," *Journal of Neurology Neurosurgery & Psychiatry*, vol. 86, no. 10, pp. 1082–1088, 2003.
- [24] K. Uchida, H. Nakajima, T. Takamura et al., "Gene expression profiles of neurotrophic factors in rat cultured spinal cord cells under cyclic tensile stress," *Spine*, vol. 33, no. 24, pp. 2596–2604, 2008.
- [25] H. X. Cai, T. Yayama, K. Uchida et al., "Cyclic tensile strain facilitates the ossification of ligamentum flavum through β -catenin signaling pathway: in vitro analysis," *Spine*, vol. 37, no. 11, pp. E639–E646, 2012.
- [26] K. J. Livak and T. D. Schmittgen, "Analysis of relative gene expression data using real-time quantitative PCR and the 2^{(-delta delta C(T))} method," *Methods*, vol. 25, no. 4, pp. 402–408, 2001.
- [27] Y. Zhang, J. Chen, Z. M. Zhong, D. Yang, and Q. Zhu, "Is platelet-derived growth factor-BB expression proportional to fibrosis in the hypertrophied lumbar ligamentum flavum?," *Spine*, vol. 35, no. 25, pp. E1479–E1486, 2010.
- [28] H. Kosaka, K. Sairyo, A. Biyani et al., "Pathomechanism of loss of elasticity and hypertrophy of lumbar ligamentum flavum in elderly patients with lumbar spinal canal stenosis," *Spine*, vol. 32, no. 25, pp. 2805–2811, 2007.
- [29] Y. Yabe, Y. Hagiwara, A. Ando et al., "Chondrogenic and fibrotic process in the ligamentum flavum of patients with lumbar spinal canal stenosis," *Spine*, vol. 40, no. 7, pp. 429–435, 2015.

- [30] K. Sairyo, A. Biyani, V. K. Goel et al., "Lumbar ligamentum flavum hypertrophy is due to accumulation of inflammation-related scar tissue," *Spine*, vol. 32, no. 11, pp. E340–E347, 2007.
- [31] J. O. Park, B. H. Lee, Y. M. Kang et al., "Inflammatory cytokines induce fibrosis and ossification of human ligamentum flavum cells," *Journal of Spinal Disorders & Techniques*, vol. 26, no. 1, pp. E6–E12, 2013.
- [32] B. J. Kim, J. W. Hur, J. S. Park et al., "Expression of matrix metalloproteinase-2 and -9 in human ligamentum flavum cells treated with tumor necrosis factor- α and interleukin-1 β ," *Journal of Neurosurgery Spine*, vol. 24, no. 3, pp. 428–435, 2016.
- [33] S. Lakemeier, M. D. Schofer, L. Foltz et al., "Expression of hypoxia-inducible Factor-1 α , vascular endothelial growth factor, and matrix metalloproteinases 1, 3, and 9 in hypertrophied ligamentum flavum," *Journal of Spinal Disorders & Techniques*, vol. 26, no. 7, pp. 400–406, 2013.
- [34] M. Löhr, J. A. Hampl, J. Y. Lee, R. I. Ernestus, M. Deckert, and W. Stenzel, "Hypertrophy of the lumbar ligamentum flavum is associated with inflammation-related TGF- β expression," *Acta Neurochirurgica*, vol. 153, no. 1, pp. 134–141, 2011.
- [35] Y. L. Cao, Y. Duan, L. X. Zhu, Y. N. Zhan, S. X. Min, and A. M. Jin, "TGF- β 1, in association with the increased expression of connective tissue growth factor, induce the hypertrophy of the ligamentum flavum through the p38 MAPK pathway," *International Journal of Molecular Medicine*, vol. 38, no. 2, pp. 391–398, 2016.
- [36] J. W. Hur, T. Bae, S. Ye et al., "Myofibroblast in the ligamentum flavum hypertrophic activity," *European Spine Journal*, vol. 26, pp. 1–10, 2017.
- [37] H. C. Chuang, K. L. Tsai, K. J. Tsai et al., "Oxidative stress mediates age-related hypertrophy of ligamentum flavum by inducing inflammation, fibrosis, and apoptosis through activating Akt and MAPK pathways," *Aging*, vol. 12, no. 23, pp. 24168–24183, 2020.
- [38] H. Habibi, A. Suzuki, K. Hayashi et al., "Expression and function of fibroblast growth factor 1 in the hypertrophied ligamentum flavum of lumbar spinal stenosis," *Journal of Orthopaedic Science*, vol. S0949-2658, no. 21, article id 00037-3, 2021.
- [39] Z. M. Zhong and J. T. Chen, "Phenotypic characterization of ligamentum flavum cells from patients with ossification of ligamentum flavum," *Yonsei Medical Journal*, vol. 50, no. 3, pp. 375–379, 2009.

Research Article

Neu5Ac Induces Human Dental Pulp Stem Cell Osteo-/Odontoblastic Differentiation by Enhancing MAPK/ERK Pathway Activation

Changzhou Li,^{1,2} Xinghuan Xie,¹ Zhongjun Liu,³ Jianhua Yang^{ID},⁴ Daming Zuo^{ID},^{1,5} and Shuaimei Xu^{ID}³

¹Department of Medical Laboratory, School of Laboratory Medicine and Biotechnology, Southern Medical University, Guangzhou, Guangdong 510515, China

²Department of Immunology, School of Basic Medical Sciences, Southern Medical University, Guangzhou, China

³Department of Endodontics, Stomatological Hospital, Southern Medical University, Guangzhou, China

⁴Department of Orthopaedics, Longgang District People's Hospital of Shenzhen, Shenzhen, China

⁵Microbiome Medicine Center, Department of Laboratory Medicine, Zhujiang Hospital, Southern Medical University, Guangzhou, China

Correspondence should be addressed to Jianhua Yang; jianhua01@163.com, Daming Zuo; zdaming@smu.edu.cn, and Shuaimei Xu; xushuaimei@smu.edu.cn

Received 9 January 2021; Revised 26 April 2021; Accepted 9 August 2021; Published 23 September 2021

Academic Editor: Liang Gao

Copyright © 2021 Changzhou Li et al. This is an open access article distributed under the Creative Commons Attribution License, which permits unrestricted use, distribution, and reproduction in any medium, provided the original work is properly cited.

Dental pulp stem cells (DPSCs) must undergo odontoblastic differentiation in order to facilitate the process of dentin-pulp complex repair. Herein, we sought to explore the ability of Neu5Ac (one form of sialic acid) to influence DPSC osteo-/odontoblastic differentiation via modulating mitogen-activated protein kinase (MAPK) signaling. *Methodology.* DPSCs were isolated from human third permanent teeth and were grown *in vitro*. Fluorescent microscopy was used to detect the existence of sialic acid on the DPSC membrane. Following the treatment of different concentrations of Neu5Ac and removing sialic acid from the cell surface by neuraminidase, the osteo-/odontoblastic differentiation of these cells was evaluated via mineralization, alkaline phosphatase, and *in vivo* assays. In addition, the expression of genes related to osteo-/odontoblastic differentiation and MAPK signaling at different stages of this differentiation process was analyzed in the presence or absence of Neu5Ac. *Results.* The existence of sialic acid on the DPSC membrane was confirmed by fluorescent microscopy, and the ability of osteo-/odontoblastic differentiation was decreased after removing sialic acid by neuraminidase. Treatment of DPSCs with Neu5Ac (0.1 mM or 1 mM) significantly enhanced their mineralization ability and alkaline phosphatase activity. The expression levels of DMP1, DSPP, BSP, and RUNX2 were also increased. Treatment of nude mice with ManNAc (the prerequisite form of Neu5Ac) also enhanced DPSC mineralization activity *in vivo*. Furthermore, Neu5Ac treatment enhanced p-ERK expression in DPSCs, while ERK pathway inhibition disrupted the ability of Neu5Ac to enhance the osteo-/odontoblastic differentiation of these cells. *Conclusions.* Neu5Ac can promote DPSC osteo-/odontoblastic differentiation through a process associated with the modulation of the ERK signaling pathway activity.

1. Introduction

Stem cells from oral cavity are easily harvestable and have shown a great plasticity towards the main lineages, specifically towards bone tissues [1]. Dental pulp stem cells (DPSCs) are the most investigated and commonly evaluated in the context

of tissue engineering and regenerative medicine [2]. Their clinical utility, however, is limited by the fact that relatively few of these cells are available, and they lose their ability to differentiate over the course of *in vitro* expansion [3]. Enhancing the utility of these cells in clinical tissue engineering contexts will therefore necessitate the development of novel approaches

to improving DPSC osteo-/odontoblastic differentiation capacity. Many factors to date have been found to impact this differentiation capacity, such as proinflammatory cytokines [4], growth factors [5], mechanical stretch, bioscaffolds/biomaterials [6, 7], and donor age [8]. Previous studies suggested that tissue inflammation may act against the tooth/bone formation/repair, and some natural compounds may be useful to alleviate this effect [9, 10]. These findings underscore the fact that the external microenvironment is a key determinant of DPSC fate, indicating that accurately recapitulating these conditions may represent a viable approach to apply these cells in the context of tissue regeneration.

Sialic acid (SA) is a component of cell surface sugar moieties that are associated with N- and O-glycan chains and glycolipids wherein it can be attached via α 2-3, α 2-6, and α 2-8 linkages [11]. SA expression is evident across vertebrate and nonvertebrate species and in mammals. It was primarily found in two major forms: N-acetylneuraminic acid (Neu5Ac) and N-glycolylneuraminic acid (Neu5Gc) [12]. Of these forms, only Neu5Ac is found in healthy humans [13], wherein it serves as an important regulator of interactions between cells and of signaling, enzymatic, and antibody-related activities [14].

The functional roles of sialic acid in many experimental contexts are well understood. Li et al. explored its role in the context of tumor cell proliferation and migration by removing sialic acid from the AGS gastric cancer cell line [15]. This led these authors to discover that MAL-II could specifically recognize and interact with terminal sialic acid residues within glycoprotein chains. Furthermore, they found that the treatment of AGS cells with α 2,3-neuraminidase, which cleaved cell surface sialic acid, enhanced the repair and migratory capabilities of these cells, highlighting the ability of sialic acid to drive cell-related signaling and behavior. Xu et al. further found that reductions in the SA expression on an osteoblast cell line were associated with decreases in both bone mineralization and the expression of bone sialoprotein (BSP), osteoprotegerin (OPG), and vitamin D receptor, indicating that SA plays key roles in the context of osteogenesis [16]. SA is closely related to many oral diseases such as recurrent aphthous ulcer, oral potentially malignant disorders (OPMD), and oral cancers [17]. Patients with OPMD and oral cancers exhibit a high SA concentration in the serum and saliva [17], while patients with recurrent aphthous stomatitis and other oral inflammations exhibit a low concentration of sialic acid [18]. As a kind of mesenchymal stem cells, DPSC has a great potential in oral clinical treatment. The specific role played by sialic acid in the context of DPSC osteo-/odontoblastic differentiation, however, has yet to be explored.

The present study was thus designed to assess whether Neu5Ac treatment was sufficient to enhance DPSC osteo-/odontoblastic differentiation, and if so, what signaling pathways and molecular mechanisms underlie such enhancement.

2. Methodology

2.1. DPSC Isolation and Culture. Caries-free third molars from 10 healthy patients (20–24 years old) were collected

immediately following the extraction and were used to isolate DPSCs. Dental pulp was isolated under sterile conditions and rinsed with PBS, after which they were minced using a ophthalmological scissors, and pulp aliquots were transferred into 6-well plates containing general medium (GM) composed of α -MEM containing 10% FBS and 1% penicillin-streptomycin (Gibco, USA). Cells were cultured in a 37°C with 5% CO₂ incubator, with media being changed every other day until cells reached confluence, at which time cells were passaged. Cells were used for experimentation following 3–5 passages. Osteo-/odontoblastic differentiation was induced in GM supplemented with 50 mg/ml ascorbic acid, 10 mM β -glycerol phosphates, and 10⁻⁷ mol/l dexamethasone. DPSC cell surface expression of stem cell markers (CD29, CD31, CD34, CD44, CD45, CD90, and CD105) was assessed via flow cytometry using antibodies from BD Biosciences (USA). The ethics committee of the Stomatological Hospital of Southern Medical University approved this study.

2.2. Treatment of DPSC with Neuraminidase or Neu5Ac. To evaluate the role of cell surface sialic acid in the odontoblastic differentiation process, DPSCs were treated with Neu5Ac or neuraminidase, which desialylated cell surface glycoconjugates. The impact of Neu5Ac on DPSCs was assessed by treating them with 0 mM, 0.1 mM, or 1 mM of Neu5Ac (Sigma-Aldrich, St Louis, MO, USA) added to the cell culture media. With regard to neuraminidase, DPSCs were exposed to neuraminidase (0 mU/ml, 1 mU/ml, 10 mU/ml, or 100 mU/ml, Sigma-Aldrich).

2.3. Cell Viability Assay (CCK-8 Assay). The cell viability was detected by Cell Counting Kit-8 (CCK-8) (Dojindo Laboratories, Kumamoto, Japan). Briefly, the cells were exposed to 0 mM, 0.1 mM, or 1 mM of Neu5Ac or 0 mU/ml, 1 mU/ml, 10 mU/ml, or 100 mU/ml of neuraminidase in 96-well plates for 1, 3, 5, or 7 days, and six wells were prepared for each dose of Neu5Ac and neuraminidase. After treatment, 10 μ l of CCK-8 solution was added to each well, and the 96-well plate was continuously incubated at 37°C for 1 hour; then, the OD value for each well was read at wavelength 450 nm to determine the cell viability on a microplate reader (Multiskan, Thermo, USA).

2.4. qRT-PCR. Cells were plated at 2 \times 10⁵ cells/well and were treated for 4, 7, or 14 days with neuraminidase (0 mU/ml, 1 mU/ml, 10 mU/ml, or 100 mU/ml) or Neu5Ac (0 mM, 0.1 mM, or 1 mM), after which TRIzol (Invitrogen, CA, USA) was used to extract total cell RNA based on provided instructions. A First-Strand cDNA Synthesis Kit (Gibco, USA) was then used to prepare cDNA from 1 g of total RNA per sample, after which qRT-PCR was conducted with SYBR green (Takara, Japan) and a thermocycler instrument (ABI7500, Applied Biosystems, USA). The 2^{- $\Delta\Delta$ Ct} method was employed to evaluate relative gene expression, with GAPDH being used as a normalization control. Primers used in this analysis are shown in Table 1.

2.5. Western Blotting. Western blotting was used to assess the MAPK signaling pathway and odontoblastic

TABLE 1: RT-PCR primers for the target genes.

Target gene	Primer sequence (5' to 3')
DMP1	F: TGAGTGAGTCCAGGGGAGATAA
DMP1	R: TTTTGTGAGTGGGAGAGTGTGTG C
DSPP	F: TTAAATGCCAGTGGAAACCAT
DSPP	R: ATTCCTTCTCCCTTGTGAC
BSP	F: CCCACCTTTTGGGAAAACCA
BSP	R: TCCCCGTTCTCACTTTCATAGAT
RUNX2	F:TGGTTACTGTCATGGCGGGTA
RUNX2	R: TCTCAGATCGTTGAACCTTGCTA
GAPDH	F: TGTTTCGTCATGGGTGTGAAC
GAPDH	R: ATGGCATGGACTGTGGTCAT

F: forward; R: reverse.

differentiation-related protein expression in DPSCs that were (1) treated with neuraminidase (0, 1, 10, or 100 mU/ml) for 4 days; (2) treated with Neu5Ac (0, 0.1, or 1 mM) for 4, 7, or 14 days; (3) treated with Neu5Ac (1 mM) for 0, 10, 30, 60, 90 minutes or for 3 days; and (4) pretreated with the extracellular signal-related kinase (ERK) inhibitor cobimetinib (1 μ M) for 4 hours and then treated with or without Neu5Ac (1 mM) for 4 days.

Following the above treatments, DPSCs were washed twice with PBS before resuspension in lysis buffer (Cell Signaling Technology, MA, USA) supplemented with phenylmethylsulfonyl fluoride (R&D Systems, Minneapolis, MN, USA) to facilitate protein extraction. A BCA assay was used to quantify protein levels in these extracts, after which samples were separated via SDS-PAGE and transferred to PVDF membranes. Blots were blocked for 1 hour with 5% nonfat milk, after which they were probed overnight with anti-DSPP, anti-DMP1, anti-RUNX2, anti-phospho-ERK, anti-ERK, anti-phospho-p38, anti-p38, anti-phospho-JNK, or anti-JNK (Cell Signaling Technology, MA, USA) at 4°C. Blots were then probed with appropriate secondary antibodies for 1 hour, after which protein bands were detected via a chemiluminescent approach.

2.6. ALP Staining. DPSCs were initially cultured in 6-well plates (1×10^5 /well) in the presence or absence of Neu5Ac or neuraminidase for 7 days. Culture media were then removed, and cells were fixed for 1 hour with 70% ethanol, after which they were stained with 300 μ l of ALP staining reagent (1-Step NBT/BCIP solution, Thermo Fisher Scientific) per well. Water was then added to terminate staining, and the stain was extracted via the addition of 10% (*w/v*) cetylpyridinium chloride (Sigma-Aldrich) for 15 minutes. Staining intensity was then quantified using a VERSA max Multiplate Reader by assessing absorbance at 540 nm.

2.7. Alizarin Red Staining. DPSCs were initially grown for 21 days in the presence of neuraminidase, Neu5Ac and/or cobimetinib, after which culture media were removed and cells were rinsed with PBS. Cells were then fixed for 1 hour using 70% chilled ethanol, followed by staining for 15 minutes with 40 mM Alizarin S (pH 4.2) at room temperature with

gentle stirring. Cells were then washed five times using PBS, after which staining was quantified via extracting the stain for 15 minutes with 10% (*w/v*) cetylpyridinium chloride (Sigma-Aldrich, St. Louis, MO, USA) and evaluating absorbance at 540 nm with a VERSA max Multiplate Reader.

2.8. Fluorescent Microscopy. The existence of sialic acid on the DPSC membrane was detected as described previously [19]. Neuraminidase-treated (100 mU/ml, 3 hour) and untreated DPSCs were washed with PBS three times, fixed with 4% paraformaldehyde for 30 minutes at room temperature (RT), rinsed with PBS for three times, and then blocked with 3% bovine serum albumin (BSA; Solarbio) for 1 hour. Washed with PBS three times, incubated with 10 μ g/ml fluorescein isothiocyanate- (FITC-) labeled lectin A. hypogaea (PNA) (Sigma-Aldrich, St. Louis, MO, USA) overnight in a moist chamber at 4°C. PNA can bind to the galactose moiety exposed on cell surface glycoconjugates after removing the terminal sialic acid. The next day, samples were incubated with DAPI (1:200) for 15 minutes at room temperature. Fluorescence microscopy images were captured under a fluorescence microscope (IX71 FL, Olympus).

2.9. In Vivo Osteogenesis Assay. *In vivo* ectopic osteogenesis was evaluated by subcutaneously implanting passage 3 DPSCs that had been mixed with 40 mg of 1.0 mm hydroxyapatite/ β -tricalcium phosphate (HA/ β -TCP) particles (ratio 3:8; Sichuan University Biomaterials Engineering Research Center, Chengdu, China) into the backs of nude mice (BALB/c, 6-weeks-old; Bianco, Kuznetsov, Riminucci, & Gehron Robey, 2006). A total of 8 mice were randomly divided into two groups with 4 mice per group; each group contains 2 female mice and 2 male mice. Mice were gavaged for 6 consecutive weeks with ManNAc (2 g/kg/animal/day) every day. The reason for choosing ManNAc over Neu5Ac is because ManNAc is the prerequisite form of Neu5Ac and can only transform to Neu5Ac in the animal organism. In addition, the absorption of ManNAc *in vivo* is better than that of Neu5Ac [20], beginning on day 2 following implantation. Control animals were administered PBS in lieu of ManNAc every day. Following the 6-week treatment period, the transplanted region was fixed, demineralized with 10% EDTA solution for 7 days, paraffin-embedded, and cut into 2 μ m sections that were then subjected to hematoxylin and eosin staining. DSPP and RUNX2 were then detected via immunohistochemical (IHC) staining with an appropriate antibody (1:50; ab122321; Abcam). The immunostained images were analyzed and scored by two pathologists independently in a blinded manner, based on the *H*-score method, which considers the percentage of cells staining positively together with the staining intensity [21, 22]. 10 fields at 400x magnification were chosen randomly. The staining intensity of weak, intermediate, and strong staining was scored as 0, 1, 2, and 3, corresponding to the negative control. The total number of cells and cells stained at each intensity were counted in each field. The *H*-score was calculated according to the formula: (%of cells stained at intensity category 1 \times 1) + (%of cells stained at intensity

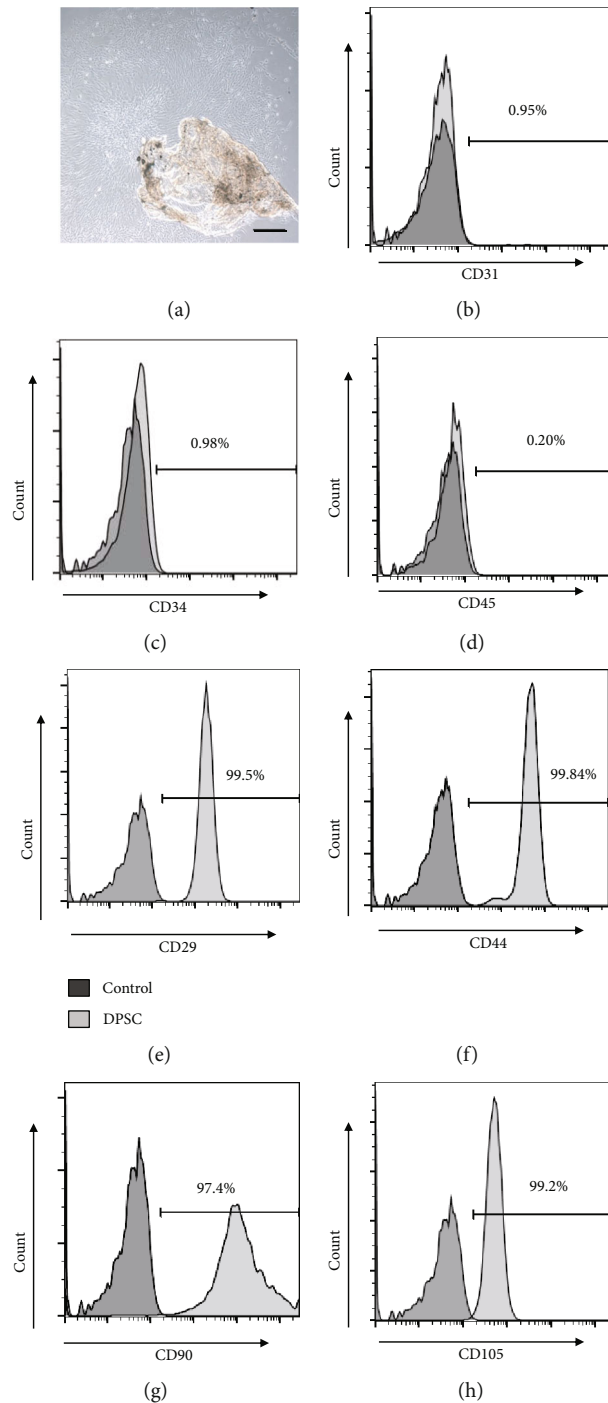


FIGURE 1: Primary human DPSC identification. (a) Primary DPSCs were isolated from dental pulp tissue. (b–h) Isolated DPSCs were CD29, CD44, CD90, and CD105 positive and were CD31, CD34, and CD45 negative in flow cytometry analyses. All the experiments were repeated at least three times independently. Scale bar = 100 μm .

category 2×2) + (% of cells stained at intensity category 3×3). *H*-scores ranged from 0 to 300 where 300 indicated 100% of cells strongly stained (3+). *H*-scores of cells ≥ 200 were defined as a high expression. The Ethics Committee of Southern Medical University approved these animal studies. *In vivo* cell viability assay, KI67 was detected via immunohistochemical (IHC) staining with an appropriate antibody

(1 : 50; ab122321; Abcam). The immunostained images were analyzed and scored by two pathologists independently in a blinded manner based on the *H*-score method which has mentioned above.

2.10. Statistical Analysis. Experiments were conducted in triplicate, and data are means \pm SD. SPSS v17.0 was

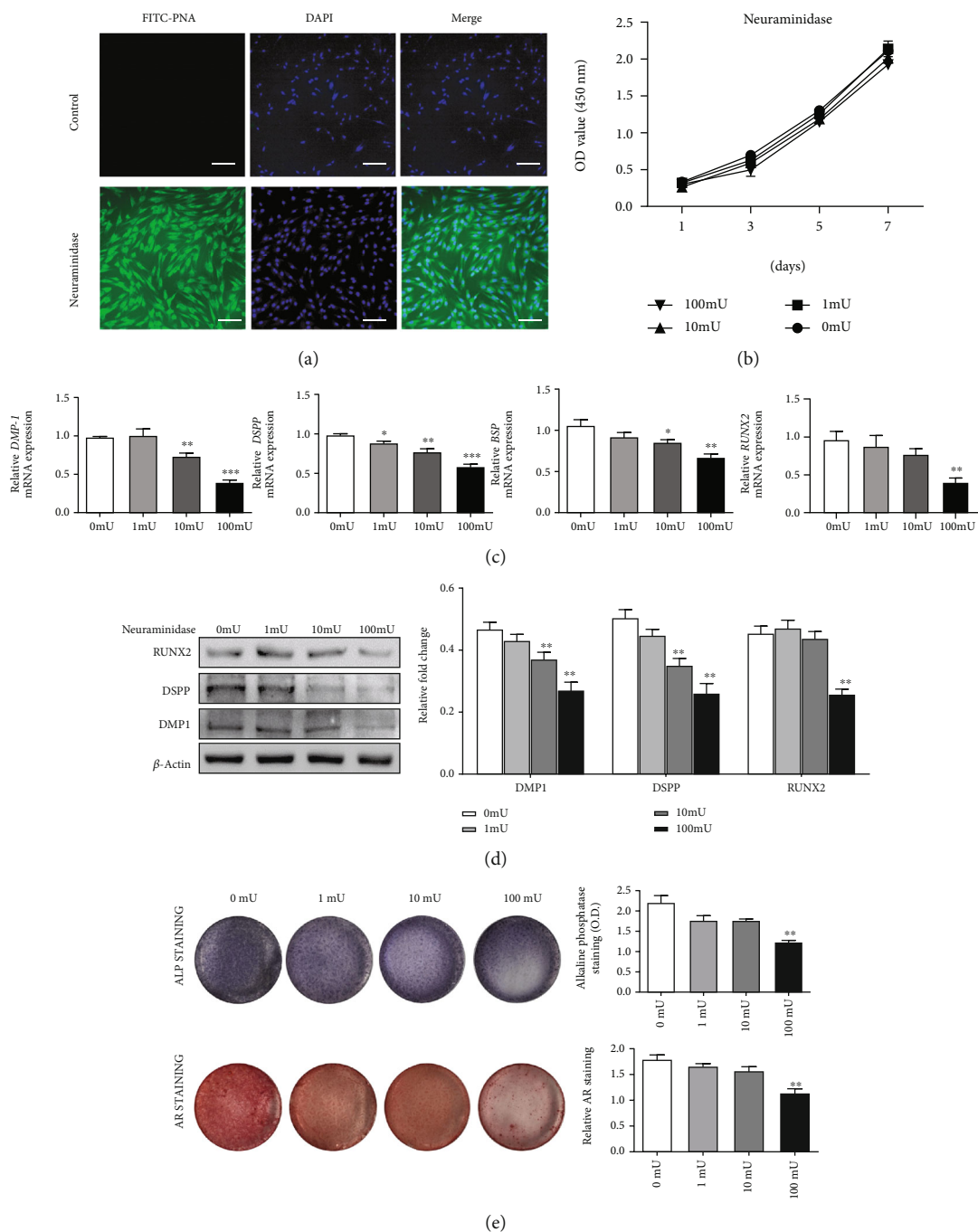
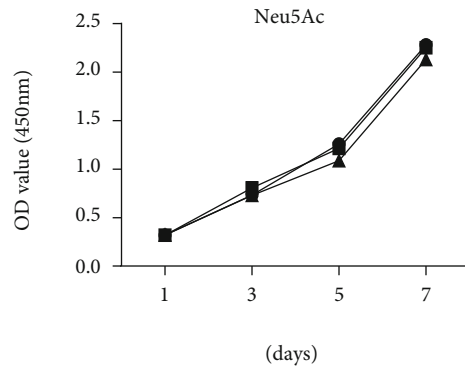


FIGURE 2: The effect of neuraminidase on DPSC osteo-/odontoblastic differentiation. (a) FITC-PNA lectin staining of DPSCs with or without neuraminidase (100 mU/ml) treatment. (b) CCK-8 assay results of neuraminidase-treated DPSC. (c) mRNA expression of DMP1, DSPP, BSP, and RUNX2 in DPSCs treated with neuraminidase (0, 1, 10, and 100 mU/ml) for 4 days. (d) Protein expression of DSPP, DMP1, and RUNX2 in DPSCs treated with neuraminidase (0, 1, 10, and 100 mU/ml) for 4 days. (e) ALP activity and Alizarin red staining after DPSCs were treated with neuraminidase (0, 1, 10, and 100 mU/ml). Scale bars = 50 μ m. * $p < 0.05$, ** $p < 0.01$, and *** $p < 0.001$. All the experiments were repeated at least three times independently.

used for all statistical testing. Data were statistically analyzed using Student's t -test, with $p < 0.05$ as the significance threshold. All graphs were plotted using GraphPad Prism 8 (GraphPad Software, Inc., La Jolla, CA, USA).

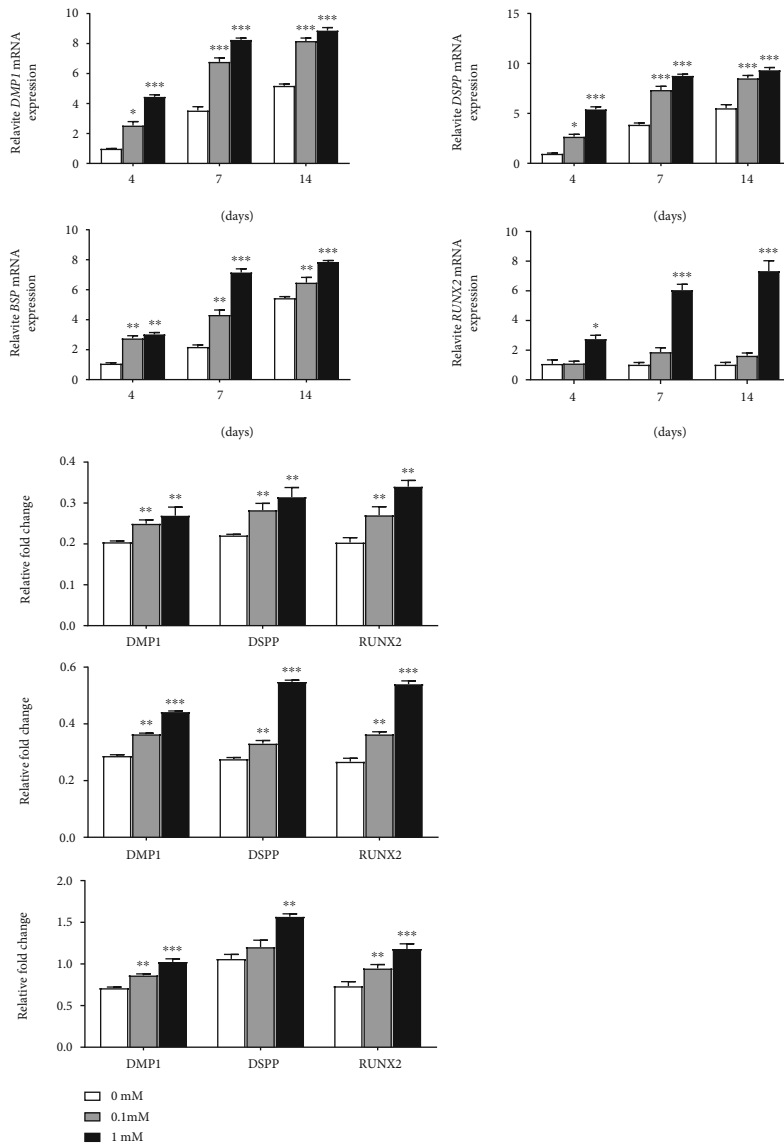
3. Results

3.1. DPSC Identification. We first validated the identity of the DPSCs used in the present study via flow cytometry. This analysis confirmed that these cells were positive for



▲ 1 mM
 ■ 0.1 mM
 ● 0 mM

(a)



(b)

FIGURE 3: Continued.

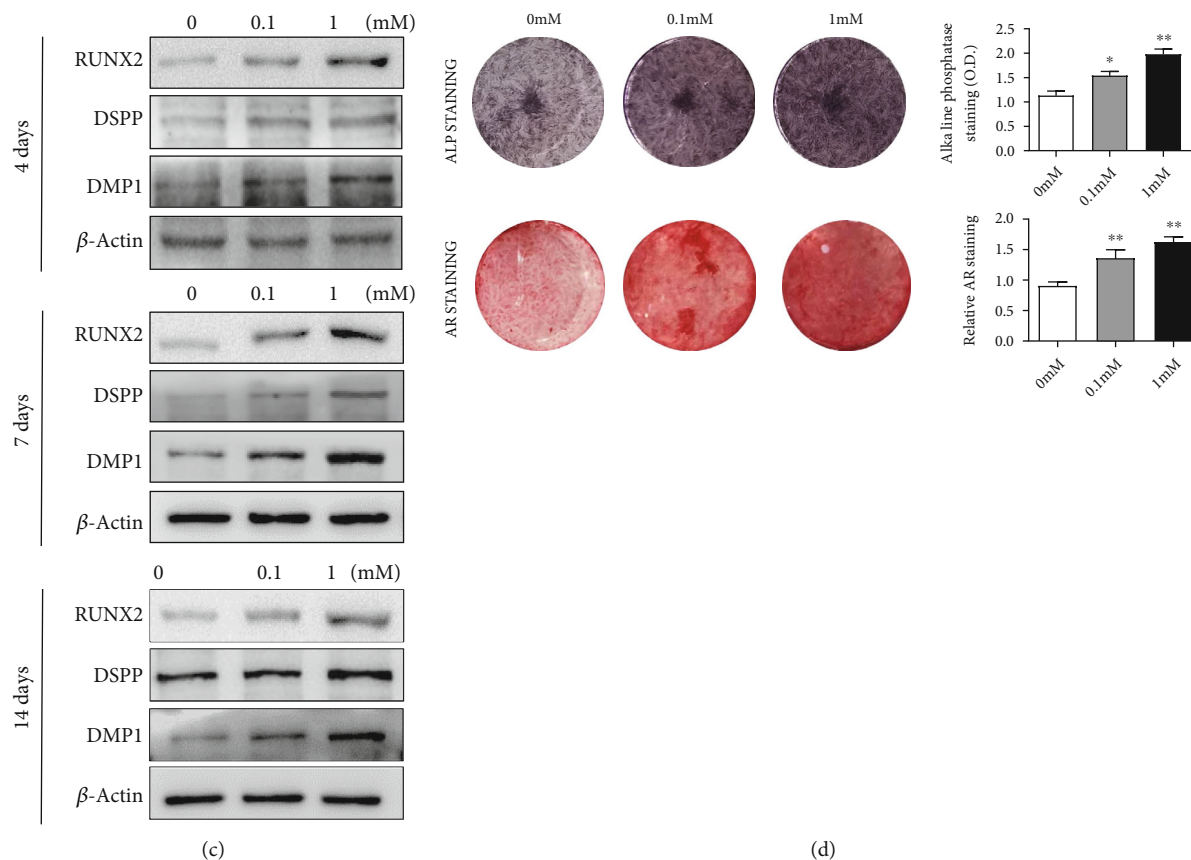


FIGURE 3: The impact of Neu5Ac on DPSC osteo-/odontoblastic differentiation. (a) CCK-8 assay results of Neu5Ac-treated DPSC. (b) qRT-PCR detected the expressions of DMP1, DSPP, BSP, and RUNX2 after treating DPSCs with Neu5Ac (0.1 or 1 mM) for 4, 7, or 14 days, with GAPDH used as a normalization control. (c) DMP1, DSPP, and RUNX2 protein expressions were detected by western blotting. (d) The ability of DPSC with Neu5Ac treatment (0.1 and 1 mM) assessed via ALP activity and Alizarin red staining. Data are means \pm SD. * $p < 0.05$, ** $p < 0.01$, or *** $p < 0.001$. All the experiments were repeated at least three times independently.

mesenchymal stem cell markers CD29, CD44, CD90, and CD105 while negative for the hematopoietic stem cell markers CD31, CD34, and CD45. These results suggested that we successfully isolated and cultured the DPSCs (Figure 1).

3.2. Desialylation of DPSC by Neuraminidase Inhibits Osteo-/Odontoblastic Differentiation of DPSC. FITC-PNA fluorescent staining was used to detect the existence of sialic acid on the DPSC surface. We observed no FITC-PNA fluorescent staining in untreated DPSCs, while FITC-PNA fluorescent staining was significantly enhanced in neuraminidase-treated DPSCs (Figure 2(a)). This proved that neuraminidase can effectively remove the sialic acid on the DPSC surface and indirectly proved the existence of sialic acid on the DPSC membrane. After we treated DPSC with different concentrations (0, 1, 10, and 100 mU/ml) of neuraminidase for 1, 3, 5, or 7 days, the CCK-8 assay showed that there was no significant difference in the OD value of each group of cells, indicating that the concentrations of neuraminidase used in this study had no significant effect on the viability of DPSC (Figure 2(b)). Removing sialic acid from the DPSC membrane by neuraminidase reduced the mRNA expression levels of osteo-/odontogenic markers DMP1, DSPP, BSP,

and RUNX2 (Figure 2(c)). Western blot analysis showed that neuraminidase also inhibited the protein levels of RUNX2, DMP1, and DSPP (Figure 2(d)). Consistent with the results of protein and mRNA expressions, neuraminidase could reduce the staining of ALP and Alizarin red, as indicated that neuraminidase could inhibit the formation of calcified nodules (Figure 2(e)). Together, these results suggested that DPSC odontoblastic differentiation was decreased in the absence of Neu5Ac.

3.3. The Impact of Neu5Ac on DPSC Odontoblastic Differentiation. In order to evaluate the impact of Neu5Ac on DPSC odontoblastic differentiation, we firstly treated DPSC with different concentrations (0, 0.1, or 1 mM) of Neu5Ac for an indicated time point, and the CCK-8 assay showed that the concentrations of Neu5Ac used in this study had no significant effect on the viability of DPSC (Figure 3(a)). Next, we assessed the expression of key osteo-/odontogenic marker genes in cells. The data revealed that Neu5Ac treatment was associated with significant increases in the mRNA expressions of DSPP, DMP1, BSP, and RUNX2 (Figure 3(b)). This was further supported by the protein level expressions of DMP1, DSPP, and RUNX2 in Neu5Ac-treated cells (Figure 3(c)).

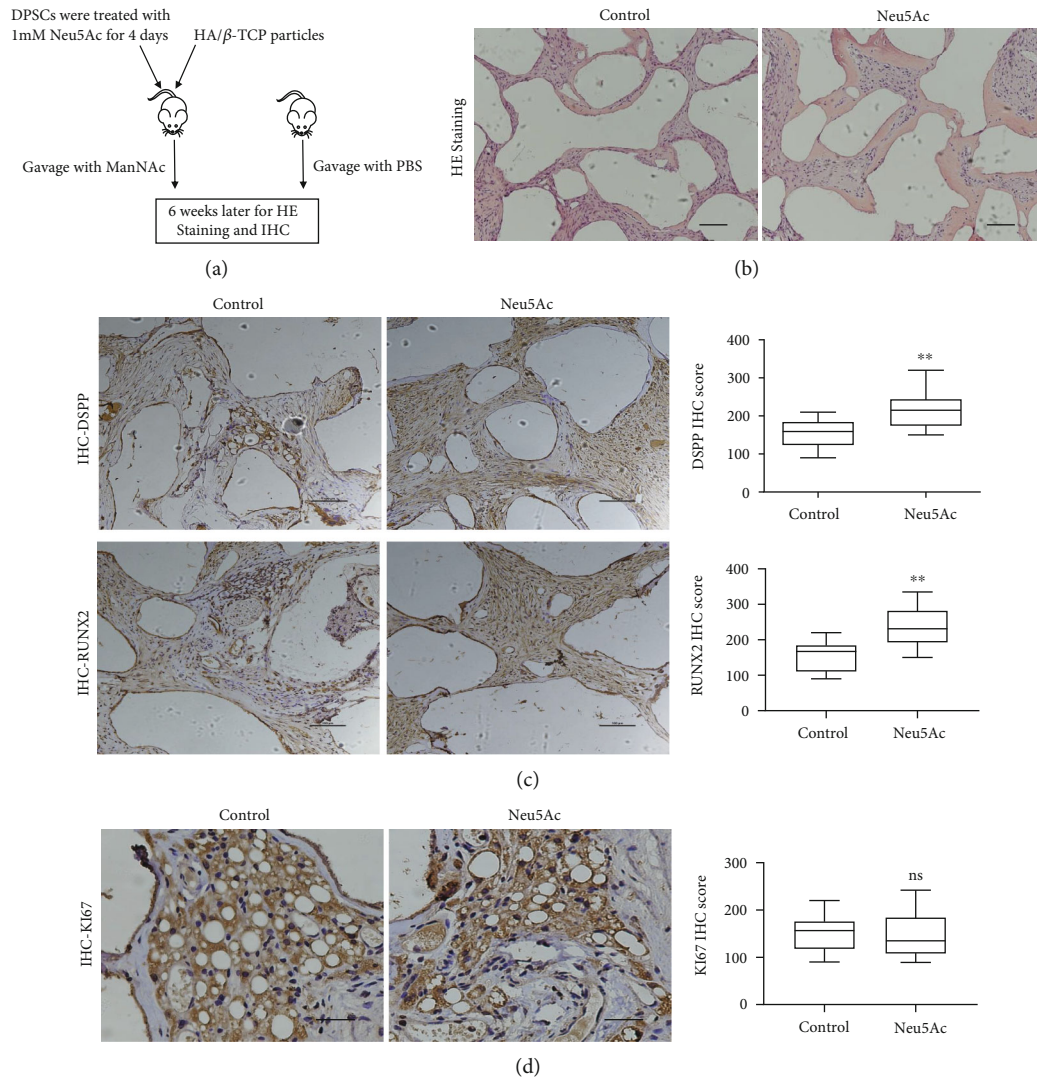


FIGURE 4: The method and impact of the ManNAc on DPSCs *in vivo*. (a) Flow chart of *in vivo* ectopic osteogenesis of DPSCs. (b) Hematoxylin and eosin stain showed enhanced osteogenesis in the ManNAc group than in the control group. (c, d) Immunohistochemistry and statistical analysis of the average *H*-score showed the effect of ManNAc on proliferation and differentiation of DPSCs. Scale bar = 100 μ m, ** $p < 0.01$. All the experiments were repeated at least three times independently.

We additionally observed clear evidence of dose-dependent enhancement of ALP activity in Neu5Ac-treated cells on day 7 after the induction of osteo-/odontoblastic differentiation. Additionally, Alizarin red staining conducted on day 14 was used to evaluate the impact of Neu5Ac on mineralization activity. The result exhibited enhanced mineralization activity in response to Neu5Ac treatment at this time point compared to control treatment (Figure 3(d)). Furthermore, we conducted *in vivo* osteogenesis assays and observed enhanced osteogenesis in ManNAc-treated mice compared to control animals, determined by HE staining and IHC staining with DSPP and RUNX2. Notably, Ki67 immunohistochemistry showed no significant difference in cell viability between the two groups (Figure 4). Taken together, *in vitro* and *in vivo* experiments indicated that Neu5Ac positively correlated with the osteo-/odontoblastic differentiation of DPSCs.

3.4. Neu5Ac Activates ERK Signaling to Drive DPSC Mineralization. Lastly, we evaluated the relationship between the MAPK signaling pathway and Neu5Ac-mediated enhancement of DPSC osteo-/odontoblastic differentiation. We observed no changes in the protein level expressions of total ERK, JNK, or p38 following Neu5Ac treatment. Interestingly, we observed significant increases in p-ERK levels that peaked at 30 minutes post-Neu5Ac treatment and remained elevated for at least 90 minutes. Even on day 3 posttreatment, the p-ERK/ERK ratio was obviously higher for cells treated with Neu5Ac (0.1 and 1mM) relative to that in untreated control cells (Figures 5(a) and 5(b)). No changes in p-JNK or p-p38 levels were detected throughout treatment. To evaluate the role of ERK pathway signaling on Neu5Ac-mediated enhancement of DPSC mineralization, we next pretreated DPSCs with the ERK inhibitor cobimetinib. This analysis revealed that ERK inhibition abrogated the Neu5Ac-

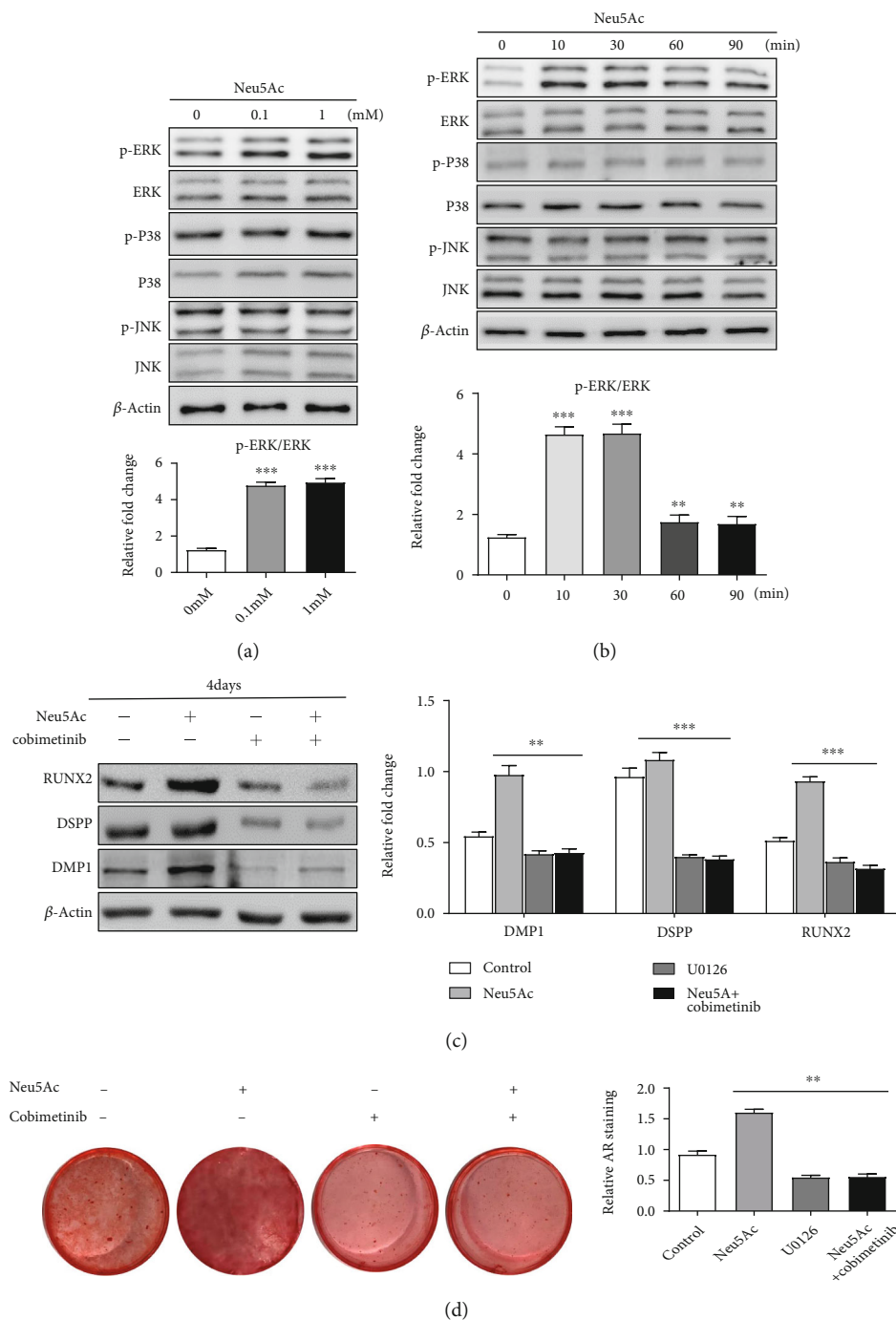


FIGURE 5: Neu5Ac enhances DPSC osteo-/odontoblastic differentiation via activating ERK signaling. (a) ERK, p-ERK, p38, p-p38, JNK, and p-JNK levels in DPSCs were evaluated following a 3-day treatment with Neu5Ac (0, 0.1, or 1 mM) via Western blotting. (b) The p-ERK/total ERK, p-p38/total p38, and p-JNK/total JNK ratios were determined for DPSCs following treatment with 1 mM Neu5Ac for 0, 10, 30, 60, or 90 minutes via Western blotting. (c) DMP1, DSPP, and RUNX2 protein levels in DPSCs treated with either Neu5Ac and/or cobimetinib were measured. (d) Alizarin red staining of DPSCs was conducted following a 14-day treatment period with cobimetinib and/or Neu5Ac. ** $p < 0.01$, *** $p < 0.001$. All the experiments were repeated at least three times independently.

induced upregulation of DMP1, DSPP, and RUNX2 in these DPSCs (Figures 5(c) and 5(d)). These findings indicated that Neu5Ac influences DPSC differentiation mainly via the ERK pathway.

4. Discussion

In recent years, with the in-depth studies of stem cells, many types of stem cells have shown their clinical therapeutic

potential [23–27]. The stable and reliable sources of stem cells is particularly important [28]. DPSCs can be readily isolated following the extraction of healthy teeth, and these cells are highly amenable to proliferating and differentiating into osteo-/odontoblasts [29], making them ideally suited to use in bone and dental tissue engineering. However, the clinical applicability of these cells has been limited to date because they rapidly lose their ability to proliferate and undergo multipotent differentiation throughout prolonged *in vitro* culture [30]. Therefore, it is vital that novel strategies capable of stimulating prolonged DPSC proliferation and differentiation be developed. As such, we herein evaluated the ability of Neu5Ac to enhance DPSC odontoblastic differentiation. To determine whether there is SA on the surface of DPSCs, we firstly assumed that there was SA on the surface of the cells. After treatment with neuraminidase, FITC-PNA fluorescent staining was significantly enhanced. This proved that neuraminidase can effectively remove the sialic acid on the DPSC surface and indirectly proved the existence of sialic acid on the DPSC membrane.

ALP activity and expression are an early indicator of osteoblastogenesis [31], whereas Alizarin red staining can reliably detect mineralized nodules [32]. We found that treating DPSCs with Neu5Ac was sufficient to enhance both ALP activity and the formation of mineralized nodules. We also evaluated the expression of key odontoblastic differentiation-related genes, including the dentin-specific DSPP [33], and the osteogenesis marker genes DMP1, BSP, and RUNX2 [34]. We observed clear increases in DSPP, DMP1, and RUNX2 protein levels as well as BSP mRNA level in DPSCs that had been treated with Neu5Ac, thus emphasizing the ability of Neu5Ac to enhance the osteo-/odontoblastic differentiation of these cells.

The results of the present study suggested that sialic acid played an important role in DPSC odontoblast differentiation. Removing SA from cell surface appeared to strongly inhibit odontoblast differentiation, while treatment with a high concentration of Neu5Ac presented the opposite tendency. These data indicated that SA was involved in the DPSC odontoblast differentiation process. Considering that SA played an important role in the cell-cell adhesion process [35, 36], SA may influence the DPSC odontoblast differentiation through cell-cell fusion.

MAPK are cytoplasmic serine/threonine kinases that are universally expressed in mammalian cells. Many cytokines and other stimuli can induce ERK1/2 activation, thereby modulating cellular proliferation and division. Owing to the ability of ERK pathway signaling to enhance tumor cell proliferation, ERK inhibitors have been considered potential anticancer drugs [37]. p38 MAPK serves as a regulator of cytokine expression and is in turn activated in response to inflammatory cytokine signaling [38]. As such, p38 is a central regulator of the immune system activity in pathological and physiological contexts. JNKs are stress-activated kinases that control cell survival or apoptotic death in response to diverse stress-related stimuli [37]. MAPK pathway activation has been shown to be a key regulator of mesenchymal stem cell differentiation [39]. Treatment of human DPSCs with LPS induced p38 and ERK activation and downstream

IL-8 production [40], and ERK activity is also vital for DMP1, DSPP, and RUNX2 activation within DPSCs [41]. Previous research suggested that sialic acid-binding lectin can induce the intracellular activation of signaling cascades, including the MAPK cascades [42]. We speculated that SA-binding lectin and SA may have something in common, so we tested whether sialic acid (Neu5Ac) affected the MAPK pathway. Herein, we observed no changes in total ERK, JNK, or p38 levels in Neu5Ac-treated DPSCs, whereas p-ERK expression was significantly enhanced in these cells. This suggests that ERK pathway activation is crucial for the SA treatment of DPSCs. We detected no changes in p38 or JNK phosphorylation as a function of Neu5Ac treatment, indicating that these pathways were unaffected by Neu5Ac. To further confirm the relevance of ERK signaling in the context of Neu5Ac-induced DPSC osteo-/odontoblastic differentiation, we treated these cells with the ERK inhibitor cobimetinib. Inhibition of ERK activity reduced DSPP, DMP1, and RUNX2 protein expressions compared to the Neu5Ac group, thus confirming that ERK pathway activation is necessary in order for Neu5Ac to enhance DPSC odontoblastic differentiation.

In summary, the results of the present study revealed that desialylation of DPSC by neuraminidase inhibited osteo-/odontoblastic differentiation while Neu5Ac treatment was able to enhance DPSC osteo-/odontoblastic differentiation. We further determined that ERK signaling was necessary for Neu5Ac to mediate such enhanced differentiation in DPSCs. However, this research only studied the effect of Neu5Ac on the osteo-/odontoblastic differentiation of DPSC. Investigations of Neu5Ac on the development and clinical values of the teeth require further scrutiny.

Data Availability

The data, used during the study, is available from the corresponding author upon reasonable request.

Conflicts of Interest

The authors declare that they have no conflicts of interest.

Authors' Contributions

Changzhou Li and Xinghuan Xie contributed equally to this work.

Acknowledgments

The work was supported by the National Natural Science Foundation of China (grant no. 81800957).

References

- [1] G. Spagnuolo, B. Codispoti, M. Marrelli, C. Rengo, S. Rengo, and M. Tatullo, "Commitment of oral-derived stem cells in dental and maxillofacial applications," *Dentistry journal*, vol. 6, no. 4, p. 72, 2018.
- [2] B. C. Kim, H. Bae, I. K. Kwon et al., "Osteoblastic/cementoblastic and neural differentiation of dental stem cells and their

- applications to tissue engineering and regenerative medicine,” *Tissue Engineering. Part B, Reviews*, vol. 18, no. 3, pp. 235–244, 2012.
- [3] J. Yu, H. He, C. Tang et al., “Differentiation potential of STRO-1+ dental pulp stem cells changes during cell passaging,” *BMC Cell Biology*, vol. 11, no. 1, p. 32, 2010.
 - [4] X. Yang, S. Zhang, X. Pang, and M. Fan, “Pro-inflammatory cytokines induce odontogenic differentiation of dental pulp-derived stem cells,” *Journal of Cellular Biochemistry*, vol. 113, no. 2, pp. 669–677, 2012.
 - [5] S. G. Kim, J. Zhou, C. Solomon et al., “Effects of growth factors on dental stem/progenitor cells,” *Dental Clinics of North America*, vol. 56, no. 3, pp. 563–575, 2012.
 - [6] M. Hata, K. Naruse, S. Ozawa et al., “Mechanical stretch increases the proliferation while inhibiting the osteogenic differentiation in dental pulp stem cells,” *Tissue Engineering Part A*, vol. 19, no. 5-6, pp. 625–633, 2013.
 - [7] A. Ballini, A. Boccaccio, R. Saini, P. Van Pham, and M. Tatullo, “Dental-derived stem cells and their secretome and interactions with bioscaffolds/biomaterials in regenerative medicine: from the in vitro research to translational applications,” *Stem Cells International*, vol. 2017, Article ID 6975251, 3 pages, 2017.
 - [8] D. Ma, Z. Ma, X. Zhang et al., “Effect of Age and Extrinsic Microenvironment on the Proliferation and Osteogenic Differentiation of Rat Dental Pulp Stem Cells *In Vitro*,” *Journal of Endodontics*, vol. 35, no. 11, pp. 1546–1553, 2009.
 - [9] F. Inchingolo, M. Tatullo, M. Marrelli et al., “Clinical trial with bromelain in third molar exodontia,” *European Review for Medical and Pharmacological Sciences*, vol. 14, no. 9, pp. 771–774, 2010.
 - [10] M. Tatullo, M. Marrelli, M. Amantea et al., “Bioimpedance detection of oral lichen planus used as preneoplastic model,” *Journal of Cancer*, vol. 6, no. 10, pp. 976–983, 2015.
 - [11] N. M. Varki and A. Varki, “Diversity in cell surface sialic acid presentations: implications for biology and disease,” *Lab Invest*, vol. 87, no. 9, article BF3700656, pp. 851–857, 2007.
 - [12] R. Schauer and J. P. Kamerling, “Exploration of the sialic acid world,” *Advances in Carbohydrate Chemistry and Biochemistry*, vol. 75, pp. 1–213, 2018.
 - [13] Z. Virion, S. Doly, K. Saha et al., “Sialic acid mediated mechanical activation of β_2 adrenergic receptors by bacterial pili,” *Nature Communications*, vol. 10, no. 1, p. 4752, 2019.
 - [14] M. S. Macauley, P. R. Crocker, and J. C. Paulson, “Siglec-mediated regulation of immune cell function in disease,” *Nature Reviews Immunology*, vol. 14, no. 10, pp. 653–666, 2014.
 - [15] X. Zhou, Y. Zhai, C. Liu et al., “Sialidase NEU1 suppresses progression of human bladder cancer cells by inhibiting fibronectin-integrin $\alpha 5 \beta 1$ interaction and Akt signaling pathway,” *Cell Communication and Signaling: CCS*, vol. 18, no. 1, p. 44, 2020.
 - [16] L. Xu, W. Xu, G. Xu et al., “Effects of cell surface $\alpha 2-3$ sialic acid on osteogenesis,” *Glycoconjugate Journal*, vol. 30, no. 7, pp. 677–685, 2013.
 - [17] M. Dadhich, V. Prabhu, V. R. Pai, J. D’Souza, S. Harish, and M. Jose, “Serum and salivary sialic acid as a biomarker in oral potentially malignant disorders and oral cancer,” *Indian Journal of Cancer*, vol. 51, no. 3, pp. 214–218, 2014.
 - [18] M. Zad, S. A. Flowers, M. Bankvall, M. Jontell, and N. G. Karlsson, “Salivary mucin MUC7 oligosaccharides in patients with recurrent aphthous stomatitis,” *Clinical Oral Investigations*, vol. 19, no. 8, pp. 2147–2152, 2015.
 - [19] N. M. Stamatou, S. Curreli, D. Zella, and A. S. Cross, “Desialylation of glycoconjugates on the surface of monocytes activates the extracellular signal-related kinases ERK 1/2 and results in enhanced production of specific cytokines,” *Journal of Leukocyte Biology*, vol. 75, no. 2, pp. 307–313, 2004.
 - [20] T. K. Niethamer, T. Yardeni, P. Leoyklang et al., “Oral monosaccharide therapies to reverse renal and muscle hyposialylation in a mouse model of *GNE* myopathy,” *Molecular Genetics and Metabolism*, vol. 107, no. 4, pp. 748–755, 2012.
 - [21] M. Früh and M. Pless, “EGFR IHC score for selection of cetuximab treatment: ready for clinical practice?,” *Translational lung cancer research*, vol. 1, no. 2, pp. 145–146, 2012.
 - [22] S. Detre, G. Saclani Jotti, and M. Dowsett, “A “quickscore” method for immunohistochemical semiquantitation: validation for oestrogen receptor in breast carcinomas,” *Journal of Clinical Pathology*, vol. 48, no. 9, pp. 876–878, 1995.
 - [23] I. Kuehnle and M. A. Goodell, “The therapeutic potential of stem cells from adults,” *BMJ (Clinical Research Ed)*, vol. 325, no. 7360, pp. 372–376, 2002.
 - [24] G. Cossu, M. Birchall, T. Brown et al., “Lancet Commission: Stem cells and regenerative medicine,” *Lancet (London, England)*, vol. 391, pp. 883–910, 2018.
 - [25] L. Gao, R. Guo, Z. Han, J. Liu, and X. Chen, “Clinical trial reporting,” *Lancet (London, England)*, vol. 396, no. 10261, pp. 1488–1489, 2020.
 - [26] A. Xiong, Y. He, L. Gao et al., “Smurf1-targeting miR-19b-3p-modified BMSCs combined PLLA composite scaffold to enhance osteogenic activity and treat critical-sized bone defects,” *Biomaterials Science*, vol. 8, no. 21, pp. 6069–6081, 2020.
 - [27] R. Guo, L. Gao, and B. Xu, “Current evidence of adult stem cells to enhance anterior cruciate ligament treatment: a systematic review of animal trials,” *Arthroscopy : the journal of arthroscopic & related surgery: official publication of the Arthroscopy Association of North America and the International Arthroscopy Association*, vol. 34, no. 1, pp. 331–340.e2, 2018.
 - [28] W. E. Fibbe, “Mesenchymal stem cells. A potential source for skeletal repair,” *Annals of the Rheumatic Diseases*, vol. 61, Supplement 2, pp. 29ii–293i, 2002.
 - [29] S. Gronthos, M. Mankani, J. Brahimi, P. G. Robey, and S. Shi, “Postnatal human dental pulp stem cells (DPSCs) in vitro and in vivo,” *Proceedings of the National Academy of Sciences of the United States of America*, vol. 97, no. 25, pp. 13625–13630, 2000.
 - [30] H. Horibe, M. Murakami, K. Iohara et al., “Isolation of a stable subpopulation of mobilized dental pulp stem cells (MDPSCs) with high proliferation, migration, and regeneration potential is independent of age,” *PLoS One*, vol. 9, no. 5, article e98553, 2014.
 - [31] P. Magnusson and J. R. Farley, “Differences in sialic acid residues among bone alkaline phosphatase isoforms: a physical, biochemical, and immunological characterization,” *Calcified Tissue International*, vol. 71, no. 6, pp. 508–518, 2002.
 - [32] Q. Wang, G. Wang, B. Wang, and H. Yang, “Activation of TGR5 promotes osteoblastic cell differentiation and mineralization,” *Biomedicine & pharmacotherapy = Biomedecine & pharmacotherapie*, vol. 108, pp. 1797–1803, 2018.
 - [33] Y. Chen, Y. Zhang, A. Ramachandran, and A. George, “DSPP is essential for normal development of the dental-craniofacial complex,” *Journal of Dental Research*, vol. 95, no. 3, pp. 302–310, 2016.

- [34] N. Zhou, Q. Li, X. Lin et al., "BMP2 induces chondrogenic differentiation, osteogenic differentiation and endochondral ossification in stem cells," *Cell and Tissue Research*, vol. 366, no. 1, pp. 101–111, 2016.
- [35] O. T. Keppler, S. Hinderlich, J. Langner, R. Schwartz-Albiez, W. Reutter, and M. Pawlita, "UDP-GlcNAc 2-epimerase: a regulator of cell surface sialylation," *Science (New York, NY)*, vol. 284, no. 5418, pp. 1372–1376, 1999.
- [36] A. Hartnell, J. Steel, H. Turley, M. Jones, D. G. Jackson, and P. R. Crocker, "Characterization of human sialoadhesin, a sialic acid binding receptor expressed by resident and inflammatory macrophage populations," *Blood*, vol. 97, no. 1, pp. 288–296, 2001.
- [37] G. L. Johnson and R. Lapadat, "Mitogen-activated protein kinase pathways mediated by ERK, JNK, and p38 protein kinases," *Science (New York, NY)*, vol. 298, no. 5600, pp. 1911–1912, 2002.
- [38] Y. Su, S. Zong, C. Wei et al., "Salidroside promotes rat spinal cord injury recovery by inhibiting inflammatory cytokine expression and NF- κ B and MAPK signaling pathways," *Journal of Cellular Physiology*, vol. 234, no. 8, pp. 14259–14269, 2019.
- [39] B. Binétruy, L. Heasley, F. Bost, L. Caron, and M. Aouadi, "Concise review: regulation of embryonic stem cell lineage commitment by mitogen-activated protein kinases," *Stem cells (Dayton, Ohio)*, vol. 25, no. 5, pp. 1090–1095, 2007.
- [40] W. He, T. Qu, Q. Yu et al., "LPS induces IL-8 expression through TLR4, MyD88, NF-kappaB and MAPK pathways in human dental pulp stem cells," *International Endodontic Journal*, vol. 46, no. 2, pp. 128–136, 2013.
- [41] M. Huang, R. G. Hill, and S. C. F. Rawlinson, "Strontium (Sr) elicits odontogenic differentiation of human dental pulp stem cells (hDPSCs): a therapeutic role for Sr in dentine repair?," *Acta Biomaterialia*, vol. 38, pp. 201–211, 2016.
- [42] Y. Kariya, T. Tatsuta, S. Sugawara, Y. Kariya, K. Nitta, and M. Hosono, "RNase activity of sialic acid-binding lectin from bullfrog eggs drives antitumor effect via the activation of p38 MAPK to caspase-3/7 signaling pathway in human breast cancer cells," *International Journal of Oncology*, vol. 49, no. 4, pp. 1334–1342, 2016.

Research Article

Bone Mesenchymal Stem Cells Contribute to Ligament Regeneration and Graft–Bone Healing after Anterior Cruciate Ligament Reconstruction with Silk–Collagen Scaffold

Fanggang Bi ¹, Yangdi Chen ², Junqi Liu ³, Wenhao Hu ⁴, and Ke Tian ¹

¹Department of Orthopedic Surgery, The First Affiliated Hospital of Zhengzhou University, No. 1 Jianshe East Road, Zhengzhou, China 450001

²Henan University of Chinese Medicine, No. 156 Jinshui East Road, Zhengzhou, China 450001

³Department of Radiation Oncology, The First Affiliated Hospital of Zhengzhou University, No. 1 Jianshe East Road, Zhengzhou, China 450001

⁴Spine Division, Department of Orthopedics, The Fourth Medical Center of PLA General Hospital, No. 51 Fucheng Road, Beijing, China

Correspondence should be addressed to Fanggang Bi; 163bfg@163.com

Received 10 November 2020; Revised 25 January 2021; Accepted 15 April 2021; Published 24 April 2021

Academic Editor: Gianpaolo Papaccio

Copyright © 2021 Fanggang Bi et al. This is an open access article distributed under the Creative Commons Attribution License, which permits unrestricted use, distribution, and reproduction in any medium, provided the original work is properly cited.

Anterior cruciate ligament (ACL) reconstruction was realized using a combination of bone mesenchymal stem cells (BMSCs) and silk–collagen scaffold, and an *in vivo* evaluation of this combination was performed. By combining type I collagen and degummed silk fibroin mesh, silk–collagen scaffolds were prepared to simulate ligament components. BMSCs isolated from bone marrow of rabbits were cultured for a homogenous population and seeded on the silk–collagen scaffold. In the scaffold and BMSC (S/C) group, scaffolds were seeded with BMSCs for 72 h and then rolled and used to replace the ACL in 20 rabbits. In the scaffold (S) group, scaffolds immersed only in culture medium for 72 h were used for ACL reconstruction. Specimens were collected at 4 and 16 weeks postoperatively to assess ligament regeneration and bone integration. HE and immunohistochemical staining (IHC) were performed to assess ligament regeneration in the knee cavity. To assess bone integration at the graft–bone interface, HE, Russell–Movat staining, micro-CT, and biomechanical tests were performed. After 4 weeks, vigorous cell proliferation was observed in the core part of the scaffold in the S/C group, and a quantity of fibroblast-like cells and extracellular matrix (ECM) was observed in the center part of the graft at 16 weeks after surgery. At 4 and 16 weeks postoperatively, the tenascin-C expression in the S/C group was considerably higher than that in the S group (4 w, $p < 0.01$; 16 w, $p < 0.01$). Furthermore, bone integration was better in the S/C group than in the S group, with histological observation of trabecular bone growth into the graft and more mineralized tissue formation detected by micro-CT (4 w, bone volume fraction (BV/TV), $p = 0.0169$, bone mineral density (BMD), $p = 0.0001$; 16 w, BV/TV, $p = 0.1233$, BMD, $p = 0.0494$). These results indicate that BMSCs promote ligament regeneration in the knee cavity and bone integration at the graft–bone interface. Silk–collagen scaffolds and BMSCs will likely be combined for clinical practice in the future.

1. Introduction

The anterior cruciate ligament (ACL) is a main structure that maintains stability of the knee [1]. As a common athletic injury, ACL rupture can cause serious damage such as knee joint instability, injury to other ligaments, dislocation, and osteoarthritis [2, 3]. ACL reconstruction is currently consid-

ered the gold standard for treating ACL rupture, and grafts including autografts, allografts, and synthetic grafts are used for this purpose [4–6]. However, these grafts have some limitations. Shortcomings of autografts include long surgery time, donor site complications, long rehabilitation time, and decrease in knee range of motion [7]. Disadvantages of allografts include higher cost, higher infection rates, and a

higher failure rate compared to autografts [8]. The complications of permanent synthetic grafts include osteoarthritis, chronic synovitis, foreign-body response, and long-term rupture [9]. Bone mesenchymal stem cells (BMSCs) and ligament tissue engineering have become promising techniques for addressing these drawbacks.

To reconstruct the ACL well, tissue engineering needs to meet the following criteria: provide immediate joint stability after surgery, assure good ligament regeneration in the knee cavity as the engineered tissue gradually degrades and diminishes, and establish good bone integration at the graft–bone interface for long-term stability after surgery [10]. In a previous study, we designed a graft by combining collagen matrix with knitted degummed silk fibroin to reconstruct the ACL in a rabbit model [11]. The silk–collagen scaffold was discovered to have good biocompatibility and biomechanical properties [12]. However, in the early postoperative period, limited ingrowth of the newly regenerated connective tissue in the knee cavity restricted ligament regeneration, and bone tissue in the bone tunnel disrupted graft–bone healing [13, 14].

BMSCs are pluripotent cells and have become a very important source of cells for cell therapy and engineered tissue repair [15]. Their multiple differentiation potential for therapeutic application when implanted with biodegradable scaffolds has been demonstrated in several previous studies [16–19]. Although which cell types initiate and regulate the ligament regeneration and graft–bone healing process has not been clarified [20], it seems that BMSCs in the marrow from the bone tunnel promote ligament regeneration and repair at the graft–bone interface [21]. Lim et al. demonstrated that the failure load and stiffness of MSC-enhanced hamstring tendons were obviously greater at 8 weeks after ACL reconstruction surgery in a rabbit model [22]. According to Soon et al., MSCs may form an intermediate fibrocartilage zone between bone and the allograft tendon after reconstruction surgery [23].

No unified and widely accepted approach has been available to guide how BMSCs are applied. BMSC application approaches include local injection [24], BMSCs sheet technology [25], combination with fibrin glue or collagen gel [17, 26], and implantation on a scaffold for tissue engineering [27, 28]. Implanting BMSCs on a tissue-engineering scaffold seems more reliable because of its small distraction on the growing status and environment of BMSCs. Based on this background, we seeded BMSCs on a silk–collagen scaffold, attempting to determine whether BMSCs could promote ligament regeneration in the knee cavity and graft–bone healing. In the present study, a rabbit ACL reconstruction model with silk–collagen scaffold with or without BMSCs was established. We hypothesized that BMSCs could improve knee ligament regeneration and bone integration at the graft–bone interface, as demonstrated by histological assessment, micro-CT, and a biomechanical test.

2. Materials and Methods

2.1. Scaffold Preparation. The raw silk fibers were provided by Zhejiang Cathaya International, Ltd. The degumming pro-

cess was completed using 0.02 M Na_2CO_3 (100°C for 60 min, 3 times) to extract sericin, as described in a previous study [11]. Isolation and purification of the collagen matrix from pigs' Achilles tendons were performed with dilute acid and neutral salt extractions [29]. The knitted silk mesh extracted from sericin was soaked in acidic collagen solution (type I, pH 3.2, w/v 1%), freeze-dried (–80°C for 12 h followed by Heto PowerDry LL1500 for 24 h), and subjected to dehydrothermal crosslinking in a vacuum oven (30 mTorr, 105°C for 24 h) [11]. Observation of the surface microstructures of the raw silk, degummed silk, and silk–collagen scaffold was performed using a scanning electron microscope (SEM). Finally, cobalt-60-sterilized silk–collagen scaffolds were prepared for the following evaluations.

2.2. Isolation, Culture, and Identification of BMSCs. Bone marrow aspirates extracted from New Zealand White rabbits (2.5 ± 0.2 kg, 12 weeks old) were used to isolate and culture BMSCs, as previously described [17]. Mononuclear cells were gathered in Ficoll–Hypaque gradient (Sigma) after centrifugation and then suspended in cell culture medium containing 10% fetal bovine serum (FBS, Gibco). As the culture medium changed, the suspended cells were removed after culture at 37°C in 5% CO_2 for 72 h. When the adherent cells reached 70–80% confluence, subculture was performed. After culture for 2 weeks, a homogenous BMSC population was obtained, and the third passage was collected and seeded on the silk–collagen scaffold. BMSCs adherent on the scaffold were observed by SEM after being seeded for 72 h. The osteogenic, adipogenic, and chondrogenic differentiation abilities of passage 3 cells were identified after culture with special inducing media (Gibco) for 3 weeks. Finally, alizarin red (Sangon), oil red O (Sangon), and alcian blue staining (Sangon) were performed according to the manufacturer's protocols.

2.3. Flow Cytometry. To confirm the homogeneous property of passage 3 BMSCs cultured at 2 weeks, a characterization for stemness markers was performed. Sheep anti-rabbit antibodies of CD29, CD73, CD105, and phycoerythrin-(PE-) labeled IgG secondary antibody were purchased from the eBioscience (San Diego, CA). Approximately 3×10^5 cells were harvested and resuspended in 100 μL phosphate-buffered saline (PBS). Cells were incubated with primary antibodies of CD29 (1:100), CD73 (1:100), and CD105 (1:100) for 1 hour at 4°C. Subsequently, the cells were washed with PBS for 3 times, and the supernatant was discarded by centrifugation at $250 \times g$ for 5 minutes. And the cells were resuspended in 100 μL PBS and incubated with PE-labeled secondary sheep antibody (1:200) for 40 minutes at 4°C in the dark. The cells were washed with PBS for 3 times, and the supernatant was discarded by centrifugation at $250 \times g$ for 5 minutes. The cells were immediately tested on the machine (BD LSRFortessa) after resuspended with 400 μL PBS. The data were analyzed with FlowJo 10.0 software.

2.4. Animal Model Study Design. The present study used 40 male New Zealand white rabbits provided by Hualan Biology (2.5 – 3.0 kg, 12 weeks old, certification No.:

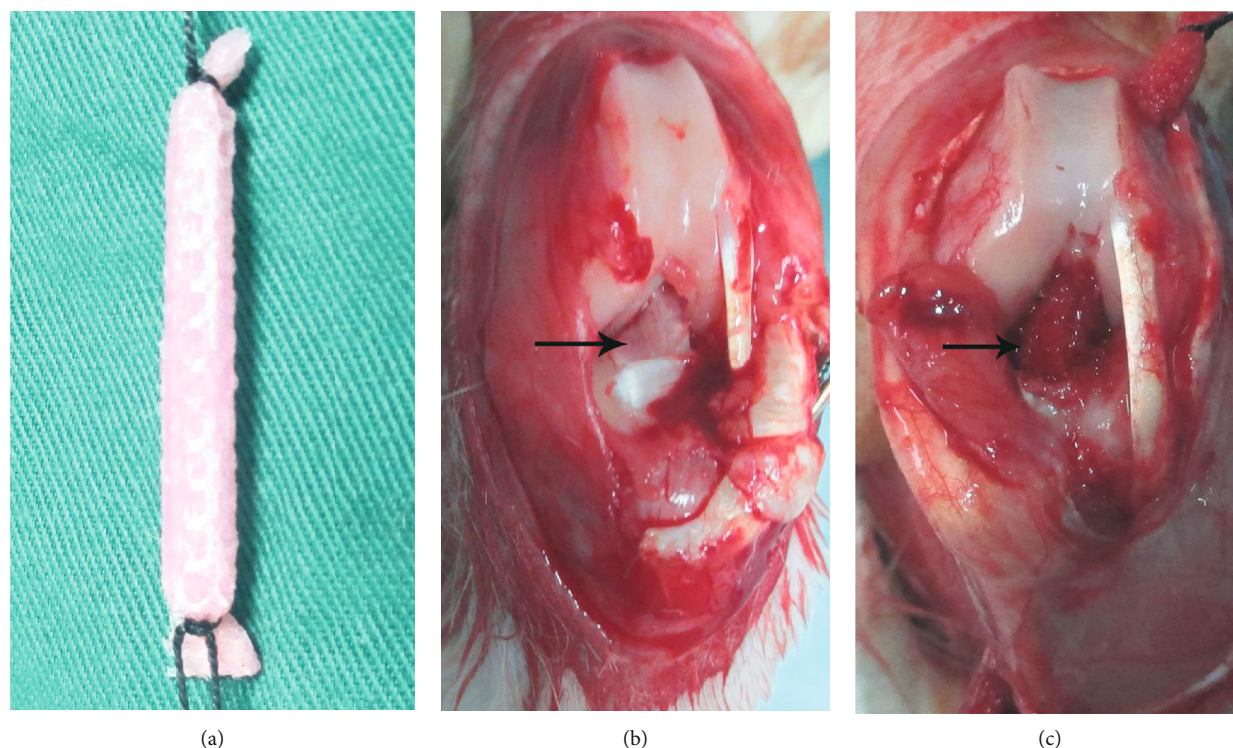


FIGURE 1: (a) After coculture with BMSCs in the S/C group and immersion only in culture medium in the S group for 72 h, the scaffold was rolled for use as a graft to replace the native ACL in a rabbit model. (b) General observation of the native ACL: the arrow points to the native ACL. (c) General observation of the knee after ACL reconstruction with the scaffold: the arrow points to the implanted graft.

SYDW20190409). The ethics committee of the First Affiliated Hospital of Zhengzhou University approved the experimental protocol (ethics review No.: 2020-KY-012). Two equal-numbered groups (scaffold group, S; scaffold and BMSCs group, S/C) were formed by dividing the rabbits at random, and ACL reconstruction was carried out in the knee of the left hind leg. In the S group, silk scaffolds were immersed in culture medium for 72 h, whereas in the S/C group, silk scaffolds were seeded with BMSCs for 72 h; then both types of scaffold were rolled and used for ACL reconstruction (Figure 1(a)). At 4 and 16 weeks after the operation, 10 rabbits from each group were sacrificed. Five specimens in each group were assessed for ligament regeneration by hematoxylin and eosin (HE) staining and immunohistochemical (IHC) staining and for bone integration at the graft–bone interface by HE and Russell–Movat (RM) staining. Graft–bone healing was assessed in the remaining specimens ($n = 5$) using micro-CT and the biomechanical test.

2.5. Surgical Procedure. ACL reconstruction was carried out under strict aseptic conditions, and all operations were performed by one person (Bi). After general anesthesia was achieved by pentobarbital (Kyoritsu-seiyaku, 30 mg/kg body weight), the surgical area was shaved, disinfected, and covered. Exposure of the knee cavity was achieved by a 3 cm incision along the patellar tendon, and then the native ACL was removed (Figure 1(b)). A 2.0 mm Kirschner wire was used to make tunnels in the femur and tibia. The graft was inserted through the bone tunnels, and its ends were attached to the

surrounding soft tissue and the periosteum with 1–0 Ethibond suture (Figure 1(c)). Then, the rabbits were raised in their cages without restriction after surgery.

2.6. Ligament Regeneration Assessment. After collection, the tibia–graft–femur complexes ($n = 5$ per group at each point in time) were immediately put in paraformaldehyde (4%; Sangon) for 24 h. The graft in the knee cavity was collected, dehydrated, and embedded. After sectioning, the slices were stained with HE. Ligament regeneration was analyzed by immunohistochemistry staining for tenascin-C. Image-Pro Plus 6.0 software (IPP6.0) was used to calculate the average immunoreactivity density of tenascin-C in the graft.

2.7. Graft–Bone Healing Assessment. After the graft was dissected from the tibia–graft–femur complex, bone integration at the graft–bone interface was assessed using the remaining bone samples. The bone samples were decalcified by ethylenediaminetetraacetic acid (EDTA; 10%) until they could be easily sectioned with a blade. The samples were sectioned after dehydration and embedding, and the slices were stained with HE and RM to evaluate bone integration.

2.8. Micro-CT Evaluations. The tibia–graft–femur complexes ($n = 5$ per group at each point in time) were prepared for micro-CT scan (36 μm thickness; Skyscan 1176, Bruker, Antwerp, Belgium) and immediately stored at -80°C after collection. The specimens were placed in a refrigerator (4°C) overnight to thaw before testing. Detection of mineralized tissue regeneration at the graft–bone interface was

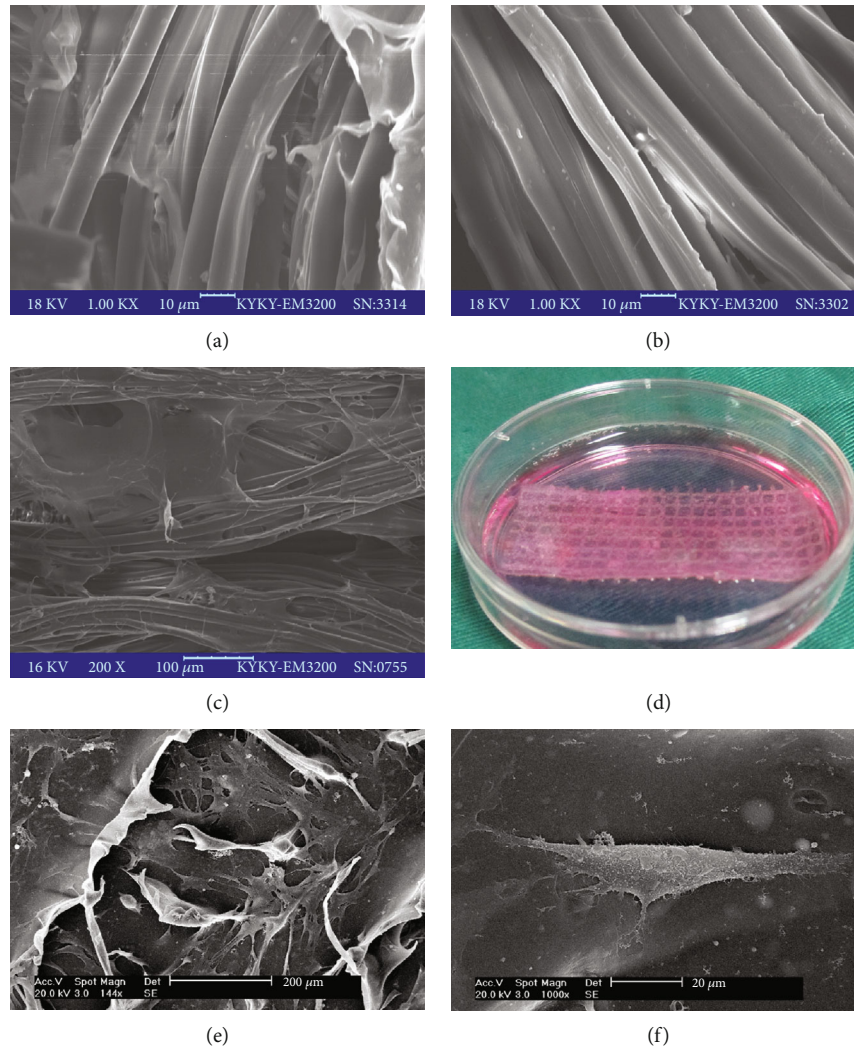


FIGURE 2: (a) The microstructure of silk fibers before degumming: the surface is coated with the glue-like protein sericin. (b) Under SEM, the surface of silk fibroins becomes smooth after complete degumming; the average diameter is about $10\ \mu\text{m}$. (c) The microstructure of silk-collagen scaffold after the dehydrothermal crosslinking process: the collagen sponge permeated into the rings of knitted mesh. (d) BMSCs were seeded on the scaffold and cocultured for 72 h for further use. (e) BMSCs exhibited vigorous proliferation on the scaffold. (f) BMSCs retained good cellular morphology on the scaffold observed by SEM.

performed using radiograph images. Calculation of the bone mineral density (BMD), trabecular number (Tb.N), bone volume fraction (BV/TV), trabecular thickness (Tb.Th), and trabecular separation (Tb.Sp) of a 2.0 mm diameter cylinder scope including the graft–bone interface was carried out by 3-dimensional standard microstructural analyses [30].

2.9. Biomechanical Test. The next step was to carry out the biomechanical test. The tibia–graft–femur complex ($n = 5$ per group at each point in time) was created by dissecting all soft tissue around the knee joint except for the graft. The femur and tibia were screwed into custom-made steel pipes, and the steel pipes were secured to an Instron 553A biomechanical testing system (Instron). The crosshead speed of the tensile load during the biomechanical test was 5 mm/min. The elongation (mm) and failure load (N) were documented, and the slope of the recorded curve indicated stiffness

(N/mm). The tibia–graft–femur complexes were kept moist with normal saline.

2.10. Statistical Analyses. The data collected in the present study are expressed as mean \pm standard deviation (SD). SPSS 16.0 software was used for the statistical analyses. Differences were considered statistically significant at $p < 0.05$. Independent-sample *t*-tests were used to detect differences between groups.

3. Results

3.1. SEM Observation. The surface of raw silk fibers was irregular due to the sericin coating on the silk fibroin (Figure 2(a)). The silk fibroins, which were about $10\ \mu\text{m}$ in diameter and had a smooth surface, were visible after complete degumming (Figure 2(b)). After the process of freeze-drying and dehydrothermal crosslinking, the collagen sponge

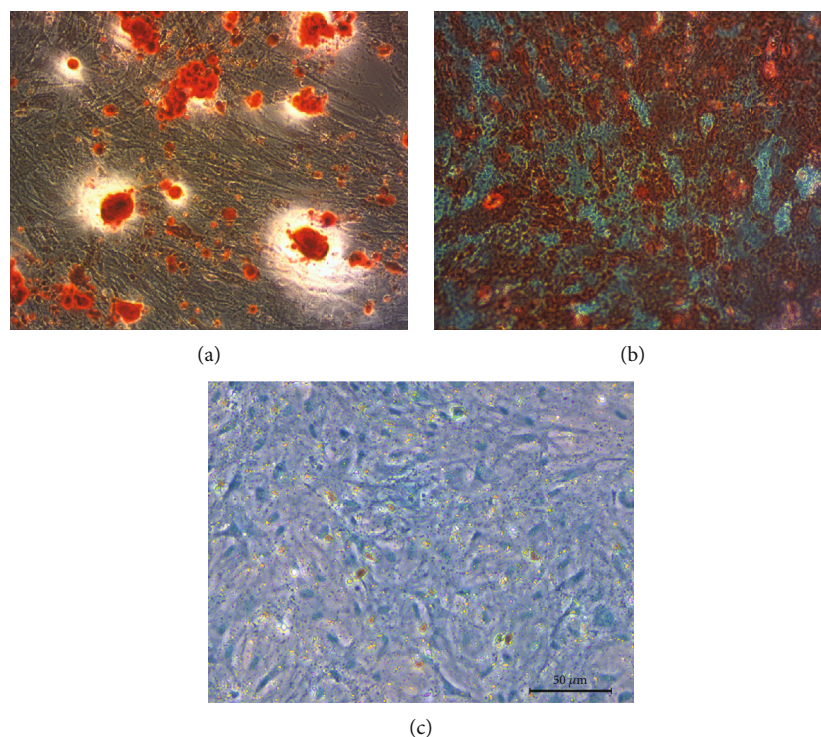


FIGURE 3: Representative images from alizarin red (a), oil red O (b), and alcian blue (c) staining to detect the osteogenic, adipogenic, and chondrogenic differentiation abilities of passage 3 cells.

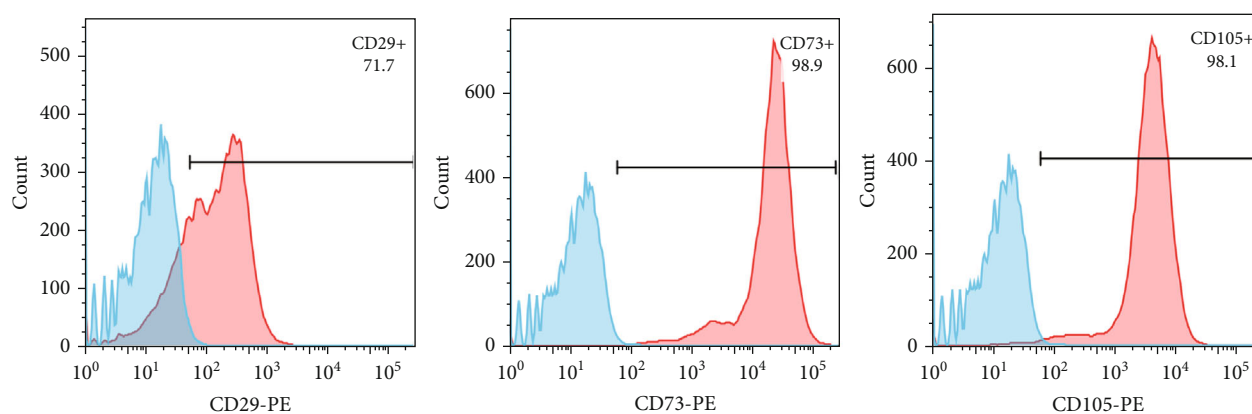


FIGURE 4: The third passage cells had high expression of CD29 (71.7%), CD73 (98.9%), and CD105 (98.1%).

distributed on the silk fibroin surface entered into the rings of knitted mesh, resulting in a fuzzier surface (Figure 2(c)). BMSCs adhered to the collagen surface after being seeded onto the scaffold for 72 h in Petri dishes (Figure 2(d)) and maintained good cellular morphology (Figures 2(e) and 2(f)).

3.2. Identification of BMSCs. Alizarin red, oil red O, and alcian blue staining were performed after cells were cultured in the inducing medium for 3 weeks. Mineralized nodules, lipid droplets, and green cytoplasm were observed under the microscope after staining with alizarin red, oil red O, and alcian blue (Figure 3). The results of flow cytometry showed that the third passage cells had high expression of

CD29 (71.7%), CD73 (98.9%), and CD105 (98.1%) (Figure 4).

3.3. Ligament Regeneration Assessment. Cellular infiltration and tenascin-C production were evaluated by HE and immunohistochemical staining. In the S/C group, considerable cells were observed in the core part of the graft, whereas in the S group, only a few cells could be observed in the graft at 4 weeks postoperatively (Figures 5(a) and 5(b)). At 16 weeks after surgery, fibroblast-like cells became more regular and denser in the S/C than in the S group (Figures 5(c) and 5(d)). The tenascin-C expression in the S group was obviously lower than that in the S/C group at 4 and 16 weeks after surgery (Figures 6(a) and 6(b)).

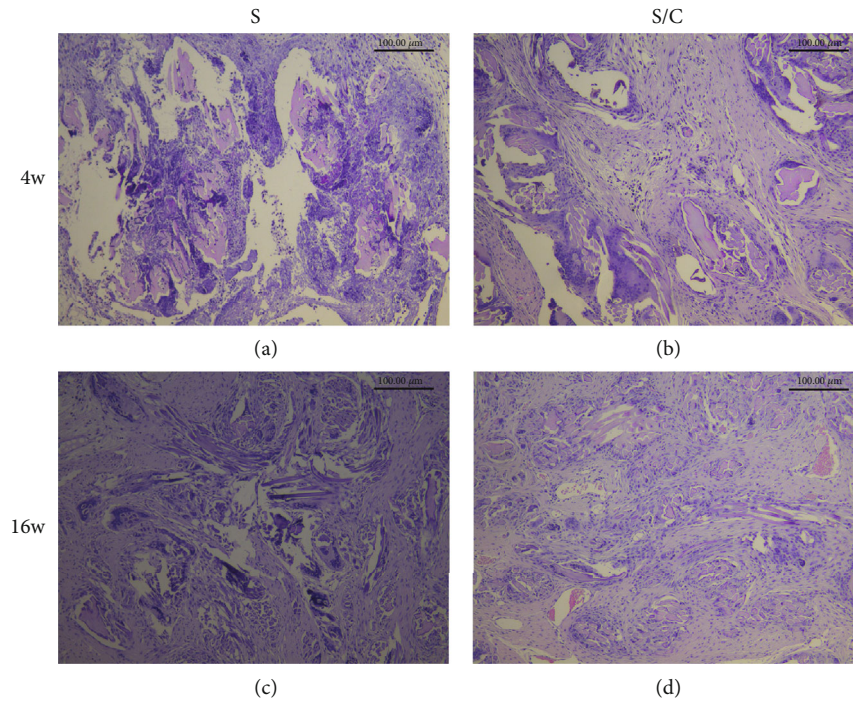


FIGURE 5: At 4 weeks after surgery, HE staining of grafts in the knee cavity in the S group (a) revealed few cells, whereas considerable cells were observed in the core part of the graft in the S/C group (b). At 16 weeks after surgery, fibroblast-like cells became more regular and denser in the S/C group (d) than in the S group (c).

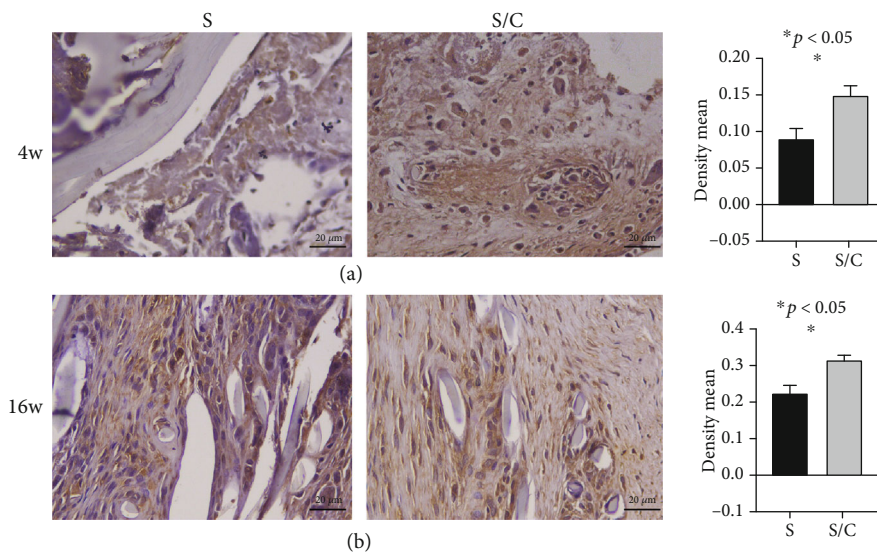


FIGURE 6: Immunohistochemistry staining of grafts in the knee cavity specific for tenascin-C in the S group and S/C group to assess ligament regeneration: the density mean of immunoreactivity was higher in the S/C group than in the S group at 4 weeks (a) and 16 weeks (b) after the operation.

3.4. Graft-Bone Healing Assessment. Histological staining revealed connective tissue with a thin chondrocyte layer at the graft-bone interface at 4 weeks after the reconstruction surgery. No obvious bone integration was noticed in the two groups; although, more cells were distributed in the core part in the S/C group than in the S group (Figures 7(a) and 7(b); Figure 8(a) and 8(b)). By 16 weeks after surgery, the mature trabecular bone and considerable cell invasion in

the scaffold could be noticed at the graft-bone interface in the S group, while integration with the trabecular bone in the graft was observed in the S/C group (Figures 7(c) and 7(d); Figures 8(c) and 8(d)).

3.5. Micro-CT Evaluations. Micro-CT reconstructed the high-resolution transverse sectional images of the tibia and femur. The formation of the mineralized tissue at the graft-

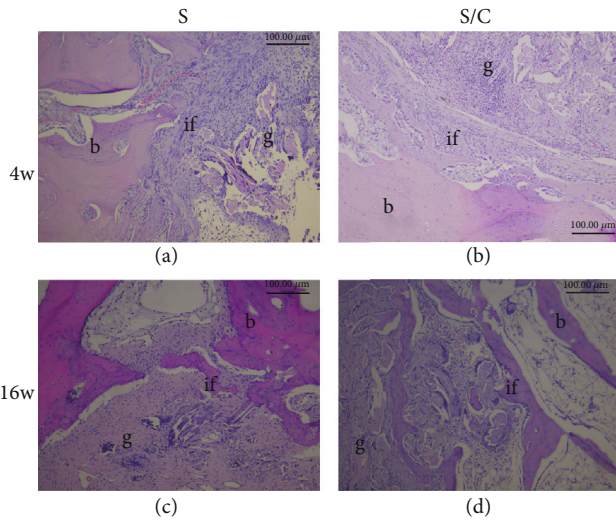


FIGURE 7: HE staining of the graft–bone interface for histological observation. At 4 weeks after the reconstruction surgery, no obvious bone integration was noticed in the two groups; although, more cells were distributed in the core part in the S/C group (b) than in the S group (a). At week 16, mature trabecular bone and considerable cell invasion in the scaffold could be noticed at the graft–bone interface in the S group (c). In the S/C group, integration of the trabecular bone into the graft was observed (d). g: graft; b: bone; if: interface.

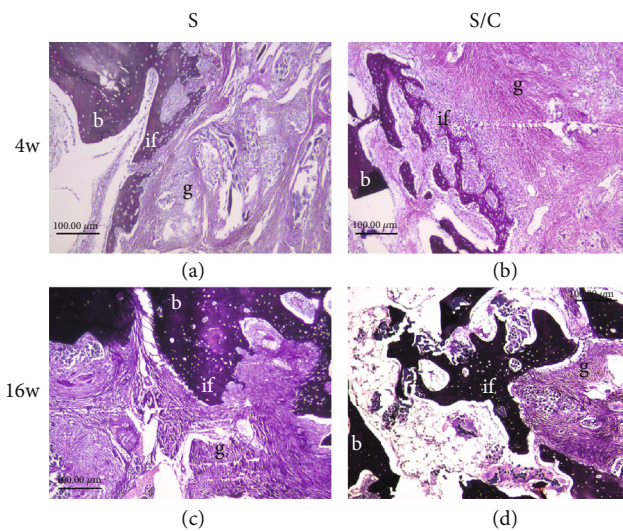


FIGURE 8: Russell–Movat staining of the graft–bone interface. At 4 weeks after the reconstruction surgery, no obvious bone integration was noticed in the two groups (a, b). At week 16, the mature trabecular bone could be noticed at the graft–bone interface in the S group (c), whereas in the S/C group, osteointegration with the trabecular bone into the graft was observed (d). g: graft; b: bone; if: interface.

bone interface could be easily observed. In both groups, few mineralized tissues were detected at the graft–bone interface at 4 weeks postoperatively (Figures 9(a) and 9(b)). BV/TV, Tb.Th, and BMD values were increased significantly more in the S/C than in the S group (Table 1). However, at 16

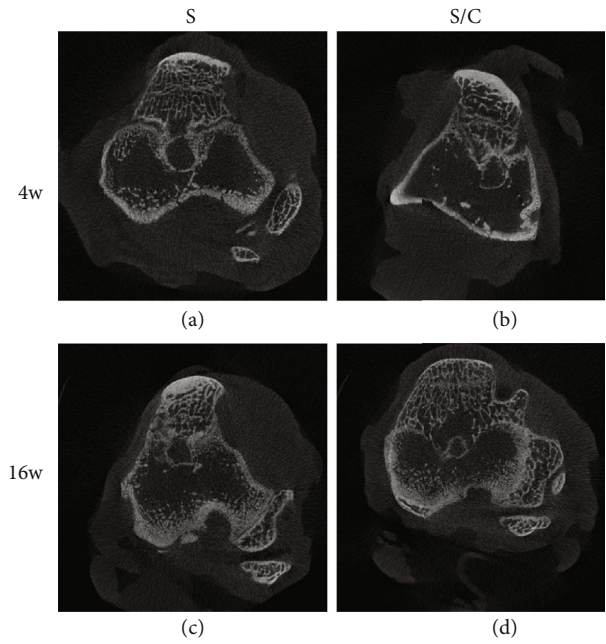


FIGURE 9: Representative micro-CT images. Few mineralized tissues were detected at the graft–bone interface at 4 weeks postoperatively (a, S group; b, S/C group). At 16 weeks postoperatively, distinct signals appeared indicating new mineralized tissue regeneration at the graft–bone interface of each group (c, S group; d, S/C group). The mineralized tissue signal and average bone tunnel area may indicate bone integration at the graft–bone interface.

TABLE 1: Micro-CT evaluations (mean ± SD). BV/TV, Tb.Th, and BMD increased significantly more in the S/C group than in the S group at 4 weeks after reconstruction surgery. Significant increases in Tb.Th and BMD were observed in the S/C group relative to the S group. * indicates a notable distinction between the two comparison groups.

Time point	Items	S	S/C	p value
4 w	BV/TV (%)	14.04 ± 0.41	15.53 ± 0.90	0.0169*
	Tb.Th (mm)	0.27 ± 0.02	0.32 ± 0.02	0.0198*
	Tb.N (1/mm)	0.24 ± 0.07	0.30 ± 0.01	0.0883
	Tb.Sp (mm)	1.21 ± 0.01	1.13 ± 0.07	0.0426*
	BMD (mg/cm ³)	0.08 ± 0.01	0.10 ± 0.00	0.0001*
16 w	BV/TV (%)	22.29 ± 1.01	23.50 ± 0.98	0.1233
	Tb.Th (mm)	0.29 ± 0.05	0.36 ± 0.03	0.0406*
	Tb.N (1/mm)	0.39 ± 0.10	0.47 ± 0.07	0.2725
	Tb.Sp (mm)	0.91 ± 0.03	0.83 ± 0.07	0.0887
	BMD (mg/cm ³)	0.19 ± 0.02	0.22 ± 0.02	0.0494*

weeks after reconstruction surgery, distinct signals appeared indicating new mineralized tissue regeneration at the graft–bone interface in both groups (Figures 9(c) and 9(d)), with greater increases in Tb.Th and BMD observed in the S/C than in the S group (Table 1).

3.6. Biomechanical Test. All grafts in both groups failed through rupture in the knee cavity or pullout from the bone

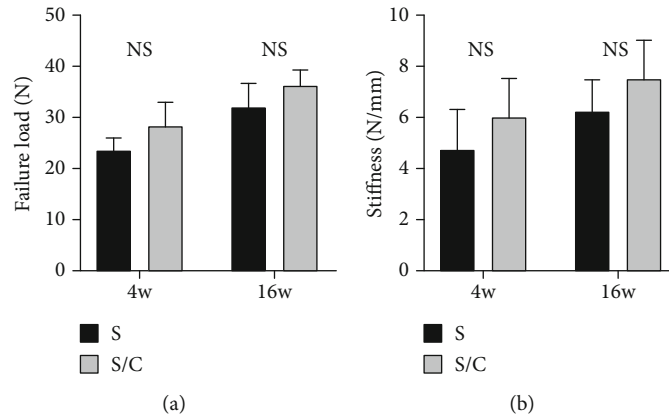


FIGURE 10: No significant differences were found in failure load (a) or stiffness (b) between the S group and S/C group at 4 and 16 weeks after the reconstruction surgery. NS indicates no significant difference between groups.

tunnel. No obvious differences in the failure load were found between the two groups at 4 and 16 weeks after surgery (4 w, S 23.24 ± 2.18 vs. S/C 28.38 ± 4.07 , $p = 0.06$; 16 w, S 31.85 ± 4.24 vs. 36.36 ± 2.58 , $p = 0.11$; Figure 10(a)). Stiffness was calculated by recording the displacement and failure load from the load–deformation curve. The stiffness was not considerably different between the groups at 4 and 16 weeks after surgery (4 w, S 4.71 ± 1.42 vs. S/C 4.71 ± 1.42 , $p = 0.21$; 16 w, S 6.18 ± 1.17 vs. 7.52 ± 1.31 , $p = 0.16$; Figure 10(b)).

4. Discussion

Tissue engineering grafts for ACL reconstruction have focused on ligament regeneration in the knee cavity and bone integration at the graft–bone interface [31]. The present study revealed that BMSCs promoted ligament regeneration and graft–bone healing after reconstruction surgery using a silk–collagen scaffold. The scaffold was infiltrated by great many fibroblast-like cells and tenascin-C depositions at 4 and 16 weeks after surgery. The graft–bone interface exhibited good bone integration at 16 weeks after surgery. The results showed that BMSCs combined with silk–collagen scaffolds represent a good prospect in ACL tissue engineering and future clinical use.

Ideally, a tissue engineering scaffold for ACL reconstruction needs to simulate biological functions as well as the geometric structures of ligaments [32]. The ECM is important in guiding tissue ingrowth, maintaining homeostasis, and providing mechanical support during the ligament regeneration process. The silk–collagen scaffold takes advantage of silk's inherent mechanical properties and its suitability for knitting as well as the favorable biocompatibility of collagen matrix. Collagen matrix dominated the space between the silk fibroins and provided an attachment point for seeded cells.

The synovium layer covers the knee cavity, providing a less vascular microenvironment. At 4 and 16 weeks after surgery, fewer cells were attracted into the scaffold, and less ECM deposition occurred in the S group compared to the S/C group. According to the results, few cells migrated from surrounding tissues into the scaffold, and implanted BMSCs contributed proliferated cells to the scaffold and regenerated

ECM. Fan and colleagues found that the production of tenascin-C, collagen-II, and collagen-I from stem cells was greatly improved after cocultivation with silk scaffolds after 7 and 14 days [33]. Tenascin-C, one of the extracellular matrix glycoproteins in intra-articular grafts, is always expressed in the actively remodeling tissue and has a highly restricted gene expression model [34]. The tenascin-C expression in the S group was obviously lower than that in the S/C group at 4 and 16 weeks postoperatively. Results demonstrated that grafts in the S/C group exhibited more vibrant ligament regeneration than did those in the S group, and implanted BMSCs contributed to cell proliferation and ECM deposition.

Successful ACL reconstruction requires solid graft–bone healing [17]. Graft–bone healing in the bone tunnel requires that bone grow inward into the graft–bone interface. Kanaya and colleagues [35] reported that transected sections shrank over time, and the interface in the MSC(-) group still lacked tissue at all points in time postoperatively, whereas in the MSC(+) group, GFP-positive cells were found at 2 and 4 weeks postoperatively in healing tissues covering the transected section. The histologic score of the MSC(+) group was obviously better than that of the MSC(-) group. As reported by Hong and colleagues, BMSCs may promote the graft–bone healing process, as cartilage-like cells proliferated and perpendicular collagen fibers increasingly formed at 4 weeks postoperatively in a rabbit model [36]. In the present study, cartilage-like cells proliferated, and less fibrocartilage-like tissue formed at the graft–bone interface in the S group than in the S/C group at 4 weeks after surgery. The mature trabecular bone was found in the core part of the graft in the S/C group at 16 weeks postoperatively, whereas only the mature trabecular bone was found at the interface in the S group. The graft–bone healing process may be promoted by the host stem cells from the circumambient bone marrow in the bone tunnel [37–39], but the host cell infiltration into the graft might take more than 4 weeks after surgery [20]. Based on the present study, it is considered that the implanted BMSCs mostly promoted bone integration between the graft and bone.

Oka and colleagues found that bone integration at the graft–bone interface determined micro-CT parameters [40]. Micro-CT could discern subtle changes in bone tunnels and collect gross information of newly formed mineralized tissue through imaging [41]. This study evaluated bone integration using micro-CT. More mineralized tissues were detected in the bone tunnel in the S/C group than in the S group at 4 and 16 weeks postoperatively; this finding corresponded to the histological findings.

The two main parameters of a ligament regenerated by tissue engineering are failure load and stiffness. Previous studies have shown that silk degraded via proteolytic degradation, resulting in a decrease in the scaffold mechanical strength [42, 43]. The speed of decrease in mechanical strength depends primarily on the physiological status, mechanical environment, implantation site, and scaffold structure. ECM including collagen fibers and proteoglycans could be produced by the infiltrated cells, which makes up for the mechanical strength decrease due to degradation. The mean failure load and stiffness in the S/C group were greater than those in the S group at 4 and 16 weeks after the procedure. The absence of a notable distinction between the two might be attributable to the small specimen dimensions.

One limitation of the present study was that we did not quantify the number of BMSCs implanted on the silk–collagen scaffold, and the optimal number of implanted cells remains unknown. Furthermore, the seeded BMSCs were not labeled and tracked, which represents another limitation. Although BMSCs seeded on the scaffold maintained good cellular morphology in vitro, the environments of the joint cavity and bone tunnel are different from that of a Petri dish. In a previous study, autologous BMSCs transfected with lentivirus vector expressing enhanced green fluorescent protein (Lv-eGFP) were seeded on a decellularized semitendinous tendon graft for ACL reconstruction [44]. The eGFP-positive cells could be observed at 12 weeks postoperatively; although, the eGFP-positive cell number at week 12 was significantly lower than that at week 4. The conclusions of the present study were based on cell infiltration and tenascin-C deposition and on graft–bone healing observed histologically. More data will be needed to confirm the fate of the implanted cells in a future study.

5. Conclusion

BMSCs may promote ligament regeneration in the cavity and bone integration at the graft–bone interface. Silk–collagen scaffold and BMSCs are very likely to be combined for clinical practice in the future.

Data Availability

The data used to support the findings of this study are included within the article.

Conflicts of Interest

The authors declare that they have no conflicts of interest.

Authors' Contributions

Fanggang Bi conceived and designed the experiment. Fanggang Bi, Yangdi Chen, Junqi Liu, and Wenhao Hu performed the experiment. Fanggang Bi and Yangdi Chen analyzed data. Ke Tian contributed reagents/materials/analysis tools. Fanggang Bi wrote the manuscript. All authors read and approved the final manuscript.

Acknowledgments

This work was supported by the Foundation of Henan Educational Committee (19A320011) and the Key Project of Science and Technology Department of Henan Province-2020 (22170139).

References

- [1] M. J. Price, M. Tuca, F. A. Cordasco, and D. W. Green, “Non-modifiable risk factors for anterior cruciate ligament injury,” *Current Opinion in Pediatrics*, vol. 29, no. 1, pp. 55–64, 2017.
- [2] R. B. Frobell, E. M. Roos, H. P. Roos, J. Ranstam, and L. S. Lohmander, “A randomized trial of treatment for acute anterior cruciate ligament tears,” *The New England Journal of Medicine*, vol. 363, no. 4, pp. 331–342, 2010.
- [3] R. Vaishya, A. K. Agarwal, S. Ingole, and V. Vijay, “Current trends in anterior cruciate ligament reconstruction: a review,” *Cureus*, vol. 7, no. 11, article e378, 2015.
- [4] T. Diermeier, R. Tisherman, J. Hughes et al., “Quadriceps tendon anterior cruciate ligament reconstruction,” *Knee Surgery, Sports Traumatology, Arthroscopy*, vol. 28, no. 8, pp. 2644–2656, 2020.
- [5] S. Shumborski, L. J. Salmon, C. Monk, E. Heath, J. P. Roe, and L. A. Pinczewski, “Allograft donor characteristics significantly influence graft rupture after anterior cruciate ligament reconstruction in a young active population,” *The American Journal of Sports Medicine*, vol. 48, no. 10, pp. 2401–2407, 2020.
- [6] S. J. Tulloch, B. M. Devitt, C. J. Norsworthy, and C. Mow, “Synovitis following anterior cruciate ligament reconstruction using the LARS device,” *Knee Surgery, Sports Traumatology, Arthroscopy*, vol. 27, no. 8, pp. 2592–2598, 2019.
- [7] S. Rai, S. Y. Jin, B. Rai et al., “A single bundle anterior cruciate ligament reconstruction (ACL-R) using hamstring tendon autograft and tibialis anterior tendon allograft: a comparative study,” *Current Medical Science*, vol. 38, no. 5, pp. 818–826, 2018.
- [8] N. K. Paschos and S. M. Howell, “Anterior cruciate ligament reconstruction: principles of treatment,” *EFORT Open Reviews*, vol. 1, no. 11, pp. 398–408, 2016.
- [9] W. Shen, X. Chen, Y. Hu et al., “Long-term effects of knitted silk–collagen sponge scaffold on anterior cruciate ligament reconstruction and osteoarthritis prevention,” *Biomaterials*, vol. 35, no. 28, pp. 8154–8163, 2014.
- [10] C. T. Laurencin and J. W. Freeman, “Ligament tissue engineering: an evolutionary materials science approach,” *Biomaterials*, vol. 26, no. 36, pp. 7530–7536, 2005.
- [11] F. Bi, Z. Shi, A. Liu, P. Guo, and S. Yan, “Anterior cruciate ligament reconstruction in a rabbit model using silk–collagen scaffold and comparison with autograft,” *PLoS One*, vol. 10, no. 5, article e0125900, 2015.

- [12] D. L. Barreiro, J. Yeo, A. Tarakanova, F. J. Martin-Martinez, and M. J. Buehler, "Multiscale modeling of silk and silk-based biomaterials—a review," *Macromolecular Bioscience*, vol. 19, no. 3, article e1800253, 2019.
- [13] R. P. A. Janssen and S. U. Scheffler, "Intra-articular remodeling of hamstring tendon grafts after anterior cruciate ligament reconstruction," *Knee Surgery, Sports Traumatology, Arthroscopy*, vol. 22, no. 9, pp. 2102–2108, 2014.
- [14] K. Ficek, J. Rajca, M. Stolarz et al., "Bioresorbable stent in anterior cruciate ligament reconstruction," *Polymers*, vol. 11, no. 12, p. 1961, 2019.
- [15] D. Chanda, S. Kumar, and S. Ponnazhagan, "Therapeutic potential of adult bone marrow-derived mesenchymal stem cells in diseases of the skeleton," *Journal of Cellular Biochemistry*, vol. 111, no. 2, pp. 249–257, 2010.
- [16] B. A. Tucker, S. S. Karamsadkar, W. S. Khan, and P. Pastides, "The role of bone marrow derived mesenchymal stem cells in sports injuries," *Journal of Stem Cells*, vol. 5, no. 4, pp. 155–166, 2010.
- [17] C. Teng, C. Zhou, D. Xu, and F. Bi, "Combination of platelet-rich plasma and bone marrow mesenchymal stem cells enhances tendon-bone healing in a rabbit model of anterior cruciate ligament reconstruction," *Journal of Orthopaedic Surgery and Research*, vol. 11, no. 1, p. 96, 2016.
- [18] C. S. Linsley, B. M. Wu, and B. Tawil, "Mesenchymal stem cell growth on and mechanical properties of fibrin-based biomimetic bone scaffolds," *Journal of Biomedical Materials Research. Part A*, vol. 104, no. 12, pp. 2945–2953, 2016.
- [19] T. Wang, X. Yang, X. Qi, and C. Jiang, "Osteoinduction and proliferation of bone-marrow stromal cells in three-dimensional poly (ϵ -caprolactone)/ hydroxyapatite/collagen scaffolds," *Journal of Translational Medicine*, vol. 13, no. 1, p. 152, 2015.
- [20] H. Komiyama, Y. Arai, Y. Kajikawa et al., "The fate and role of bone graft-derived cells after autologous tendon and bone transplantation into the bone tunnel," *Journal of Orthopaedic Science*, vol. 18, no. 6, pp. 994–1004, 2013.
- [21] M. Kobayashi, N. Watanabe, Y. Oshima, Y. Kajikawa, M. Kawata, and T. Kubo, "The fate of host and graft cells in early healing of bone tunnel after tendon graft," *The American Journal of Sports Medicine*, vol. 33, no. 12, pp. 1892–1897, 2005.
- [22] J. K. Lim, J. Hui, L. Li, A. Thambyah, J. Goh, and E. H. Lee, "Enhancement of tendon graft osteointegration using mesenchymal stem cells in a rabbit model of anterior cruciate ligament reconstruction," *Arthroscopy*, vol. 20, no. 9, pp. 899–910, 2004.
- [23] M. Y. H. Soon, A. Hassan, J. H. P. Hui, J. C. H. Goh, and E. H. Lee, "An analysis of soft tissue allograft anterior cruciate ligament reconstruction in a rabbit model: a short-term study of the use of mesenchymal stem cells to enhance tendon osteointegration," *The American Journal of Sports Medicine*, vol. 35, no. 6, pp. 962–971, 2007.
- [24] C. C. Ude, B. S. Shamsul, M. H. Ng et al., "Long-term evaluation of osteoarthritis sheep knee, treated with TGF- β 3 and BMP-6 induced multipotent stem cells," *Experimental Gerontology*, vol. 104, pp. 43–51, 2018.
- [25] M. Chen, Y. Xu, T. Zhang et al., "Mesenchymal stem cell sheets: a new cell-based strategy for bone repair and regeneration," *Biotechnology Letters*, vol. 41, no. 3, pp. 305–318, 2019.
- [26] W. Zhang, Y. Yang, K. Zhang, Y. Li, and G. Fang, "Weft-knitted silk-poly(lactide-co-glycolide) mesh scaffold combined with collagen matrix and seeded with mesenchymal stem cells for rabbit Achilles tendon repair," *Connective Tissue Research*, vol. 56, no. 1, pp. 25–34, 2015.
- [27] W. Li, R. Xu, J. Huang, X. Bao, and B. Zhao, "Treatment of rabbit growth plate injuries with oriented ECM scaffold and autologous BMSCs," *Scientific Reports*, vol. 7, no. 1, article 44140, 2017.
- [28] S. Q. Ruan, J. Deng, L. Yan, and W. L. Huang, "Composite scaffolds loaded with bone mesenchymal stem cells promote the repair of radial bone defects in rabbit model," *Biomedicine & Pharmacotherapy*, vol. 97, pp. 600–606, 2018.
- [29] J. S. Pieper, A. Oosterhof, P. J. Dijkstra, J. H. Veerkamp, and T. van Kuppevelt, "Preparation and characterization of porous crosslinked collagenous matrices containing bioavailable chondroitin sulphate," *Biomaterials*, vol. 20, no. 9, pp. 847–858, 1999.
- [30] M. L. Boussein, S. K. Boyd, B. A. Christiansen, R. E. Guldborg, K. J. Jepsen, and R. Müller, "Guidelines for assessment of bone microstructure in rodents using micro-computed tomography," *Journal of Bone and Mineral Research*, vol. 25, no. 7, pp. 1468–1486, 2010.
- [31] A. J. Lee, W. H. Chung, D. H. Kim et al., "Anterior cruciate ligament reconstruction in a rabbit model using canine small intestinal submucosa and autologous platelet-rich plasma," *The Journal of Surgical Research*, vol. 178, no. 1, pp. 206–215, 2012.
- [32] F. Wang, Y. Hu, D. He, G. Zhou, and E. Ellis III, "Scaffold-free cartilage cell sheet combined with bone-phase BMSCs-scaffold regenerate osteochondral construct in mini-pig model," *American Journal of Translational Research*, vol. 10, no. 10, pp. 2997–3010, 2018.
- [33] H. Fan, H. Liu, E. J. W. Wong, S. L. Toh, and J. C. H. Goh, "In vivo study of anterior cruciate ligament regeneration using mesenchymal stem cells and silk scaffold," *Biomaterials*, vol. 29, no. 23, pp. 3324–3337, 2008.
- [34] E. J. Mackie and S. Ramsey, "Expression of tenascin in joint-associated tissues during development and postnatal growth," *Journal of Anatomy*, vol. 188, pp. 157–165, 1996.
- [35] A. Kanaya, M. Deie, N. Adachi, M. Nishimori, S. Yanada, and M. Ochi, "Intra-articular injection of mesenchymal stromal cells in partially torn anterior cruciate ligaments in a rat model," *Arthroscopy*, vol. 23, no. 6, pp. 610–617, 2007.
- [36] H. W. Ouyang, J. C. H. Goh, and E. H. Lee, "Use of bone marrow stromal cells for tendon graft-to-bone healing: histological and immunohistochemical studies in a rabbit model," *The American Journal of Sports Medicine*, vol. 32, no. 2, pp. 321–327, 2004.
- [37] S. Kawamura, L. Ying, H. J. Kim, C. Dynybil, and S. A. Rodeo, "Macrophages accumulate in the early phase of tendon-bone healing," *Journal of Orthopaedic Research*, vol. 23, no. 6, pp. 1425–1432, 2005.
- [38] M. Hevesi, M. LaPrade, D. B. F. Saris, and A. J. Krych, "Stem cell treatment for ligament repair and reconstruction," *Current Reviews in Musculoskeletal Medicine*, vol. 12, no. 4, pp. 446–450, 2019.
- [39] Z. C. Hao, S. Z. Wang, X. J. Zhang, and J. Lu, "Stem cell therapy: a promising biological strategy for tendon-bone healing after anterior cruciate ligament reconstruction," *Cell Proliferation*, vol. 49, no. 2, pp. 154–162, 2016.

- [40] S. Oka, T. Matsumoto, S. Kubo et al., “Local administration of low-dose simvastatin-conjugated gelatin hydrogel for tendon-bone healing in anterior cruciate ligament reconstruction,” *Tissue Engineering. Part A*, vol. 19, no. 9-10, pp. 1233–1243, 2013.
- [41] M. Bellido, L. Lugo, J. A. Roman-Blas et al., “Improving subchondral bone integrity reduces progression of cartilage damage in experimental osteoarthritis preceded by osteoporosis,” *Osteoarthritis and Cartilage*, vol. 19, no. 10, pp. 1228–1236, 2011.
- [42] G. H. Altman, F. Diaz, C. Jakuba et al., “Silk-based biomaterials,” *Biomaterials*, vol. 24, no. 3, pp. 401–416, 2003.
- [43] D. Greenwald, S. Shumway, P. Albear, and L. Gottlieb, “Mechanical comparison of 10 suture materials before and after *in vivo* incubation,” *The Journal of Surgical Research*, vol. 56, no. 4, pp. 372–377, 1994.
- [44] W. Lu, J. Xu, S. Dong et al., “Anterior cruciate ligament reconstruction in a rabbit model using a decellularized allogenic semitendinous tendon combined with autologous bone marrow-derived mesenchymal stem cells,” *Stem Cells Translational Medicine*, vol. 8, no. 9, pp. 971–982, 2019.

Research Article

Potency of Bone Marrow-Derived Mesenchymal Stem Cells and Indomethacin in Complete Freund's Adjuvant-Induced Arthritic Rats: Roles of TNF- α , IL-10, iNOS, MMP-9, and TGF- β 1

Eman A. Ahmed ¹, Osama M. Ahmed ¹, Hanaa I. Fahim ¹, Tarek M. Ali ^{2,3},
Basem H. Elesawy ^{4,5} and Mohamed B. Ashour ¹

¹Physiology Division, Zoology Department, Faculty of Science, Beni-Suef University, P.O. Box 62521, Beni-Suef, Egypt

²Department of Physiology, College of Medicine, Taif University, P.O. Box 11099, Taif 21944, Saudi Arabia

³Department of Physiology, Faculty of Medicine, Beni-Suef University, Beni-Suef, Egypt

⁴Department of Clinical Laboratory Sciences, College of Applied Medical Sciences, Taif University, P.O. Box 11099, Taif 21944, Saudi Arabia

⁵Department of Pathology, Faculty of Medicine, Mansoura University, Egypt

Correspondence should be addressed to Eman A. Ahmed; eman.mohsen2012@yahoo.com

Received 26 December 2020; Revised 21 January 2021; Accepted 20 March 2021; Published 5 April 2021

Academic Editor: Liang Gao

Copyright © 2021 Eman A. Ahmed et al. This is an open access article distributed under the Creative Commons Attribution License, which permits unrestricted use, distribution, and reproduction in any medium, provided the original work is properly cited.

Rheumatoid arthritis (RA) is an autoimmune syndrome affecting joint spaces, leading to the disabled state. Currently, there is no optimal therapy for RA except for systemic immunosuppressants that have variable undesirable effects after long-term use. Hence, the need for other treatment modalities has emerged in an attempt to develop a treating agent that is effective but without bad effects. Bone marrow-derived mesenchymal stem cells (BM-MSCs) may be an alternative medicine since they may differentiate into a variety of mesenchymal tissues including bone and cartilage. Indomethacin (IMC) could be suggested as an analgesic, anti-inflammatory, and antirheumatic potential agent against the course of RA since it possesses significant palliative effects and antipyretic properties. Therefore, our target of this study was to explore and compare the effect of BM-MSCs (1×10^6 cells/rat at the 1st, 6th, 12th, and 18th days) and IMC (2 mg/kg b.w./day for 3 weeks) either alone or in combination on arthritic rats. The model of rheumatoid arthritis in rats was induced by subcutaneous injection of 0.1 mL/rat CFA into the footpad of the right hind paw. The BM-MSC intravenous injection and IMC oral administration significantly reduced the elevated right hind leg paw diameter and circumference, serum anti-CCP, and ankle joint articular tissue expressions of TNF- α , iNOS, MMP-9, and TGF- β 1 while they significantly increased the lowered articular IL-10 expression in CFA-induced arthritic rats. The combinatory effect of the two treatments was the most potent. In conclusion, the treatment of RA with BM-MSCs and IMC together is more effective than the treatment with either BM-MSCs or IMC. The Th1 cytokine (TNF- α), Th2 cytokine (IL-10), iNOS, MMP-9, and TGF- β 1 are important targets for mediating the antiarthritic effects of BM-MSCs and IMC in CFA-induced arthritis in rats.

1. Introduction

Rheumatoid arthritis (RA) is a syndrome of ongoing inflammation that is categorized with joint rubefaction, edema, and impairment of synovial joints. Such phase is correlated with inflammatory cell proliferation and penetration of the synovium, in addition to bone as well as periarticular cartilage

dysfunction [1]. RA is considered a chief cause of permanent disability, augmented mortality, and socioeconomic costs [2]. Its prevalence is around 1% of the global population and is in continuous increase with time [3] and propagates in females 3 times more than males which could be attributed to sex hormones. It is also linked with the extra-articular manifestations involving renal, pulmonary, and cardiovascular

problems [4]. Former research and studies suggested that the imbalanced immunological responses in addition to genetic factors play a fundamental role in RA development. The mechanism of RA pathogenesis and its etiology remains generally indefinite. However, it primarily is activated by T cell immunological responses that release various proinflammatory mediators [5] such as tumor necrosis factor- α (TNF- α), matrix metalloproteinase-9 (MMP-9), inducible nitric oxide synthase (iNOS), and transforming growth factor- β 1 (TGF- β 1). Also, the anticyclic citrullinated protein antibodies (anti-CCP) are subsequently produced inducing local edema, inflammation, and ultimately joint destruction [6]. In comparison, a compensatory anti-inflammatory response in the RA synovia is also evidenced by producing anti-inflammatory cytokines such as IL-10 that is believed to suppress RA progression [7]. Accordingly, it became so critical to explore promising mechanisms and seek potential safer alternative therapies to improve the inflammatory pathological progress in RA patients [8].

There are many common drugs administered for pain relief and delay of RA progression including traditional nonsteroidal anti-inflammatory drugs (NSAIDs) combined with those steroids or disease-modifying antirheumatic drugs (DMARDs), also hormonal-based drugs or corticosteroids, and the novel biological therapeutic agents, such as the tumor necrosis factor- α (TNF- α) antibody and the decoy TNF- α receptor [9]. However, the application of these available medicines is frequently limited and undesired by patients due to their high costs, and their administration for a long time is accompanied by the incidence of harm and extensive side effects [10]. In this regard, unconventional therapies or anti-inflammatory substances from other different sources that provide an effective but safer treatment of arthritis have aroused great public interest in recent years [11]. Various experimental animal models have been well known in rats to study the disease initiation and propagation as well as determine the probable efficacy of antiarthritic and anti-inflammatory agents [12]. The arthritis model induced *via* complete Freund's adjuvant (CFA) reagent is one of the best available models for chronic inflammation and polyarthritis with features that resemble human RA and is still widely used in the preclinical testing of arthritis [13–15]. Mesenchymal stem cells (MSCs) are multipotent cells that differentiate into various kinds of cells including adipocytes, osteoclasts, and chondrocytes. They could be extracted from numerous mesodermal tissues such as the dental pulp, placenta, umbilical cord blood, menstrual fluid, umbilical cord, adipose tissue, and bone marrow [16]. They were found to exert immunosuppressive purposes on both the innate and adaptive immune cells [17]. Consequently, MSCs have an interesting therapeutic cell candidate for tissue engineering and repair of damaged structures in autoimmune diseases such as RA. This could be attributed to their anti-inflammatory and regenerative functions besides their capacity to attenuate the exacerbated pathogenic immune response observed in these patients [17].

Moreover, indomethacin (IMC), 1-(p-chlorobenzoyl)-5-methoxy-2-methylindole-3-acetic acid, is considered a nonsteroidal indole derivative with anti-inflammatory activity

and chemopreventive properties. As a nonsteroidal anti-inflammatory drug (NSAID), indomethacin reduces prostaglandins by inhibiting cyclooxygenase (COX) enzymes, COX-1 and COX-2, with greater selectivity for COX-1. IMC inhibits COX enzymes by binding to them, forming COX-IMC complexes [18, 19]. Also, IMC exhibits potent antipyretic effects and analgesic properties that may enable it to relieve the pain of patients and overcome the inflammatory reactions of the disease. The Food and Drug Administration (FDA) approved its use for many diseases including primary dysmenorrhea, pericarditis, juvenile arthritis, pseudogout, and Paget's disease [20]. It has acquired an established place in the treatment of osteoarthritis of the hip. It was introduced in 1963 for the treatment of ankylosing spondylitis and seems to be effective in degenerative joint diseases. Also, it showed benefit in treating acute gout and musculoskeletal disorders, inflammation, and edema [21]. Additionally, IMC has been used by clinicians in treating RA and preventing its progression. However, it is rarely used solely but usually showed greater efficacy in conjunction with DMARDs such as adalimumab, etanercept, infliximab, and methotrexate [20].

In conductance with the previous publications, this study was designed to evaluate the convenience and bioavailability of BM-MSCs and IMC administered in combination to associate the advantages of both of them in relation to each treatment (BM-MSCs or IMC) alone, *via* their role in suppressing the Th1 (TNF- α , iNOS, MMP-9, and TGF- β 1) pathway while promoting the Th2 (IL-10) pathway and subsequently overcoming the course of the disease in the CFA-arthritis rat model.

2. Materials and Methods

2.1. Animal Procurement and Maintenance. Our experiment included 50 male Wistar rats (120–150 g, weight; 10–12 weeks, specific pathogen-free) that were obtained from VAC-SERA (Helwan Station, Cairo, Egypt). The animals were kept in an animal facility at temperature $22 \pm 2^\circ\text{C}$, relative humidity $55 \pm 5\%$, and 12-hour (h)/12 h light/dark cycle. The animal experiment was approved by the local committee for animal experimentation, Faculty of Science, Beni-Suef University, Egypt (ethical approval number: BSU/FS/2017/11).

2.1.1. Induction of Arthritis. For arthritis induction, animals were inoculated by subcutaneous injection of 0.1 mL/rat CFA solution (Sigma Chemical Co., St. Louis, MO, USA) into the footpad of the right hind paw as described by Ahmed et al. [13] for two consecutive days. Each 1 mL of CFA contains 1 mg of *Mycobacterium tuberculosis*, heat-killed and dried, 0.85 mL paraffin oil, and 0.15 mL mannide monooleate.

2.1.2. Animal Grouping. The experimental model was designed as described in our recent study [22] as follows:

Group 1 (normal). It consists of healthy rats that were given the equivalent volumes of carboxymethylcellulose (CMC) daily and orally for 3 weeks and Dulbecco's modified

Eagle's medium (DMEM) intravenously at the 1st, 6th, 12th, and 18th days.

Group 2 (CFA). It is composed of CFA-induced arthritic rats and was orally given the equivalent volumes of CMC daily and orally for 3 weeks and DMEM intravenously at the 1st, 6th, 12th, and 18th days.

Group 3 (CFA+BM-MSCs). This group consists of CFA-induced arthritic rats that received four doses of BM-MSCs (1×10^6 cells/rat/dose) by intravenous injection through the lateral tail vein per rat [23]. Each dose was suspended in 0.2 mL DMEM (Dulbecco's modified Eagle's medium). Doses were given on the 1st, 6th, 12th, and 18th days after CFA injection.

Group 4 (CFA+IMC). This group is composed of CFA-induced arthritic rats supplemented orally with IMC in a dose of 2 mg/kg body weight (b.w.)/day for 3 weeks after CFA injection. IMC was freshly prepared immediately before administration by dissolving in 5 mL of 1% CMC for three weeks. IMC was acquired from Sigma Chemical Company (Sigma Chemical Co., St. Louis, MO, USA).

Group 5 (CFA+BM-MSCs+IMC). This group consists of CFA-induced arthritic rats that were concurrently supplemented with BM-MSCs and IMC as described in groups 3 and 4.

2.2. Isolation and Culture of BM-MSCs. The isolating and culturing technique of the BM-MSCs is established on the approach of Chaudhary and Rath [24] and our former publications [22, 25].

2.3. Evaluation of Paw Edema and Swelling Rate in Arthritis. In the present study, for evaluating the arthritis development, the paw circumference (cm) and the paw diameter (mm) of the right hind paw were used as indicators of the rate of swelling and joint edema. Measurements were obtained at various times on days 0, 7, 14, and 21 after CFA induction. The joint diameter was recorded with a micrometer screw gauge [26], while the paw circumference was evaluated by wrapping a string around the paw and then measuring its length on a ruler. Edema and the swelling rate for the CFA rats were compared to those for a normal control group, while those for the treated rats were compared to those for the CFA group. The rats were anesthetized by ether inhalation before measurement.

2.4. Measurement of Anti-CCP and IL-10 Using the ELISA Technique. Serum anti-CCP and IL-10 levels were determined in different groups using specific enzyme-linked immunosorbent assay (ELISA) kits purchased from R&D Systems (R&D Systems, Inc., Minneapolis, MN, USA) according to the manufacturer's instructions.

2.5. Determination of the Expression of Various Genes by RT-PCR. The mRNA expression levels of TNF- α , MMP-9, and iNOS in relation to the housekeeping gene beta-actin (β -actin) were determined using reverse transcription polymerase chain reaction (RT-PCR).

2.5.1. Ribonucleic Acid (RNA) Isolation. The RNA product was extracted totally from ankle joints using the Thermo Sci-

entific GeneJET RNA extraction kit purchased from Thermo Fisher Scientific Inc., Rochester, New York, USA [27]. In liquid nitrogen, samples were homogenized and then lysed using a lysis buffer solution that consists of guanidine thiocyanate and a chaotropic salt which protects RNA from endogenous RNases. The lysate was then mixed with ethyl alcohol and mounted on a purification column. Both the chaotropic salt and the ethyl alcohol made RNA bind to the silica membrane as the lysate is spun through the column. Impurities were subsequently removed away from the membrane by washing the column with a washing buffer solution. Then, pure RNA was eluted with a nuclease-free water reagent in low-ionic strength conditions. And the amount of purified RNA was quantified by using a UV spectrophotometer according to the following formula: $\text{RNA } \mu\text{g}/\mu\text{L} = \text{O.D.}_{260 \text{ nm}} \times (40 \mu\text{g RNA/mL}) \times \text{dilution factor}/1000$. To ensure the high purity of the isolated RNA, we checked the purity of RNA that ranged between 1.8 and 2.0. By the end, 0.5 μg of purified RNA was used for the production of complementary deoxyribonucleic acid (cDNA) that was kept at -20°C, for further assay of the mRNA.

2.5.2. Reverse Transcription Polymerase Chain Reaction (RT-PCR) Analysis. RT-PCR analysis was performed as described in Ahmed et al.'s [22] research work, and the relative expression level of TNF- α , iNOS, and MMP-9 was normalized to the β -actin housekeeping gene. All the primers used in this experiment were synthesized by Sangon Biotech (Shanghai, China) (Table 1).

2.6. Western Blot Analysis. The amount of TGF- β 1 protein was assayed using the Western blot technique. Briefly, we used the ice-cold RIPA lysis buffer to extract the proteins from joint tissue. The Bradford Protein Assay Kit (SK3041) for quantitative protein analysis was provided by Bio Basic Inc. (Markham, Ontario, L3R 8T4, Canada). A Bradford assay was performed according to the manufacturer's instructions to determine protein concentration in each sample. Equivalent amounts (30 μg) of protein were divided using 10% sodium dodecyl sulfate-polyacrylamide gel electrophoresis (SDS-PAGE). Next, the proteins loaded on the gel were shifted onto membranes of polyvinylidene fluoride (PVDF). Then, overnight, the membrane was probed at 4°C with the TGF- β 1-specific primary antibody (cat. no. 9574; Thermo Fisher Scientific). After washing with Tris-buffered saline with Tween 20 (TBST) three times, the blots were prepared for incubation with horseradish peroxidase-conjugated secondary antibodies (1:5000, Santa Cruz Biotechnology, CA) at RT 25°C for 30 minutes. The blots were washed again, and then, the signal of the chemiluminescence was visualized with an X-ray film [22, 28].

2.7. Histopathological Examination. On day 21 of arthritis induction and after euthanization, the right hind leg ankle joints of 4 rats from each group were detached and conserved for 48 hours in 10% buffered formalin. Decalcification of the sample tissues was performed using paraffin blocks with 10% nitric acid for 2 weeks. Finally, 5 μm thick cross sections of these blocks were dyed with hematoxylin-eosin and viewed

TABLE 1: The forward and reverse primer sequences of various mRNA genes.

Gene	Primer sequence	Amplicon size (bp)
β -Actin (housekeeping gene)	F: 5'-TCACCCTGAAGTACCCCATGGAG-3'	151
	R: 5'-TTGGCCTTGGGGTTCAGGGGG-3'	
TNF- α	F: 5'-AAAATCCTGCCCTGTCACAC-3'	323
	R: 5'-GCTGAGGTTGGACGGATAAA-3'	
iNOS	F: 5'-ATGGAACAGTATAAGGCCAAACACC-3'	220
	R: 5'-GTTTCTGGTGCATGTCATGAGCAAAGG-3'	
MMP-9	F: 5'-CTGGGCTTGATGCCTGTTT-3'	331
	R: 5'-TTGTGGTGGTGCCACTTGA-3'	

using a light microscope to determine the histopathological changes and severity of arthritis.

2.8. Statistical Analysis. Statistical tests were performed utilizing IBM SPSS Statistics program version 22.0 (IBM, Armonk, NY, USA). All values were represented as the mean and standard error of the mean (mean \pm SE). Differences among groups were estimated for statistical significance using the one-way analysis of variance (ANOVA) test followed by the Tukey–Kramer post hoc test for comparisons between groups, and $p < 0.05$ was considered the minimal level of significance [29].

3. Results

3.1. Effect of Treatments on Paw Edema. All rats developed arthritis after adjuvant injection. The CFA-induced arthritic rats showed a statistically significant ($p < 0.05$) increase in the paw diameter and circumference (edema) that was maintained for 21 days compared with a normal control group (Figures 1 and 2). However, the arthritic treated rats administered with BM-MSCs and/or IMC showed a significant ($p < 0.05$) decrease in those parameters by the end of the experiment with inhibition percentages of 8.10, 14.83, and 16.30% and 12.07, 14.60, and 13.72% for the paw diameter and circumference, respectively, in comparison with CFA rats.

3.2. Effect of Treatments on Anti-CCP and IL-10 Concentrations. Levels of anti-CCP and IL-10 were detected in serum using a standard ELISA technique (Figures 3 and 4), respectively. Rats immunized with CFA exhibited a significant ($p < 0.05$) increase in the anti-CCP autoantibody (631.71%) but a marked reduction in anti-inflammatory IL-10 cytokine levels (-51.29) compared with the normal control group. Conversely, administration of BM-MSCs, IMC, and BM-MSCs+IMC each, respectively, successfully decreased the anti-CCP level (-75.33, -73.50, and -83.33) and promoted IL-10 production (64.95, 39.55, and 78.43%) as well when compared to the normal group.

3.3. Evaluation of TNF- α , iNOS, and MMP-9 mRNA Expression Level and Protein Level of TGF- β 1 in Ankle Joint Articular Tissues. As represented in Figures 5–7, the TNF- α , MMP-9, and iNOS mRNA expression levels, respectively,

in ankle joint articular tissues, were determined by the PCR technique. The arthritic untreated rats noticeably showed upregulation of their mRNA expression levels as compared to the normal ones. On the other hand, the rats treated with BM-MSCs and/or IMC showed apparent downregulation of their levels. Likewise, the TGF- β 1 protein level was highly elevated in the arthritic group with a change percentage of 512.87% when compared with the normal control. However, the animals treated with BM-MSCs, IMC, and BM-MSCs +IMC, respectively, showed a significant reduction of its level with a change percentage of -56.22%, -51.53%, and -70.92%, respectively, concerning the arthritic control group (Figure 8).

3.4. Effect of Treatments on Gross Lesions (Macroscopic Changes) of the Right Hind Paw and Ankle Joint. Macroscopic changes such as edema and the swelling rate of the right hind paw and ankle joints acted as external features and inflammatory signs for evaluating the arthritic inflammatory model intensity. The CFA control group showed severe inflammation as well as paw and ankle joint swelling; on the other side, both of which gradually decreased following BM-MSC and/or IMC treatments by the end of the experiment (on day 21 post-CFA injection) (Figure 9).

3.5. Histopathological (Microscopic) Changes. Histological sections of the right hind ankle joint obtained from normal rats showed a clear and complete histological architecture with the normal synovial membrane and normal articular (cartilage and bone) surfaces. The CFA-induced arthritic rats exhibited severe histological alterations including focal proliferation and degeneration of the synovial membrane forming the pannus that infiltrated with a massive number of mononuclear inflammatory cells, extensive and widespread erosion in the cartilage surface, and hypercellularity and hyperplasia of myeloid cells of the bone. On the contrary, sections of the CFA-induced arthritic rats treated with BM-MSCs and/or IMC presented highly improved histological configuration with nearly normal cartilage and bone surfaces except for slight inflammation of synovia that was moderate in IMC-treated rats and mild in both groups treated with BM-MSCs and those concurrently administered rats (BM-MSCs+IMC) (Figure 10).

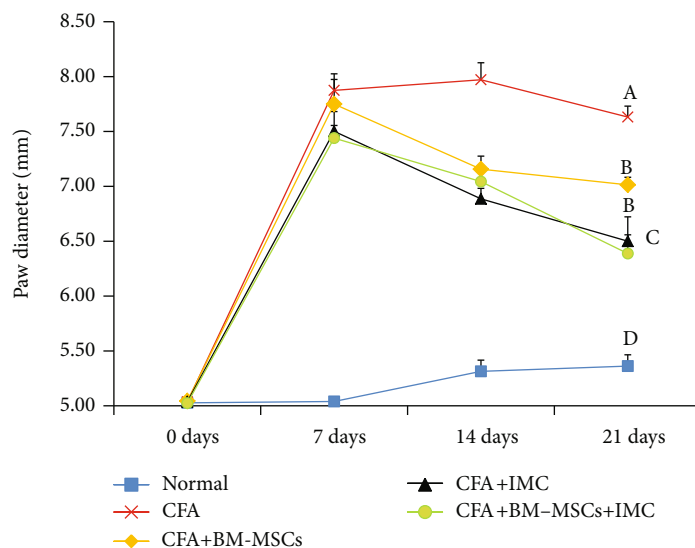


FIGURE 1: Effect of BM-MSCs and/or IMC on the right hind paw diameter (mm) in CFA-induced rats. Means, which have different symbols, A, B, C, and D, are significantly different at $p < 0.05$.

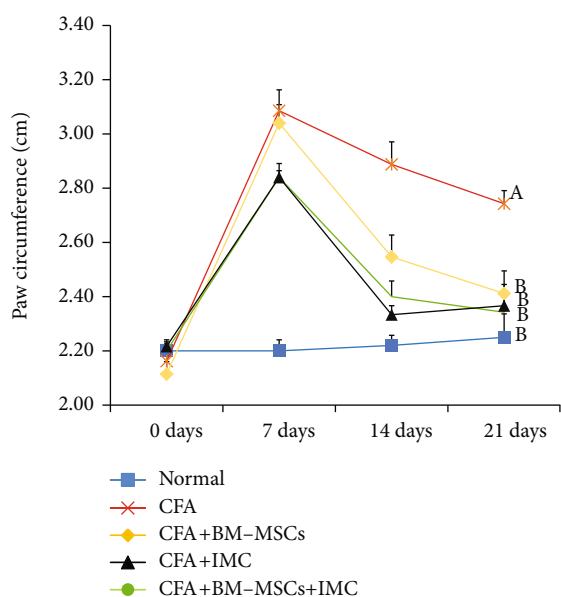


FIGURE 2: Effect of BM-MSCs and/or IMC on the right hind paw circumference (cm) in CFA-induced rats. Means, which have different symbols, A and B, are significantly different at $p < 0.05$.

4. Discussion

RA is regarded as a disabling autoimmune syndrome that is related to long-lasting joint inflammation besides extensive cartilage and bone impairment [30]. CFA is a widely used animal model for both researching pathogenesis and discovering novel therapies to treat RA in humans [31]. In the CFA-induced arthritis model, rats experience persistent swelling in several joints followed by inflammatory cell inflow, joint cartilage degradation, and bone integrity erosion and dysfunction. Herein, the diameter and the circumference of the right hind paw were estimated weekly and for 3 weeks as an index of the joint swelling, subsequently monitoring disease

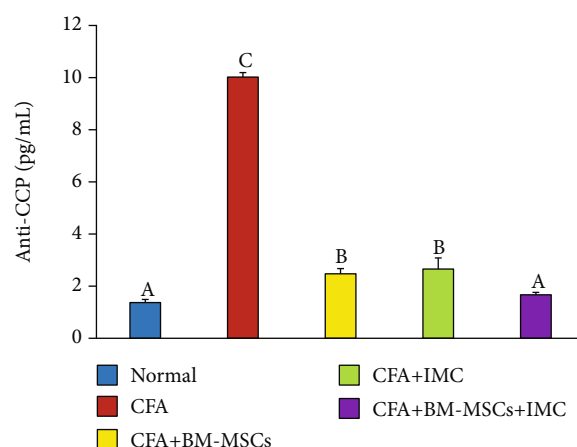


FIGURE 3: Effect of BM-MSCs and/or IMC on anti-CCP concentration in CFA-induced rats. Means, which have different symbols, A, B, and C, are significantly different at $p < 0.05$.

development besides the response to the tested drugs. In complete agreement with the study of Nagai et al. [32], our data displayed that paw edema and swelling reached the maximum on day 7 of arthritis induction in the acute phase (primary inflammation) and gradually declined until day 14 and then began the chronic phase of arthritis (secondary inflammation). By the end of the experiment (3rd week), the arthritic control rats exhibited a significant increase in the paw diameter and circumference comparable to the normal rats. On the contrary, the BM-MSC- and/or IMC-treated rats efficiently inhibited the elevation about the arthritic control rats and were approximated to normal ranges. Consistent with our findings, the study of Porth [33] reported that edema of the right hind foot of adjuvant and arthritic rats immunized with low-dose IMC nanoparticle (0.4 mg/kg) oral administration was significantly lower regarding those immunized with a vehicle. Furthermore, these outcomes

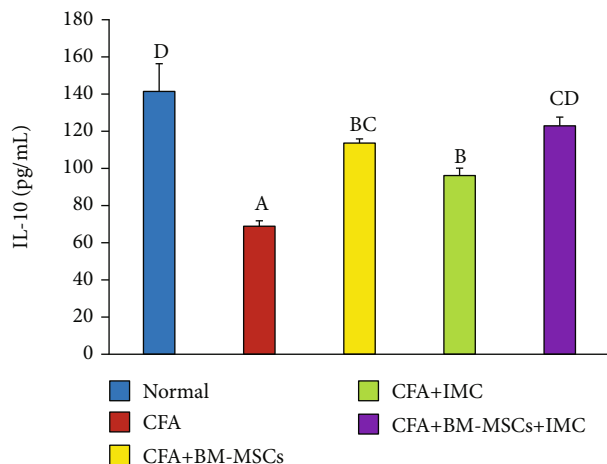


FIGURE 4: Effect of BM-MSCs and/or IMC on IL-10 concentration in CFA-induced rats. Means, which have different symbols, A, B, C, and D, are significantly different at $p < 0.05$.

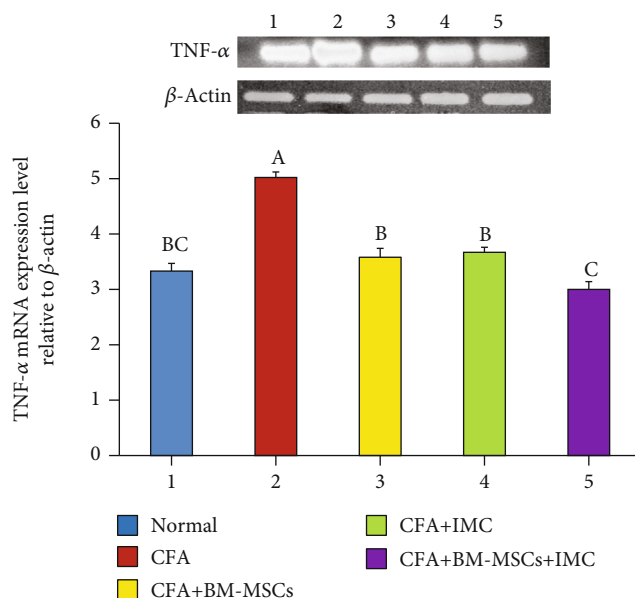


FIGURE 5: Effect of BM-MSCs and/or IMC on the TNF- α expression level relative to β -actin in CFA-induced rats. Means, which have different symbols, A, B, and C, are significantly different at $p < 0.05$.

were strongly supported by the results of biochemical assays and revealed the anti-inflammatory efficacy of the tested drugs against CFA-induced arthritis.

Preceding research papers revealed that RA is initiated chiefly through immunological responses of T cells which induce cytokine release [33] and facilitate the development of autoantibodies, leading to joint destruction. Concerning the autoantibodies formed during the course of the disease, the anticitrullinated protein antibodies (ACPA) are the most common RA biomarker for diagnostics. It is produced as a response to the occurrence of autoantigens, named citrullinated peptides. These autoantigens could prompt local edema and inflammation *via* developing an immune response within the localized region of the joint [6]. Besides,

the presence of ACPA is predictive for the development of a worse disease effect with more joint erosions along with time [34]. The recent investigation demonstrated that the sera of arthritic control rats showed a remarkable increase in the anti-CCP concentration level as compared to the normal group. Principally, the BM-MSC+IMC group besides BM-MSC- and IMC-supplemented rats clearly declined the elevated anti-CCP level compared to the arthritic control rats. Such an anti-CCP level proves the capabilities of the tested agents to modulate immune responses induced in RA, hence recommending them as promising antirheumatic drugs.

Similarly, RA is considered an autoimmune disorder characterized by infiltration of immune cells (monocytes and lymphocytes). These inflammatory cells are deemed substantial in initiating and perpetuating RA as represented in Figure 11; it produces interleukins (ILs), as well as inflammatory mediators such as tumor necrosis factor-alpha (TNF- α), nitric oxide (NO), MMP-9, and prostaglandin E2 (PGE2) [35]. Those mediators are implicated in the inflammatory response and have various roles through many pathways. Therefore, modulating or blocking these pathways became the target of the new therapeutic tested drugs against the disease. In this study, we focused on TNF- α , iNOS, MMPs, and TGF-1 β as originators of inflammation besides IL-10 as an inhibitor of inflammation within tissues.

Specifically, TNF- α is a principal cytokine that induces apoptosis in some cells and proliferative reactions in others and plays a crucial role in both acute and chronic inflammation [36]. It prompts the production of inducible nitric oxide synthase (iNOS) that in turn enhances the release of matrix metalloproteinases (MMPs). MMPs are a family of inflammatory mediators (MMP-3, MMP-13, and MMP-9) responsible for promoting extracellular matrix degradation and cartilage damage [37]. Therefore, when the TNF- α pathway is specifically blocked, the severity of inflammation is accordingly reduced; that is why it became a key therapeutic target to cease the evolution toward the chronic form of the disease [38]. In parallel, transforming growth factor- β 1 (TGF- β 1) is a component of the TGF- β superfamily of cytokines contributing to various cellular responses, such as apoptosis, proliferation, differentiation, and extracellular matrix production [39]. TGF- β 1 is essential for the induction of RA-related fibrosis [40]. On the contrary, a compensatory anti-inflammatory response is also observed in RA synovial membranes. IL-10 is an upstream regulator and anti-inflammatory marker that is thought to control the progression of RA negatively. Several animal model studies of arthritis have illustrated the beneficial impact of IL-10 on reducing arthritis severity [7]. Similar to the explanation displayed in Figure 11 illustrating the IL-10 role in the course of the disease, Hisadome et al. [41] demonstrated that it controls the functioning of APCs and prevents cytokine release from activated macrophages. Also, van Roon et al. [42] established that IL-10 suppresses the production of protein lysing enzymes *via* monocytes that produced the inhibitor of metalloproteinase-1 (TIMP-1). Furthermore, it antagonized osteoclast formation (osteoclastogenesis) by suppressing the production of IL-6 in osteoclast precursors, hence overcoming the bone resorption induced by arthritis [43].

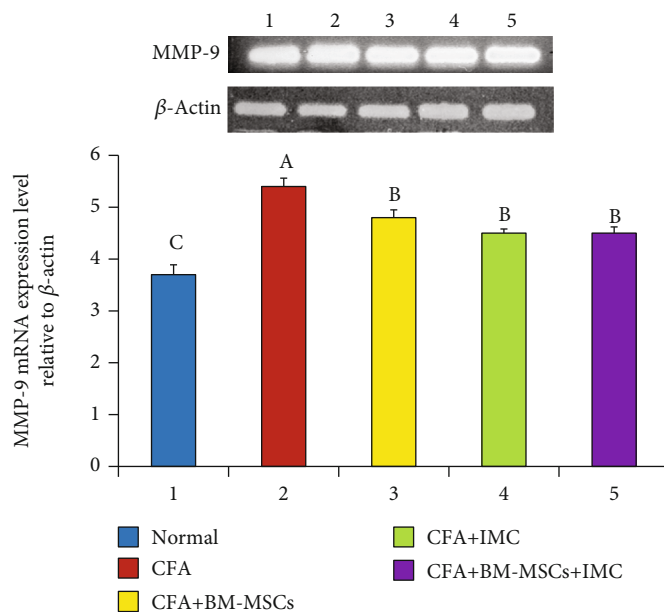


FIGURE 6: Effect of BM-MSCs and/or IMC on the MMP-9 expression level relative to β -actin in CFA-induced rats. Means, which have different symbols, A, B, and C, are significantly different at $p < 0.05$.

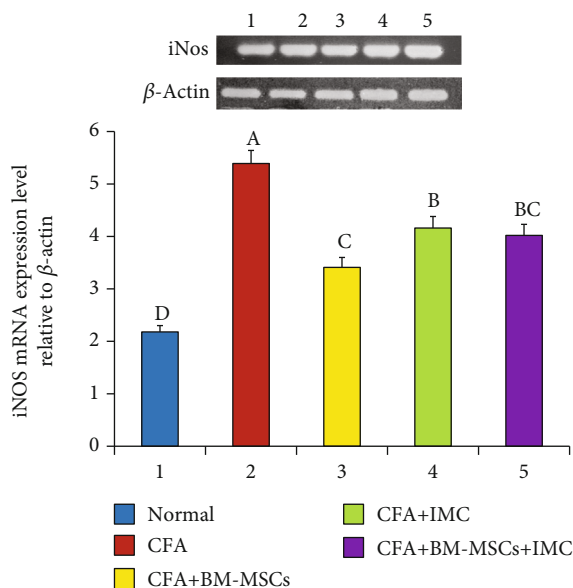


FIGURE 7: Effect of BM-MSCs and/or IMC on the iNOS level mRNA expression relative to β -actin in CFA-induced rats. Means, which have different symbols, A, B, C, and D, are significantly different at $p < 0.05$.

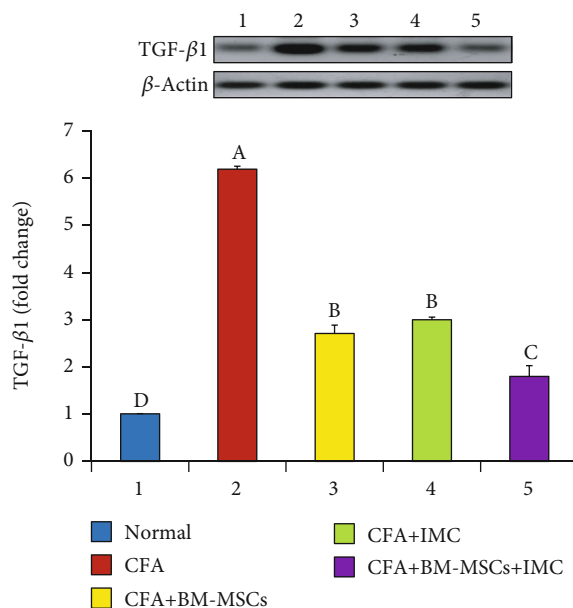


FIGURE 8: Effect of BM-MSCs and/or IMC on the TGF- β 1 level in CFA-induced rats. Means, which have different symbols, A, B, C, and D, are significantly different at $p < 0.05$.

In addition to the former measurements, the anti-inflammatory impact of treatments on the CFA-induced arthritis model was more investigated macroscopically *via* evaluating the gross lesion changes and microscopically by demonstrating the histopathological changes on the right hind paw and ankle joint. Initially, histopathological or microscopic lesions of rats in the CFA control group exhibited an obvious synovial degradation and proliferation accompanied by cartilage erosion and bone mass resorption. Conversely, the BM-MSC-treated arthritic group and BM-

MSC+IMC-treated arthritic group afforded significant protection against those alterations and exhibited a mild stage of inflammation while those supplemented by IMC displayed a moderate stage of inflammation. Correspondingly, the macroscopic lesions displayed intensive edema and paw swelling in the CFA-induced control rats that were interestingly improved in the BM-MSC+IMC-, BM-MSC-, and IMC-treated groups in respect to CFA.

Overall, in the current research, our data demonstrated a marked elevation of the proinflammatory TNF- α cytokine as



FIGURE 9: Effect of BM-MSCs and/or IMC on gross lesions on the right hind leg paw and ankle joint on day 21 post-CFA induction showing (a) normal rats, (b) CFA-induced arthritic control rats, (c) CFA+BM-MSC-treated rats, (d) CFA+IMC-treated rats, and (e) CFA+BM-MSC+IMC-treated rats.

well as the iNOS, MMP-9, and TGF- β 1 gene expression levels in paw tissues of CFA-induced rats; however, the anti-inflammatory IL-10 levels in sera conversely declined as compared with the normal rats. As exhibited schematically in Figure 11, BM-MSC and IMC therapies either concurrently or alone received by the rats essentially downregulated

the reported proinflammatory cytokines whereas promoted evidently the anti-inflammatory cytokine (IL-10) in comparison with the CFA-induced arthritic group. These results illustrated the ability of BM-MSCs and IMC to protect against cartilage and bone destruction, preventing further development of the disease through such immunoregulatory

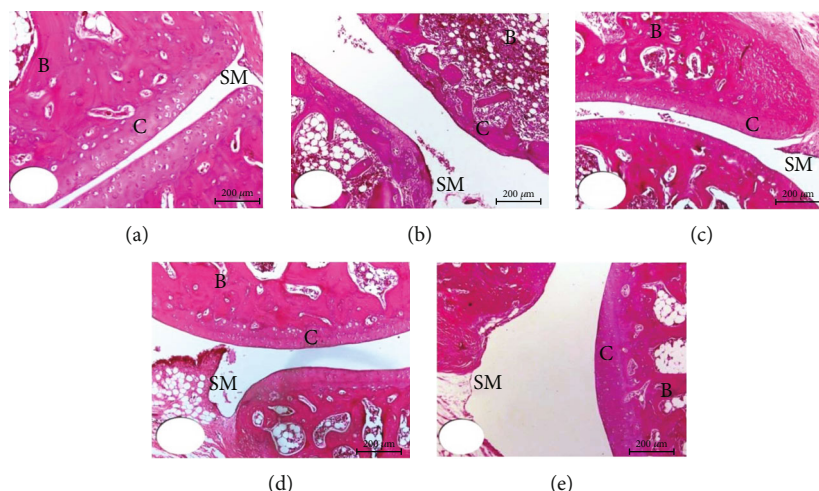


FIGURE 10: Photomicrographs (200x) of HE-stained sections showing the effect of BM-MSCs and/or IMC treatments on the histopathological changes in the ankle joints of CFA-induced arthritic rats. (a) Normal group. (b) CFA-arthritic control group. (c) CFA+BM-MSC-treated group. (d) CFA+IMC-treated group. (e) CFA+BM-MSC+IMC-treated group. SM: synovial membrane; C: cartilage; B: bone.

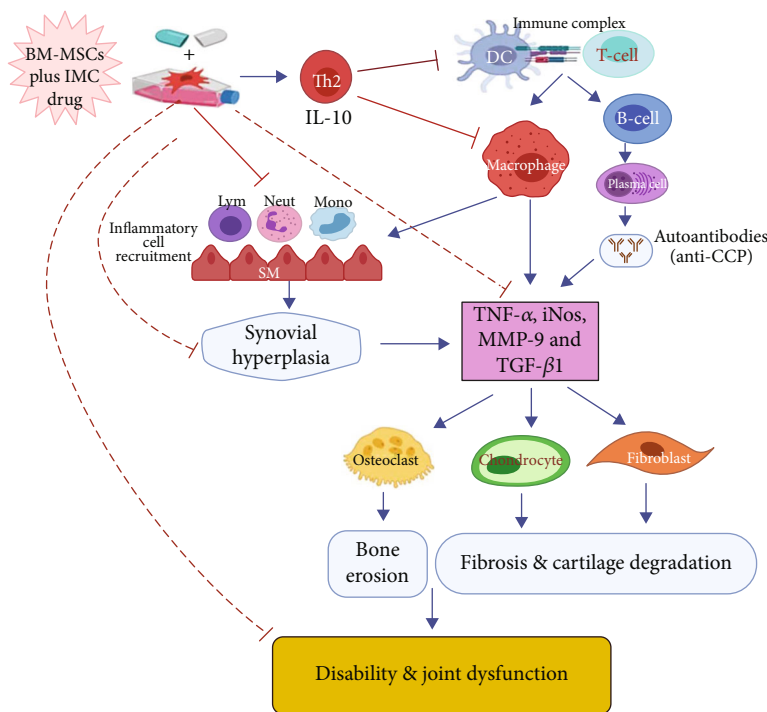


FIGURE 11: Schematic diagram showing the immunomodulatory effect of BM-MSCs+IMC administered concurrently in CFA-induced arthritis. IMC: indomethacin; BM-MSCs: bone marrow-derived mesenchymal stem cells; Th2: T helper 2; DC: dendritic cell; IL-10: interleukin 10; T cell: T lymphocytes; B cell: B lymphocytes; Mono: monocytes; Neut: neutrophils; SM: synovial membrane; iNos: inducible nitric oxide synthase; TGF-β1: transforming growth factor-beta-1; TNF-α: tumor necrosis factor-alpha; anti-CCP: anticyclic citrullinated peptide antibody; MMP-9: matrix metalloproteinase-9.

pathways. In the same regard, the findings of the present study were strongly approved by Abo-Aziza et al. [44] that documented a marked decrease in serum TNF-α levels at week 2 and week 4, respectively, of transplantation with BM-MSC+albendazole (ABZ) therapy, whereas the level of IL-10 was considerably elevated only at week 4 after transplantation. Additionally, our outcomes are inconsistent with

Wei et al. [45] who revealed that BM-MSCs successfully lowered the expression level of TNF-α as well as other inflammatory cytokines in blood and hippocampus tissues. Overall, the results of the current study provide evidence for the successful effects of BM-MSCs and IMC in downregulating Th1 cytokine (TNF-α), iNOS, MMP-9, and TGF-β1 and upregulating Th2 cytokine (IL-10), and all of these effects may have

important roles in relieving the manifestations of the experimentally induced rheumatoid arthritis in Wistar rats (Figure 11).

5. Summary and Conclusion

Generally, all preceding data proved the validity of BM-MSC +IMC as a promising therapy for RA more than each treatment alone. This was evidenced by their effectiveness in inhibiting paw swelling, reducing anti-CCP concentration, downregulating the proinflammatory Th1 cytokine (TNF- α), iNOS, MMP-9, and TGF- β 1, and upregulating the anti-inflammatory Th2 cytokine (IL-10). Th1 cytokine (TNF- α), Th2 cytokine (IL-10), iNOS, MMP-9, and TGF- β 1 are possible targets of BM-MSCs and IMC to mediate the antiarthritic effects in CFA-induced arthritic rats.

Data Availability

The data used to support the findings of this study are available from the corresponding author upon reasonable request.

Conflicts of Interest

The authors declare that they have no competing interests.

Acknowledgments

The authors acknowledged Taif University, Taif, Saudi Arabia, for supporting the study (Taif University Researchers Supporting Project number: TURSP-2020/127).

References

- [1] Q. Fang, C. Zhou, and K. S. Nandakumar, "Molecular and cellular pathways contributing to joint damage in rheumatoid arthritis," *Mediators of Inflammation*, vol. 2020, 20 pages, 2020.
- [2] O. Sangha, "Epidemiology of rheumatic diseases," *Rheumatology*, vol. 39, Supplement 2, pp. 3–12, 2000.
- [3] G. Huang, T. Guan, P. Wang, and S. Qin, "Anti-arthritis effect of baicalein exert on complete Freund's adjuvant-induced arthritis in rats by reducing the inflammatory reaction," *International Journal of Pharmacology*, vol. 15, no. 7, pp. 880–890, 2019.
- [4] J. T. Giles, "Extra-articular manifestations and comorbidity in rheumatoid arthritis: potential impact of pre-rheumatoid arthritis prevention," *Clinical Therapeutics*, vol. 41, no. 7, pp. 1246–1255, 2019.
- [5] A. F. Edrees, S. N. Misra, and N. I. Abdou, "Anti-tumor necrosis factor (TNF) therapy in rheumatoid arthritis: correlation of TNF-alpha serum level with clinical response and benefit from changing dose or frequency of infliximab infusions," *Clinical and Experimental Rheumatology*, vol. 23, no. 4, pp. 469–474, 2005.
- [6] J. M. Berthelot, B. Le Goff, and Y. Maugars, "Bone marrow mesenchymal stem cells in rheumatoid arthritis, spondyloarthritis, and ankylosing spondylitis: problems rather than solutions?," *Arthritis Research and Therapy*, vol. 21, no. 1, p. 239, 2019.
- [7] S. Mateen, S. Moin, S. Shahzad, and A. Q. Khan, "Level of inflammatory cytokines in rheumatoid arthritis patients: correlation with 25-hydroxy vitamin D and reactive oxygen species," *PLoS One*, vol. 12, no. 6, p. e0178879, 2017.
- [8] L. Ouyang, Y. Dan, Z. Shao et al., "Effect of umbelliferone on adjuvant-induced arthritis in rats by MAPK/NF- κ B pathway," *Drug Design, Development and Therapy*, vol. - Volume 13, pp. 1163–1170, 2019.
- [9] A. Gaffo, K. G. Saag, and J. R. Curtis, "Treatment of rheumatoid arthritis," *American Journal of Health-System Pharmacy*, vol. 63, no. 24, pp. 2451–2465, 2006.
- [10] L. Bevaart, M. J. Vervoordeldonk, and P. P. Tak, "Evaluation of therapeutic targets in animal models of arthritis: how does it relate to rheumatoid arthritis?," *Arthritis and Rheumatism*, vol. 62, no. 8, pp. 2192–2205, 2010.
- [11] C. Nasuti, D. Fedeli, L. Bordoni et al., "Anti-inflammatory, anti-arthritis and anti-nociceptive activities of Nigella sativa oil in a rat model of arthritis," *Antioxidants*, vol. 8, no. 9, p. 342, 2019.
- [12] C. Vingsbo, P. Sahlstrand, J. G. Brun, R. Jonsson, T. Saxne, and R. Holmdahl, "Pristane-induced arthritis in rats: a new model for rheumatoid arthritis with a chronic disease course influenced by both major histocompatibility complex and non-major histocompatibility complex genes," *The American Journal of Pathology*, vol. 149, no. 5, pp. 1675–1683, 1996.
- [13] O. M. Ahmed, H. A. Soliman, B. Mahmoud, and R. R. Ghergany, "Ulva lactuca hydroethanolic extract suppresses experimental arthritis via its anti-inflammatory and antioxidant activities," *Beni-Suef University Journal of Basic and Applied Sciences*, vol. 6, no. 4, pp. 394–408, 2017.
- [14] O. M. Ahmed, M. B. Ashour, H. I. Fahim, and N. A. Ahmed, "The role of Th1/Th2/Th17 cytokines and antioxidant defense system in mediating the effects of lemon and grapefruit peel hydroethanolic extracts on adjuvant-induced arthritis in rats," *Journal of Applied Pharmaceutical Science*, vol. 8, no. 10, pp. 69–081, 2018.
- [15] A. Saleem, M. Saleem, M. F. Akhtar, M. Shahzad, and S. Jahan, "Polystichum braunii extracts inhibit complete Freund's adjuvant-induced arthritis via upregulation of I- κ B, IL-4, and IL-10, downregulation of COX-2, PGE2, IL-1 β , IL-6, NF- κ B, and TNF- α , and subsiding oxidative stress," *Inflammopharmacology*, vol. 28, no. 6, pp. 1633–1648, 2020.
- [16] R. A. Contreras, F. E. Figueroa, F. Djouad, and P. Luz-Crawford, "Mesenchymal stem cells regulate the innate and adaptive immune responses dampening arthritis progression," *Stem Cells International*, vol. 2016, Article ID 3162743, 10 pages, 2016.
- [17] K. Le Blanc and D. Mouggiakakos, "Multipotent mesenchymal stromal cells and the innate immune system," *Nature Reviews Immunology*, vol. 12, no. 5, pp. 383–396, 2012.
- [18] A. L. Blobaum, M. J. Uddin, A. S. Felts, B. C. Crews, C. A. Rouzer, and L. J. Marnett, "The 2'-trifluoromethyl analogue of indomethacin is a potent and selective COX-2 inhibitor," *ACS Medicinal Chemistry Letters*, vol. 4, no. 5, pp. 486–490, 2013.
- [19] A. L. Blobaum and L. J. Marnett, "Structural and functional basis of cyclooxygenase inhibition," *Journal of Medicinal Chemistry*, vol. 50, no. 7, pp. 1425–1441, 2007.
- [20] A. Munjal and A. E. Allam, *Indomethacin*, StatPearls Publishing, Treasure Island, FL, USA, 2021, <https://www.ncbi.nlm.nih.gov/books/NBK555936>.

- [21] S. Khan, F. N. K. Yusufi, and A. N. K. Yusufi, "Comparative effect of indomethacin (IndoM) on the enzymes of carbohydrate metabolism, brush border membrane and oxidative stress in the kidney, small intestine and liver of rats," *Toxicology Reports*, vol. 6, pp. 389–394, 2019.
- [22] E. A. Ahmed, O. M. Ahmed, H. I. Fahim et al., "Combinatory Effects of Bone Marrow-Derived Mesenchymal Stem Cells and Indomethacin on Adjuvant-Induced Arthritis in Wistar Rats: Roles of IL-1 β , IL-4, Nrf-2, and Oxidative Stress," *Evidence-Based Complementary and Alternative Medicine*, vol. 2021, Article ID 8899143, 15 pages, 2021.
- [23] T. A. Mohamed and M. F. Abouel-Nour, "Therapeutic effects of bone marrow stem cells in diabetic rats," *Journal of Computer Science & Systems Biology*, vol. 9, no. 2, 2015.
- [24] J. K. Chaudhary and P. C. Rath, "A simple method for isolation, propagation, characterization, and differentiation of adult mouse bone marrow-derived multipotent mesenchymal stem cells," *Journal of Cell Science & Therapy*, vol. 8, no. 1, 2016.
- [25] O. M. Ahmed, M. A. Hassan, and A. S. Saleh, "Combinatory effect of hesperetin and mesenchymal stem cells on the deteriorated lipid profile, heart and kidney functions and antioxidant activity in STZ-induced diabetic rats," *Biocell*, vol. 44, no. 1, pp. 27–29, 2020.
- [26] S. S. Chaudhari, S. R. Chaudhari, and M. J. Chavan, "Analgesic, anti-inflammatory and anti-arthritic activity of *Cassia uniflora* Mill.," *Asian Pacific Journal of Tropical Biomedicine*, vol. 2, no. 1, pp. S181–S186, 2012.
- [27] P. CHOMZYNSKI, "Single-step method of RNA isolation by acid guanidinium thiocyanate–phenol–chloroform extraction," *Analytical Biochemistry*, vol. 162, no. 1, pp. 156–159, 1987.
- [28] J. Chu, X. Wang, H. Bi, L. Li, M. Ren, and J. Wang, "Dihydromyricetin relieves rheumatoid arthritis symptoms and suppresses expression of pro-inflammatory cytokines via the activation of Nrf2 pathway in rheumatoid arthritis model," *International Immunopharmacology*, vol. 59, pp. 174–180, 2018.
- [29] N. Gözel, M. Çakirer, A. Karataş et al., "Sorafenib reveals anti-arthritic potentials in collagen induced experimental arthritis model," *Arch. Rheumatol.*, vol. 33, no. 3, pp. 309–315, 2018.
- [30] E. Silvagni, A. Giollo, G. Sakellariou et al., "One year in review 2020: novelties in the treatment of rheumatoid arthritis," *Clinical and experimental rheumatology*, vol. 38, no. 2, pp. 181–194, 2020.
- [31] V. Kelly and M. Genovese, "Novel small molecule therapeutics in rheumatoid arthritis," *Rheumatology*, vol. 52, no. 7, pp. 1155–1162, 2013.
- [32] N. Nagai, T. Fukuhata, Y. Ito, S. Usui, and K. Hirano, "Involvement of interleukin 18 in indomethacin-induced lesions of the gastric mucosa in adjuvant-induced arthritis rat," *Toxicology*, vol. 255, no. 3, pp. 124–130, 2009.
- [33] C. Porth, "White blood cell response," in *Essentials of Pathophysiology: Concepts of Altered Health States*, pp. 64–65, Wolters Kluwer/Lippincott Williams & Wilkins, 2011.
- [34] M. A. M. van Delft and T. W. J. Huizinga, "An overview of autoantibodies in rheumatoid arthritis," *Journal of Autoimmunity*, vol. 110, 2020.
- [35] A. T. Peana, F. Bennardini, L. Buttu et al., "Effect of simulated microgravity on PGE2-induced edema and hyperalgesia in rat paws: pharmacological data and biochemical correlates," *Journal of gravitational physiology*, vol. 11, no. 2, 2004.
- [36] G. Pentón-Rol, M. Cervantes-Llanos, G. Martínez-Sánchez et al., "TNF- α and IL-10 downregulation and marked oxidative stress in neuromyelitis optica," *Journal of Inflammation*, vol. 6, no. 1, p. 18, 2009.
- [37] Z. Szekanecz, M. M. Halloran, M. V. Volin et al., "Temporal expression of inflammatory cytokines and chemokines in rat adjuvant-induced arthritis," *Arthritis and Rheumatism*, vol. 43, no. 6, pp. 1266–1277, 2000.
- [38] J. C. Shanahan, L. W. Moreland, and R. H. Carter, "Upcoming biologic agents for the treatment of rheumatic diseases," *Current Opinion in Rheumatology*, vol. 15, no. 3, pp. 226–236, 2003.
- [39] S. M. Wahl, "Transforming growth factor- β : innately bipolar," *Current Opinion in Immunology*, vol. 19, no. 1, pp. 55–62, 2007.
- [40] D. Pohlers, J. Brenmoehl, I. Löffler et al., "TGF- β and fibrosis in different organs – molecular pathway imprints," *Biochimica et Biophysica Acta - Molecular Basis of Disease*, vol. 1792, no. 8, pp. 746–756, 2009.
- [41] M. Hisadome, T. Fukuda, H. Sumichika, T. Hanano, and K. Adachi, "A novel anti-rheumatic drug suppresses tumor necrosis factor- α and augments interleukin-10 in adjuvant arthritic rats," *European Journal of Pharmacology*, vol. 409, no. 3, pp. 331–335, 2000.
- [42] J. A. G. van Roon, F. P. J. G. Lafeber, and J. W. J. Bijlsma, "Synergistic activity of interleukin-4 and interleukin-10 in suppression of inflammation and joint destruction in rheumatoid arthritis," *Arthritis & Rheumatism*, vol. 44, no. 1, pp. 3–12, 2001.
- [43] M. H. Hong, H. Williams, C. H. Jin, and J. W. Pike, "The inhibitory effect of interleukin-10 on mouse osteoclast formation involves novel tyrosine-phosphorylated proteins," *Journal of Bone and Mineral Research*, vol. 15, no. 5, pp. 911–918, 2000.
- [44] F. A. M. Abo-Aziza, A. K. A. Zaki, and A. M. Abo El-Maaty, "Bone marrow-derived mesenchymal stem cell (BM-MSC): a tool of cell therapy in hydatid experimentally infected rats," *Cell Regen.*, vol. 8, no. 2, pp. 58–71, 2019.
- [45] Y. Wei, Z. Xie, J. Bi, and Z. Zhu, "Anti-inflammatory effects of bone marrow mesenchymal stem cells on mice with Alzheimer's disease," *Experimental and Therapeutic Medicine*, vol. 16, no. 6, pp. 5015–5020, 2018.

Review Article

Research Progress on Stem Cell Therapies for Articular Cartilage Regeneration

Shuangpeng Jiang ^{1,2} **Guangzhao Tian** ^{1,3} **Xu Li**² **Zhen Yang**^{1,3} **Fuxin Wang**¹ **Zhuang Tian**¹ **Bo Huang**¹ **Fu Wei**¹ **Kangkang Zha**^{1,3} **Zhiqiang Sun**^{1,3} **Xiang Sui**¹ **Shuyun Liu** ¹ **Weimin Guo** ^{1,4} and **Quanyi Guo** ¹

¹*Institute of Orthopedics, The First Medical Center, Chinese PLA General Hospital, Beijing Key Lab of Regenerative Medicine in Orthopedics, Key Laboratory of Musculoskeletal Trauma and War Injuries PLA, No. 28 Fuxing Road, Haidian District, Beijing 100853, China*

²*Department of Orthopedics, The First Hospital of China Medical University, 155 Nanjing North Street, Heping District, Shenyang 110001 Liaoning Province, China*

³*School of Medicine, Nankai University, Tianjin 300071, China*

⁴*Department of Orthopedic Surgery, First Affiliated Hospital, Sun Yat-sen University, Guangzhou, Guangdong, China*

Correspondence should be addressed to Shuyun Liu; clear_ann@163.com, Weimin Guo; guowm5@mail.sysu.edu.cn, and Quanyi Guo; doctorguo_301@163.com

Received 25 September 2020; Revised 11 January 2021; Accepted 28 January 2021; Published 12 February 2021

Academic Editor: Liang Gao

Copyright © 2021 Shuangpeng Jiang et al. This is an open access article distributed under the Creative Commons Attribution License, which permits unrestricted use, distribution, and reproduction in any medium, provided the original work is properly cited.

Injury of articular cartilage can cause osteoarthritis and seriously affect the physical and mental health of patients. Unfortunately, current surgical treatment techniques that are commonly used in the clinic cannot regenerate articular cartilage. Regenerative medicine involving stem cells has entered a new stage and is considered the most promising way to regenerate articular cartilage. In terms of theories on the mechanism, it was thought that stem cell-mediated articular cartilage regeneration was achieved through the directional differentiation of stem cells into chondrocytes. However, recent evidence has shown that the stem cell secretome plays an important role in biological processes such as the immune response, inflammation regulation, and drug delivery. At the same time, the stem cell secretome can effectively mediate the process of tissue regeneration. This new theory has attributed the therapeutic effect of stem cells to their paracrine effects. The application of stem cells is not limited to exogenous stem cell transplantation. Endogenous stem cell homing and in situ regeneration strategies have received extensive attention. The application of stem cell derivatives, such as conditioned media, extracellular vesicles, and extracellular matrix, is an extension of stem cell paracrine theory. On the other hand, stem cell pretreatment strategies have also shown promising therapeutic effects. This article will systematically review the latest developments in these areas, summarize challenges in articular cartilage regeneration strategies involving stem cells, and describe prospects for future development.

1. Introduction

Articular cartilage is an important weight-bearing tissue of synovial joints. Due to the lack of blood vessels, nerves, and lymphatic vessels and the restriction of the dense extracellular matrix (ECM) on cartilage cells, the self-healing ability of articular cartilage after injury is very limited. If left untreated, damage to articular cartilage can lead to osteoarthritis (OA) [1]. OA has a high incidence and disability rate, affecting

250 million patients worldwide [2]. Unfortunately, none of the cartilage repair techniques currently in clinical use can completely regenerate hyaline cartilage [3].

Stem cells are an important milestone in the field of tissue engineering and regenerative medicine. Stem cell therapy is considered to be a promising method to solve the regeneration of articular cartilage [4, 5]. A large number of preclinical and clinical studies have shown that compared with traditional repair techniques such as microfractures, stem cell

therapy can form more typical hyaline cartilage and can better control symptoms [6–8]. On the other hand, compared with autologous chondrocytes, stem cells have a wider source and stronger ability to expand *in vitro*, which makes tissue-engineered cartilage involving stem cells more advantageous than tissue-engineered cartilage involving autologous chondrocytes. Tissue engineering strategies involving stem cells involve the implantation of exogenous stem cells and homing of endogenous stem cells to achieve cartilage regeneration *in situ*. The basis of the exogenous stem cell implantation strategy is finding suitable types of stem cells. Mesenchymal stem cells (MSCs) derived from various tissues are currently the most studied tissue engineering articular cartilage seed cell type [9]. Embryonic stem cells (ESCs) have the potential to differentiate into any cell type, but due to ethical disputes, ESCs are in only the preclinical experimental stage. Induced pluripotent stem cells (iPSCs) can theoretically be obtained by reprogramming any type of terminally differentiated cell, removing limitations of the cell source and reducing ethical disputes, thus becoming a new type of seed cell that is gradually emerging. However, stem cell transplantation also poses the risk of tumorigenesis, immune rejection, disease transmission, and the functional heterogeneity of cells from different individuals [10–13].

In this review, we first introduced the two main theories of stem cell-mediated articular cartilage regeneration and then reviewed the application of exogenous stem cell implantation strategies and endogenous stem cell homing and *in situ* cartilage regeneration strategies. Second, we reviewed the research progress of stem cell pretreatment strategies, derivatives, and delivery scaffolds. Finally, we summarized problems in stem cell research related to articular cartilage regeneration and looked toward the future directions of this field.

2. Theories on Cartilage Regeneration Involving Stem Cells

As immature tissue precursor cells, stem cells can self-renew and have the ability to form clonal cell populations and differentiate into multiple cell lineages [14]. These special properties are particularly attractive for restoring the functions of a variety of organs. At present, stem cells can be divided into three general categories: (1) ESCs derived from early embryos, (2) iPSCs, and (3) adult stem cells, including hematopoietic stem cells, neural stem cells, and MSCs. A large number of studies have confirmed the beneficial role of stem cells in the regeneration of articular cartilage, and their potential mechanisms are mainly divided into two theories (Figure 1): the first is the “differentiation theory,” which states that stem cells directly differentiate into chondrocytes and repair damaged cartilage by adding or replacing chondrocytes [15]. The other is the “paracrine theory,” in which stem cells secrete bioactive factors, extracellular vesicles (EVs), and ECM [16], changing the biological behavior of receptor cells (including endogenous stem cells, chondrocytes, and macrophages), such as proliferation, differentiation, migration, polarization, metabolism, and apoptosis, and regulating the local microenvironment to repair and regenerate articular cartilage. Early studies focused on the

direct differentiation and replacement of stem cells. In recent years, there has been an increasing amount of evidence that the therapeutic benefits of stem cells may be attributed to their paracrine effects.

2.1. Differentiation Theory. From the perspective of chondrogenesis, cartilage formation begins with mesenchymal condensation, which causes MSCs to differentiate into cartilage. Then, a dense matrix forms, which serves as a template for the subsequent formation of subchondral bone and cartilage [17]. In addition, a large number of studies have indicated that MSCs maintain pluripotency after repeated proliferation cycles *in vitro* and can differentiate into matrix-producing chondrocytes [18, 19]. Based on these findings, most previous studies attributed the role of stem cells in regenerating articular cartilage to their ability to differentiate into multiple lineages [20, 21]. A large number of studies focused on the development of materials and methods to induce stem cells to differentiate into cells with a chondrocyte phenotype [22]. Abir and colleagues demonstrated that autologous MSCs that were intra-articularly injected differentiated into mature chondrocyte-like cells [23]. This conclusion strongly supports this theory. Researchers suspended donkey autologous bone marrow-derived MSCs (BMSCs) labeled with green fluorescent protein (GFP) in hyaluronic acid (HA) for intra-articular injections in an attempt to treat wrist OA induced by amphotericin B. The results of up to 6 months of follow-up showed that the intra-articular injection of autologous BMSCs combined with HA resulted in an improved therapeutic effect compared with that of HA injections alone. GFP-labeled MSCs were detected in all the examined articular cartilage. Some cells showed a chondrocyte-like phenotype (round and surrounded by cavities), which proved that the injected MSCs differentiated into chondrocytes. To further verify this conclusion, similar work in a dog knee cartilage defect model also proved that injected MSCs differentiated into mature chondrocytes [24]. The same results were obtained in a study by Kotaka et al., who found that human iPSCs can repair knee cartilage defects in nude mice. The immunofluorescence of antihuman mitochondrial antibodies was found in newborn chondrocytes, which suggested that implanted iPSCs differentiated into chondrocytes [25]. In a recent study in a rat KOA model, researchers injected fluorescein-labeled human adipose-derived MSCs (ADSCs) into the articular cavity and found that the injected cells had a good therapeutic effect on OA. The existence of human cells in the rat meniscus and cartilage was confirmed by immunohistochemistry with antihuman mitochondria and antihuman Ki67 antibodies, and some of the cells were in the proliferative phase [26]. Although this study did not explore whether injected cells differentiated into mature chondrocytes, the fluorescence signal in OA rats lasted for approximately 10 weeks, which at least indicated that the implanted stem cells could be retained in the articular cavity for a long time. The above studies provide strong evidence for the “differentiation theory” of stem cells.

2.2. Paracrine Theory. Researchers have long known that the conditioned medium (CM) of stem cells can promote cell

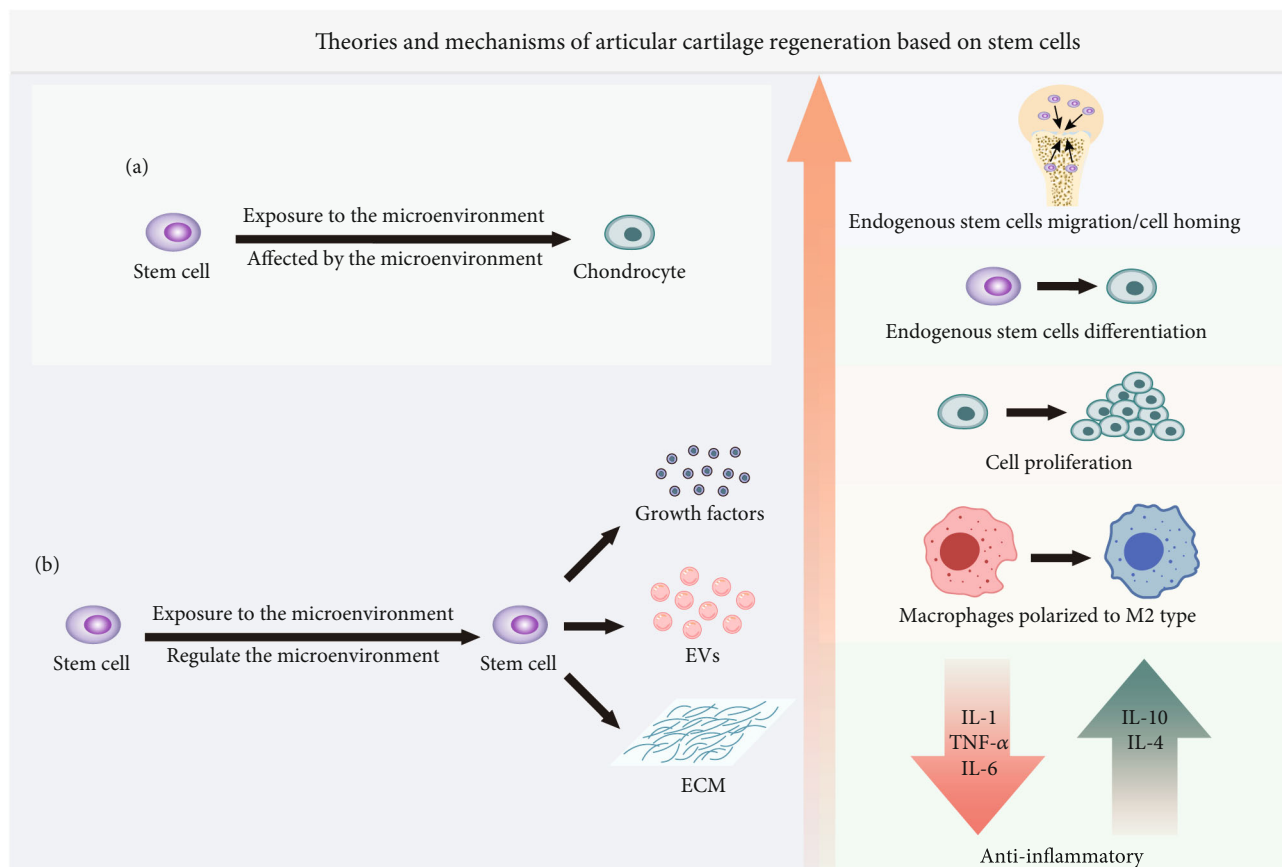


FIGURE 1: Two theories of articular cartilage regeneration involving stem cells. (a) Stem cell differentiation theory. Stem cells are affected by the microenvironment and directly differentiate into chondrocytes. (b) Paracrine theory of stem cells. Stem cells are affected by the microenvironment and secrete various derivatives, including growth factors, EVs, and ECM. These derivatives have been proven to induce homing of endogenous stem cells, promote the differentiation of endogenous stem cells into chondrocytes, promote the proliferation of chondrocytes, induce macrophages to polarize to the M2 type, and regulate the level of inflammatory factors to exert anti-inflammatory effects. EVs: extracellular vesicles; ECM: extracellular matrix.

proliferation and differentiation *in vitro* and can promote tissue repair and regeneration *in vivo* [27]. It has been shown that stem cells secrete many cytokines and proteins. The synergistic effect of small molecules secreted by MSCs can reduce cell damage and improve the repair ability of tissue [28]. Second, the immunomodulatory effect of stem cells has been increasingly reported. Stem cells can regulate the immune microenvironment during the process of tissue repair and provide a good environment for tissue regeneration [29]. MSCs in the immune microenvironment can promote chondrogenesis through immune regulation [30]. At the same time, a large number of studies on the coculture of MSCs and chondrocytes *in vitro* have proven that paracrine signaling is an important feature of MSCs [31–33]. The nutritional function of MSCs has led researchers to increasingly regard them as therapeutic delivery agents, and it has been recommended to rename them “medicinal signaling cells” [34]. Their paracrine signaling drives the endogenous response [35]. On the other hand, some *in vitro* studies [36–38] found that the differentiation of MSCs is not as strong as originally thought, and it is difficult to achieve stable and effective differentiation. Especially in the case of differentiation into chondrocytes, the progres-

sion of stem cells to terminal hypertrophy is a frustrating problem [39]. Early *in vivo* follow-up studies showed that few cells can survive for more than a few weeks after implantation [40, 41]. A recent clinical study described the ultimate results of stem cell implantation. Tommy et al. implanted allogeneic MSCs into full-thickness femoral cartilage defects. After a 12-month repair period, histological samples were examined, and no allogeneic MSC DNA was detected in the repaired tissue. This indicated that implanted MSCs provided the initial stimulation but then died and were cleared from the tissue [42]. The above studies suggest that the function of stem cells in tissue repair and regeneration is mediated by active components secreted by stem cells rather than by their direct differentiation into target cells.

At present, the mechanism of stem cell-mediated cartilage regeneration is still unclear, and the above theory provides some insights. The complete regeneration process may be coordinated by multiple mechanisms, and stem cells may play different roles in different stages of the actual repair process. The precise control of the changing roles of stem cells may be an effective way to achieve the desired regeneration effect.

3. Cartilage Regeneration Strategies Involving Stem Cells

Stem cells used for tissue engineering and cell therapy are usually obtained from four basic sources: (1) embryonic tissue; (2) fetal tissue, such as fetus, amniotic fluid, and umbilical cord (Wharton jelly, blood); (3) a specific location in adult organisms (such as fat, bone marrow, and synovium); and (4) somatic cells after genetic reprogramming, i.e., iPSC [43, 44]. Among the sources of stem cells, adipose tissue seems to be the most promising choice. It has many unparalleled advantages. Specifically, adipose tissue is available in relatively high quantity in many patients and can be collected by “waste tissue” produced by surgical procedures (such as liposuction or abdominal plastic surgery), which can effectively solve problems with local morbidity, safety, and ethical issues. Moreover, compared with other tissues, adipose tissue produces a large number of living stem cells. Studies have shown that ADSCs in lipoaspiration account for 2% of nuclear cells, and the output per gram of adipose tissue is approximately 5000 fibroblast colony forming units (CFU-F). In contrast, the production of bone marrow MSCs (BMSCs) is only 100–1000 CFU-F/ml bone marrow [45]. Due to the tissue diversity and individual differences of MSC sources, the MSC population has obvious heterogeneity. Adult MSCs have obvious differences in their cartilage differentiation ability due to their different inherent tissue sources. Studies have compared adult MSCs derived from different tissues, and the results show that MSCs derived from joint synovium (SMSCs) have the strongest cartilage differentiation ability, which may be determined by their inherent cell characteristics and growth characteristics [46]. Researchers found high expression of proline arginine-rich end leucine-rich repeat protein (PRELP) in SMSCs, which is a glycoprotein rich in cartilage, but little or no content in stem cells outside the joints [47]. In addition, SMSCs remained multidirectional in 10 generations *in vitro*, and cell senescence was limited [48]. However, the acquisition of synovium is accompanied by invasive operation of the joint cavity, and the source of synovium is limited, which greatly limits the application of SMSCs. Compared with cells isolated from adult tissues, embryonic or neonatal-derived stem cells are characterized by faster proliferation and more passages *in vitro* before aging [49]. There is no study to compare the chondrogenic differentiation ability of neonatal/ESCs and adult stem cells, but studies have shown that single-cell-derived colonies of marrow stromal cells contained three morphologically distinct cell types: spindle-shaped cells, large flat cells, and very small round cells, and the small cells had a greater potential for multipotential differentiation [50].

With the development of high-throughput analysis technology, the heterogeneity of stem cells has become more obvious at the genetic molecular level [51]. Cell surface molecules that may be markers of stem cell pluripotency have been identified including but not limited to CD34 [52], CD146 [53], and CD49f [54]. Animal experiments show that CD146⁺ ADSCs can inhibit the inflammation of the joint cavity and promote the regeneration of articular cartilage [55]. Although no studies have confirmed the special role of

CD34 and CD49f-specific stem cells in cartilage regeneration, the beneficial effects of CD34⁺ stem cells on cardiac repair and regeneration have been confirmed [56]. Studies have also found that the CM of CD34⁺ stem cells contains 32 soluble factors related to cell proliferation, survival, tissue repair, and wound healing, which can promote liver repair and regeneration *in vivo* [57]. MSCs with high expression of CD49f play an important role in the maintenance of hair follicle epithelial cells [58]. Directly implanting exogenous stem cells into joint cavities or articular cartilage defects seems to be the most direct stem cell application strategy. However, the strategy of stem cell homing and *in situ* regeneration was the first to be applied. Its history can even be traced back to 1959. Pridie [59] reported for the first time the subchondral bone drilling method used to treat cartilage injury. The bone marrow (containing BMSCs) was drained to the cartilage defect to form a blood clot, and then, cartilage tissue formed. However, there was no concept of “homing” stem cells at that time. This chapter will discuss these two strategies in detail.

3.1. Exogenous Stem Cell Implantation Strategy. We searched for studies applying exogenous stem cell implantation strategies to treat articular cartilage defects or OA on PubMed from the past 4 years (2017–2020) and summarized the representative studies in Table 1 (animal experiments) and Table 2 (clinical research). According to the search results, most studies showed good therapeutic effects. Most of the animal models used in animal experiments involved rats, rabbits, pigs, sheep, and horses. The pathological process of OA in these quadrupeds may be quite different from that in humans. One study used a model of OA in primates (rhesus monkeys) [60]. Encouragingly, the results of this study showed that both xenogenic ESC-derived MSCs (EMSCs) and allogeneic BMSC transplantation had therapeutic effects on knee joint OA in rhesus monkeys, and the results were better than those in the control group. There are relatively few clinical studies, and there are only 2 clinical studies with a large sample (more than 100 cases) [61, 62]. In terms of the follow-up time, the evaluation time for animal experiments ranged from 3 weeks to 64 weeks. The shortest follow-up time for a clinical study was 6 months, and the longest follow-up time was more than 36 months. Because articular cartilage is in an ischemic and hypoxic environment that relies on only synovial fluid to supply nutrients, the regeneration of articular cartilage often takes a long time [63]. Therefore, long-term follow-up has more reference value. In terms of the stem cell dose, the single dose used in most studies was 10^6 – 10^7 cells. Although a higher number of cells would theoretically increase the number of successful stem cell transplants, there may be a plateau, beyond which the results will not continue to improve. For example, a study by Wu et al. confirmed that the intravenous injection of 1×10^6 MSCs improved the neurological function of rats with brain injury, but increasing the dose to 3×10^6 cells did not lead to a greater improvement in function [64]. In addition, some studies have shown that the repeated delivery of stem cells can have a better therapeutic effect [65], and no serious adverse events, such as tumorigenesis, were found during

TABLE 1

Cell types	References	Animal model	Carrier/scaffold material/delivery method	Groups	Cell source	Single dose	Transplant number	Time point (W)	Conclusion
BMSCs	Lang Li [70]	Canines (n = 24) Full-thickness cartilage defects	HA Intra-articular injection	(1) HA (2) BMSCs+HA (3) Control: saline	Allogeneic	1 × 10 ⁷	1	28	BMSCs+HA can regenerate articular cartilage better than HA alone.
	Wu et al. [71]	Rabbits (n = 24) Osteochondral defect	PBS Intra-articular injection	(1) BMSCs (2) PRFr (3) BMSCs+PRFr (4) Control: untreated	Autologous	3 × 10 ⁶	2	12	The BMSCs+PRFr group had better results in histological evaluation and GAG production. MSCs-primed+LRS improved clinical symptoms and reduced synovial inflammation, but there was no significant difference from the control group.
	Barrachina et al. [72]	Equine (n = 18) Chemically induced OA	LRS Intra-articular injection	(1) MSCs-primed+LRS (2) MSCs-naive+LRS (3) Control: LRS	Allogeneic	1 × 10 ⁷	2	8 and 24	
	Vayas et al. [73]	Rabbits (n = 36) Full-thickness cartilage defects	PLGA microspheres dispersed in a pluronic F-127 solution Intra-articular injection	(1) MF (2) MSCs (3) BMP (3) (4) MF-BMP (3) (5) MSCs-BMP (3) (6) BMP (12) (7) MF-BMP (12) (8) MSCs-BMP (12) (9) Control: untreated	Allogeneic	2.5 × 10 ⁵	1	12 and 24	Compared with MF, BMP-2 and MSCs repaired articular cartilage defects better and were less invasive.
	Xia et al. [66]	Pigs (n = 6) Bilateral medial meniscectomy-induced OA	SPIO nanoparticles Intra-articular injection	(1) SPIO-BMSCs (2) Control: untreated	Allogenic	1 × 10 ⁷	4	11	The treatment effect of the MSC group was not significantly different from that of the control group.
	Jiang et al. [74]	Rats (n = 60) Cartilage defect	PCL-PTHF Cell-scaffold construct implantation	(1) PCL-PTHF with rat tail-derived collagen nanofibers+BMSCs (2) PCL-PTHF with chondroitin sulfate (3) Control: untreated	Allogenic	3.14 × 10 ⁵	1	4 and 8	The PCL-PTHF with rat tail-derived collagen nanofiber group showed better chondrogenesis potential <i>in vitro</i> and <i>in vivo</i> .

TABLE 1: Continued.

Cell types	References	Animal model	Carrier/scaffold material/delivery method	Groups	Cell source	Single dose	Transplant number	Time point (W)	Conclusion
ADSCs	Kohli et al. [75]	Athymic nude rats ($n = 15$) Osteochondral defect	Alpha Chondro Shield Cell-scaffold construct implantation	(1) PA MSCs+Alpha Chondro Shield	Xenogenic (human)	5×10^4	1	3	CD271+ADSCs had a stronger ability to promote cartilage regeneration <i>in vivo</i> .
				(2) CD271 ⁺ MSCs+Alpha Chondro Shield					
	Li et al. [55]	Rabbits ($n = 60$) Cartilage defect	AECM scaffold Cell-scaffold construct implantation	(3) Control: Alpha Chondro Shield	Xenogenic (human)	5×10^5	1	12 and 24	CD146+ ADSCs promoted better cartilage regeneration than that in the control group.
				(1) ADSCs+scaffold					
				(2) CD146 ⁺ ADSCs+scaffold					
Mei et al. [76]	Rats ($n = 60$) ACLT-induced OA	PBS Intra-articular injection	(3) Scaffold	Allogenic	1×10^6	1	8 and 12	ADSCs had anti-inflammatory effects and inhibited articular cartilage degeneration.	
			(4) Positive control: sham-operated						
Mei et al. [76]	Rats ($n = 60$) ACLT-induced OA	PBS Intra-articular injection	(5) Negative control: untreated	Allogenic	1×10^6	1	8 and 12	ADSCs had anti-inflammatory effects and inhibited articular cartilage degeneration.	
			(1) ADSCs+PBS						
Crichtley et al. [77]	Caprine ($n = 14$) Osteochondral defect	3D-printed PCL alginate hydrogel biphasic scaffold Cell-scaffold construct implantation	(2) Control: PBS	Allogenic	3×10^6 ADSCs+ 1×10^6 chondrocytes	1	24	The biphasic constructs regenerated hyaline cartilage <i>in vivo</i> .	
			(1) The biphasic constructs						
Yan et al. [78]	Mice ($n = 20$) Bovine type II collagen-induced OA	PBS Intra-articular injection	(2) Matrogen scaffolds (Finceramica)	Xenogenic (human)	1×10^6	3	10	SMSCs prevented arthritis development and suppressed immune responses.	
			(1) SMSCs+PBS						
Kondo et al. [79]	Pigs ($n = 13$) Full-thickness osteochondral defects	No carrier or scaffold MSC aggregate implantation	(2) Control: PBS	Autologous	4×10^6	1	4 and 12	Autologous synovial MSC aggregates promoted articular cartilage regeneration <i>in vivo</i> .	
			(1) MSC aggregates						
Neybecker et al. [80]	Nude rats ($n = 48$) ACLT-induced OA	Saline Intra-articular injection	(2) Control: untreated	Xenogenic (human)	1×10^6	2	4 and 8	Xenogenic SFMSCs exerted neither chondroprotection nor inflammation in ACLT-induced OA.	
			(1) SFMSCs+ saline						
Neybecker et al. [80]	Nude rats ($n = 48$) ACLT-induced OA	Saline Intra-articular injection	(3) Control: sham + saline	Xenogenic (human)	1×10^6	2	4 and 8	Xenogenic SFMSCs exerted neither chondroprotection nor inflammation in ACLT-induced OA.	
			(1) SFMSCs+ saline						

TABLE 1: Continued.

Cell types	References	Animal model	Carrier/scaffold material/delivery method	Groups	Cell source	Single dose	Transplant number	Time point (W)	Conclusion
UCBMSCs/WJMSCs	Li et al. [81]	Rats ($n = 30$) Full-thickness cartilage defects	Hyperbranched poly-PEGDA/HA hydrogel Injected into the cartilage defect site	(1) AFF-MSCs/hydrogel (2) Hydrogel (3) Control: PBS	Xenogeneic (human)	1×10^6	1	4 and 8	The composite material significantly repaired articular cartilage defects. The cell-scaffold constructs maintained the integrity of subchondral bone and regenerated hyaline cartilage.
	Zhang et al. [6]	Goats ($n = 6$) Full-thickness cartilage defects	AECM scaffold Cell-scaffold construct implantation	(1) MSCs+ scaffold (2) MF	Xenogeneic (human)	1×10^6	1	24 and 36	WJMSC composite ECM scaffold regenerated hyaline cartilage <i>in vivo</i> . Undifferentiated WJMSCs had a better repair effect.
	Liu et al. [82]	Rabbits ($n = NS$) Full-thickness cartilage defects	ECM scaffold Cell-scaffold construct implantation	(1) hWJMSCs-scaffold (2) hWJMSCs-C-scaffold (3) Scaffold (4) Control: untreated	Xenogeneic (human)	NS	1	12, 24, 28, and 64	At 6 weeks, the therapeutic effect of the HA+MSCs group was significantly better than that of other groups, but there was no significant difference between the groups at 12 weeks.
	Xing et al. [83]	Rats ($n = 18$) ACLT and medial meniscectomy-induced OA	HA Intra-articular injection	(1) HA+MSCs (2) HA (3) Control: saline	Xenogeneic (human)	1×10^6	1	6 and 12	Both the chondropellets and the chondrocytes derived from iPSCs had therapeutic effects on osteochondral defects.
iPSCs	Rim et al. [84]	Rats ($n = NS$) Full-thickness cartilage defects	hiChondroPellet group: no carrier or scaffold Transplant directly to the defect site hiChondrocytes group: PBS Injected into the cartilage defect site	(1) hiChondroPellet (2) hiChondrocytes+PBS (3) Defect control: untreated (4) Normal control	Xenogeneic (human)	hiChondroPellets or 1×10^6 hiChondrocytes	1	8	Both the chondropellets and the chondrocytes derived from iPSCs had therapeutic effects on osteochondral defects.
	Kotaka et al. [25]	Nude rats ($n = 54$) Full-thickness cartilage defects	Atelocollagen Transplant directly to the defect site by an external magnetic field	(1) Magnetic force+iPS+ atelocollagen (2) iPS+ atelocollagen (3) Control: atelocollagen	Xenogeneic (human)	1×10^5	1	4, 6, and 8	The histological score of the treatment group was significantly better than that of the control group.

TABLE 1: Continued.

Cell types	References	Animal model	Carrier/scaffold material/delivery method	Groups	Cell source	Single dose	Transplant number	Time point (W)	Conclusion
ESCs/EMSCs	Jiang et al. [60]	Rhesus macaques ($n = 8$) Spontaneous OA	Saline Intra-articular injection	(1) EMSCs (2) BMSCs (3) Control: saline	EMSC group: xenogeneic (human) BMSC group: allogeneic	5×10^6	3	4, 8, 12, 16, 24, and 36	The degrees of joint swelling and imaging examination results in the EMSC group and BMSC group were significantly improved.
	Gibson et al. [85]	Nude rats ($n = 15$) Cartilage defects	No carrier or scaffold Transplant MSC pellets directly to the defect site	(1) MSC pellets (untreated) (2) MSC pellets (pretreated with BMP-2 and Wnt5a) (3) Control: empty defects	Xenogeneic (human)	2.5×10^5	1	4 and 8	Cartilage progenitor cell particles derived from hESCs pretreated with BMP-2 and Wnt5a induced hyaline cartilage regeneration <i>in vivo</i> .

TABLE 2

Cell types	References	Cell source	Single dose	Transplant number	K-L grade	Age	Sample size	Carrier/scaffold material	Follow-up (M)	Conclusion
BMSCs/BMACs	Chahal et al. [86]	Autologous	1×10^6 1×10^7 5×10^7	1	III-IV	40-65	12	Excipient	12	The clinical symptoms significantly improved in the 5×10^7 cell group. BMACs relieved pain caused by OA. However, at 12 months, BMACs had no significant advantage compared with saline.
	Shapiro et al. [87]	Autologous	5 mL BMAC (1.7×10^5 cells)	1	I-III	42-68	25	Platelet-poor bone marrow plasma	12	BMSCs significantly relieved the pain of patients with OA.
	Emadedin et al. [88]	Autologous	4×10^7	1	II-IV	18-65	43	Saline +2% human serum albumin	6	BMSCs alleviated clinical symptoms, but their efficacy at 12 months was not significantly different from that of the placebo.
ADSCs	Shadmanfar et al. [89]	Autologous	4×10^7	1	II-IV	18-65	30	Saline	12	HTO combined with ADSCs improved IKDC and Lysholm scores in patients with OA.
	Kim and Koh [61]	Autologous	4.26×10^6	1	III-IV	53-65	100	NS	At least 36	Autologous ADSCs were safe and significantly improved the symptoms of OA. The effect of repeated injections of high-dose cells was more obvious.
	Song et al. [65]	Autologous	1×10^7 2×10^7 5×10^7	3	\geq II	40-70	14	NS	24	HTO+autologous MSCs+ allogeneic cartilage implantation more effectively treated OA.
	Kim et al. [67]	Autologous	4.7×10^6	1	III-IV	42-68	70	Allogenic cartilage (MegaCartilage) or fibrin glue (Greenplast kit®)	27.6	

TABLE 2: Continued.

Cell types	References	Cell source	Single dose	Transplant number	K-L grade	Age	Sample size	Carrier/scaffold material	Follow-up (M)	Conclusion
UCBMSCs/WJMSCs	Sadlik et al. [68]	Allogenic	NS	1	NS	NS	5	Porcine type I/II collagen matrix scaffold (Chondro-Gide)	12	WJMSCs can be used to induce articular cartilage regeneration.
	Matas et al. [90]	Allogenic	2×10^7	2	I-III	40-65	26	Saline with 5% AB plasma	13	Repeated injection of WJMSCs was safe and significantly improved the clinical symptoms of OA.
	Song et al. [62]	Allogenic	2.5×10^6 cells/cm ²	1	I-III	>40	128	4% HA (CARTISTEM®)	24	Allogenic UCBMSCs significantly reduced the pain of OA joints and improved joint function.
ESCs or PLMSCs	Khalifeh Soltani et al. [91]	Allogenic	$5 - 6 \times 10^7$	1	II-IV	35-75	20	NS	6	Allogenic PLMSCs relieved the symptoms of OA joints.

BMAC: bone marrow aspiration and concentration; SMSCs/SFMSCs: synovial-derived mesenchymal stem cells/synovial fluid-derived mesenchymal stem cells; UCBMSCs/WJMSCs: umbilical cord blood-derived mesenchymal stem cells/umbilical cord Wharton's jelly derived mesenchymal stem cells; iPSCs: induced pluripotent stem cells; ESCs/EMSCs: embryonic stem cells/ESC-derived mesenchymal stem cells; LRS: lactate's ringier solution; MF: microfracture; SPIO: superparamagnetic iron oxide; PAMSCs: plastic adherent MSCs; AECM: articular cartilage extracellular matrix; HTO: high tibial osteotomy; RA: rheumatoid arthritis; WOMAC: the Western Ontario and McMaster Universities Arthritis Index; VAS: visual analog scale; PLMSCs: placenta-derived MSCs; PCL-PTHF: electrospun nanofibers composed of cartilage matrix components (collagen or chondroitin sulfate) and poly(ϵ -caprolactone)-polytetrahydrofuran; NS: not specified; PRFr: platelet-rich fibrin releasate; K-L grade: Kellgren-Lawrence grade.

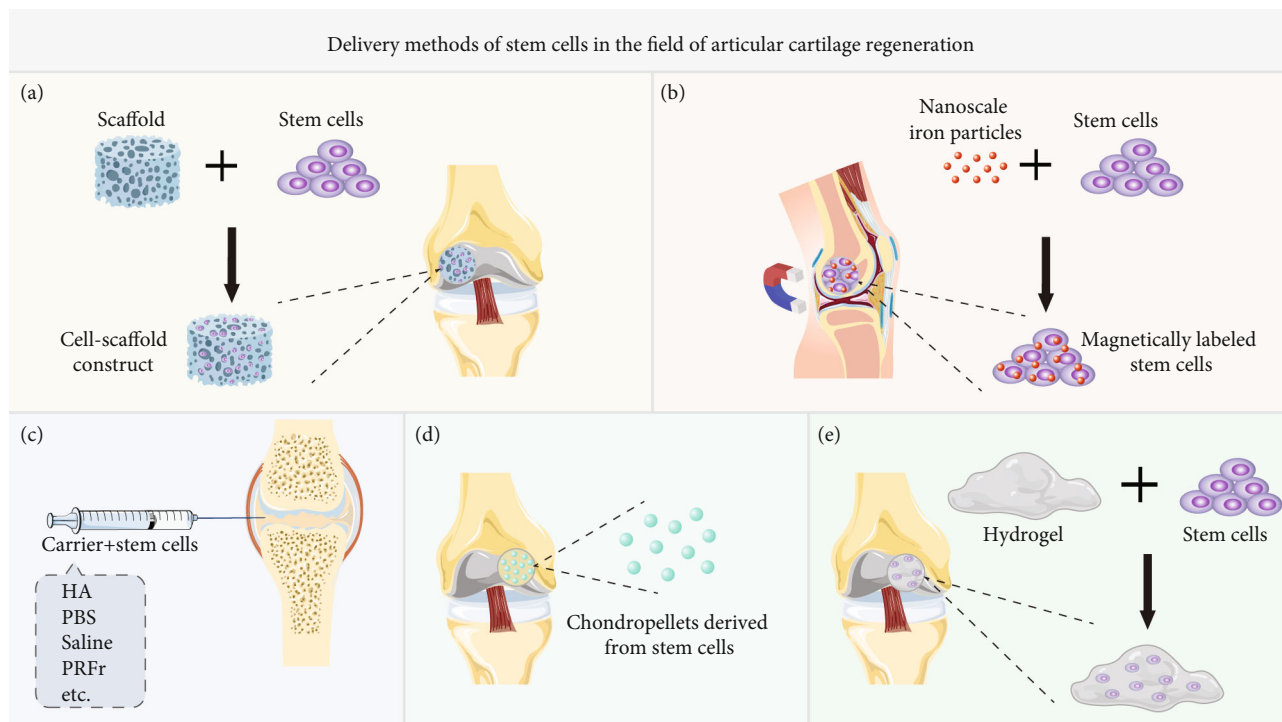


FIGURE 2: Stem cell delivery for repairing articular cartilage defects or treating OA. (a) Cell-scaffold construct. Stem cells are planted on a tissue engineering scaffold, cultured *in vitro* until the cells adhere to the scaffold, and then, the cell-scaffold construct is implanted into the cartilage defect. (b) Magnetic targeting. Place a magnet on the back of the cartilage defect (popliteal fossa), use nanoiron particles to label stem cells, and then implant the stem cells into the cartilage defect. Under the attraction of the magnet, the stem cells are tightly fixed to the bottom of the cartilage defect. (c) Intra-articular injection. The stem cells are resuspended in hyaluronic acid (HA), phosphate-buffered saline (PBS), physiological saline or platelet-rich fibrin releasate (PRFr), and other carriers and then injected into the joint cavity. (d) Chondrocyte pellets. The stem cells are cultured and differentiated *in vitro* to form cartilage pellets, and then, the cartilage pellets are implanted into the cartilage defect. (e) Cell-hydrogel construct. The stem cells are mixed into the injectable hydrogel material, and then, the cell-hydrogel construct is injected into the cartilage defect.

the 2-year follow-up. However, increased treatment costs, tedious cell culture and expansion procedures, and potential infection risks are problems that cannot be ignored. The delivery mode of stem cells determines the success rate of stem cell transplantation to some extent. We summarize the commonly used delivery methods in Figure 2. Because of the lack of blood vessels in articular cartilage, it is difficult to deliver drugs through the intravenous or arterial system. Most studies directly inject stem cells into the articular cavity, usually using normal saline, phosphate-buffered saline (PBS), or HA as cell carriers. After the direct injection of stem cells into the articular cavity, it is impossible to accurately target the area of cartilage injury. Although studies by Xia et al. [66] and others have shown that superparamagnetic iron oxide-labeled BMSCs gather at the location of cartilage defects after injection into the articular cavity, the practicability of the technique needs to be further verified. Magnetic targeted delivery and cell-scaffold constructs may solve this problem, but magnetic targeted delivery is still in the preclinical research stage [25], and the long-term effect of magnetic iron particles on cell and tissue regeneration is unclear. The cell-scaffold construct strategy has been used in the clinic. According to the search results, three commercial scaffold products have been used [62, 67, 68]. This may be due to the incomplete supervision and management policies of var-

ious countries on cell products, especially stem cell products, which restricts the translation of related products into clinical practice. Although there are still few commercial products of stem cell-scaffold constructs at present, commercial products of autologous chondrocyte-scaffold constructs have been widely used, and their therapeutic effects are ideal [69]. We have reason to believe that stem cells with stronger proliferation and differentiation ability have better application prospects.

A large amount of clinical follow-up evidence has proven that MF, cartilage transplantation, ACI, etc., can regenerate fibrocartilage, but the long-term treatment effects are not good. An increasing number of scholars have attempted to combine stem cell transplantation with these traditional repair methods. Song et al. [62] combined human umbilical cord blood-derived MSC transplantation with MF, and Kim et al. [67] combined autologous ADSC transplantation with allogeneic cartilage transplantation (MegaCartilage, particulate allogeneic cartilage, L&CBio, Seoul, KR), which significantly improved the clinical symptoms of OA patients. These results provide a reference for the combined use of stem cells and traditional cartilage repair techniques.

However, the limitations of exogenous stem cell implantation strategies cannot be ignored, such as the risk of tumorigenesis, the risk of disease transmission, the risk of immune

rejection, and the restrictions on stem cell regulatory policies in different countries.

3.2. Stem Cell Homing and In Situ Regeneration Strategy. The term “homing” was first proposed by Gallatin et al. [92] in 1983. It was first used to describe the phenomenon in which lymphocytes in circulating blood tend to migrate to the sites that they were originally derived from, such as lymph nodes, which is referred to as “lymphocyte homing,” and then was gradually extended to stem cells. The term has recently been used to emphasize the ability of stem cells to respond to extracellular signals, such as migration stimuli and guidance cues, for targeted transport and migration [93]. Most tissues initiate the recruitment of stem cells to a certain extent when they are injured or inflamed, which promotes the homing of stem cells to the damaged area and exerts the potential for a variety of repair types, including ECM reconstruction and microenvironment regulation [94, 95]. Recruited stem cells can come directly from the stem cell pool of the tissue around the injury or be recruited from the circulatory system. As endogenous stem cells/progenitor cells do not need to be cultured and expanded *in vitro* and there is no risk of immunogenicity and disease transmission, researchers have focused on *in situ* cartilage regeneration by triggering endogenous stem cells/progenitor cells to undergo “homing” [96].

To enhance the homing behavior of stem cells, researchers tested the following strategies.

3.2.1. Artificially Increasing the Concentration of Chemokines in the Injured Site. For example, the stromal cell-derived factor (SDF-1)/CXCR4 signaling pathway has been shown to play a key role in endogenous stem cell homing [97, 98]. Zhang et al. successfully repaired part of a thickness cartilage defect in a rabbit knee joint with a type I collagen scaffold containing SDF-1 and confirmed that increasing the concentration of chemokines at the injured site promoted the homing of endogenous stem cells and mediated cartilage regeneration [99]. In another recent study, researchers embedded transforming growth factor β 1 (TGF- β 1) in photocrosslinked glycidyl methacrylate (GM-HPCH) to repair articular cartilage defects in rats. The results showed that compared with GM-HPCH alone, GM-HPCH+TGF- β 1 could repair cartilage defects more effectively through its ability to recruit stem cells [100]. In similar studies, increases in interleukin 8 (IL-8) and macrophage inflammatory protein 3 α (MIP-3 α) were shown to promote stem cell homing to articular cartilage injury sites and mediate articular cartilage regeneration [101].

3.2.2. Increasing the Number of Stem Cells in the Damaged Local Microenvironment. For example, MF can stimulate and release BMSCs. Min and others demonstrated that the MF channel caused by the hollow cone is more unobstructed than that caused by a traditional blunt cone and can mobilize more BMSCs to the location of a cartilage defect [102]. Baboolal et al. stirred joint synovium with a special stem cell mobilization device (StemDevice) for 1 minute and collected joint cavity lavage fluid for cell culture. Compared with ordinary cytological brushes, this stem cell mobilization device

greatly increased the number of synovial stem cells in the lavage fluid [103]. Encouragingly, both of these techniques have been applied in the clinic, and both are arthroscopic-assisted operations with the advantages of being minimally invasive.

3.2.3. Construct Scaffolds Conducive to Stem Cell Homing, Adhesion, Proliferation, and Differentiation. For example, Sun et al. combined self-assembled peptide nanofiber hydrogels (RAD/SKP) with acellular cartilage matrix (DCM) scaffolds. It was confirmed in animal experiments that the DCM-RAD/SKP functional scaffold system significantly promoted the recruitment of endogenous stem cells and regenerated hyaline cartilage [104].

It is worth noting that at present, many studies are not limited to the application of one of these strategies, but a variety of strategies can be combined to improve the repair effect. In a recent study, researchers first used 3D-bioprinting technology to construct a silk fibroin-gelatin composite scaffold (SFG), which had a porous structure suitable for cell adhesion and good mechanical strength. The scaffold was then combined with a BMSC-specific affinity peptide (E7), which was shown to have the ability to recruit BMSCs. In the rabbit knee articular cartilage defect model, the SFG-E7 composite scaffold was combined with MF. After 24 weeks, the cartilage defect was completely filled, and the new tissue had obvious characteristics of hyaline cartilage [105]. The research team modified the acellular porcine peritoneal matrix (APM) scaffold with the E7 polypeptide, which had good biocompatibility and a surface suitable for cell growth. The combined application of the APM-E7 scaffold and MF greatly enhanced the recruitment of endogenous stem cells and regenerated rabbit knee cartilage [106].

Endogenous stem cell recruitment and *in situ* regeneration strategies also face many limitations. The biologically active ingredients used to recruit stem cells often require high synthesis techniques and conditions. At the same time, in order to exert a sustained recruitment effect, the delivery materials need to have a slow-release function.

4. Stem Cell Pretreatment Strategy

The microenvironment of damaged articular cartilage is adverse, with inflammation, hypoxia, and insufficient blood supply. In addition, most stem cells used in clinical applications come from adults, and the functions of these cells are compromised. The above factors lead to a very low survival rate of transplanted cells [107], and the use of stem cells for cartilage regeneration has not yet achieved the desired effect. Studies have shown that pretreatment is an effective way to enhance the ability of stem cells to resist adverse microenvironments. Stem cell pretreatment can improve cell survival and differentiation potential, regulate the immune response, inhibit fibrosis, and enhance cell secretion of anti-inflammatory factors. These effects promote the regeneration and functional recovery of organs and tissues after cell implantation [108, 109]. Stem cell pretreatment strategies reported in the field of cartilage regeneration mainly include the following aspects:

4.1. Hypoxia. In natural cartilage, cells are exposed to very low oxygen pressure: approximately 7% (53 mmHg) in the superficial area and only 1% (5-8 mmHg) in the deep area [110]. Hypoxic pretreatment not only enhances the survival and migration ability of stem cells after implantation but also promotes the proliferation and differentiation of stem cells [111]. Under the same conditions for cartilage-induced differentiation, compared with MSCs without hypoxia pretreatment, MSCs with hypoxia pretreatment have been shown to enhance matrix deposition and reduce the expression of hypertrophy markers such as type X collagen [112]. Additionally, hypoxic pretreatment can also upregulate genes related to growth, cell signaling, metabolism, and cellular stress response pathways [113]. In a rabbit knee joint trauma and focal early OA model, hypoxia-pretreated MSC+HA hydrogel caused a significant improvement in the cartilage repair score [114]. The mechanism through which hypoxia affects cells is mainly regulated by HIF-1. The latest evidence shows that HIF-1 α promotes cartilage matrix gene expression and upregulation and that HIF-3 α can help stabilize the cartilage phenotype. In contrast, HIF-2 α upregulates hypertrophy genes and matrix-degrading enzymes [112]. Some studies have explored the specific mechanism of hypoxia that regulates HIF. Studies have shown that hypoxia can induce an increase in phosphorylated AKT and p38 MAPK to stabilize HIF-1 α [115], resulting in the upregulation of the glucose-6-phosphate transporter and an increase in the MSC survival rate [116].

4.2. Pharmacological or Chemical Agents. The use of pharmacological or chemical reagents to protect stem cells and improve the effect of stem cells on cartilage regeneration is another pretreatment strategy. For example, vitamin E pretreatment can make MSCs resistant to H₂O₂-induced oxidative stress, upregulate the expression of proliferation markers and transforming growth factor- β (TGF- β), and downregulate the expression of apoptosis-related genes. After the above pretreatment, MSCs increased the content of proteoglycan in the cartilage matrix in a surgically induced OA rat model, upregulated a chondrogenesis marker, and promoted the differentiation of MSCs into cartilage [117]. Kartogenin (KGN) has been proven to be a chondrogenesis and cartilage protective agent that is more effective in inducing cartilage regeneration than growth factors [118]. Jing and colleagues found that KGN pretreatment may improve the chondrogenesis and differentiation of human WJMSCs by promoting human WJMSCs to enter the prechondral phase, enhancing JNK phosphorylation and inhibiting β -catenin [119]. A recent study found that EVs derived from human WJMSCs pretreated with KGN contain a unique miRNA, miR-381-3p. Researchers found that miR-381-3p directly inhibited TAOK1 by targeting the 3' untranslated region of TAOK1, thus inhibiting the Hippo signaling pathway and mediating cartilage formation [120].

4.3. Trophic Factors and Cytokines. The interaction between specific nutritional factors and their receptors can activate downstream signal transduction and promote cell survival and differentiation. Therefore, the pretreatment of stem cells

with nutritional factors and cytokines is a promising strategy for improving the therapeutic effect of stem cells. Stem cells pretreated with FGF-2 have been shown to have an enhanced proliferation ability and to retain the potential to differentiate into cartilage after 30 population doublings, while stem cells that were not pretreated lost their ability to differentiate into cartilage after approximately 20 doublings [121]. The pretreatment of stem cells with specific growth factors can promote their chondrogenic differentiation potential and their ability to repair cartilage defects *in vivo* [111]. For example, pretreatment with an appropriate concentration of IL-1 β can not only promote proliferation but also enhance the chondrogenic potential of synovial MSCs. However, high concentrations of IL-1 β adversely affected synovial MSCs by reducing their adhesion and pluripotency [122]. BMSCs pretreated with soluble IL-6R effectively repaired articular cartilage defects *in vivo* [123].

4.4. Physical Factors. Articular cartilage is a load-bearing tissue, so mechanical stimulation is very important for the development and maintenance of articular cartilage. A 3D culture model can mimic the natural growth state of cells *in vivo*, provide enough space for stem cell proliferation, and produce more biochemical and biomechanical clues by providing intensive cell-to-cell interactions. Therefore, with these advantages, a variety of physical factors can be applied to the 3D microenvironment *in vitro* or *in vivo* to improve the performance of stem cells [124]. For example, Zhang et al. found that radial shock waves not only significantly improved the proliferation and self-renewal ability of MSCs *in vitro* but also safely promoted the repair cartilage defects by MSCs *in vivo* [125]. The articular cartilage matrix contains a large amount of collagen type II (COLII), and the expression of the SOX9 gene is positively correlated with COLII. Continuous low-intensity ultrasound pretreatment upregulated SOX9 gene expression and enhanced the nuclear localization of SOX9 protein in MSCs compared with control stimulation by discontinuous low-intensity ultrasound [126]. In addition, a new method involves combining cells with carriers/scaffolds before physical stimulation. To date, researchers have designed different types of cell carriers with appropriate physical and chemical properties for cell transplantation, such as injectable hydrogels, large scaffolds, microcarriers, and microspheres [127]. Cheng et al. loaded BMSCs onto an autologous platelet-rich fibrin (PRF) membrane scaffold and applied hydrostatic pressure to the cell-scaffold construct before transplantation. The results showed that the cell scaffold pretreated by hydrostatic pressure significantly increased the formation rate and matrix content of new cartilage and enhanced its mechanical properties [128].

4.5. Genetic Modification. A large number of studies have genetically engineered stem cells to reduce their tendency to differentiate into a hypertrophic phenotype or to induce the overexpression of transcription factors and growth factors to promote the formation of new cartilage *in vivo* [129, 130]. The overexpression of specific growth factors before implantation is a controllable and effective way to improve the efficacy of stem cell therapy. Genes for specific factors

can be introduced into cells by nonviral or viral techniques. For example, compared with simple cellular or acellular scaffolds, BMSCs overexpressing TGF- β 1 can be implanted into polylactic acid (PLA) scaffolds to achieve good cartilage tissue repair in a rabbit knee osteochondral defect model [131]. With regard to the specific progress of gene modification in cartilage repair, please refer to relevant reviews [129, 130].

There are still few *in vivo* animal experiments on stem cell pretreatment strategies, and there is currently a lack of standard protocols. The optimal length and dosage of stem cells need to be explored in depth. At the same time, it is necessary to clarify the molecular mechanism of physical, chemical, and genetic processing methods to promote cartilage regeneration.

5. Composition and Characteristics of Stem Cell Derivatives for Cartilage Regeneration

Stem cell derivatives are an extension of the paracrine theory of stem cells (Figure 1), in which the secretome is considered to be the mechanism through which stem cells exert their tissue repair and regeneration effects [132]. The secretome is a general term for bioactive factors and EVs secreted from the cell to the extracellular space. The secretome of cells is specific but changes in physiological or pathological conditions that directly affect it [133]. Bioactive factors include growth factors, cytokines, chemokines, and enzymes [134]. EVs are considered an important component of the therapeutic efficacy of MSCs. According to the size, composition, and origin of EVs, they can be divided into three types: apoptotic bodies, microvesicles, and exosomes [135, 136]. There are relatively few studies on apoptotic bodies, which are generated only during apoptosis, have a diameter of 50-5000 nm, and carry nuclear fragments and organelles. Microvesicles are small vesicles with a diameter of 50-1000 nm released by cells in the form of budding, which can be obtained by 10,000-20,000 g centrifugation. Exosomes are formed by the multivesicular endosomal pathway and are usually a complex of proteins, nucleic acids, and lipids with a diameter of 50-200 nm that can be obtained from very high-speed centrifugation at or above 100,000 g. Although stem cells have become powerful tools for clinical applications, they still have limitations in terms of delivery, safety, and the heterogeneity of therapeutic responses. The secretome composed of cytokines, chemokines, growth factors, proteins, and EVs may represent an effective alternative [16]. Notably, MSC-derived EVs (MSC-EVs) have been demonstrated to have a similar effect to MSCs and may have advantages over parent cells because of their specific miRNA load [135]. The focus of current research has shifted from stem cells to their secretome while attempting to overcome the limitations of cell-based therapies.

In addition, stem cell-derived ECM can be obtained by decellularizing stem cells cultured *in vitro*, and the ECM is a noncellular component that contains macromolecules secreted by various cells. The ECM may vary among cell type sources, but it is mainly composed of proteoglycans, such as growth factors, glycosaminoglycan (GAG), and matrix pro-

teins, as well as collagen, fibronectin, elastin, vitronectin, and laminin [137]. After removing cellular components, such as DNA and cellular components that trigger an immune response, the ECM retains natural biochemical and biophysical signals [138]. Recent studies have shown that the ECM can promote cell proliferation and chondrogenic potential and is a potential biomaterial for tissue-engineered articular cartilage [139, 140].

The following sections will discuss in detail three aspects of the application of stem cell derivatives in cartilage regeneration and OA treatment: stem cell-derived CM, purified EVs (microvesicles and exosomes), and stem cell-derived ECM.

5.1. Stem Cell-Derived CM. Compared with stem cells, CM can be stored in a low-temperature environment, which is convenient for transportation, and does not have the risk of tumorigenesis. Compared with EVs and certain growth factors, CM components are more complex, including all components of the cell secretome, and do not need to be isolated and extracted, making it is convenient to use. Recently, Islam et al. studied the secretome of stromal cells obtained from the Hoffa fat pad (HFSPCs), synovial (SMSCs), umbilical cord (UCSCs), and cartilage (ACs) by quantitative liquid chromatography-mass spectrometry (LC-MS/MS) proteomics [141]. They identified more than 1000 proteins in each type of cell-derived CM. The secretome contained a large number of growth factors and cytokines. More importantly, compared with stromal cells from adult tissues, UCSCs had stronger anti-inflammatory and immunosuppressive properties. Recent studies reported that stem cell-derived CM plays a role in anti-inflammation and immune regulation and increases the synthesis of cartilage matrix in arthritis and osteochondral defect models. Ishikawa et al. intravenously injected CM derived from human dental pulp stem cells into the joint cavity of rheumatoid arthritis mice and found that CM relieved joint symptoms and synovial inflammation. The histological scores of bone erosion and cartilage damage in the CM group were significantly better than those in the control group, and the gene expression levels of proinflammatory cytokines were significantly reduced [142]. Alasdair found that the intra-articular injection of MSC-CM reduced cartilage damage and inhibited the immune response by reducing the cleavage of aggrecan, enhancing Treg function, and regulating the ratio of Treg:Th17 [143]. In addition, the application of BMSC-CM in a rat model of antigen-induced arthritis significantly reduced edema and thermal hyperalgesia as well as serum levels of TNF- α [144]. The anti-inflammatory effect of CM is related to its various immunomodulatory factors, including TGF- β , thrombospondin 1 (TSP1), and prostaglandin E2 (PGE2) [134]. Moreover, MSC-CM can also inhibit the progression of OA by balancing the ratio of MMP-13 to TIMP-1 in cartilage, inhibiting chondrocyte apoptosis and enhancing autophagy [145]. In a rabbit osteochondral defect repair experiment, the application of BMSC-CM led to only fibrocartilage regeneration [146]. Widhiyanto et al. composited ADSC-CM into porous scaffolds to repair rabbit trochlear cartilage defects, and new hyaline cartilage was observed at 12 weeks [147]. Interestingly, contradictory

results were reported in a rabbit ear cartilage regeneration study. Researchers subcutaneously injected ADSCs, ADSC-CM, and PBS and found that there was no significant difference between the ADSC-CM and PBS groups at 4 or 8 weeks [148]. The above studies preliminarily proved that stem cell-derived CM repaired articular cartilage defects and relieved OA. The differences in experimental results *in vivo* may be related to the application method. When using scaffolds as carriers, CM can be retained in the defect area and gradually released. Stem cell-derived CM contains the whole secretome, and different stem cells and pretreatments can significantly affect the composition of CM. Researchers need to find more effective CM collection conditions to promote cartilage regeneration and to ensure that there are effective concentrations of effector substances at the target location to achieve better cartilage regeneration. Researchers also need to determine the exact biological mechanism of CM *in vivo*.

5.2. Stem Cell-Derived EVs. Unlike the direct use of stem cell-derived CM, EVs need to be separated and purified. The current methods used to obtain EVs include but are not limited to ultrafiltration and size-exclusion chromatography [149, 150], ultracentrifugation [151], and immunoaffinity [152]. Recently, an increasing number of reports have indicated that exosomes are the main therapeutic agents secreted by MSCs that enhance the regeneration and immunomodulatory ability of MSCs during tissue repair [135]. It has been reported that stem cell-derived EVs can promote cartilage regeneration and prevent cartilage degeneration induced by OA [153–156]. In a rat model of osteochondral defects, the weekly injection of human ESC-derived exosomes into the joint cavity induced cartilage and subchondral bone tissue regeneration within 2 weeks, and the orderly regeneration of the two tissues was observed at 12 weeks [153]. Compared with MSC injection, a single intra-articular injection of exosomes or microvesicles derived from mouse BMSCs had similar effects in preventing the development of collagenase-induced OA in mice [154]. Exosomes derived from human ESCs also showed cartilage protective effects in a mouse OA model [155]. Another study compared the therapeutic effects of iPSC-derived exosomes and synovial-derived exosomes in a collagenase-induced mouse OA model. The results showed that iPSC-derived exosomes could more effectively delay the progression of OA [157]. The biodistribution of EVs after intra-articular injection is not clear. Encapsulating EVs in a suitable biomaterial can prevent the rapid clearance of EVs and achieve a sustained release effect. Liu et al. encapsulated hiPSC-MSC-derived exosomes in a photocrosslinked hydrogel, which resulted in the retention of exosomes *in vitro* and achieved cartilage regeneration and repair in a rabbit femoral condylar cartilage defect model [63]. Chen et al. used desktop stereolithography to fabricate 3D-printed cartilage ECM/methacrylic acid gelatin (GelMA)/exosome scaffolds with radial channels. *In vivo* experiments showed that the 3D-printed scaffolds significantly promoted cartilage regeneration [158]. *In vitro* mechanistic studies showed that EVs derived from MSCs mediate cartilage repair by enhancing proliferation, reducing cell apoptosis, and regulating the immune response [159].

With the in-depth study of the therapeutic mechanism of EVs, the anti-inflammatory effects of EVs have been reviewed in detail [160, 161]. A growing number of scholars believe that the therapeutic efficacy of EVs can be attributed to their nucleic acid composition [162]. An increasing number of studies have described a complex picture of how miRNA regulates or influences OA [163]. Wu et al. reported that ADSC-derived exosomes from the human subpatellar fat pad protected articular cartilage from damage and improved gait abnormalities in OA mice by maintaining cartilage homeostasis, which may have been related to the inhibition of the mTOR autophagy pathway regulated by miR100-5p [156]. Another study proved that exosomes derived from SMSCs with high miR-140 expression promoted articular cartilage regeneration in rats [164]. In addition, early molecular mechanism studies showed that miR-92a regulates the PI3K/AKT/mTOR signaling pathway by targeting noggin3, thus upregulating chondrocyte proliferation and matrix synthesis [165, 166]. Exosome miR-23b induced human MSCs to differentiate into chondrocytes by inhibiting the protein kinase A (PKA) signaling pathway [167]. On the other hand, miR-125b and miR-320 reduced ECM damage by downregulating the expression of aggrecanase-1 (ADAMTS-4) and MMP-13, while these two ECM proteases were significantly upregulated in human OA chondrocytes [168]. Recently, Enrico et al. conducted high-throughput screening of the human adipose-derived MSC secretome and identified 60 kinds of miRNAs that can protect cartilage and induce macrophages to polarize to an M2 phenotype through bioinformatics analysis [169]. Increasing evidence indicates that stem cell-derived EVs may promote cartilage regeneration and treat OA by regulating a complex miRNA network [163]. Finally, the application of stem cell-derived EVs in treatment may have more advantages than using stem cells alone, mainly for the following reasons: (1) they cannot proliferate and are easy to preserve and transport [170]; (2) EVs are nontoxic, have no risk of tumorigenesis, low immunogenicity, and higher safety [171]; and (3) compared with the regulatory and ethical restrictions on stem cell products, the application of EVs is less restricted. However, in the field of cartilage repair, there are still many questions about the therapeutic effect, biodynamics, biodistribution, and delivery methods of stem cell-derived EVs that need to be answered in large animal experiments.

5.3. Stem Cell-Derived ECM. Stem cell-derived ECM is a natural biomaterial with strong biological activity and good biocompatibility. A large number of studies have shown that stem cell-derived ECM can enhance cell proliferation, prevent chondrocyte dedifferentiation, and maintain the stemness of stem cells [172, 173]. Stem cell-derived ECM provides a better platform for the expansion of chondrocytes/stem cells *in vitro*. Many studies have shown that compared with tissue culture polystyrene (TCPS), stem cell-derived ECM can significantly improve the proliferation of chondrogenic cells. At the same time, chondrogenic cells expanded on stem cell-derived ECM have stronger chondrogenic potential [174, 175]. Pei et al. showed that compared with cell culture plates, porcine synovial stem cell-derived

ECM increased the proliferation of chondrocytes and delayed the dedifferentiation of porcine chondrocytes [174]. At the same time, stem cell-derived ECM can be used as a substrate for stem cell culture *in vitro*, which can restore the lineage differentiation ability of stem cells in aging mice [176]. Research by Yang et al. showed that compared with chondrocytes grown on TCP, chondrocytes inoculated on human BMSC-ECM showed a significantly increased proliferation rate and maintained a better cartilage phenotype. After expanding to the same number of cells and placing them in high-density micromass culture, chondrocytes from the BMSC-ECM group showed better cartilage differentiation characteristics than those from the TCP group [175]. Interestingly, the age of host that cells were derived from and different cell sources seem to be important factors affecting the ECM. Chee et al. found that fetal BMSC-ECM was superior to adult BMSC-ECM or human neonatal dermal fibroblasts in promoting the proliferation and pluripotency of adult BMSCs [177]. In addition to promoting cell proliferation and lineage-specific differentiation, recent studies have shown that SMSC-ECM enhanced the anti-inflammatory properties of rabbit articular chondrocytes through the SIRT1 pathway [178].

In addition to being used as a cell culture substrate, stem cell ECM can also be used alone or in combination with polymer materials to make 3D scaffolds to promote cartilage formation *in vivo/in vitro*. Tang et al. evaluated the cartilage repair ability of autologous BMSC-derived ECM scaffolds in two kinds of cartilage defect animal models. Six months after surgery, the histological characteristics and biochemical content of the bone marrow stimulation + ECM group were similar to those of normal hyaline cartilage [179]. Makiko et al. inoculated human amniotic MSCs on PLGA, successfully prepared an ECM-PLGA scaffold by removing cellular components, and implanted the scaffold into an osteochondral defect in the rat femoral trochlea. The results showed that ECM-PLGA induced gradual tissue regeneration and resulted in hyaline cartilage repair that was superior to that in the empty control group [180].

Current research shows that various stem cell derivatives play beneficial roles in cartilage regeneration and OA treatment. However, compared with the direct application of stem cells, the most substantial problem faced by stem cell derivatives is the cumbersome collection process, which undoubtedly increases the cost of treatment. In addition, how to increase the yield of exosomes and other derivatives and ensure the unity between batches is an urgent problem to be solved.

6. Stem Cell Delivery Biomaterials and Scaffolds

The key factor determining the effectiveness of stem cell therapy is the survival rate of stem cells during and after transplantation. Biomaterials used for cartilage repair not only provide mechanical support for cartilage defects but also provide support matrix for stem cells to induce cell growth, diffusion, and differentiation [181]. Biomaterial-based cell delivery systems can be extracted from naturally occurring materials, such as HA [182], gelatin [183], alginate [184], col-

lagen, and decellularized matrix [185, 186] or based on synthetic materials, such as poly(ethylene glycol) (PEG) [187], poly(N-isopropylacrylamide) (PNIPAM) [188], poly(lactico-glycolic acid) (PLGA) [189], and polycaprolactone (PCL) [190]. The material is usually made into a porous structure to facilitate cell inoculation or hydrated polymeric networks, hydrogels for cell encapsulation [191]. Natural materials have better biological effects such as promoting cell adhesion, proliferation, and cartilage differentiation [192]. However, the mechanical properties and degradation rate of synthetic materials are more adjustable, and it is easier to customize according to cartilage or bone cartilage [193]. By combining biomaterials or natural ECM components with synthetic polymers, it is beneficial to highlight their respective advantages while limiting their disadvantages [194–197].

Early researchers used the material as a stem cell delivery platform to ensure the survival rate of stem cell transplantation to the defect and enhance the cell retention and therapeutic effect at the local administration site. Vahedi et al. inoculated adipose-derived stem cells into PCL scaffolds, and the ASC-PCL construct treated with low-intensity ultrasound achieved effective cartilage regeneration in a sheep model of a femoral condylar cartilage defect [198]. Collagen exists widely in a variety of biological tissues, has good biocompatibility and biodegradability, and has good plasticity [199]. Shi et al. successfully fabricated silk-fibroin-gelatin composite scaffolds using 3D printing technology and introduced BMSC-specific-affinity peptide [105]. This composite scaffold not only provides a suitable three-dimensional structure for stem cell proliferation, differentiation, and extracellular matrix synthesis but also achieves articular cartilage regeneration by recruiting endogenous BMSCs. In cartilage tissue engineering, the use of decellularized ECM is a relatively new concept. Our study group has proven that decellularized cartilage ECM porous scaffolds can promote stem cell adhesion, proliferation, and cartilage differentiation. At the same time, preclinical studies have proven that decellularized cartilage scaffolds have an excellent cartilage repair effect [200–203].

Although collagen type II and HA are key components of cartilage ECM, mainly type I collagen and HA have been developed as hydrogels for experimental and clinical cartilage repair [204]. To develop injectable scaffolds for the treatment of cartilage, the effects of HA hydrogel on chondrogenic differentiation and cartilage repair of hMSCs have been evaluated *in vitro* and *in vivo*. Result showed that the hydrogels reduce the fast leakage of the encapsulated growth factors, leading to the enhanced chondrogenesis of hMSCs and neo-cartilage formation [205]. Hydrogel can also achieve better cartilage repair by encapsulating functional biological small molecules. Xu et al. demonstrated that hydrogel encapsulation resulted in more sustained release of kartogenin and TGF- β 1, which led to enhanced chondrogenesis of encapsulated human bone marrow MSCs *in vitro* and *in vivo* [206]. For the treatment of cartilage and osteochondral defects, the exact size and shape can be determined only after debridement. Therefore, methods such as *in situ* 3D bio-printing or hydrogel application are the most appropriate procedures for providing personalized treatment. The

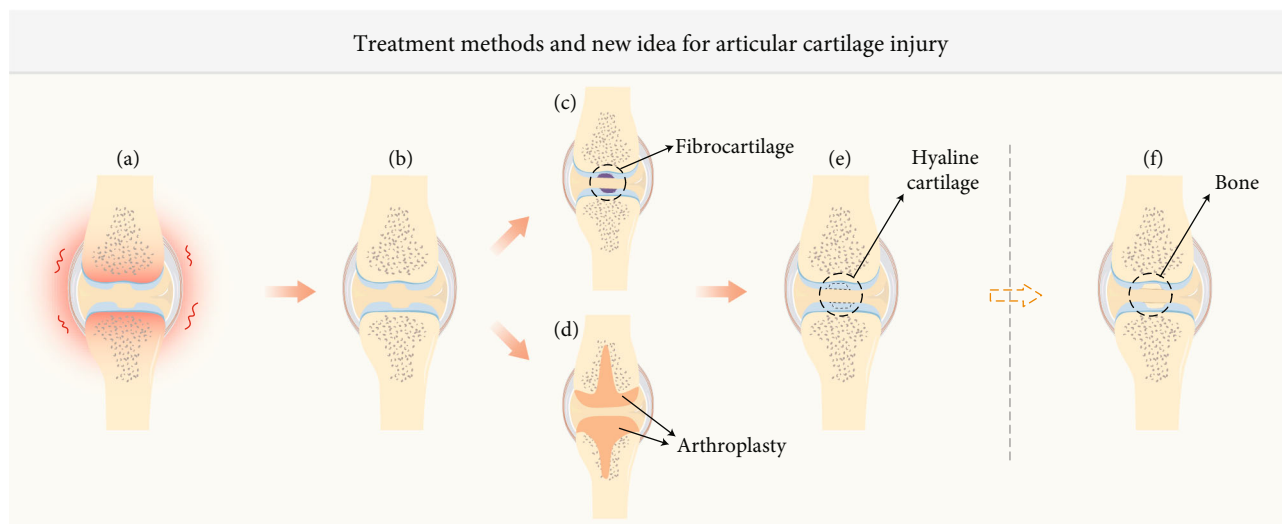


FIGURE 3: Treatment methods and new idea for articular cartilage injury. (a) Joint cartilage defects cause joint inflammation. (b) Medication can relieve symptoms. (c) Traditional repair techniques such as MF form fibrocartilage. (d) Artificial joint replacement surgery reconstructs the articular surface. (e) Ideal form of cartilage regeneration. (f) New ideas for cartilage regeneration.

customizability of traditional solid scaffolds is weak, while the limitations of hydrogels include poor mechanical integrity and rapid degradation when exposed to inflammatory environment [207]. With the deepening of the intersection of biology and material manufacturing disciplines, any strategy aimed at imitating the composition and regional organization of articular cartilage will be more likely to reconstruct engineering tissue with the potential for successful clinical application [208].

The current biomaterials and scaffolds used for the delivery of stem cells still have many problems to be solved. For example, the biocompatibility of polymer materials is poor, and their degradation products may cause changes in the pH of the microenvironment. The mechanical properties and degradation rate of natural biomaterials are difficult to control, and its activity and functionality in the body are still to be clarified.

7. Conclusions and Future Perspectives

In the field of articular cartilage regeneration and OA treatment, research involving stem cells has moved from the laboratory to the clinic [209, 210]. However, several problems remain that restrict the application of tissue-engineered cartilage involving stem cells.

First, the functional heterogeneity of stem cells is a substantial obstacle to their clinical transformation [211]. Therefore, before using stem cells, it is necessary to screen out specific subgroups to more accurately explore the molecular mechanism of cartilage regeneration. Second, the problem of premature differentiation of stem cells *in vitro* expansion has not been resolved. Finding specific targets that regulate stem cell differentiation may solve this problem. For example, methyltransferase inhibitors can inhibit Setd7 protein, prevent cell differentiation, and maintain cell division. Researchers used stem cells containing methyltransferase inhibitors to treat muscle atrophy mice, and the

results showed that the strength of regenerating muscle was significantly improved [212]. Finally, standard animal models of articular cartilage defects and OA have not yet been established [213]. Rodents such as mice and rats maintain open endochondral ossification throughout their lives, and the healing of cartilage defects may be greatly affected by spontaneous internal healing [214]. Using large animals such as pigs and horses often limits the number of samples due to high prices. Therefore, finding a balance between effectiveness and economic benefits is necessary in the choice of animal models.

The use of stem cell derivatives to regenerate articular cartilage is a promising development direction [133]. miRNA is considered to be the main component that mediates the biological effects of EVs. However, the main problem currently encountered is that it is technically challenging to produce a sufficient number of EVs, and the amount of nucleic acid packages for EVs is too low [215, 216]. Cell nanoporation biochips can not only increase the production of exosomes but also realize the encapsulation of specific miRNAs [217]. This new technology may help translate the EV-based cartilage regeneration strategy into clinical practice.

The treatment of articular cartilage defects has gone through several stages of development: drug treatment can only relieve symptoms (Figures 3(a) and 3(b)). MF and other techniques often use fibrocartilage to temporarily fill cartilage defects (Figures 3(b) and 3(c)) [218]. Artificial joint replacement surgery temporarily restores the smooth joint surface (Figures 3(b) and 3(d)). The use of hyaline cartilage to restore the joint surface (Figure 3(e)) is the consummate appeal [219]. A recent study suggested that we might not consider hyaline cartilage as a “final” goal, but as an intermediate stage (Figures 3(e) and 3(f)), and try to stay at this stage. The cells go through the hyaline cartilage stage before forming bone tissue [220]. Researchers used bone morphogenetic protein 2 (BMP2) to initiate the bone formation process after MF

and then used an antagonist (VEGFR1) to block the vascular endothelial growth factor, thereby stopping the bone formation process and leaving the new tissue in the hyaline cartilage stage [221].

In summary, the articular cartilage regeneration strategy involving stem cells has achieved encouraging results. The joint cooperation of practitioners from multiple disciplines and fields will help overcome current challenges, and the change in thinking style may open up new strategies for articular cartilage regeneration.

Conflicts of Interest

The authors declare that they have no conflicts of interest.

Authors' Contributions

Shuangpeng Jiang and Guangzhao Tian contributed equally to this work.

Acknowledgments

This work was supported by the National Key R&D Program of China (2019 YFA 0110600), the National Natural Science Foundation of China (81772319), and the China Postdoctoral Science Foundation Grant (2019TQ0379, 2019M663262).

References

- [1] R. F. Loeser, S. R. Goldring, C. R. Scanzello, and M. B. Goldring, "Osteoarthritis: a disease of the joint as an organ," *Arthritis and rheumatism*, vol. 64, no. 6, pp. 1697–1707, 2012.
- [2] R. Barnett, "Osteoarthritis," *Lancet*, vol. 391, no. 10134, pp. 1985–2078, 2018.
- [3] S. Jiang, W. Guo, G. Tian et al., "Clinical application status of articular cartilage regeneration techniques: tissue-engineered cartilage brings new hope," *Stem Cells International*, vol. 2020, Article ID 5690252, 16 pages, 2020.
- [4] Y. Nam, Y. A. Rim, J. Lee, and J. H. Ju, "Current therapeutic strategies for stem cell-based cartilage regeneration," *Stem cells international*, vol. 2018, Article ID 8490489, 20 pages, 2018.
- [5] E. V. Medvedeva, E. A. Grebenik, S. N. Gornostaeva et al., "Repair of damaged articular cartilage: current approaches and future directions," *International journal of molecular sciences*, vol. 19, no. 8, 2018.
- [6] Y. Zhang, S. Liu, W. Guo et al., "Human umbilical cord Wharton's jelly mesenchymal stem cells combined with an acellular cartilage extracellular matrix scaffold improve cartilage repair compared with microfracture in a caprine model," *Osteoarthritis Cartilage*, vol. 26, no. 7, pp. 954–965, 2018.
- [7] Y. G. Koh, O. R. Kwon, Y. S. Kim, Y. J. Choi, and D. H. Tak, "Adipose-derived mesenchymal stem cells with microfracture versus microfracture alone: 2-year follow-up of a prospective randomized Trial," *Arthroscopy*, vol. 32, no. 1, pp. 97–109, 2016.
- [8] A. T. Wang, Y. Feng, H. H. Jia, M. Zhao, and H. Yu, "Application of mesenchymal stem cell therapy for the treatment of osteoarthritis of the knee: a concise review," *World journal of stem cells*, vol. 11, no. 4, pp. 222–235, 2019.
- [9] C. R. Harrell, B. S. Markovic, C. Fellabaum, A. Arsenijevic, and V. Volarevic, "Mesenchymal stem cell-based therapy of osteoarthritis: current knowledge and future perspectives," *Biomedicine & pharmacotherapy*, vol. 109, pp. 2318–2326, 2019.
- [10] J. Houghton, C. Stoicov, S. Nomura et al., "Gastric cancer originating from bone marrow-derived cells," *Science*, vol. 306, no. 5701, pp. 1568–1571, 2004.
- [11] Ž. Večerić-Haler, A. Cerar, and M. Perše, "(Mesenchymal) stem cell-based therapy in cisplatin-induced acute kidney injury animal model: risk of immunogenicity and tumorigenicity," *Stem Cells International*, vol. 2017, Article ID 7304643, 17 pages, 2017.
- [12] A. Stolzing, E. Jones, D. McGonagle, and A. Scutt, "Age-related changes in human bone marrow-derived mesenchymal stem cells: consequences for cell therapies," *Mechanisms of ageing and development*, vol. 129, no. 3, pp. 163–173, 2008.
- [13] J. M. Murphy, K. Dixon, S. Beck, D. Fabian, A. Feldman, and F. Barry, "Reduced chondrogenic and adipogenic activity of mesenchymal stem cells from patients with advanced osteoarthritis," *Arthritis & Rheumatism*, vol. 46, no. 3, pp. 704–713, 2002.
- [14] G. Kolios and Y. Moodley, "Introduction to stem cells and regenerative medicine," *Respiration*, vol. 85, no. 1, pp. 3–10, 2013.
- [15] L. Daneshmandi, S. Shah, T. Jafari et al., "Emergence of the stem cell secretome in regenerative engineering," *Trends in Biotechnology*, vol. 38, no. 12, pp. 1373–1384, 2020.
- [16] P. K. L., S. Kandoi, R. Misra, V. S., R. K., and R. S. Verma, "The mesenchymal stem cell secretome: a new paradigm towards cell-free therapeutic mode in regenerative medicine," *Cytokine & growth factor reviews*, vol. 46, no. 1–9, pp. 1–9, 2019.
- [17] J. C. Bernhard and G. Vunjak-Novakovic, "Should we use cells, biomaterials, or tissue engineering for cartilage regeneration?," *Stem cell research & therapy*, vol. 7, no. 1, 2016.
- [18] S. Zhou, S. Chen, Q. Jiang, and M. Pei, "Determinants of stem cell lineage differentiation toward chondrogenesis versus adipogenesis," *Cellular and Molecular Life Sciences*, vol. 76, no. 9, pp. 1653–1680, 2019.
- [19] T. Wang, P. Nimkingratana, C. A. Smith, A. Cheng, T. E. Hardingham, and S. J. Kimber, "Enhanced chondrogenesis from human embryonic stem cells," *Stem cell research*, vol. 39, p. 101497, 2019.
- [20] J. U. Yoo, T. S. Barthel, K. Nishimura et al., "The chondrogenic potential of human bone-marrow-derived mesenchymal progenitor cells," *The Journal of Bone and Joint Surgery*, vol. 80, no. 12, pp. 1745–1757, 1998.
- [21] H. Kang, S. Lu, J. Peng et al., "In vivo construction of tissue-engineered cartilage using adipose-derived stem cells and bioreactor technology," *Cell Tissue Bank*, vol. 16, no. 1, pp. 123–133, 2015.
- [22] K. L. Caldwell and J. Wang, "Cell-based articular cartilage repair: the link between development and regeneration," *Osteoarthritis and cartilage*, vol. 23, no. 3, pp. 351–362, 2015.
- [23] A. N. Mokbel, O. S. El Tookhy, A. A. Shamaa, L. A. Rashed, D. Sabry, and A. M. El Sayed, "Homing and reparative effect of intra-articular injection of autologous mesenchymal stem cells in osteoarthritic animal model," *BMC Musculoskeletal Disord*, vol. 12, no. 1, 2011.

- [24] A. Mokbel, O. El-Tookhy, A. A. Shamaa, D. Sabry, L. Rashed, and A. Mostafa, "Homing and efficacy of intra-articular injection of autologous mesenchymal stem cells in experimental chondral defects in dogs," *Clinical and Experimental Rheumatology-Incl Supplements*, vol. 29, no. 2, pp. 275–284, 2011.
- [25] S. Kotaka, S. Wakitani, A. Shimamoto et al., "Magnetic targeted delivery of induced pluripotent stem cells promotes articular cartilage repair," *Stem cells international*, vol. 2017, Article ID 9514719, 7 pages, 2017.
- [26] M. Li, X. Luo, X. Lv et al., "In vivo human adipose-derived mesenchymal stem cell tracking after intra-articular delivery in a rat osteoarthritis model," *Stem cell research & therapy*, vol. 7, no. 1, 2016.
- [27] J. A. Pawitan, "Prospect of stem cell conditioned medium in regenerative medicine," *BioMed research international*, vol. 2014, Article ID 965849, 14 pages, 2014.
- [28] A. I. Caplan and J. E. Dennis, "Mesenchymal stem cells as trophic mediators," *Journal of cellular biochemistry*, vol. 98, no. 5, pp. 1076–1084, 2006.
- [29] H. J. Li, S. Shen, H. T. Fu et al., "Immunomodulatory functions of mesenchymal stem cells in tissue engineering," *Stem Cells International*, vol. 2019, 18 pages, 2019.
- [30] J. Ding, B. Chen, T. Lv et al., "Bone Marrow Mesenchymal Stem Cell-Based Engineered Cartilage Ameliorates Polyglycolic Acid/Polylactic Acid Scaffold-Induced Inflammation Through M2 Polarization of Macrophages in a Pig Model," *STEM CELLS Translational Medicine*, vol. 5, no. 8, pp. 1079–1089, 2016.
- [31] L. Wu, J. C. Leijten, N. Georgi, J. N. Post, C. van Blitterswijk, and M. Karperien, "Trophic effects of mesenchymal stem cells increase chondrocyte proliferation and matrix formation," *Tissue Eng Part A*, vol. 17, no. 9-10, pp. 1425–1436, 2011.
- [32] C. Acharya, A. Adesida, P. Zajac et al., "Enhanced chondrocyte proliferation and mesenchymal stromal cells chondrogenesis in coculture pellets mediate improved cartilage formation," *Cellular Physiology*, vol. 227, no. 1, pp. 88–97, 2012.
- [33] Y. Zhang, W. Guo, M. Wang et al., "Co-culture systems-based strategies for articular cartilage tissue engineering," *Journal of Cellular Physiology*, vol. 233, no. 3, pp. 1940–1951, 2018.
- [34] A. I. Caplan, "Mesenchymal Stem Cells: Time to Change the Name!," *STEM CELLS Translational Medicine*, vol. 6, no. 6, pp. 1445–1451, 2017.
- [35] M. J. Stoddart, J. Bara, and M. Alini, "Cells and secretome—towards endogenous cell re-activation for cartilage repair," *Advanced Drug Delivery Reviews*, vol. 84, pp. 135–145, 2015.
- [36] Q. Liu, J. Wang, Y. Chen et al., "Suppressing mesenchymal stem cell hypertrophy and endochondral ossification in 3D cartilage regeneration with nanofibrous poly(L-lactic acid) scaffold and matrilin-3," *Acta Biomaterialia*, vol. 76, pp. 29–38, 2018.
- [37] K. Pelttari, A. Winter, E. Steck et al., "Premature induction of hypertrophy during in vitro chondrogenesis of human mesenchymal stem cells correlates with calcification and vascular invasion after ectopic transplantation in SCID mice," *Arthritis Rheum*, vol. 54, no. 10, pp. 3254–3266, 2006.
- [38] M. B. Mueller and R. S. Tuan, "Functional characterization of hypertrophy in chondrogenesis of human mesenchymal stem cells," *Arthritis Rheum*, vol. 58, no. 5, pp. 1377–1388, 2008.
- [39] D. Studer, C. Millan, E. Öztürk, K. Maniura-Weber, and M. Zenobi-Wong, "Molecular and biophysical mechanisms regulating hypertrophic differentiation in chondrocytes and mesenchymal stem cells," *European Cells and Materials*, vol. 24, pp. 118–135, 2012.
- [40] P. J. Emans, J. Pieper, M. M. Hulsbosch et al., "Differential cell viability of chondrocytes and progenitor cells in tissue-engineered constructs following implantation into osteochondral defects," *Tissue Engineering*, vol. 12, no. 6, pp. 1699–1709, 2006.
- [41] J. Quintavalla, S. Uziel-Fusi, J. Yin et al., "Fluorescently labeled mesenchymal stem cells (MSCs) maintain multilineage potential and can be detected following implantation into articular cartilage defects," *Biomaterials*, vol. 23, no. 1, pp. 109–119, 2002.
- [42] T. S. de Windt, L. A. Vonk, I. C. Slaper-Cortenbach et al., "Allogeneic mesenchymal stem cells stimulate cartilage regeneration and are safe for single-stage cartilage repair in humans upon mixture with recycled autologous chondrons," *Stem Cells*, vol. 35, no. 1, pp. 256–264, 2017.
- [43] A. Andrzejewska, B. Lukomska, and M. Janowski, "Concise Review: Mesenchymal Stem Cells: From Roots to Boost," *Stem Cells*, vol. 37, no. 7, pp. 855–864, 2019.
- [44] L. Bacakova, J. Zarubova, M. Travnickova et al., "Stem cells: their source, potency and use in regenerative therapies with focus on adipose-derived stem cells - a review," *Biotechnology Advances*, vol. 36, no. 4, pp. 1111–1126, 2018.
- [45] A. Bajek, N. Gurtowska, J. Olkowska, L. Kazmierski, M. Maj, and T. Drewa, "Adipose-derived stem cells as a tool in cell-based therapies," *Archivum Immunologiae et Therapiae Experimentalis*, vol. 64, no. 6, pp. 443–454, 2016.
- [46] T. Pizzute, K. Lynch, and M. Pei, "Impact of tissue-specific stem cells on lineage-specific differentiation: a focus on the musculoskeletal system," *Stem Cell Reviews and Reports*, vol. 11, no. 1, pp. 119–132, 2015.
- [47] Y. Segawa, T. Muneta, H. Makino et al., "Mesenchymal stem cells derived from synovium, meniscus, anterior cruciate ligament, and articular chondrocytes share similar gene expression profiles," *Journal of Orthopaedic Research*, vol. 27, no. 4, pp. 435–441, 2009.
- [48] C. De Bari, F. Dell'Accio, P. Tylzanowski, and F. P. Luyten, "Multipotent mesenchymal stem cells from adult human synovial membrane," *Arthritis Rheum*, vol. 44, no. 8, pp. 1928–1942, 2001.
- [49] R. Hass, C. Kasper, S. Böhm, and R. Jacobs, "Different populations and sources of human mesenchymal stem cells (MSC): A comparison of adult and neonatal tissue-derived MSC," *Cell communication and signaling: CCS*, vol. 9, no. 1, pp. 12–12, 2011.
- [50] D. C. Colter, I. Sekiya, and D. J. Prockop, "Identification of a subpopulation of rapidly self-renewing and multipotential adult stem cells in colonies of human marrow stromal cells," *Proceedings of the National Academy of Sciences*, vol. 98, no. 14, pp. 7841–7845, 2001.
- [51] L. Wen and F. Tang, "Single-cell sequencing in stem cell biology," *Genome Biology*, vol. 17, no. 1, 2016.
- [52] L. E. Sidney, M. J. Branch, S. E. Dunphy, H. S. Dua, and A. Hopkinson, "Concise review: evidence for CD34 as a

- common marker for diverse progenitors,” *Stem Cells*, vol. 32, no. 6, pp. 1380–1389, 2014.
- [53] K. C. Russell, D. G. Phinney, M. R. Lacey, B. L. Barrilleaux, K. E. Meyertholen, and K. C. O’Connor, “In vitro high-capacity assay to quantify the clonal heterogeneity in trilineage potential of mesenchymal stem cells reveals a complex hierarchy of lineage commitment,” *Stem Cells*, vol. 28, no. 4, pp. 788–798, 2010.
- [54] P. H. Krebsbach and L. G. Villa-Diaz, “The Role of Integrin $\alpha 6$ (CD49f) in Stem Cells: More than a Conserved Biomarker,” *Cells and Development*, vol. 26, no. 15, pp. 1090–1099, 2017.
- [55] X. Li, W. Guo, K. Zha et al., “Enrichment of CD146+Adipose-Derived Stem Cells in Combination with Articular Cartilage Extracellular Matrix Scaffold Promotes Cartilage Regeneration,” *Theranostics*, vol. 9, no. 17, pp. 5105–5121, 2019.
- [56] T. B. Marvasti, F. J. Alibhai, R. D. Weisel, and R. K. Li, “CD34(+) stem cells: promising roles in cardiac repair and regeneration,” *Canadian Journal of Cardiology*, vol. 35, no. 10, pp. 1311–1321, 2019.
- [57] P. J. Mintz, K. W. Huang, V. Reebye et al., “Exploiting human CD34⁺ stem cell-conditioned medium for tissue repair,” *Molecular Therapy*, vol. 22, no. 1, pp. 149–159, 2014.
- [58] Z. Yang, S. Ma, R. Cao et al., “CD49^{high} Defines a Distinct Skin Mesenchymal Stem Cell Population Capable of Hair Follicle Epithelial Cell Maintenance,” *Journal of Investigative Dermatology*, vol. 140, no. 3, pp. 544–555.e9, 2020.
- [59] K. Pridie, “A method of resurfacing osteoarthritis knee joints,” *Journal of Bone and Joint Surgery*, vol. 41, 1959.
- [60] B. Jiang, X. Fu, L. Yan et al., “Transplantation of human ESC-derived mesenchymal stem cell spheroids ameliorates spontaneous osteoarthritis in rhesus macaques,” *Theranostics*, vol. 9, no. 22, pp. 6587–6600, 2019.
- [61] Y. S. Kim and Y. G. Koh, “Comparative Matched-Pair Analysis of Open-Wedge High Tibial Osteotomy With Versus Without an Injection of Adipose-Derived Mesenchymal Stem Cells for Varus Knee Osteoarthritis: Clinical and Second-Look Arthroscopic Results,” *The American Journal of Sports Medicine*, vol. 46, no. 11, pp. 2669–2677, 2018.
- [62] J. S. Song, K. T. Hong, N. M. Kim et al., “Implantation of allogenic umbilical cord blood-derived mesenchymal stem cells improves knee osteoarthritis outcomes: Two-year follow-up,” *Regenerative Therapy*, vol. 14, pp. 32–39, 2020.
- [63] X. Liu, Y. Yang, Y. Li et al., “Integration of stem cell-derived exosomes with in situ hydrogel glue as a promising tissue patch for articular cartilage regeneration,” *Nanoscale*, vol. 9, no. 13, pp. 4430–4438, 2017.
- [64] J. Wu, Z. Sun, H. S. Sun et al., “Intravenously administered bone marrow cells migrate to damaged brain tissue and improve neural function in ischemic rats,” *Cell Transplant*, vol. 16, no. 10, pp. 993–1005, 2008.
- [65] Y. Song, H. Du, C. Dai et al., “Human adipose-derived mesenchymal stem cells for osteoarthritis: a pilot study with long-term follow-up and repeated injections,” *Regenerative Medicine*, vol. 13, no. 3, pp. 295–307, 2018.
- [66] T. Xia, F. Yu, K. Zhang et al., “The effectiveness of allogeneic mesenchymal stem cells therapy for knee osteoarthritis in pigs,” *Annals of Translational Medicine*, vol. 6, no. 20, p. 404, 2018.
- [67] Y. S. Kim, P. K. Chung, D. S. Suh, D. B. Heo, D. H. Tak, and Y. G. Koh, “Implantation of mesenchymal stem cells in combination with allogenic cartilage improves cartilage regeneration and clinical outcomes in patients with concomitant high tibial osteotomy,” *Knee Surg Sports Traumatol Arthrosc*, vol. 28, no. 2, pp. 544–554, 2020.
- [68] B. Sadlik, G. Jaroslowski, D. Gladysz et al., “Knee Cartilage Regeneration with Umbilical Cord Mesenchymal Stem Cells Embedded in Collagen Scaffold Using Dry Arthroscopy Technique,” *Clinical Research and Practice*, vol. 1020, pp. 113–122, 2017.
- [69] B. J. Huang, J. C. Hu, and K. A. Athanasiou, “Cell-based tissue engineering strategies used in the clinical repair of articular cartilage,” *Biomaterials*, vol. 98, pp. 1–22, 2016.
- [70] L. Li, X. Duan, Z. Fan et al., “Mesenchymal stem cells in combination with hyaluronic acid for articular cartilage defects,” *Scientific Reports*, vol. 8, no. 1, p. 9900, 2018.
- [71] C. C. Wu, S. Y. Sheu, L. H. Hsu, K. C. Yang, C. C. Tseng, and T. F. Kuo, “Intra-articular Injection of platelet-rich fibrin releasates in combination with bone marrow-derived mesenchymal stem cells in the treatment of articular cartilage defects: An in vivo study in rabbits,” *Journal of Biomedical Materials Research Part B: Applied Biomaterials*, vol. 105, no. 6, pp. 1536–1543, 2017.
- [72] L. Barrachina, A. R. Remacha, A. Romero et al., “Assessment of effectiveness and safety of repeat administration of proinflammatory primed allogeneic mesenchymal stem cells in an equine model of chemically induced osteoarthritis,” *BMC Veterinary Research*, vol. 14, no. 1, p. 241, 2018.
- [73] R. Vayas, R. Reyes, M. R. Arnau, C. Évora, and A. Delgado, “Injectable Scaffold for Bone Marrow Stem Cells and Bone Morphogenetic Protein-2 to Repair Cartilage,” *Cartilage*, p. 194760351984168, 2019.
- [74] T. Jiang, S. Heng, X. Huang et al., “Biomimetic poly(poly(ϵ -caprolactone)-polytetrahydrofuran urethane) based nanofibers enhanced chondrogenic differentiation and cartilage regeneration,” *Journal of Biomedical Nanotechnology*, vol. 15, no. 5, pp. 1005–1017, 2019.
- [75] N. Kohli, I. R. T. Al-Delfi, M. Snow et al., “CD271-selected mesenchymal stem cells from adipose tissue enhance cartilage repair and are less angiogenic than plastic adherent mesenchymal stem cells,” *Scientific Reports*, vol. 9, no. 1, p. 3194, 2019.
- [76] L. Mei, B. Shen, P. Ling et al., “Culture-expanded allogenic adipose tissue-derived stem cells attenuate cartilage degeneration in an experimental rat osteoarthritis model,” *PLoS One*, vol. 12, no. 4, p. e0176107, 2017.
- [77] S. Critchley, E. J. Sheehy, G. Cunniffe et al., “3D printing of fibre-reinforced cartilaginous templates for the regeneration of osteochondral defects,” *Acta Biomater*, vol. 113, pp. 130–143, 2020.
- [78] M. Yan, X. Liu, Q. Dang, H. Huang, F. Yang, and Y. Li, “Intra-articular injection of human synovial membrane-derived mesenchymal stem cells in murine collagen-induced arthritis: assessment of immunomodulatory capacity in vivo,” *Stem Cells International*, vol. 2017, Article ID 9198328, 12 pages, 2017.
- [79] S. Kondo, Y. Nakagawa, M. Mizuno et al., “Transplantation of aggregates of autologous synovial mesenchymal stem cells for treatment of cartilage defects in the femoral condyle and the femoral groove in microminipigs,” *The American Journal of Sports Medicine*, vol. 47, no. 10, pp. 2338–2347, 2019.
- [80] P. Neybecker, C. Henrionnet, E. Pape et al., “In vitro and in vivo potentialities for cartilage repair from human

- advanced knee osteoarthritis synovial fluid-derived mesenchymal stem cells," *Stem Cell Res Ther*, vol. 9, no. 1, p. 329, 2018.
- [81] J. Li, Y. Huang, J. Song et al., "Cartilage regeneration using arthroscopic flushing fluid-derived mesenchymal stem cells encapsulated in a one-step rapid cross-linked hydrogel," *Acta Biomater*, vol. 79, pp. 202–215, 2018.
- [82] S. Liu, Y. Jia, M. Yuan et al., "Repair of osteochondral defects using human umbilical cord Wharton's jelly-derived mesenchymal stem cells in a rabbit model," *BioMed Research International*, vol. 2017, Article ID 8760383, 2017.
- [83] D. Xing, J. Wu, B. Wang et al., "Intra-articular delivery of umbilical cord-derived mesenchymal stem cells temporarily retard the progression of osteoarthritis in a rat model," *Int J Rheum Dis*, vol. 23, no. 6, pp. 778–787, 2020.
- [84] Y. A. Rim, Y. Nam, N. Park, J. Lee, S. H. Park, and J. H. Ju, "Repair potential of nonsurgically delivered induced pluripotent stem cell-derived chondrocytes in a rat osteochondral defect model," *Journal of Tissue Engineering and Regenerative Medicine*, vol. 12, no. 8, pp. 1843–1855, 2018.
- [85] J. D. Gibson, M. B. O'Sullivan, F. Alaee et al., "Regeneration of Articular Cartilage by Human ESC-Derived Mesenchymal Progenitors Treated Sequentially with BMP-2 and Wnt5a," *STEM CELLS Translational Medicine*, vol. 6, no. 1, pp. 40–50, 2017.
- [86] J. Chahal, A. Gómez-Aristizábal, K. Shestopaloff et al., "Bone Marrow Mesenchymal Stromal Cell Treatment in Patients with Osteoarthritis Results in Overall Improvement in Pain and Symptoms and Reduces Synovial Inflammation," *STEM CELLS Translational Medicine*, vol. 8, no. 8, pp. 746–757, 2019.
- [87] S. A. Shapiro, J. R. Arthurs, M. G. Heckman et al., "Quantitative T2 MRI mapping and 12-month follow-up in a randomized, blinded, placebo controlled trial of bone marrow aspiration and concentration for osteoarthritis of the knees," *Cartilage*, vol. 10, no. 4, pp. 432–443, 2018.
- [88] M. Emadedin, N. Labibzadeh, M. G. Liastani et al., "Intra-articular implantation of autologous bone marrow-derived mesenchymal stromal cells to treat knee osteoarthritis: a randomized, triple-blind, placebo-controlled phase 1/2 clinical trial," *Cytotherapy*, vol. 20, no. 10, pp. 1238–1246, 2018.
- [89] S. Shadmanfar, N. Labibzadeh, M. Emadedin et al., "Intra-articular knee implantation of autologous bone marrow-derived mesenchymal stromal cells in rheumatoid arthritis patients with knee involvement: Results of a randomized, triple-blind, placebo-controlled phase 1/2 clinical trial," *Cytotherapy*, vol. 20, no. 4, pp. 499–506, 2018.
- [90] J. Matas, M. Orrego, D. Amenabar et al., "Umbilical Cord-Derived Mesenchymal Stromal Cells (MSCs) for Knee Osteoarthritis: Repeated MSC Dosing Is Superior to a Single MSC Dose and to Hyaluronic Acid in a Controlled Randomized Phase I/II Trial," *STEM CELLS Translational Medicine*, vol. 8, no. 3, pp. 215–224, 2019.
- [91] S. Khalifeh Soltani, B. Forogh, N. Ahmadbeigi et al., "Safety and efficacy of allogenic placental mesenchymal stem cells for treating knee osteoarthritis: a pilot study," *Cytotherapy*, vol. 21, no. 1, pp. 54–63, 2019.
- [92] W. M. Gallatin, I. L. Weissman, and E. C. Butcher, "A cell-surface molecule involved in organ-specific homing of lymphocytes," *Nature*, vol. 304, no. 5921, pp. 30–34, 1983.
- [93] Y. Yin, X. Li, X. T. He, R. X. Wu, H. H. Sun, and F. M. Chen, "Leveraging stem cell homing for therapeutic regeneration," *Journal of Dental Research*, vol. 96, no. 6, pp. 601–609, 2017.
- [94] S. Zhang, B. Hu, W. Liu et al., "Articular cartilage regeneration: The role of endogenous mesenchymal stem/progenitor cell recruitment and migration," *Semin Arthritis Rheum*, vol. 50, no. 2, pp. 198–208, 2020.
- [95] J. M. Karp and G. S. Leng Teo, "Mesenchymal stem cell homing: the devil is in the details," *Cell Stem Cell*, vol. 4, no. 3, pp. 206–216, 2009.
- [96] X. Li, X. T. He, Y. Yin, R. X. Wu, B. M. Tian, and F. M. Chen, "Administration of signalling molecules dictates stem cell homing for in situ regeneration," *Journal of Cellular and Molecular Medicine*, vol. 21, no. 12, pp. 3162–3177, 2017.
- [97] M. Li, X. Sun, L. Ma et al., "SDF-1/CXCR4 axis induces human dental pulp stem cell migration through FAK/PI3-K/Akt and GSK3 β / β -catenin pathways," *Scientific Reports*, vol. 7, no. 1, p. 40161, 2017.
- [98] A. A. Peyvandi, N. A. Roozbahany, H. Peyvandi et al., "Critical role of SDF-1/CXCR4 signaling pathway in stem cell homing in the deafened rat cochlea after acoustic trauma," *Neural Regeneration Research*, vol. 13, no. 1, pp. 154–160, 2018.
- [99] W. Zhang, J. Chen, J. Tao et al., "The use of type 1 collagen scaffold containing stromal cell-derived factor-1 to create a matrix environment conducive to partial-thickness cartilage defects repair," *Biomaterials*, vol. 34, no. 3, pp. 713–723, 2013.
- [100] X. Ji, Z. Lei, M. Yuan et al., "Cartilage repair mediated by thermosensitive photocrosslinkable TGF β 1-loaded GM-HPCH via immunomodulating macrophages, recruiting MSCs and promoting chondrogenesis," *Theranostics*, vol. 10, no. 6, pp. 2872–2887, 2020.
- [101] M. S. Park, Y. H. Kim, Y. Jung et al., "In Situ Recruitment of Human Bone Marrow-Derived Mesenchymal Stem Cells Using Chemokines for Articular Cartilage Regeneration," *Cell Transplant*, vol. 24, no. 6, pp. 1067–1083, 2015.
- [102] B. H. Min, M. D. Truong, H. K. Song et al., "Development and Efficacy Testing of a "Hollow Awl" That Leads to Patent Bone Marrow Channels and Greater Mesenchymal Stem Cell Mobilization During Bone Marrow Stimulation Cartilage Repair Surgery," *Arthroscopy*, vol. 33, no. 11, pp. 2045–2051, 2017.
- [103] T. G. Baboolal, A. Khalil-Khan, A. A. Theodorides, O. Wall, E. Jones, and D. McGonagle, "A Novel Arthroscopic Technique for Intraoperative Mobilization of Synovial Mesenchymal Stem Cells," *The American Journal of Sports Medicine*, vol. 46, no. 14, pp. 3532–3540, 2018.
- [104] X. Sun, H. Yin, Y. Wang et al., "In situ articular cartilage regeneration through endogenous reparative cell homing using a functional bone marrow-specific scaffolding system," *ACS Applied Materials & Interfaces*, vol. 10, no. 45, pp. 38715–38728, 2018.
- [105] W. Shi, M. Sun, X. Hu et al., "Structurally and Functionally Optimized Silk-Fibroin-Gelatin Scaffold Using 3D Printing to Repair Cartilage Injury In Vitro and In Vivo," *Advanced Materials*, vol. 29, no. 29, 2017.
- [106] Q. Meng, X. Hu, H. Huang et al., "Microfracture combined with functional pig peritoneum-derived acellular matrix for cartilage repair in rabbit models," *Acta Biomater*, vol. 53, pp. 279–292, 2017.

- [107] G. Kalamegam, A. Memic, E. Budd, M. Abbas, and A. Mobasheri, "A Comprehensive Review of Stem Cells for Cartilage Regeneration in Osteoarthritis," *Advances in Experimental Medicine and Biology*, vol. 1089, pp. 23–36, 2018.
- [108] S. Liu, J. Zhou, X. Zhang et al., "Strategies to optimize adult stem cell therapy for tissue regeneration," *International Journal of Molecular Sciences*, vol. 17, no. 6, 2016.
- [109] S. P. Yu, Z. Wei, and L. Wei, "Preconditioning strategy in stem cell transplantation therapy," *Translational Stroke Research*, vol. 4, no. 1, pp. 76–88, 2013.
- [110] I. A. Silver, "Measurement of pH and ionic composition of pericellular sites," *Philosophical Transactions of the Royal Society of London. B, Biological Sciences*, vol. 271, no. 912, pp. 261–272, 1975.
- [111] M. Pei, "Environmental preconditioning rejuvenates adult stem cells' proliferation and chondrogenic potential," *Biomaterials*, vol. 117, pp. 10–23, 2017.
- [112] G. Pattappa, B. Johnstone, J. Zellner, D. Docheva, and P. Angele, "The Importance of Physioxia in Mesenchymal Stem Cell Chondrogenesis and the Mechanisms Controlling Its Response," *International Journal of Molecular Sciences*, vol. 20, no. 3, p. 484, 2019.
- [113] S. H. Peck, J. R. Bendigo, J. W. Tobias et al., "Hypoxic Preconditioning Enhances Bone Marrow-Derived Mesenchymal Stem Cell Survival in a Low Oxygen and Nutrient-Limited 3D Microenvironment," *Cartilage*, p. 194760351984167, 2019.
- [114] G. Pattappa, J. Krueckel, R. Schewior et al., "Physioxia expanded bone marrow derived mesenchymal stem cells have improved cartilage repair in an early osteoarthritic focal defect model," *Biology*, vol. 9, no. 8, p. 230, 2020.
- [115] M. Kanichai, D. Ferguson, P. J. Prendergast, and V. A. Campbell, "Hypoxia promotes chondrogenesis in rat mesenchymal stem cells: a role for AKT and hypoxia-inducible factor (HIF)-1 α ," *Journal of Cellular Physiology*, vol. 216, no. 3, pp. 708–715, 2008.
- [116] S. Lord-Dufour, I. B. Copland, L. C. Levros Jr. et al., "Evidence for transcriptional regulation of the glucose-6-phosphate transporter by HIF-1 α : Targeting G6PT with mumbaistatin analogs in hypoxic mesenchymal stromal cells," *Stem Cells*, vol. 27, no. 3, pp. 489–497, 2009.
- [117] F. U. Bhatti, A. Mehmood, N. Latief et al., "Vitamin E protects rat mesenchymal stem cells against hydrogen peroxide-induced oxidative stress *in vitro* and improves their therapeutic potential in surgically-induced rat model of osteoarthritis," *Osteoarthritis Cartilage*, vol. 25, no. 2, pp. 321–331, 2017.
- [118] G. Cai, W. Liu, Y. He et al., "Recent advances in kartogenin for cartilage regeneration," *J Drug Target*, vol. 27, no. 1, pp. 28–32, 2019.
- [119] H. Jing, X. Zhang, M. Gao et al., "Kartogenin preconditioning commits mesenchymal stem cells to a precartilaginous stage with enhanced chondrogenic potential by modulating JNK and β -catenin-related pathways," *The FASEB Journal*, vol. 33, no. 4, pp. 5641–5653, 2019.
- [120] H. Jing, X. Zhang, K. Luo et al., "miR-381-abundant small extracellular vesicles derived from kartogenin- preconditioned mesenchymal stem cells promote chondrogenesis of MSCs by targeting TAOK1," *Biomaterials*, vol. 231, p. 119682, 2020.
- [121] L. A. Solchaga, K. Penick, V. M. Goldberg, A. I. Caplan, and J. F. Welter, "Fibroblast growth factor-2 enhances proliferation and delays loss of chondrogenic potential in human adult bone-marrow-derived mesenchymal stem cells," *Tissue Eng Part A*, vol. 16, no. 3, pp. 1009–1019, 2010.
- [122] E. Matsumura, K. Tsuji, K. Komori, H. Koga, I. Sekiya, and T. Muneta, "Pretreatment with IL-1 β enhances proliferation and chondrogenic potential of synovium-derived mesenchymal stem cells," *Cytotherapy*, vol. 19, no. 2, pp. 181–193, 2017.
- [123] K. Yamagata, S. Nakayamada, T. Zhang, X. Zhang, and Y. Tanaka, "Soluble IL-6R promotes chondrogenic differentiation of mesenchymal stem cells to enhance the repair of articular cartilage defects using a rat model for rheumatoid arthritis," *Clin Exp Rheumatol*, vol. 38, no. 4, pp. 670–679, 2020.
- [124] S. Sart, S. N. Agathos, Y. Li, and T. Ma, "Regulation of mesenchymal stem cell 3D microenvironment: From macro to microfluidic bioreactors," *Biotechnol J*, vol. 11, no. 1, pp. 43–57, 2016.
- [125] H. Zhang, Z. L. Li, F. Yang et al., "Radial shockwave treatment promotes human mesenchymal stem cell self-renewal and enhances cartilage healing," *Stem Cell Research & Therapy*, vol. 9, no. 1, 2018.
- [126] N. Sahu, G. Budhiraja, and A. Subramanian, "Preconditioning of mesenchymal stromal cells with low-intensity ultrasound: influence on chondrogenesis and directed SOX9 signaling pathways," *Stem Cell Research & Therapy*, vol. 11, no. 1, p. 6, 2020.
- [127] A. R. Armiento, M. J. Stoddart, M. Alini, and D. Eglin, "Biomaterials for articular cartilage tissue engineering: Learning from biology," *Acta Biomater*, vol. 65, pp. 1–20, 2018.
- [128] B. Cheng, T. Tu, X. Shi et al., "A novel construct with biomechanical flexibility for articular cartilage regeneration," *Stem Cell Res Ther*, vol. 10, no. 1, p. 298, 2019.
- [129] X. Yan, Y. R. Chen, Y. F. Song et al., "Scaffold-based gene therapeutics for osteochondral tissue engineering," *Frontiers in Pharmacology*, vol. 10, no. 1534, 2020.
- [130] V. Graceffa, C. Vinatier, J. Guicheux et al., "State of art and limitations in genetic engineering to induce stable chondrogenic phenotype," *Biotechnology Advances*, vol. 36, no. 7, pp. 1855–1869, 2018.
- [131] X. Guo, Q. Zheng, S. Yang et al., "Repair of full-thickness articular cartilage defects by cultured mesenchymal stem cells transfected with the transforming growth factor beta1 gene," *Biomed Mater*, vol. 1, no. 4, pp. 206–215, 2006.
- [132] F. J. Vizoso, N. Eiro, S. Cid, J. Schneider, and R. Perez-Fernandez, "Mesenchymal stem cell secretome: toward cell-free therapeutic strategies in regenerative medicine," *International Journal of Molecular Sciences*, vol. 18, no. 9, p. 1852, 2017.
- [133] A. González-González, D. García-Sánchez, M. Dotta, J. C. Rodríguez-Rey, and F. M. Pérez-Campo, "Mesenchymal stem cells secretome: The cornerstone of cell-free regenerative medicine," *World Journal of Stem Cells*, vol. 12, no. 12, pp. 1529–1552, 2020.
- [134] C. R. Harrell, C. Fellabaum, N. Jovicic, V. Djonov, N. Arsenijevic, and V. Volarevic, "Molecular Mechanisms Responsible for Therapeutic Potential of Mesenchymal Stem Cell-Derived Secretome," *Cells*, vol. 8, no. 5, p. 467, 2019.
- [135] O. P. B. Wiklander, M. Brennan, J. Lötval, X. O. Breakefield, and S. El Andaloussi, "Advances in therapeutic applications of extracellular vesicles," *Science Translational Medicine*, vol. 11, no. 492, 2019.

- [136] L. M. Doyle and M. Z. Wang, "Overview of Extracellular Vesicles, Their Origin, Composition, Purpose, and Methods for Exosome Isolation and Analysis," *Cells*, vol. 8, no. 7, p. 727, 2019.
- [137] H. Järveläinen, A. Annele Sainio, M. Koulu, T. N. Wight, and R. Penttinen, "Extracellular matrix molecules: potential targets in pharmacotherapy," *Pharmacological Reviews*, vol. 6, no. 2, pp. 198–223, 2009.
- [138] C. W. Cheng, L. D. Solorio, and E. Alsberg, "Decellularized tissue and cell-derived extracellular matrices as scaffolds for orthopaedic tissue engineering," *Biotechnology Advances*, vol. 32, no. 2, pp. 462–484, 2014.
- [139] S. Pérez-Castrillo, M. L. González-Fernández, M. E. López-González, and V. Villar-Suárez, "Effect of ascorbic and chondrogenic derived decellularized extracellular matrix from mesenchymal stem cells on their proliferation, viability and differentiation," *Ann Anat*, vol. 220, pp. 60–69, 2018.
- [140] C. Tang, C. Jin, Y. Xu, B. Wei, and L. Wang, "Chondrogenic Differentiation Could Be Induced by Autologous Bone Marrow Mesenchymal Stem Cell-Derived Extracellular Matrix Scaffolds Without Exogenous Growth Factor," *Tissue Eng Part A*, vol. 22, no. 3-4, pp. 222–232, 2016.
- [141] A. Islam, I. Urbarova, J. A. Bruun, and I. Martinez-Zubiaurre, "Large-scale secretome analyses unveil the superior immunosuppressive phenotype of umbilical cord stromal cells as compared to other adult mesenchymal stromal cells," *European Cells and Materials*, vol. 37, pp. 153–174, 2019.
- [142] J. Ishikawa, N. Takahashi, T. Matsumoto et al., "Factors secreted from dental pulp stem cells show multifaceted benefits for treating experimental rheumatoid arthritis," *Bone*, vol. 83, pp. 210–219, 2016.
- [143] A. G. Kay, G. Long, G. Tyler et al., "Mesenchymal Stem Cell-Conditioned Medium Reduces Disease Severity and Immune Responses in Inflammatory Arthritis," *Scientific Reports*, vol. 7, no. 1, p. 18019, 2017.
- [144] V. Nazemian, H. Manaheji, A. M. Sharifi, and J. Zaringhalam, "Long term treatment by mesenchymal stem cells conditioned medium modulates cellular, molecular and behavioral aspects of adjuvant-induced arthritis," *Cell Mol Biol (Noisy-le-grand)*, vol. 64, no. 1, pp. 19–26, 2018.
- [145] W. Chen, Y. Sun, X. Gu et al., "Conditioned medium of mesenchymal stem cells delays osteoarthritis progression in a rat model by protecting subchondral bone, maintaining matrix homeostasis, and enhancing autophagy," *Journal of Tissue Engineering and Regenerative Medicine*, vol. 13, no. 9, pp. 1618–1628, 2019.
- [146] F. Veronesi, G. Desando, M. Fini et al., "Bone marrow concentrate and expanded mesenchymal stromal cell surnatants as cell-free approaches for the treatment of osteochondral defects in a preclinical animal model," *International Orthopaedics*, vol. 43, no. 1, pp. 25–34, 2019.
- [147] L. Widhiyanto, D. N. Utomo, A. P. Perbowo, K. D. Hernugranto, and Purwati, "Macroscopic and histologic evaluation of cartilage regeneration treated using xenogenic biodegradable porous sponge cartilage scaffold composite supplemented with allogenic adipose derived mesenchymal stem cells (ASCs) and secretome: An in vivo experimental study," *Journal of Biomaterials Applications*, vol. 35, no. 3, pp. 422–429, 2020.
- [148] S. J. Oh, K. U. Choi, S. W. Choi et al., "Comparative analysis of adipose-derived stromal cells and their secretome for auricular cartilage regeneration," *Stem Cells International*, vol. 2020, article 8595940, 2020.
- [149] M. Monguió-Tortajada, M. Morón-Font, A. Gámez-Valero, L. Carreras-Planella, F. E. Borràs, and M. Franquesa, "Extracellular-vesicle isolation from different biological fluids by size-exclusion chromatography," *Curr Protoc Stem Cell Biol*, vol. 49, no. 1, p. e82, 2019.
- [150] E. M. Guerreiro, B. Vestad, L. A. Steffensen et al., "Efficient extracellular vesicle isolation by combining cell media modifications, ultrafiltration, and size-exclusion chromatography," *PLoS One*, vol. 13, no. 9, p. e0204276, 2018.
- [151] S. Y. Kim, T. H. Phan, C. Limantoro, B. Kalionis, and W. Chrzanowski, "Isolation and characterization of extracellular vesicles from mesenchymal stromal cells," *Methods in Molecular Biology*, vol. 2029, pp. 15–23, 2019.
- [152] S. I. Brett, F. Lucien, C. Guo et al., "Immunoaffinity based methods are superior to kits for purification of prostate derived extracellular vesicles from plasma samples," *Prostate*, vol. 77, no. 13, pp. 1335–1343, 2017.
- [153] S. Zhang, S. J. Chuah, R. C. Lai, J. H. P. Hui, S. K. Lim, and W. S. Toh, "MSC exosomes mediate cartilage repair by enhancing proliferation, attenuating apoptosis and modulating immune reactivity," *Biomaterials*, vol. 156, pp. 16–27, 2018.
- [154] S. Cosenza, M. Ruiz, K. Toupet, C. Jorgensen, and D. Noël, "Mesenchymal stem cells derived exosomes and microparticles protect cartilage and bone from degradation in osteoarthritis," *Scientific Reports*, vol. 7, no. 1, p. 16214, 2017.
- [155] Y. Wang, D. Yu, Z. Liu et al., "Exosomes from embryonic mesenchymal stem cells alleviate osteoarthritis through balancing synthesis and degradation of cartilage extracellular matrix," *Stem Cell Research & Therapy*, vol. 8, no. 1, p. 189, 2017.
- [156] J. Wu, L. Kuang, C. Chen et al., "miR-100-5p-abundant exosomes derived from infrapatellar fat pad MSCs protect articular cartilage and ameliorate gait abnormalities via inhibition of mTOR in osteoarthritis," *Biomaterials*, vol. 206, pp. 87–100, 2019.
- [157] Y. Zhu, Y. Wang, B. Zhao et al., "Comparison of exosomes secreted by induced pluripotent stem cell-derived mesenchymal stem cells and synovial membrane-derived mesenchymal stem cells for the treatment of osteoarthritis," *Stem Cell Research & Therapy*, vol. 8, no. 1, p. 64, 2017.
- [158] P. Chen, L. Zheng, Y. Wang et al., "Desktop-stereolithography 3D printing of a radially oriented extracellular matrix/mesenchymal stem cell exosome bioink for osteochondral defect regeneration," *Theranostics*, vol. 9, no. 9, pp. 2439–2459, 2019.
- [159] K. H. Kim, J. H. Jo, H. J. Cho, T. S. Park, and T. M. Kim, "Therapeutic potential of stem cell-derived extracellular vesicles in osteoarthritis: preclinical study findings," *Laboratory animal research*, vol. 36, no. 1, 2020.
- [160] Y. G. Kim, J. Choi, and K. Kim, "Mesenchymal Stem Cell-derived exosomes for effective cartilage tissue repair and treatment of osteoarthritis," *Biotechnology Journal*, vol. 15, no. 12, p. 2000082, 2020.
- [161] E. Mianehsaz, H. R. Mirzaei, M. Mahjoubin-Tehran et al., "Mesenchymal stem cell-derived exosomes: a new therapeutic approach to osteoarthritis?," *Stem Cell Res Ther*, vol. 10, no. 1, 2019.
- [162] S. Eleuteri and A. Fierabracci, "Insights into the secretome of mesenchymal stem cells and its potential applications," *International journal of molecular sciences*, vol. 20, no. 18, p. 4597, 2019.

- [163] W. S. Toh, R. C. Lai, J. H. P. Hui, and S. K. Lim, "MSC exosome as a cell-free MSC therapy for cartilage regeneration: implications for osteoarthritis treatment," *Semin Cell Dev Biol*, vol. 67, pp. 56–64, 2017.
- [164] S.-C. Tao, T. Yuan, Y.-L. Zhang, W.-J. Yin, S.-C. Guo, and C.-Q. Zhang, "Exosomes derived from miR-140-5p-overexpressing human synovial mesenchymal stem cells enhance cartilage tissue regeneration and prevent osteoarthritis of the knee in a rat model," *Theranostics*, vol. 7, no. 1, pp. 180–195, 2017.
- [165] G. Ning, X. Liu, M. Dai, A. Meng, and Q. Wang, "MicroRNA-92a Upholds Bmp Signaling by Targeting *noggin3* during Pharyngeal Cartilage Formation," *Dev Cell*, vol. 24, no. 3, pp. 283–295, 2013.
- [166] C. Hou, Z. Zhang, Z. Zhang et al., "Presence and function of microRNA-92a in chondrogenic ATDC5 and adipose-derived mesenchymal stem cells," *Molecular medicine reports*, vol. 12, no. 4, pp. 4877–4886, 2015.
- [167] O. Ham, B. W. Song, S. Y. Lee et al., "The role of microRNA-23b in the differentiation of MSC into chondrocyte by targeting protein kinase A signaling," *Biomaterials*, vol. 33, no. 18, pp. 4500–4507, 2012.
- [168] F. Meng, Z. Zhang, W. Chen et al., "MicroRNA-320 regulates matrix metalloproteinase-13 expression in chondrogenesis and interleukin-1 β -induced chondrocyte responses," *Osteoarthritis Cartilage*, vol. 24, no. 5, pp. 932–941, 2016.
- [169] E. Ragni, C. Perucca Orfei, P. De Luca et al., "Inflammatory priming enhances mesenchymal stromal cell secretome potential as a clinical product for regenerative medicine approaches through secreted factors and EV-miRNAs: the example of joint disease," *Stem cell research & therapy*, vol. 11, no. 1, pp. 165–165, 2020.
- [170] S. Mardpour, A. A. Hamidieh, S. Taleahmad, F. Sharifzad, A. Taghikhani, and H. Baharvand, "Interaction between mesenchymal stromal cell-derived extracellular vesicles and immune cells by distinct protein content," *Journal of Cellular Physiology*, vol. 234, no. 6, pp. 8249–8258, 2018.
- [171] A. F. Saleh, E. Lázaro-Ibáñez, M. A. Forsgard et al., "Extracellular vesicles induce minimal hepatotoxicity and immunogenicity," *Nanoscale*, vol. 11, no. 14, pp. 6990–7001, 2019.
- [172] S. Y. Chun, J. O. Lim, E. H. Lee et al., "Preparation and characterization of human adipose tissue-derived extracellular matrix, growth factors, and stem cells: a concise review," *Tissue Engineering and Regenerative Medicine*, vol. 16, no. 4, pp. 385–393, 2019.
- [173] J. S. Choi, B. S. Kim, J. D. Kim, Y. C. Choi, H. Y. Lee, and Y. W. Cho, "In vitro cartilage tissue engineering using adipose-derived extracellular matrix scaffolds seeded with adipose-derived stem cells," *Tissue Engineering Part A*, vol. 18, no. 1-2, pp. 80–92, 2012.
- [174] M. Pei and F. He, "Extracellular matrix deposited by synovium-derived stem cells delays replicative senescent chondrocyte dedifferentiation and enhances redifferentiation," *Journal of Cellular Physiology*, vol. 227, no. 5, pp. 2163–2174, 2012.
- [175] Y. Yang, H. Lin, H. Shen, B. Wang, G. Lei, and R. S. Tuan, "Mesenchymal stem cell-derived extracellular matrix enhances chondrogenic phenotype of and cartilage formation by encapsulated chondrocytes *in vitro* and *in vivo*," *Acta Biomater*, vol. 69, pp. 71–82, 2018.
- [176] J. Li, K. C. Hansen, Y. Zhang et al., "Rejuvenation of chondrogenic potential in a young stem cell microenvironment," *Biomaterials*, vol. 35, no. 2, pp. 642–653, 2014.
- [177] C. P. Ng, A. R. Sharif, D. E. Heath et al., "Enhanced *ex vivo* expansion of adult mesenchymal stem cells by fetal mesenchymal stem cell ECM," *Biomaterials*, vol. 35, no. 13, pp. 4046–4057, 2014.
- [178] J. Yan, X. Chen, C. Pu et al., "Synovium stem cell-derived matrix enhances anti-inflammatory properties of rabbit articular chondrocytes via the SIRT1 pathway," *Materials Science and Engineering: C*, vol. 106, p. 110286, 2020.
- [179] C. Tang, C. Jin, X. Li et al., "Evaluation of an autologous bone mesenchymal stem cell-derived extracellular matrix scaffold in a rabbit and minipig model of cartilage repair," *Medical Science Monitor*, vol. 25, pp. 7342–7350, 2019.
- [180] M. Nogami, T. Kimura, S. Seki et al., "A human amnion-derived extracellular matrix-coated cell-free scaffold for cartilage repair: *in vitro* and *in vivo* studies," *Tissue Engineering Part A*, vol. 22, no. 7-8, pp. 680–688, 2016.
- [181] N. Ashammakhi, S. Ahadian, M. A. Darabi et al., "Minimally invasive and regenerative therapeutics," *Advanced Materials*, vol. 31, no. 1, p. e1804041, 2019.
- [182] G. D. Prestwich, "Hyaluronic acid-based clinical biomaterials derived for cell and molecule delivery in regenerative medicine," *Journal of Controlled Release*, vol. 155, no. 2, pp. 193–199, 2011.
- [183] B. J. Klotz, D. Gawlitta, A. Rosenberg, J. Malda, and F. P. W. Melchels, "Gelatin-methacryloyl hydrogels: towards biofabrication-based tissue repair," *Trends Biotechnol*, vol. 34, no. 5, pp. 394–407, 2016.
- [184] P. Rastogi and B. Kandasubramanian, "Review of alginate-based hydrogel bioprinting for application in tissue engineering," *Biofabrication*, vol. 11, no. 4, p. 042001, 2019.
- [185] X. Yang, Z. Lu, H. Wu, W. Li, L. Zheng, and J. Zhao, "Collagen-alginate as bioink for three-dimensional (3D) cell printing based cartilage tissue engineering," *Materials Science and Engineering: C*, vol. 83, pp. 195–201, 2018.
- [186] C. Xia, S. Mei, C. Gu et al., "Decellularized cartilage as a prospective scaffold for cartilage repair," *Materials Science and Engineering: C*, vol. 101, pp. 588–595, 2019.
- [187] G. Musumeci, C. Loreto, S. Castorina, R. Imbesi, R. Leonardi, and P. Castrogiovanni, "New perspectives in the treatment of cartilage damage. Poly(ethylene glycol) diacrylate (PEGDA) scaffold. A review," *Italian Journal of Anatomy and Embryology*, vol. 118, no. 2, pp. 204–210, 2013.
- [188] R. Suntornnond, J. An, and C. K. Chua, "Bioprinting of thermoresponsive hydrogels for next generation tissue engineering: a review," *Macromolecular Materials and Engineering*, vol. 302, no. 1, p. 1600266, 2017.
- [189] Z. Pan and J. Ding, "Poly(lactide-co-glycolide) porous scaffolds for tissue engineering and regenerative medicine," *Interface Focus*, vol. 2, no. 3, pp. 366–377, 2012.
- [190] D. Mondal, M. Griffith, and S. S. Venkatraman, "Polycaprolactone-based biomaterials for tissue engineering and drug delivery: current scenario and challenges," *International Journal of Polymeric Materials and Polymeric Biomaterials*, vol. 65, no. 5, pp. 255–265, 2016.
- [191] M. Cucchiari and H. Madry, "Biomaterial-guided delivery of gene vectors for targeted articular cartilage repair," *Nature Reviews Rheumatology*, vol. 15, no. 1, pp. 18–29, 2019.

- [192] W. S. Toh, M. Spector, E. H. Lee, and T. Cao, "Biomaterial-mediated delivery of microenvironmental cues for repair and regeneration of articular cartilage," *Molecular Pharmaceutics*, vol. 8, no. 4, pp. 994–1001, 2011.
- [193] K. Rezwan, Q. Z. Chen, J. J. Blaker, and A. R. Boccaccini, "Biodegradable and bioactive porous polymer/inorganic composite scaffolds for bone tissue engineering," *Biomaterials*, vol. 27, no. 18, pp. 3413–3431, 2006.
- [194] Y. L. Cui, A. D. Qi, W. G. Liu et al., "Biomimetic surface modification of poly(L-lactic acid) with chitosan and its effects on articular chondrocytes in vitro," *Biomaterials*, vol. 24, no. 21, pp. 3859–3868, 2003.
- [195] G. Chen and N. Kawazoe, "Porous scaffolds for regeneration of cartilage, bone and osteochondral tissue," *Advances in Experimental Medicine and Biology*, vol. 1058, pp. 171–191, 2018.
- [196] G. Chen, T. Sato, T. Ushida, N. Ochiai, and T. Tateishi, "Tissue engineering of cartilage using a hybrid scaffold of synthetic polymer and collagen," *Tissue Engineering*, vol. 10, no. 3-4, pp. 323–330, 2004.
- [197] J. Liao, Y. Qu, B. Chu, X. Zhang, and Z. Qian, "Biodegradable CSMA/PECA/graphene porous hybrid scaffold for cartilage tissue engineering," *Sci Rep*, vol. 5, no. 1, 2015.
- [198] P. Vahedi, L. Roshangar, S. Jarolmasjed, H. Shafaei, N. Samadi, and J. Soleimanirad, "Effect of low-intensity pulsed ultrasound on regenerative potential of transplanted ASCs -PCL construct in articular cartilage defects in sheep," *Indian Journal of Animal Sciences*, vol. 86, no. 10, pp. 1111–1114, 2016.
- [199] N. Fu, T. Dong, A. Meng, Z. Meng, B. Zhu, and Y. Lin, "Research progress of the types and preparation techniques of scaffold materials in cartilage tissue engineering," *Current Stem Cell Research & Therapy*, vol. 13, no. 7, pp. 583–590, 2018.
- [200] Q. Yang, J. Peng, Q. Guo et al., "A cartilage ECM-derived 3-D porous acellular matrix scaffold for in vivo cartilage tissue engineering with PKH26-labeled chondrogenic bone marrow-derived mesenchymal stem cells," *Biomaterials*, vol. 29, no. 15, pp. 2378–2387, 2008.
- [201] X. Zheng, F. Yang, S. Wang et al., "Fabrication and cell affinity of biomimetic structured PLGA/articular cartilage ECM composite scaffold," *Journal of Materials Science: Materials in Medicine*, vol. 22, no. 3, pp. 693–704, 2011.
- [202] X.-F. Zheng, S.-B. Lu, W.-G. Zhang, S.-Y. Liu, J.-X. Huang, and Q.-Y. Guo, "Mesenchymal stem cells on a decellularized cartilage matrix for cartilage tissue engineering," *Biotechnology and Bioprocess Engineering*, vol. 16, no. 3, pp. 593–602, 2011.
- [203] H. Kang, J. Peng, S. Lu et al., "In vivocartilage repair using adipose-derived stem cell-loaded decellularized cartilage ECM scaffolds," *Journal of Tissue Engineering and Regenerative Medicine*, vol. 8, no. 6, pp. 442–453, 2014.
- [204] S. L. Vega, M. Y. Kwon, and J. A. Burdick, "Recent advances in hydrogels for cartilage tissue engineering," *Eur Cell Mater*, vol. 33, pp. 59–75, 2017.
- [205] K. Wei, M. Zhu, Y. Sun et al., "Robust biopolymeric supramolecular "Host-Guest Macromer" hydrogels reinforced by in situ Formed multivalent nanoclusters for cartilage regeneration," *Macromolecules*, vol. 49, no. 3, pp. 866–875, 2016.
- [206] J. Xu, Q. Feng, S. Lin et al., "Injectable stem cell-laden supramolecular hydrogels enhance in situ osteochondral regeneration via the sustained co-delivery of hydrophilic and hydrophobic chondrogenic molecules," *Biomaterials*, vol. 210, pp. 51–61, 2019.
- [207] A. K. Jha, K. M. Tharp, S. Browne et al., "Matrix metalloproteinase-13 mediated degradation of hyaluronic acid-based matrices orchestrates stem cell engraftment through vascular integration," *Biomaterials*, vol. 89, pp. 136–147, 2016.
- [208] P. D. Tatman, W. Gerull, S. Sweeney-Easter, J. I. Davis, A. O. Gee, and D. H. Kim, "Multiscale biofabrication of articular cartilage: bioinspired and biomimetic approaches," *Tissue Engineering Part B: Reviews*, vol. 21, no. 6, pp. 543–559, 2015.
- [209] J. A. McIntyre, I. A. Jones, B. Han, and C. T. Vangsness Jr., "Intra-articular mesenchymal stem cell therapy for the human joint: a systematic review," *The American Journal of Sports Medicine*, vol. 46, no. 14, pp. 3550–3563, 2018.
- [210] A. Vega, M. A. Martín-Ferrero, F. Del Canto et al., "Treatment of knee osteoarthritis with allogeneic bone marrow mesenchymal stem cells: a randomized controlled trial," *Transplantation*, vol. 99, no. 8, pp. 1681–1690, 2015.
- [211] L. A. Costa, N. Eiro, M. Fraile et al., "Functional heterogeneity of mesenchymal stem cells from natural niches to culture conditions: implications for further clinical uses," *Cellular and Molecular Life Sciences*, 2020.
- [212] R. N. Judson, M. Quarta, M. J. Oudhoff et al., "Inhibition of Methyltransferase Setd7 Allows the In Vitro Expansion of Myogenic Stem Cells with Improved Therapeutic Potential," *Cell Stem Cell*, vol. 22, no. 2, pp. 177–190.e7, 2018.
- [213] I. Tessaro, V. T. Nguyen, A. Di Giancamillo et al., "Animal models for cartilage repair," *Journal of Biological Regulators & Homeostatic Agents*, vol. 32, no. 6, Supplemet. 1, pp. 105–116, 2018.
- [214] A. B. Dawson, "The age order of epiphyseal union in the long bones of the albino rat," *The Anatomical Record*, vol. 31, no. 1, pp. 1–17, 1925.
- [215] S. Kamerkar, V. S. LeBleu, H. Sugimoto et al., "Exosomes facilitate therapeutic targeting of oncogenic KRAS in pancreatic cancer," *Nature*, vol. 546, no. 7659, pp. 498–503, 2017.
- [216] S. el Andaloussi, I. Mäger, X. O. Breakefield, and M. J. A. Wood, "Extracellular vesicles: biology and emerging therapeutic opportunities," *Nature Reviews Drug Discovery*, vol. 12, no. 5, pp. 347–357, 2013.
- [217] Z. Yang, J. Shi, J. Xie et al., "Large-scale generation of functional mRNA-encapsulating exosomes via cellular nanoporation," *Nature Biomedical Engineering*, vol. 4, no. 1, pp. 69–83, 2020.
- [218] G. Knutsen, L. Engebretsen, T. C. Ludvigsen et al., "Autologous chondrocyte implantation compared with microfracture in the knee. A randomized trial," *The Journal of Bone & Joint Surgery*, vol. 86, no. 3, pp. 455–464, 2004.
- [219] A. R. Armiento, M. Alini, and M. J. Stoddart, "Articular fibrocartilage - why does hyaline cartilage fail to repair?," *Adv Drug Deliv Rev*, vol. 146, pp. 289–305, 2019.
- [220] A. D. Berendsen and B. R. Olsen, "Bone development," *Bone*, vol. 80, pp. 14–18, 2015.
- [221] M. P. Murphy, L. S. Koepke, M. T. Lopez et al., "Articular cartilage regeneration by activated skeletal stem cells," *Nature Medicine*, vol. 26, no. 10, pp. 1583–1592, 2020.

Review Article

Bioengineering Approaches to Accelerate Clinical Translation of Stem Cell Therapies Treating Osteochondral Diseases

Meng Wang , Yixuan Luo , Yin Yu , and Fei Chen 

CAS Key Laboratory of Quantitative Engineering Biology, Shenzhen Institute of Synthetic Biology, Shenzhen Institutes of Advanced Technology, Chinese Academy of Sciences, Shenzhen 518055, China

Correspondence should be addressed to Yin Yu; yin.yu@siat.ac.cn and Fei Chen; fei.chen1@siat.ac.cn

Received 25 September 2020; Revised 17 November 2020; Accepted 12 December 2020; Published 24 December 2020

Academic Editor: Zhenxing Shao

Copyright © 2020 Meng Wang et al. This is an open access article distributed under the Creative Commons Attribution License, which permits unrestricted use, distribution, and reproduction in any medium, provided the original work is properly cited.

The osteochondral tissue is an interface between articular cartilage and bone. The diverse composition, mechanical properties, and cell phenotype in these two tissues pose a big challenge for the reconstruction of the defected interface. Due to the availability and inherent regenerative therapeutic properties, stem cells provide tremendous promise to repair osteochondral defect. This review is aimed at highlighting recent progress in utilizing bioengineering approaches to improve stem cell therapies for osteochondral diseases, which include microgel encapsulation, adhesive bioinks, and bioprinting to control the administration and distribution. We will also explore utilizing synthetic biology tools to control the differentiation fate and deliver therapeutic biomolecules to modulate the immune response. Finally, future directions and opportunities in the development of more potent and predictable stem cell therapies for osteochondral repair are discussed.

1. Introduction

Despite four decades of advances and achievements in the field of tissue engineering, reconstructing interfacial tissues such as bone-articular cartilage remains a significant challenge. Bone-articular cartilage, also known as osteochondral tissue, consists of cartilage, a calcified cartilage layer, and the subchondral bone with a proportion of 90%, 5%, and 5%, respectively. In severe traumatic incidents, both the cartilage and the subchondral bone are affected. Due to the ready availability and multipotent character, stem cells, especially mesenchymal stem cells, have become a focus in the field of osteochondral tissue engineering. However, the major obstacles to the construction of clinically useful osteochondral tissue are our inability to control the stem cell fate, differentiation to the extent needed, and the poor integration between engineered and host tissues after construct implantation.

In this review, we explore major clinical challenges for stem cell therapies toward joint preservation including administration and distribution, control of stem cell differentiation, and modulating a regenerative microenvironment. Under these challenges, we discuss several examples that

leverage bioengineering approaches to improve stem cell therapies for osteochondral diseases. We will first discuss approaches of engineering biomimetic microenvironments to improve cell delivery and patterning, which include microgel encapsulation, bioadhesive inks, and 3D bioprinting to achieve accurate cell deposition and gradient living constructs. We will then discuss several examples of bioengineering strategies to engineer cells to control the differentiation fate and deliver therapeutic biomolecules to modulate the immune response. Finally, we will share our perspectives on the future endeavor to develop more potent and predictable MSC therapies.

2. Overcoming Clinical Challenges from Administration and Distribution

2.1. Challenges Associated with Local Administration and Distribution. The damage of osteochondral tissue is one of the major causes of osteoarthritis (OA), which is affecting the life quality of ~61.2 million people in China alone [1]. To repair and reconstruct osteochondral lesions for preventing OA progression, the replication of the innate physiological structure, function, and living milieu of cartilage and the

subchondral bone is of significant importance. Currently, clinical strategies for the regeneration of osteochondral tissue such as abrasion arthroplasty, microfracture, and articular chondrocyte transplantation have received positive results in midterm follow-up periods. However, the long-term efficacy of these approaches is still unsatisfying due to the generation of fibrocartilage and poor integration between transplants and resident tissue [2]. In addition, adult cell-based therapies, such as autologous chondrocyte implantation (ACI), are restricted by cell availability and expansion potency. Stem cells, most commonly found in the embryo, bone marrow, adipose tissue, and synovium, have differentiation capability toward chondrocytes and osteoblasts under specific biochemical and biomechanical stimulation, which have offered a new platform for osteochondral regeneration and OA treatment in both preclinical and clinical situations. Local administration of MSCs, providing a straight path to the target site, is commonly utilized in OA clinical indications. For example, Mayo Clinic is using single and multiple injections of the culture-expanded autologous adipose-derived mesenchymal stromal cells (AMSCs) for investigating the safety and feasibility of treatment in mild to severe knee OA, which is currently in Phase I of the interventional clinical trial. Researchers from Ren Ji Hospital and the cooperating unit established a preclinical study to explore the efficacy and safety of human AMSC injection in intra-articular cartilage for the relief of OA symptoms (5×10^7 MSCs showed the best improvement) [3]. However, the therapeutic efficacy is still hampered; the dominant barriers are (1) the need for large dosages of cells (the dose normally ranges from 10^6 to 10^9 cells/injection), partly because of the short residence time after depositing to tissue sites [4, 5], and (2) the low cell survival rate caused by multireasons, including severe shear stress formed in the process of viscous hydrogel precursor injection [6, 7], hostile and immune microenvironment at the disease site, and insufficient nutrients and oxygen supply, which have been reviewed elsewhere [8]. In this section, we will first discuss different bioengineering strategies used to improve the survival rate and retention of stem cells in osteochondral lesions and further discuss the potential of employing various biomanufacture systems, such as 3D bioprinting, to accurately deposit stem cells and form gradient complex tissues.

2.2. Strategies to Improve Viability of MSCs by Encapsulation.

Local administration of MSCs is a favored delivery approach compared to systemic delivery as it is easier to access the disease site and results in better therapeutic outcomes. However, insufficient retention and survival of transplanted MSCs at the diseased sites hampered its therapeutic efficacy. Using biomaterials to encapsulate MSCs is a promising approach to increase the retention and viability at the infarction site [9].

Cell encapsulation within microgels (~ 1 - $1000 \mu\text{m}$) offers many advantages compared to encapsulation in bulk hydrogels [10] as it can supply an ECM-like 3D milieu for cell culture and expansion [11]; the micrometer-sized pockets of interstitial space between microgels can provide good diffusion of nutrients and oxygen [12]; most importantly, it can

physically protect encapsulated cells from shear stress during injection. For example, under the same injection rate (15 ml/h), cell viability of BMSCs encapsulated in gelatin/hyaluronic acid hybrid microgels (67.5%) was higher than the medium suspended one (15%), meanwhile maintaining normal cellular functions, such as cell proliferation and chondrogenic abilities (Figures 1(a) and 1(b)) [13]. Similar phenomena were also observed in the bone regeneration study. In Hou and coworkers' work, poly(vinyl alcohol)-based microgels were developed for encapsulating MSCs and BMP-2 growth factor (GF) to induce osteogenic differentiation; high cell bioactivity and sustained release of GF were obtained by optimizing the crosslinking conditions of microgels, which ensured a specific and upregulated osteogenic differentiation and hence more efficient bone regeneration [14]. In terms of immune response, one interesting study found that geometry of implanted microgels could affect foreign body immune response and fibrosis in rodent and nonhuman primate models [15].

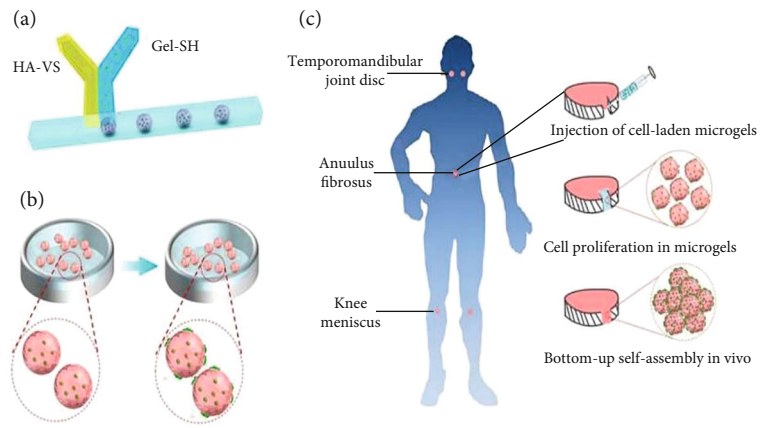
Although microgels can improve stem cell viability and enhance regeneration efficacy of cartilage and bone through physical protection and increased nutrition diffusion, the mechanical properties of assembled microgels are usually weak which cannot withstand physiological mechanical loads in osteochondral interfaces. Researchers recently reported a new strategy called triggered micropore-forming bioprinting (Figure 1(c)), to improve cell viability through microscopic pore formation in bulk hydrogel while preserving superior mechanical robustness (Figure 1(d)) [16]. The micropores were formed by temperature-triggered microphase separation and stabilized by hydrogen bonds of chitosan. Without sacrificing mechanical robustness, the bioprinted scaffold with interconnected pores ($\sim 17.8 \mu\text{m}$) supports cell spreading, migration, and proliferation. Impressively, the stiffness and viscoelasticity of the scaffold can be orthogonally controlled through a slight change of pH and the amount of PEG in the bioink. Though this system is yet to be applied in cartilage or osteochondral regeneration, it demonstrated potential of improving stem cell viability and maintaining mechanical robustness of porous hydrogel simultaneously.

Collectively, the approaches of microencapsulation and micropore-forming bioprinting may promote the efficacy of stem cell therapy via increasing the survival rate and reducing needed dosages of stem cells.

2.3. Strategies to Improve the Persistence of MSCs in the Host.

Cartilage is surrounded by synovial fluid and acts as a load-bearing buffer which protects the bone and disperses shock and stress. To achieve the regenerative properties of stem cells, retention of injected stem cells at the dynamic defect site is vital for successful tissue regeneration. Strategies have been developed to improve stem cell retention in situ through different forms and types of biomaterials [17].

One strategy is to incorporate mussel-inspired adhesives into the stem cell-based grafts. For example, Han et al. developed a polydopamine (PDA) modified chondroitin sulfate-(CS-) polyacrylamide (PAM) hydrogels with tissue adhesiveness for cartilage regeneration (see Figures 2(a) and 2(b)). The composite hydrogel exhibited good resilience and

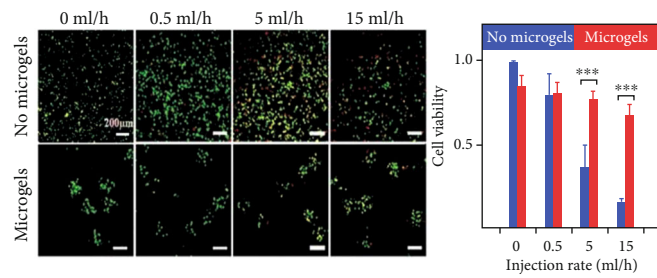


(a)

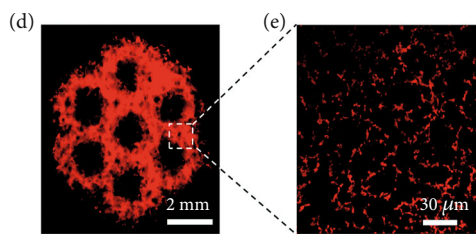
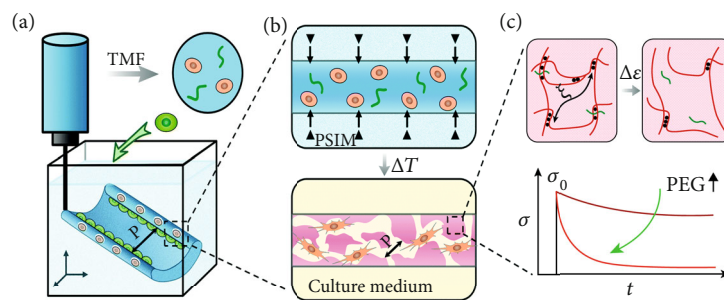
(a) Injection and self-assembly of BMSC-laden microgels in vitro



(b) BMSC viability after injection



(b)



- Cell-laden bioink
- PSIM
- Cell in macropores
- Phase separation inducer
- PEG
- Polymeric chain

(c)

FIGURE 1: Continued.

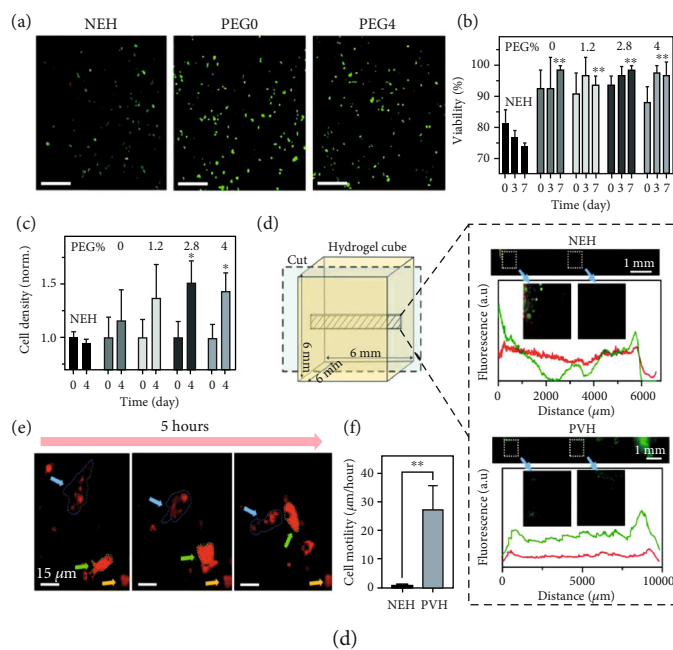


FIGURE 1: Encapsulation techniques for improving stem cell viability. (a) Microgel encapsulating stem cells can self-assemble into 3D microporous scaffold and (b) maintain high cell viability and chondrogenic differentiation potential. (c) Triggered micropore-forming bioprinting strategy improved cell viability compared to bulk hydrogel and (d) cell migration in micropore hydrogels. Reproduced with permission [13, 16].

toughness because of the noncovalent interaction between PDA and CS and covalently crosslinked PAM network [18].

Similar to mussel-inspired catechol chemistry, gallol moieties which possess aromatic rings with three hydroxyl groups have recently been incorporated into cell-carrying hydrogels to achieve adhesive property. Shin et al. [19] developed gallol-modified ECM hydrogel inks which exhibited fast covalent crosslinking and tissue adhesion. The manufactured bioink maintained ~95% of cell viability after printing and can be printed on tissue substrates due to the adhesion of gallol groups to ECM. However, the mechanical property of gallol modified ECM hydrogel is much lower than the native cartilage. Furthermore, a high dose of the gallol group is cytotoxic to cells, which has been reported in previous research by the same research group [20]. Thus, the usage of gallol to synthesizing adhesive cell-loading inks should be further carefully evaluated in preclinical studies.

Another mechanism employed to prolong the residence time of stem cells is to develop a cell carrier with specific functional groups (e.g., aldehyde) which could react with amino groups on the surface of cartilage tissue. Zhou et al. studied an oxidized dextran- (ODex-) based construct for cartilage defect repair [21]. In this study, ODex not only make up the scaffold network via reacting with gelatin for superior mechanical performance but also formed good tissue adhesion by reacting with amino groups existing on the cartilage, which further promoted the integration of transplants and host osteochondral lesions. However, a high degree of aldehyde substitution to the dextran backbone is harmful to cells; thus, it is essential to shorten the duration of stem cells in the aldehyde environment. Yang et al. and colleagues prepared a novel phototriggered imine reaction

to resolve the above limitations (see Figure 2(c)). In this system, o-nitrosobenzene (NB) can be transferred to NB-aldehyde under the exposure of 365 nm light and immediately crosslink with $-NH_2$ in the polymer or surface of surrounding tissue [22]. This kind of phototriggered adhesive mechanism offers a good spatiotemporal control on cell viability, tissue adhesion, and tissue integration, providing a new strategy to prolong the retention time of stem cells in host tissue and facilitate seamless tissue integration for osteochondral regeneration.

In the future, there are opportunities to endow adhesive features to the microgel systems. It would be interesting and meaningful for endogenous repair as the adhesive microgels could adhere to the target tissue while facilitating endogenous cell infiltration to the microgel scaffold.

2.4. Accurate Cell Patterning to Improve Osteochondral Tissue Regeneration. Osteochondral tissue exhibits spatial gradients from the articulating surface to the underlying bone, with graded densities of chondrocytes, hypertrophic chondrocytes, and osteoblasts. These graded cell populations in osteochondral tissue secrete different ECM components that provide the tissue with spatial gradient mechanical properties to withstand the dynamic load-bearing environment. Thus, fabricating biomaterials and cell gradients to replicate the native gradient structures of osteochondral tissue is of critical importance in functional osteochondral tissue engineering [5].

3D bioprinting (3DBP), in which cells can be printed in either biomaterial-based or biomaterial-free bioink, has been extensively investigated in manufacturing desired topographies of osteochondral tissues [23, 24]. 3DBP uses

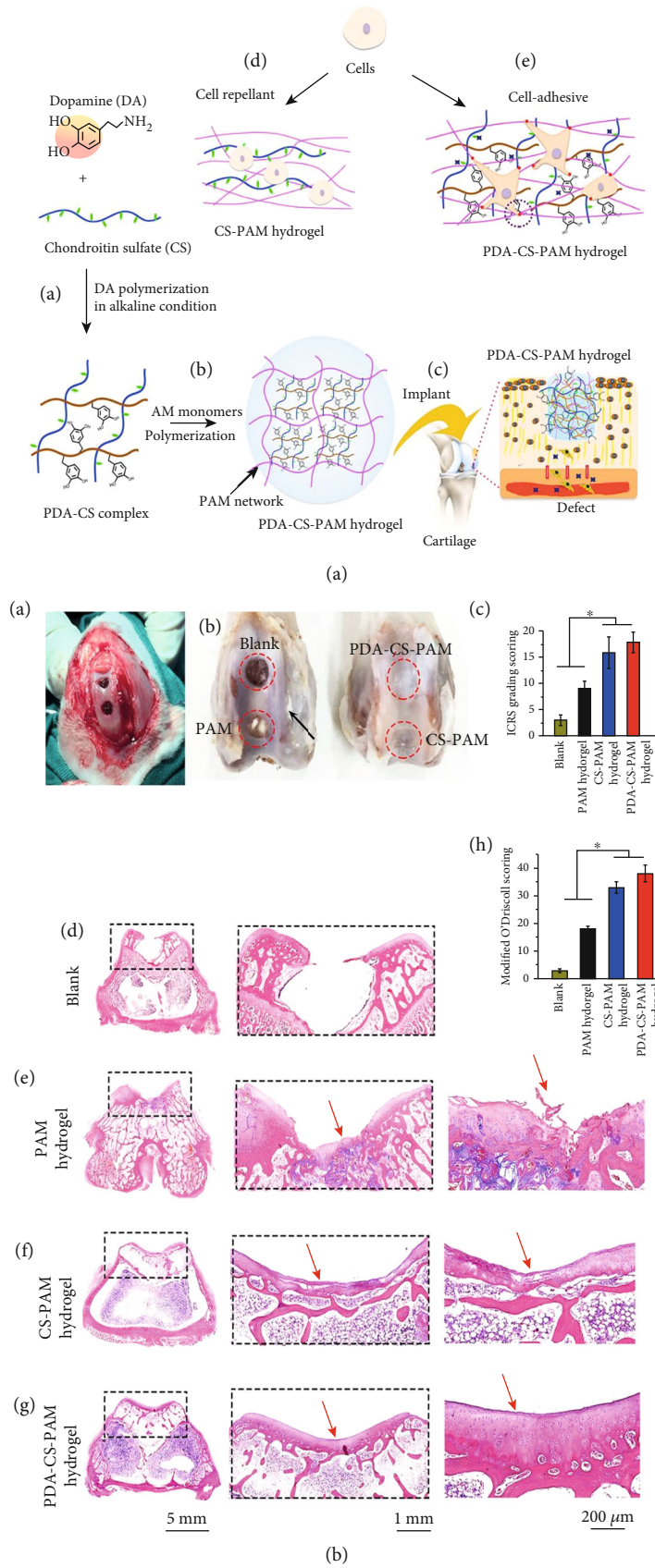


FIGURE 2: Continued.

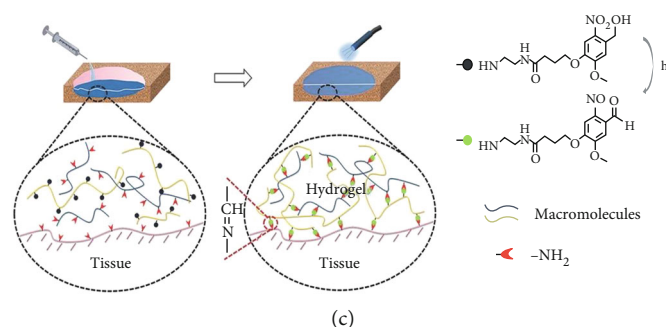


FIGURE 2: Adhesive hydrogels for improving the persistence of MSCs in the host. (a) Mussel-inspired tissue-adhesive cell carriers; (b) assessment of mussel-inspired tissue-adhesive cell carriers used in cartilage regeneration; (c) phototriggered tissue-integrable hydrogel developed for prolonging stem cell retention in situ. Reproduced with permission [18, 22].

multiheads to precisely deposit multibiopinks; thus, diverse growth factors and cell types can be printed to the defect site according to the defined pattern and layer. For instance, a specific amount of MSCs and chondrocytes were accurately deposited in well-designed and printed microchambers to form cartilage, which possess comparable architecture, composition, and biomechanical performances to the native cartilage tissue according to histological, immunohistochemical, and mechanical analysis. Furthermore, this system was also applied in the building of entire articular osteochondral tissue based on the construct of endochondral bone, which showed a stratified region of cartilage and bone by significant distinct content of GAG and calcium deposition [25].

The inclusion of cells within the bioink is capable of directly fabricating defined cellular gradients, although spatiotemporal control of cell differentiation toward chondrocytes and osteoblast in bioink is still a big challenge. As an alternative, MSCs can be first differentiated into chondrogenic and osteogenic spheroids, respectively, and then accurately positioned to mimic the osteochondral structure. Ayan and coworkers recently developed a scaffold-free bioprinting approach to fabricate a dual-layered fused osteochondral interface through a homemade aspiration-assisted bioprinting (AAB) apparatus (Figure 3(a)) [26]. To reconstruct the osteochondral tissue, osteogenic spheroids and chondrogenic spheroids were first separately generated by the differentiation of human adipose-derived stem cells (ADSCs) in 3D culture. The OC interface was then bioprinted by first deposition of a layer of osteogenic spheroids onto a sacrificial support material (alginate crosslinked by CaCl_2 vapor). Subsequently, another layer of chondrogenic spheroids was deposited onto a previous osteogenic layer. It is worth noting that the spheroids in individual layers can fuse together and the phenotypes in both zones can maintain through the study (Figure 3(b)) [27]. Similar to cell spheroids, different microgels encapsulating stem cells can be utilized as building blocks to form a predefined tissue with a spatial controlled cell type and gradient structure [12, 28, 29].

In short, biomaterial-based or biomaterial-free 3D bioprinting is promising in recreating gradient biochemical or biomechanical structures of osteochondral tissues. However, few challenges remain for applications of these artificial osteochondral constructs in the clinic. For example, Young's

modulus [13] of most biomaterial-based stem cell implants is significantly lower than the natural articular cartilage (0.5–1.5 MPa) and bone tissue (15–20 MPa) [30, 31]. Integration force between engineered cartilage and subchondral bone as well as engineered osteochondral tissue with underlying native tissue is insufficient. In addition, facile and large-scale stem cell assembly techniques need to be developed for the creation of personalized constructs in clinic. Nevertheless, the precise assembly of stem cells with or without the aid of biomaterial provides a promising means to mimic the spatial complexity of the osteochondral tissue, which can be utilized not only in tissue engineering but also in drug testing and disease modeling.

3. Overcoming Clinical Challenges from Controlling Stem Cell Differentiation

3.1. Challenges Associated with Stem Cell Differentiation. The multidirectional differentiation potential makes MSCs become a sufficient source of seed cells for osteochondral tissue engineering and other disease therapies, but the precise control of cell differentiation in vitro and in vivo has been a huge challenge [32, 33]. The successful differentiation of stem cells involves many aspects, such as the interactions of MSCs to biomaterial scaffold, which we discussed in Section 2, biomolecular cues (growth factors, cytokines, trophic factors, etc.), and the applied culture systems [34, 35]. During developing an integrated multiphase tissue, crosstalk of signaling or potential interference between the different phases has a significant impact on the quality of engineered tissue. For instance, codelivery of genes of BMP-2 and TGF- β 3 and to build an osteochondral construct may obtain insufficient cartilage forming or calcium deposition compared to individual delivery, because there can be antagonistic effects between chondrogenic and osteogenic growth factors [36]. In this regard, cellular engineering approaches including spatiotemporal control of transgene overexpression play increasing roles to control cell growth and differentiation, and we will examine few examples below to address these important questions.

3.2. Precise Control of MSC Differentiation with Spatial Gene Delivery for Osteochondral Regeneration. The repair of osteochondral defects involves the simultaneous regeneration of

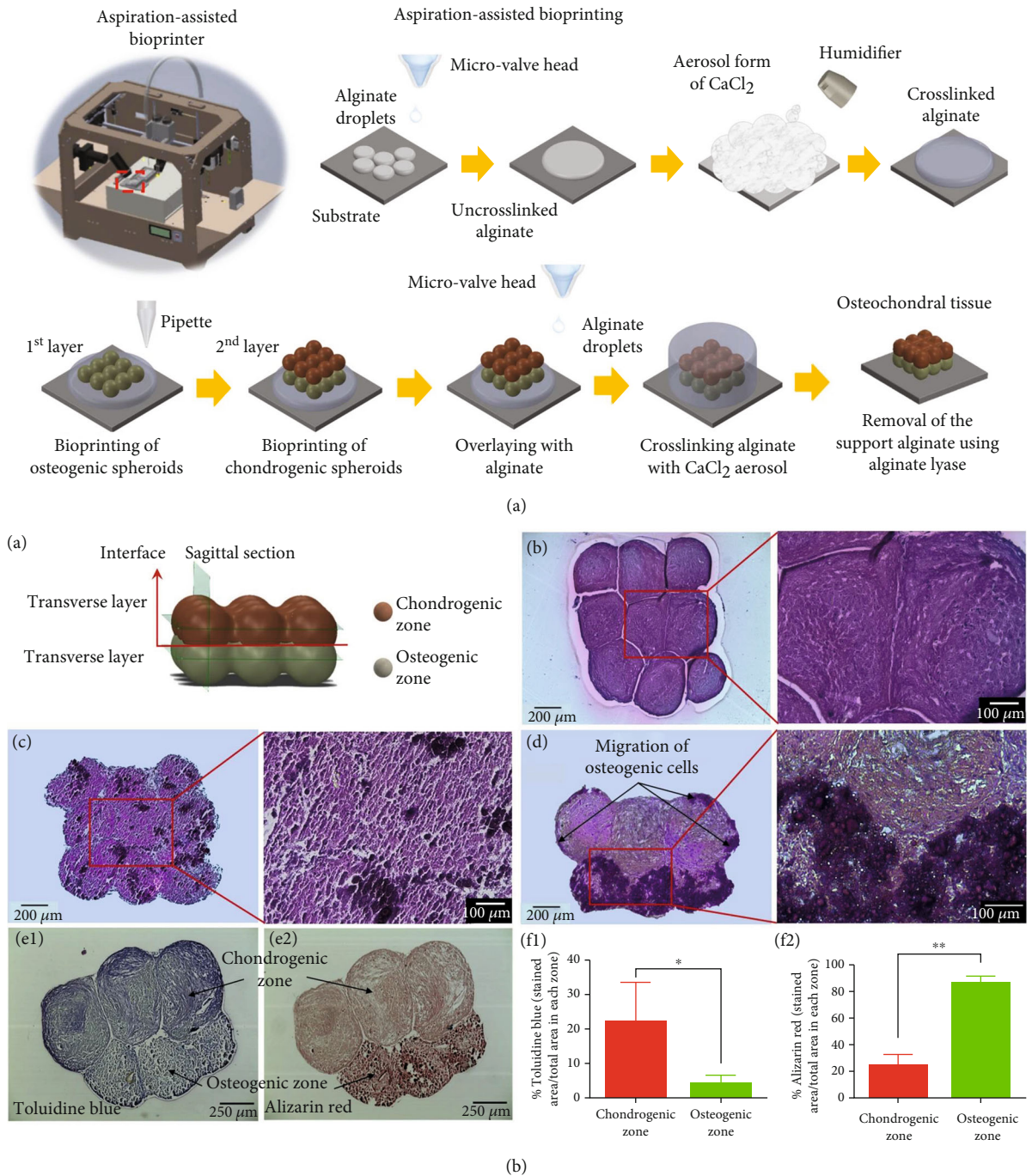


FIGURE 3: 3D biomanufacture strategy used in stem cell accurate pattern to improve the efficiency of osteochondral tissue recapitulation. (a) Aspiration-assisted bioprinting process of osteochondral (OC) interface. (b) Characteristics of the bioprinted OC interface and the zone of cartilage and subchondral bone. Reproduced with permission [26, 27].

bone and cartilage. Correspondingly, MSCs need to be differentiated into chondrocytes and osteocytes. Traditionally, MSCs were, respectively, predifferentiated by the culture media containing specific growth factors. More recently, these bioactive proteins that drive the MSCs toward specific cell types have been directly embedded into the biomaterial scaffold. However, it is difficult to control the dose and spatial distribution of the growth factor in the scaffold device, and the proteins have a relatively short half-life in vivo [37, 38].

Therefore, gene delivery via viral or nonviral approaches has attracted considerable attention. Such genetic modification has the potential to produce high levels of expression of growth and transcription factors over long periods [39]. It is still difficult to, respectively, direct cell fate into certain lineages (i.e., cartilage and bone) using only one biomaterial scaffold from the same cell source, in a single culture system. To address this challenge, Huynh et al. [40] developed a method to induce osteogenic and chondrogenic differentiation of

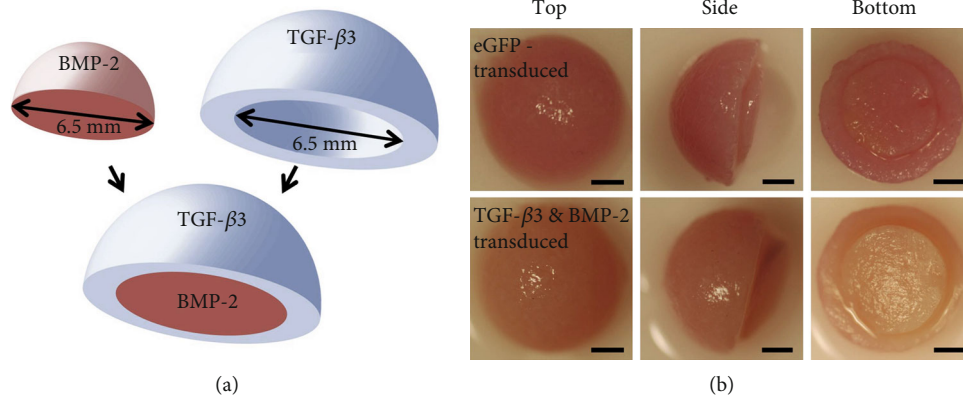


FIGURE 4: Osteochondral constructs. (a) Schematic diagram of fusing concentric hemispheres with embedded lentivirus of TGF- β 3 and BMP-2. (b) Pictures of eGFP-transduced or TGF- β 3+BMP-2-transduced constructs from 3 different angles. Scale: 2 mm. Reproduced with permission [48].

MSCs on two independent 3D woven PCL scaffolds in one single culture system. In general, TGF- β 3 and BMP-2 are used to induce MSC chondrogenesis and osteogenesis, respectively [41, 42]. However, mothers against DPP homolog 3 (SMAD3) downstream of the TGF- β 3 signaling pathway can repress Runt-related transcription factor (Runx2), which has great osteogenic capacity [43, 44]. Therefore, in this study, TGF- β 3 was supplemented in a specific chondrogenic environment to promote the production of GAG and COL II on one scaffold. On the other scaffold, to inhibit the effects of chondrogenic-inducing TGF- β 3 signaling, engineered MSCs overexpressing RUNX2 with knockdown of SMAD3 genes were prepared to generate a mineralized matrix in the same culture condition. This method could develop a bilayered scaffold with a layer of cartilage on top of a layer of bone below. In theory, the delivery of DNA plasmids coding tissue-specific inducing factors from multiphasic scaffold may be able to spatially facilitate cellular differentiation processes and further the regeneration of complex tissue structures [45]. Another research showed that the MSCs in different layers could also be induced to differentiate into chondrocytes and osteoblasts to form a bilayered osteochondral structure in vitro. This scaffold consists of one chitosan-gelatin scaffold layer activated by plasmid TGF- β 1 for chondrogenic and the other hydroxyapatite/chitosan-gelatin scaffold layer activated by plasmid BMP-2 for osteogenic, respectively. And it was able to facilitate the regeneration of articular cartilage and subchondral bone in vivo simultaneously [46].

As a further attempt to spatially and temporally control the presentation of therapeutic genes to stem cells, Gonzalez-Fernandez and colleagues [47] developed a new pore-forming bioink combined with DNA plasmids encoding for either chondrogenic or osteogenic genes. By blending fast and slow degrading hydrogels, bioinks with increased porosity over time were achieved. The researchers found that the release rate of encapsulated pDNA in pore-forming bioink was higher than in solid inks; thus, it was possible to achieve transfection of transfected or host cells in either rapid and transient manner or slower and more sustained manner by modulating the porosity of these bioinks. Furthermore,

these 3D bioprinted tissues could form a vascularized, bilayered, and stable osteochondral implant in vivo.

Another major challenge in developing successful constructs for osteochondral defect repair is to match the scaffold degradation rate with the neotissue formation. Toward this objective, Rowland and colleagues [48] recently developed constructs to suppress abnormal inflammatory response induced by the cytokine interleukin-1 (IL-1). They developed fusing concentric cartilage-derived matrix (CDM) hemispheres seeded with MSCs, overexpressing BMP-2 and TGF- β 3 in addition with a doxycycline-inducible IL-1 receptor antagonist (IL-1Ra) transgene via the delivery of lentiviral particles. Their findings demonstrated that the gene delivery and the release of IL-1Ra effectively promoted the osteochondral tissue formation and protected the structure from degradation caused by the aberrant inflammation (Figure 4).

In summary, spatiotemporal delivery of therapeutic genes to locally control the differentiation of stem cells in vivo is a promising approach for the regeneration of osteochondral tissue. However, further effort needs to be focused on improving the transfection efficiency of the transfected cells and their immobilization at the site of action. Besides, the transgene combination and control of gene delivery need to be optimized to obtain better results during the tissue regeneration processes [49, 50].

4. Overcoming Clinical Challenges from Modulating a Regenerating Microenvironment

4.1. Challenges Associated with Host Factors. Although the administration and engineering of stem cells themselves are important to cell therapies, the host factors (local or systematic cytotoxic response, inflammation conditions, microenvironment, etc.) have also been shown to have a considerable influence on the biological fate and efficacy of stem cells in clinical trials [51]. For example, recipient cytotoxic response against the infused MSCs plays an important role in mediating the cell therapies. A study showed that hMSCs were

phagocytized by monocytes after injected into a mouse model after 24 h, and this further promoted the immunotolerance by systemic immunoregulatory phenotype in the host [52]. The different stages and microenvironments of disease progression also can lead to the different effects of MSC therapies. During the progression of the disease, the internal microenvironment of inflammation, hypoxia, and many other pathological factors are dynamic, and it is difficult to take samples routinely from acutely ill patients [53]. Therefore, it is necessary to fully consider the impact of the host dynamic microenvironment on MSCs when applying them in therapies.

4.2. MSC Priming to Boost Their Potency toward Therapeutic Applications. Many studies have demonstrated that in order to exogenously boost the immunomodulatory function and clinical potency, MSC can be primed with proinflammatory cytokines or growth factors [54, 55]. For example, a soluble proinflammatory cytokine IFN- γ may affect adipogenesis and osteogenesis of MSCs [56]. Several IFN- γ -inducible genes such as Runx2 were found to upregulate during the early stage of osteogenic differentiation of BMSCs [57]. Besides, IFN- γ plays an important role in promoting the anti-inflammatory activity of MSCs. As reported, priming with IFN- γ , mouse MSCs (mMSCs) upregulated the expression of enzyme indolamine 2,3-dioxygenase (IDO), which has been shown to suppress T-cell activity in the early stage. And some important immunomodulatory molecules, including CCL2, PGE2, TGF- β , and HGF, were secreted from the primed mMSCs [58]. Another research suggested that the activation of the STAT1/STAT3 signaling pathway and inhibition of the mTOR signaling pathway facilitated the immunosuppressive properties of mMSC primed with IFN- γ . Also, the immunoregulatory ability was enhanced by the repression of the mTOR pathway in hMSCs [59]. As for the other cytokines, the alkaline phosphate activity and bone mineralization of MSCs were promoted when primed with LPS/TNF- α [60, 61]. Redondo-Castro et al. found that when treated with conditioned media of IL-1 primed MSC, murine BV2 cells secreted more trophic factors such as G-CSF and anti-inflammatory mediators such as IL-10, but less proinflammatory cytokines such as IL-6 and TNF- α [62]. Moreover, MSCs derived from AT, BM, or foreskin exhibited different expression levels of the immunoregulatory genes (IDO1, SEMA4D, FGL2, SEMA7A, and GAL) when primed with a proinflammatory cytokine mixture (IFN- γ , IL-1 β , IFN- α , and TNF- α) [63, 64].

Since MSCs are highly sensitive to the harsh environment and will get function loss after cryopreservation during the preclinical or clinical trials, priming may help to improve the therapeutic potential of MSCs to target the biological properties of MSCs. In clinical translation, MSC priming still has many limitations, such as high costs, the harm of immunogenicity, unstable effects depending on the source and donor of MSCs, and the tumorigenic potential effect of MSCs treated with priming approaches during the long-term trials.

4.3. Engineered Stem Cells for Self-Regulated Drug Delivery Responding to an Inflammatory Environment. In addition

to the osteochondral defect, both systemic and local inflammations may also have a profound impact on the pathogenesis of OA and other diseases. Although the proper pretreating with cytokines is beneficial to the immunomodulatory effect of MSCs, aberrant and continuously increased levels of proinflammatory cytokines such as interleukin-1 (IL-1), IL-6, IL-17, and tumor necrosis factor (TNF) can lead to the suppression of cartilage-specific genes and proteoglycan formation, in addition to the degeneration of the extracellular matrix (ECM). Furthermore, IL-1-mediated inflammatory environment inhibits chondrogenic differentiation of stem cells and leads to rapid degradation of cartilage derived from stem cells [65, 66]. Hence, there has been increasing investigations into therapeutics that may be beneficial in an inflammatory environment. Given the successful framework of a variety of protein therapies that are developed and applied in rheumatoid arthritis (RA), new approaches that edit the key transcripts of anticytokine molecules under endogenous promoter sequences have been applied to control the cellular response to inflammatory signals in the surrounding microenvironment dynamically. Pferdehirt et al. [67] developed a synthetic system using a designed promoter with several recognition elements of the nuclear factor kappa-light-chain-enhancer of activated B cells (NF- κ B) to amplify and induce the expression and release of anticytokine protein IL-1Ra. Transfecting the gene circuit into induced pluripotent stem cells (iPSCs) through lentiviral delivery, the engineered cells were capable of differentiating into engineered cartilage for the regeneration of diseased tissue and mitigating the inflammation in response to IL-1 in a self-regulated manner (Figure 5(a)). In recent studies, due to the highly targeted character and the low risks of tumorigenicity, the CRISPR-Cas9 system has revolutionized the applicability to mammalian cells [68]. A research showed that murine induced pluripotent stem cells (iPSCs) were engineered to functionally delete the IL-1 receptor I (*Il1r1*) using the CRISPR-Cas9 system. These modified cells produced more proteoglycan matrix and exhibited significant protection from the inflammation-induced tissue degradation compared to the wild-type cells [69]. Another similarly engineered iPSCs containing feedback-controlled gene circuits could be induced to produce bioactive drugs. Similarly, the base sequences expressing IL-1Ra or soluble TNFR1 (sTNFR1) were inserted downstream of the promoter of gene CCL2 to construct a dynamic negative feedback circuit activated by IL-1 or TNF using CRISPR gene editing (Figure 5(b)) [70]. During the latter research, the iPSCs in combination with a 3D PCL woven scaffolds were engineered to form a stable cartilaginous implant to alleviate the inflammation in a RA model [71]. The union of tissue engineering and synthetic biology promises a wide range of potential therapeutic applications for treating chronic diseases such as OA and RA by producing specially designed stem cells that not only can differentiate into tissue-specific cell types but can also regulate the expression of transgene molecules in direct response to dynamically changing pathologic signals in vivo. In the future, this highly responsive and self-regulated therapeutic strategy using designer stem cells for OA treatment could potentially overcome the limitations of

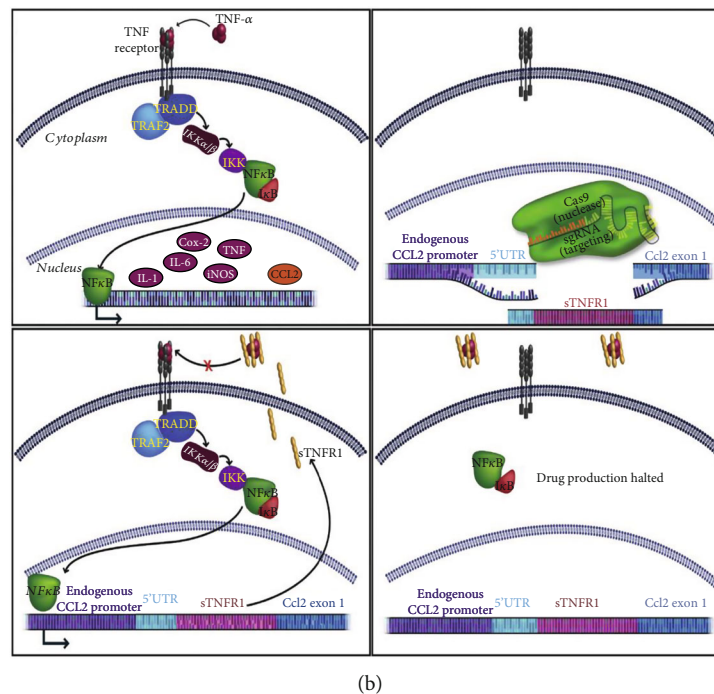
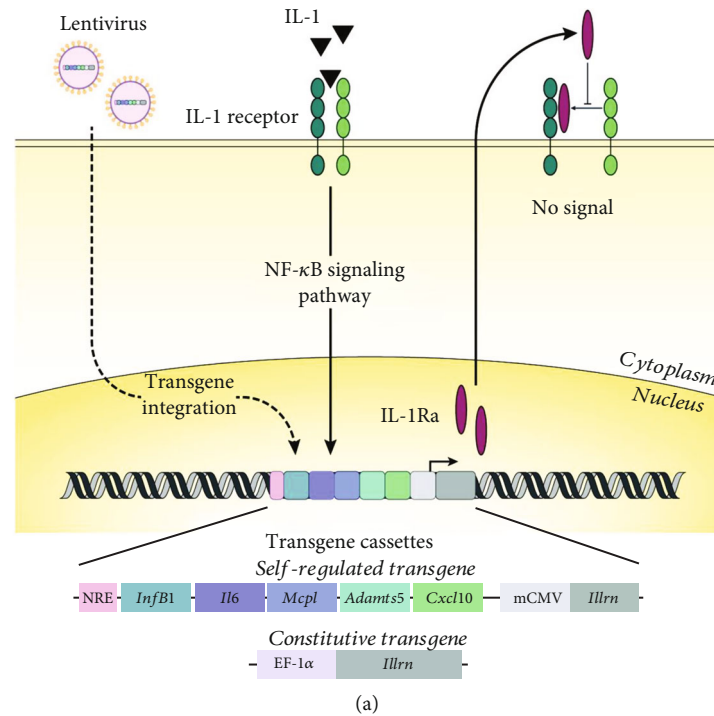


FIGURE 5: Synthetic gene circuits for self-regulated drug delivery systems. (a) IL-1 induced IL-1Ra expression through the NF- κ B signaling pathway. (b) sTNFR1 inserted in CCL2 loci can be initiated by TNF and inhibit TNF in return. Reproduced with permission [67, 70].

traditional biologic anticytokine drugs or therapies and ultimately reduce the risk of adverse events in patients.

5. Conclusion and Future Perspective

Despite the fact that stem cells have provided tremendous promise to treat orthopedic diseases due to their inherent regenerative therapeutic and immunoregulatory properties,

there still remain many challenges to realize their full therapeutic outcome, as increasing evidence indicated that in many cases, stem cells in their original state may not achieve the desired effect. Continued bioengineering approaches have improved the therapeutic efficacy; in particular, microgel assembly and 3D bioprinting techniques enable efficient cell encapsulation and improve cell survival and retention at the target site and precise cell patterning which mimics

the gradient structure of the osteochondral interface. Coupled with other technologies such as transgene delivery, CRISPR-Cas9-based gene editing, designer stem cells that can dynamically modulate the extracellular environment can be functionally achieved. In addition, for successful applications of MSCs in clinic, certain biosafety concerns such as genetic abnormality, tumor formation, and induction of host immune response need to be carefully addressed. It is reported that genomic instability and mutation may be induced during continuous and long-term cell expansion. The potential tumorigenic risk of MSC treatments may be related to the aberrant cell phenotype and malignant transformation [72]. Besides, some MSCs may undergo malignant transformation in the recipients with immune deficiency or special tumor environment [73, 74]. Therefore, it is important to optimize culture duration and monitor the chromosomal karyotype and cell growth kinetics strictly during the manufacturing of MSCs using advanced cytogenetic techniques and miRNA analysis to avoid the risk of tumorigenicity. At last, MSC-related clinical trials should be based on substantial animal experimental studies confirming its safety and effectiveness.

In the future, we believe that bioengineering approaches will continue to profoundly influence the application of stem cell therapies for osteochondral and joint relevant diseases. Intelligent stem cell therapies with self-regulating capabilities for biologic drug delivery will be widely applied in OA and many other chronic diseases.

Conflicts of Interest

The authors declare that they have no conflicts of interest.

Authors' Contributions

Meng Wang and Yixuan Luo contributed equally to this work.

Acknowledgments

F.C. acknowledges support from the Shenzhen Institutes of Advanced Technology Innovation Program for Excellent Young Researchers (Y9G075), and Y.Y. acknowledges funding from the Shenzhen Science and Technology Program (KQTD20170331160605510).

References

- [1] H. Long, X. Zeng, Q. Liu et al., "Burden of osteoarthritis in China, 1990–2017: findings from the global burden of disease study 2017," *The Lancet Rheumatology*, vol. 2, no. 3, pp. e164–e172, 2020.
- [2] H. Kwon, W. E. Brown, C. A. Lee et al., "Surgical and tissue engineering strategies for articular cartilage and meniscus repair," *Nature Reviews Rheumatology*, vol. 15, no. 9, pp. 550–570, 2019.
- [3] <https://clinicaltrials.gov/ct2/show/NCT01809769?term=cells&recrs=abcdefghijklm&cond=osteoarthritis&draw=2&rank=5>.
- [4] A. Arshi, F. A. Petrigliano, R. J. Williams, and K. J. Jones, "Stem cell treatment for knee articular cartilage defects and osteoarthritis," *Current Reviews in Musculoskeletal Medicine*, vol. 13, no. 1, pp. 20–27, 2020.
- [5] N. Nasiri, S. Hosseini, M. Alini, A. Khademhosseini, and M. Baghaban Eslaminejad, "Targeted cell delivery for articular cartilage regeneration and osteoarthritis treatment," *Drug Discovery Today*, vol. 24, no. 11, pp. 2212–2224, 2019.
- [6] L. Shang, Y. Cheng, and Y. Zhao, "Emerging droplet microfluidics," *Chemical Reviews*, vol. 117, no. 12, pp. 7964–8040, 2017.
- [7] W. Leong and D.-A. Wang, "Cell-laden polymeric microspheres for biomedical applications," *Trends in Biotechnology*, vol. 33, no. 11, pp. 653–666, 2015.
- [8] O. Levy, R. Kuai, E. M. Siren et al., "Shattering barriers toward clinically meaningful MSC therapies," *Science Advances*, vol. 6, no. 30, article eaba6884, 2020.
- [9] M. E. Sharpe, D. Morton, and A. Rossi, "Nonclinical safety strategies for stem cell therapies," *Toxicology and Applied Pharmacology*, vol. 262, no. 3, pp. 223–231, 2012.
- [10] H. Zhong, G. Chan, Y. Hu, H. Hu, and D. Ouyang, "A comprehensive map of FDA-approved pharmaceutical products," *Pharmaceutics*, vol. 10, no. 4, p. 263, 2018.
- [11] M. W. Tibbitt and K. S. Anseth, "Hydrogels as extracellular matrix mimics for 3D cell culture," *Biotechnology and Bioengineering*, vol. 103, no. 4, pp. 655–663, 2009.
- [12] A. C. Daly, L. Riley, T. Segura, and J. A. Burdick, "Hydrogel microparticles for biomedical applications," *Nature Reviews Materials*, vol. 5, no. 1, pp. 20–43, 2020.
- [13] Q. Feng, Q. Li, H. Wen et al., "Injection and self-assembly of bioinspired stem cell-laden gelatin/hyaluronic acid hybrid microgels promote cartilage repair in vivo," *Advanced Functional Materials*, vol. 29, no. 50, p. 1906690, 2019.
- [14] Y. Hou, W. Xie, K. Achazi et al., "Injectable degradable PVA microgels prepared by microfluidic technology for controlled osteogenic differentiation of mesenchymal stem cells," *Acta Biomaterialia*, vol. 77, pp. 28–37, 2018.
- [15] O. Veisheh, J. C. Doloff, M. Ma et al., "Size- and shape-dependent foreign body immune response to materials implanted in rodents and non-human primates," *Nature Materials*, vol. 14, no. 6, pp. 643–651, 2015.
- [16] G. Y. Bao, T. Jiang, H. Ravanbakhsh et al., "Triggered micropore-forming bioprinting of porous viscoelastic hydrogels," *Materials Horizons*, vol. 7, no. 9, pp. 2336–2347, 2020.
- [17] Y. Xia and K. Momot, *Biophysics and Biochemistry of Cartilage by NMR and MRI*, Royal Society of Chemistry, 2016.
- [18] L. Han, M. Wang, P. Li et al., "Mussel-inspired tissue-adhesive hydrogel based on the polydopamine–chondroitin sulfate complex for growth-factor-free cartilage regeneration," *ACS Applied Materials & Interfaces*, vol. 10, no. 33, pp. 28015–28026, 2018.
- [19] M. Shin, J. H. Galarraga, M. Y. Kwon, H. Lee, and J. A. Burdick, "Gallol-derived ECM-mimetic adhesive bioinks exhibiting temporal shear-thinning and stabilization behavior," *Acta Biomaterialia*, vol. 95, pp. 165–175, 2019.
- [20] J. H. Weisburg, D. B. Weissman, T. Sedaghat, and H. Babich, "In vitro cytotoxicity of epigallocatechin gallate and tea extracts to cancerous and normal cells from the human oral cavity," *Basic & Clinical Pharmacology & Toxicology*, vol. 95, no. 4, pp. 191–200, 2004.
- [21] F. Zhou, Y. Hong, X. Zhang et al., "Tough hydrogel with enhanced tissue integration and *in situ* forming capability

- for osteochondral defect repair,” *Applied Materials Today*, vol. 13, pp. 32–44, 2018.
- [22] Y. Yang, J. Zhang, Z. Liu et al., “Tissue-integratable and bio-compatible photogelation by the imine crosslinking reaction,” *Advanced Materials*, vol. 28, no. 14, pp. 2724–2730, 2016.
- [23] Y. Yu, K. K. Moncal, J. Li et al., “Three-dimensional bioprinting using self-assembling scalable scaffold-free “tissue strands” as a new bioink,” *Scientific Reports*, vol. 6, no. 1, p. 28714, 2016.
- [24] P. Datta, A. Dhawan, Y. Yu, D. Hayes, H. Gudapati, and I. T. Ozbolat, “Bioprinting of osteochondral tissues: a perspective on current gaps and future trends,” *International Journal of Bioprinting*, vol. 3, no. 2, pp. 109–120, 2017.
- [25] A. C. Daly and D. J. Kelly, “Biofabrication of spatially organised tissues by directing the growth of cellular spheroids within 3D printed polymeric microchambers,” *Biomaterials*, vol. 197, pp. 194–206, 2019.
- [26] B. Ayan, D. N. Heo, Z. Zhang, M. Dey, and I. T. Ozbolat, “Aspiration-assisted bioprinting for precise positioning of biologics,” *Science Advances*, vol. 6, no. 10, article eaaw5111, 2020.
- [27] B. Ayan, Y. Wu, V. Karuppagounder, F. Kamal, and I. T. Ozbolat, “Aspiration-assisted bioprinting of the osteochondral interface,” *Scientific Reports*, vol. 10, no. 1, 2020.
- [28] O. Jeon, Y. B. Lee, T. J. Hinton, A. W. Feinberg, and E. Alsborg, “Cryopreserved cell-laden alginate microgel bioink for 3D bioprinting of living tissues,” *Materials Today Chemistry*, vol. 12, pp. 61–70, 2019.
- [29] S. Xin, J. Dai, C. A. Gregory, A. Han, and D. L. Alge, “Creating physicochemical gradients in modular microporous annealed particle hydrogels via a microfluidic method,” *Advanced Functional Materials*, vol. 30, no. 6, article 1907102, 2019.
- [30] J. Liu, H. Zheng, P. S. Poh, H.-G. Machens, and A. F. Schilling, “Hydrogels for engineering of perfusable vascular networks,” *International Journal of Molecular Sciences*, vol. 16, no. 7, pp. 15997–16016, 2015.
- [31] A. M. Handorf, Y. Zhou, M. A. Halanski, and W.-J. Li, “Tissue stiffness dictates development, homeostasis, and disease progression,” *Organogenesis*, vol. 11, no. 1, pp. 1–15, 2015.
- [32] N. S. Hwang, S. Varghese, C. Puleo, Z. Zhang, and J. Elisseeff, “Morphogenetic signals from chondrocytes promote chondrogenic and osteogenic differentiation of mesenchymal stem cells,” *Journal of Cellular Physiology*, vol. 212, no. 2, pp. 281–284, 2007.
- [33] R. Yang, F. Chen, J. Guo, D. Zhou, and S. Luan, “Recent advances in polymeric biomaterials-based gene delivery for cartilage repair,” *Bioactive Materials*, vol. 5, no. 4, pp. 990–1003, 2020.
- [34] K. C. Clause, L. J. Liu, and K. Tobita, “Directed stem cell differentiation: the role of physical forces,” *Cell Communication & Adhesion*, vol. 17, no. 2, pp. 48–54, 2010.
- [35] N. Huebsch, P. R. Arany, A. S. Mao et al., “Harnessing traction-mediated manipulation of the cell/matrix interface to control stem-cell fate,” *Nature Materials*, vol. 9, no. 6, pp. 518–526, 2010.
- [36] T. Gonzalez-Fernandez, E. G. Tierney, G. M. Cunniffe, F. J. O’Brien, and D. J. Kelly, “Gene delivery of TGF- β 3 and BMP2 in an MSC-laden alginate hydrogel for articular cartilage and endochondral bone tissue engineering,” *Tissue Engineering Part A*, vol. 22, no. 9–10, pp. 776–787, 2016.
- [37] X. Wang, E. Wenk, X. Zhang, L. Meinel, G. Vunjak-Novakovic, and D. L. Kaplan, “Growth factor gradients via microsphere delivery in biopolymer scaffolds for osteochondral tissue engineering,” *Journal of Controlled Release*, vol. 134, no. 2, pp. 81–90, 2009.
- [38] X. Guo, H. Park, G. Liu et al., “In vitro generation of an osteochondral construct using injectable hydrogel composites encapsulating rabbit marrow mesenchymal stem cells,” *Biomaterials*, vol. 30, no. 14, pp. 2741–2752, 2009.
- [39] C. Evans, “Using genes to facilitate the endogenous repair and regeneration of orthopaedic tissues,” *International Orthopaedics*, vol. 38, no. 9, pp. 1761–1769, 2014.
- [40] N. P. Huynh, J. M. Brunger, C. C. Gloss, F. T. Moutos, C. A. Gersbach, and F. Guilak, “Genetic engineering of mesenchymal stem cells for differential matrix deposition on 3D woven scaffolds,” *Tissue Engineering Part A*, vol. 24, no. 19–20, pp. 1531–1544, 2018.
- [41] H. Madry, A. Rey-Rico, J. K. Venkatesan, B. Johnstone, and M. Cucchiari, “Transforming growth factor beta-releasing scaffolds for cartilage tissue engineering,” *Tissue Engineering Part B: Reviews*, vol. 20, no. 2, pp. 106–125, 2014.
- [42] D. H. Kempen, L. Lu, T. E. Hefferan et al., “Retention of in vitro and in vivo BMP-2 bioactivities in sustained delivery vehicles for bone tissue engineering,” *Biomaterials*, vol. 29, no. 22, pp. 3245–3252, 2008.
- [43] T. Alliston, L. Choy, P. Ducey, G. Karsenty, and R. Derynck, “TGF- β -induced repression of CBFA1 by Smad3 decreases cbfa1 and osteocalcin expression and inhibits osteoblast differentiation,” *The EMBO Journal*, vol. 20, no. 9, pp. 2254–2272, 2001.
- [44] C. A. Gersbach, R. E. Guldberg, and A. J. Garcia, “In vitro and in vivo osteoblastic differentiation of BMP-2- and Runx2-engineered skeletal myoblasts,” *Journal of Cellular Biochemistry*, vol. 100, no. 5, pp. 1324–1336, 2007.
- [45] A. C. Daly, F. E. Freeman, T. Gonzalez-Fernandez, S. E. Critchley, J. Nulty, and D. J. Kelly, “3D bioprinting for cartilage and osteochondral tissue engineering,” *Advanced Healthcare Materials*, vol. 6, no. 22, p. 1700298, 2017.
- [46] J. Chen, H. Chen, P. Li et al., “Simultaneous regeneration of articular cartilage and subchondral bone in vivo using MSCs induced by a spatially controlled gene delivery system in bilayered integrated scaffolds,” *Biomaterials*, vol. 32, no. 21, pp. 4793–4805, 2011.
- [47] T. Gonzalez-Fernandez, S. Rathan, C. Hobbs et al., “Pore-forming bioinks to enable spatio-temporally defined gene delivery in bioprinted tissues,” *Journal of Controlled Release*, vol. 301, pp. 13–27, 2019.
- [48] C. R. Rowland, K. A. Glass, A. R. Etyreddy et al., “Regulation of decellularized tissue remodeling via scaffold-mediated lentiviral delivery in anatomically-shaped osteochondral constructs,” *Biomaterials*, vol. 177, pp. 161–175, 2018.
- [49] R. Capito and M. Spector, “Collagen scaffolds for nonviral IGF-1 gene delivery in articular cartilage tissue engineering,” *Gene Therapy*, vol. 14, no. 9, pp. 721–732, 2007.
- [50] T. Gonzalez-Fernandez, D. J. Kelly, and F. J. O’Brien, “Controlled non-viral gene delivery in cartilage and bone repair: current strategies and future directions,” *Advanced Therapeutics*, vol. 1, no. 7, p. 1800038, 2018.
- [51] Y. Wang, X. Chen, W. Cao, and Y. Shi, “Plasticity of mesenchymal stem cells in immunomodulation: pathological and therapeutic implications,” *Nature Immunology*, vol. 15, no. 11, pp. 1009–1016, 2014.
- [52] S. F. de Witte, F. Luk, J. M. Sierra Parraga et al., “Immunomodulation by therapeutic mesenchymal stromal cells (MSC) is

- triggered through phagocytosis of MSC by monocytic cells,” *Stem Cells*, vol. 36, no. 4, pp. 602–615, 2018.
- [53] Y. Shi, Y. Wang, Q. Li et al., “Immunoregulatory mechanisms of mesenchymal stem and stromal cells in inflammatory diseases,” *Nature Reviews Nephrology*, vol. 14, no. 8, pp. 493–507, 2018.
- [54] M. Najar, M. Krayem, M. Merimi et al., “Insights into inflammatory priming of mesenchymal stromal cells: functional biological impacts,” *Inflammation Research*, vol. 67, no. 6, pp. 467–477, 2018.
- [55] C. Hu and L. Li, “Preconditioning influences mesenchymal stem cell properties in vitro and in vivo,” *Journal of Cellular and Molecular Medicine*, vol. 22, no. 3, pp. 1428–1442, 2018.
- [56] J. Croitoru-Lamoury, F. M. Lamoury, M. Caristo et al., “Interferon- γ regulates the proliferation and differentiation of mesenchymal stem cells via activation of indoleamine 2, 3 dioxygenase (IDO),” *PLoS One*, vol. 6, no. 2, article e14698, 2011.
- [57] G. Duque, D. C. Huang, M. Macoritto et al., “Autocrine regulation of interferon γ in mesenchymal stem cells plays a role in early osteoblastogenesis,” *Stem Cells*, vol. 27, no. 3, pp. 550–558, 2009.
- [58] S. F. de Witte, M. Franquesa, C. C. Baan, and M. J. Hoogduijn, “Toward development of imesenchymal stem cells for immunomodulatory therapy,” *Frontiers in Immunology*, vol. 6, p. 648, 2016.
- [59] T. Vigo, C. Procaccini, G. Ferrara et al., “IFN- γ orchestrates mesenchymal stem cell plasticity through the signal transducer and activator of transcription 1 and 3 and mammalian target of rapamycin pathways,” *Journal of Allergy and Clinical Immunology*, vol. 139, no. 5, pp. 1667–1676, 2017.
- [60] M. Croes, F. C. Oner, M. C. Kruyt et al., “Proinflammatory mediators enhance the osteogenesis of human mesenchymal stem cells after lineage commitment,” *PLoS One*, vol. 10, no. 7, article e0132781, 2015.
- [61] T. Lin, J. Pajarinen, A. Nabeshima et al., “Preconditioning of murine mesenchymal stem cells synergistically enhanced immunomodulation and osteogenesis,” *Stem Cell Research & Therapy*, vol. 8, no. 1, pp. 1–9, 2017.
- [62] E. Redondo-Castro, C. Cunningham, J. Miller et al., “Interleukin-1 primes human mesenchymal stem cells towards an anti-inflammatory and pro-trophic phenotype in vitro,” *Stem Cell Research & Therapy*, vol. 8, no. 1, p. 79, 2017.
- [63] H. Fayyad-Kazan, M. Fayyad-Kazan, B. Badran, D. Bron, L. Lagneaux, and M. Najar, “Study of the microRNA expression profile of foreskin derived mesenchymal stromal cells following inflammation priming,” *Journal of Translational Medicine*, vol. 15, no. 1, p. 10, 2017.
- [64] M. Fayyad-Kazan, M. Najar, H. Fayyad-Kazan, G. Raicevic, and L. Lagneaux, “Identification and evaluation of new immunoregulatory genes in mesenchymal stromal cells of different origins: comparison of normal and inflammatory conditions,” *Medical Science Monitor Basic Research*, vol. 23, pp. 87–96, 2017.
- [65] M. Kapoor, J. Martel-Pelletier, D. Lajeunesse, J.-P. Pelletier, and H. Fahmi, “Role of proinflammatory cytokines in the pathophysiology of osteoarthritis,” *Nature Reviews Rheumatology*, vol. 7, no. 1, pp. 33–42, 2011.
- [66] K. A. Glass, J. M. Link, J. M. Brunger, F. T. Moutos, C. A. Gersbach, and F. Guilak, “Tissue-engineered cartilage with inducible and tunable immunomodulatory properties,” *Biomaterials*, vol. 35, no. 22, pp. 5921–5931, 2014.
- [67] L. Pferdehirt, A. K. Ross, J. M. Brunger, and F. Guilak, “A synthetic gene circuit for self-regulating delivery of biologic drugs in engineered tissues,” *Tissue Engineering Part A*, vol. 25, no. 9–10, pp. 809–820, 2019.
- [68] M. L. Maeder and C. A. Gersbach, “Genome-editing technologies for gene and cell therapy,” *Molecular Therapy*, vol. 24, no. 3, pp. 430–446, 2016.
- [69] J. M. Brunger, A. Zutshi, V. P. Willard, C. A. Gersbach, and F. Guilak, “CRISPR/Cas9 editing of murine induced pluripotent stem cells for engineering inflammation-resistant tissues,” *Arthritis & Rheumatology*, vol. 69, no. 5, pp. 1111–1121, 2017.
- [70] J. M. Brunger, A. Zutshi, V. P. Willard, C. A. Gersbach, and F. Guilak, “Genome engineering of stem cells for autonomously regulated, closed-loop delivery of biologic drugs,” *Stem Cell Reports*, vol. 8, no. 5, pp. 1202–1213, 2017.
- [71] Y.-R. Choi, K. H. Collins, L. E. Springer et al., “A genome-engineered bioartificial implant for autoregulated anti-cytokine drug delivery,” *bioRxiv*, vol. 20, article 535609, p. 13, 2019.
- [72] Q. Pan, S. M. Fouraschen, P. E. D. Ruiter et al., “Detection of spontaneous tumorigenic transformation during culture expansion of human mesenchymal stromal cells,” *Experimental Biology & Medicine*, vol. 239, no. 1, pp. 105–115, 2014.
- [73] J. Liu, Y. Zhang, L. Bai, X. Cui, and J. Zhu, “Rat bone marrow mesenchymal stem cells undergo malignant transformation via indirect co-cultured with tumour cells,” *Cell Biochemistry & Function*, vol. 30, no. 8, pp. 650–656, 2012.
- [74] N. Amariglio, A. Hirshberg, B. W. Scheithauer et al., “Donor-derived brain tumor following neural stem cell transplantation in an ataxia telangiectasia patient,” *PLoS Medicine*, vol. 6, no. 2, pp. 221–231, 2009.